

b162 112 61
C.1

UV - UFS
BLOEMFONTEIN
BIBLIOTHEEK - LIBRARY

HIERDIE EASERPLAAT MAS WATERS
GEEN OMSTANDIGHEDE UIT DIE
BIBLIOTHEEK VERWYDER WORD NIE

University Free State



34300004551374

Universiteit Vrystaat

**NON-PERIPHERALLY SUBSTITUTED
PHTHALOCYANINES AS
CATALYSTS IN THE EPOXIDATION
OF ALKENES**

By

CHARLES ARREY ENOW

Thesis Submitted in fulfilment of the requirements for the degree

DOCTOR Philosophiae

in the

Faculty of Natural and Agricultural Sciences
Department of chemistry

at the
University of the Free State
Bloemfontein

Promoter: Prof. B.C.B. Bezuidenhout
Co-promoter: Dr. Charlene Marais

JUNE 2010

Universiteit van die
Vrystaat

BLOEFONTEIN

11 SEP 2012

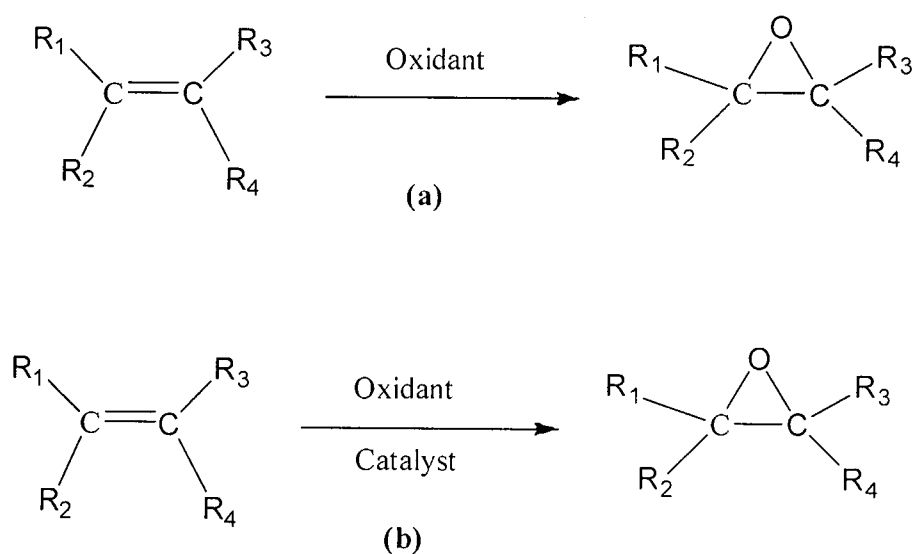
UV SASOL BIBLIOTHEK

CHAPTER ONE

Introduction and aims

1.1 Introduction

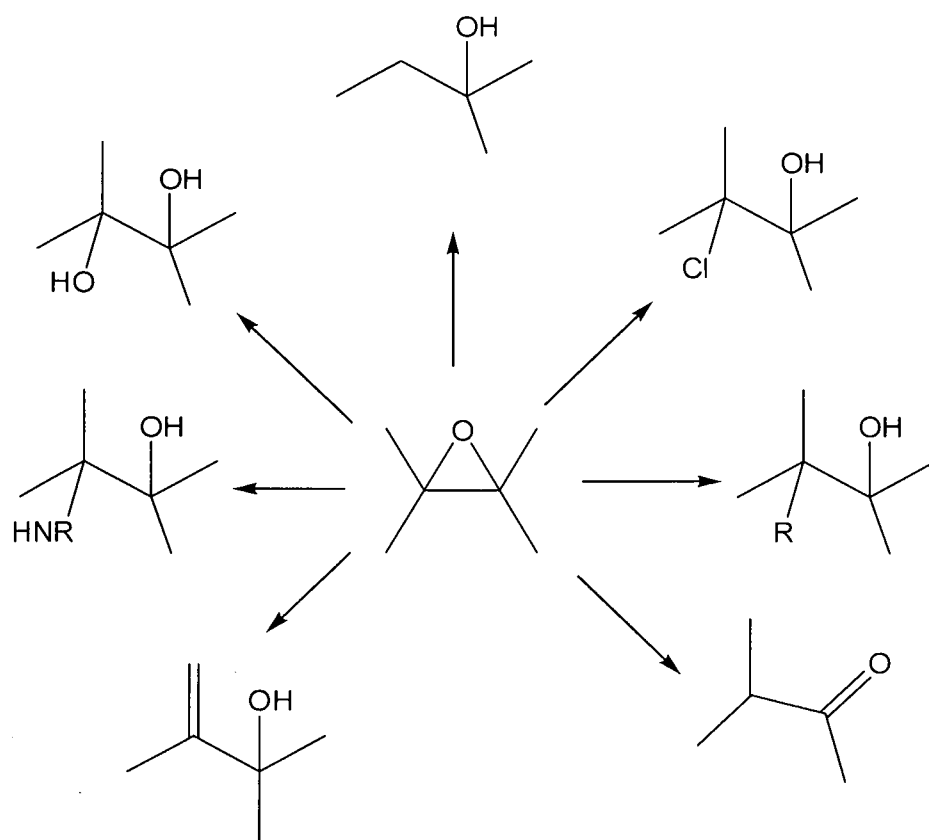
Epoxidation of alkenes (Scheme. 1.1), which is the main focus of this work, is a great reaction for converting the double bond of an alkene into an oxirane or epoxide.¹ Epoxides are an important class of functional groups found in many naturally occurring molecules as well as industrial starting materials. The epoxide unit in the structures of many naturally occurring molecules is essential for the biological activities of such molecules.



Scheme 1.1: Stoichiometric or catalytic alkene epoxidation.

Several well established systems based on a variety of oxidants have been reported for the production of epoxides.² There are basically two ways for transforming alkenes into epoxides. The traditional method [process (a) Scheme 1.1] uses stoichiometric amounts of oxidant, while a catalytic process [(b) in Scheme 1.1] in addition to the oxidant also requires a catalyst. The use of transition-metal complexes as catalysts for epoxidation and oxidation reactions in general has received considerable attention within the past three decades and most of the newly developed reactions in this field are catalytic in nature. The majority of the oxidative processes employed by industries involve catalysis by metal complexes, and an increasing variety of catalytic processes are being developed for laboratory-scale synthesis as well.

Notwithstanding the high activity, this area of chemistry continues to draw the attention of many researchers in academia and industry, because some epoxidation products such as propylene oxide, cyclohexene oxide, and ethylene oxide are valuable intermediates and precursors to many industrial products.¹⁻⁴ Propylene oxide (PO), for example, is a key industrial chemical used in the production of a variety of products such as propylene glycol (PG), PG ethers, polyurethane, unsaturated resins, etc.⁵ In fact, about 4.5 million metric tons of propylene oxide is produced annually by the epoxidation of propylene with an alkyl hydroperoxide or hydrogen peroxide, using either a heterogeneous or homogenous catalytic process.⁵ The versatility of epoxides as starting material in the synthesis of many other compounds is further illustrated by their conversion into diols, aminoalcohols, allylic alcohols, ketones, polyethers etc. as depicted in Scheme 1.2.⁷ Furthermore, since epoxidation of alkenes may lead to the generation of two chiral centres in a single reaction, there has been a heightened focus on the utilization of transition metal complexes in the synthesis of enantiomerically pure compounds.⁶ This was stimulated by a growing need towards the synthesis of optically active epoxides as starting materials for the production of a wide variety of biologically and pharmaceutically important compounds in the pharmaceutical and agrochemical industries.



Scheme 1.2: Possible conversions of epoxides (R = alkyl, aryl).⁷

While a variety of oxidants, like dioxiranes, alkylhydroperoxides, hydrogen peroxide, bleach, iodosylbenzene, pyridine *N*-oxides and molecular oxygen, have been described for laboratory epoxidations, peracids such as *m*-chloroperbenzoic acid (*m*-CPBA), are extensively used in these reactions.¹⁻⁶ Since the cost of the oxidant as well as the cost of dealing with the waste produced, are of utmost importance during industrial processes, industries strives towards chemical processes that utilize inexpensive reagents, give clean reactions, are environmentally friendly and atom-economical. Chemical processes which

involve many steps and produce, along with the target molecule, considerable amounts of other (undesirable) products and waste, have become less attractive. Oxidants are therefore generally chosen considering their economic - and environmental suitability, though the type of mechanism involved (per-oxo or oxo) also plays a role. The oxidants, except for molecular oxygen, are either expensive or produce stoichiometric amounts of by-products or waste that are difficult to remove. For example, one of the epoxidation routes for the manufacturing of propylene oxide produces huge amounts of styrene as by-product.^{1,5} Extensive efforts are therefore coming from both industry and academia towards the development of more efficient catalytic systems that utilise dioxygen, hydrogen peroxide or another environmentally benign oxidants. Unfortunately, each oxidant seems to have its own set of problems ranging from the preparation method to the type of solvent needed. Organic oxidants such as *tert*-butylhydroperoxide (TBHP) and *N*-oxides are preferred over inorganic ones, because they can often be recycled through reaction with hydrogen peroxide for example.^{2b} Furthermore, many of these oxidants show moderate reactivity towards various substrates or are unstable. From the industrial point of view oxygen is considered the ideal oxidant considering that it is cheap, its active oxygen content is high (100%) and the fact that no waste products or only water is formed after oxidation.

Compared to catalytic processes, stoichiometric reactions are usually performed under much harsher conditions, are unselective, and produce huge amounts of inorganic effluents that are difficult to dispose of.⁸ Transition metal catalysts are therefore used purposely to promote the rate of reaction, yields and selectivity. For catalytic processes, compatibility between the type of catalyst and the oxidant is important. Thus, an assortment of metal complexes of porphyrins, phenanthrolines, salens, phthalocyanines (Pcs) etc. have been developed and studied as epoxidation catalysts with various oxidants. Since catalyst decomposition is a serious concern for most of these systems, product yields based on substrate are usually low and reaction times very long.

1.2 Aim of this study

Despite the existence of numerous catalytic systems for the epoxidation of alkenes, yields based on the substrate used, are low, and the scope of substrates limited.^{2b} Furthermore, reaction times for complete consumption of the substrate are usually extensive (≥ 48 h), while significant degradation of the catalyst during the course of the reaction have been observed in many instances. Some catalysts also require the presence of a sacrificial reductant, like an aldehyde that would be converted to the corresponding acid, during the epoxidation process.^{2a}

Due to their structural similarity to porphyrins, metallophthalocyanines have received some attention as epoxidation catalysts,⁹ but the epoxidation chemistry of phthalocyanines have not been developed to the extent of that of porphyrins with respect to the type of oxygen donors and metals used, or reaction mechanisms involved. In fact only phthalocyanines containing iron, manganese, and cobalt have received extensive attention,¹⁰ while ruthenium phthalocyanines have only been applied to the oxidation of 1-octene to 2-octanone (with dioxygen and $(\text{C}_6\text{H}_5\text{CN})_2\text{PdCl}_2$ as olefin activator)¹¹ and cycloalkenes to ketones and alcohols using *tert*-butyl hydroperoxide (*t*-BuOOH) as oxidant.¹²

Although phthalocyanines have the advantage of being more stable towards oxidative degradation than porphyrins,¹⁰ development of the oxidation chemistry of ruthenium-phthalocyanines have been hampered by poor solubility in hydrocarbon solvents due to aggregation. Ruthenium phthalocyanines with alkyl substituents in the 1,4,8,11,15,18,22,25 (non-peripheral) positions would, however, make attractive catalysts in oxidation/epoxidation reactions because of their improved solubility.¹³ In order to exploit the increased stability of phthalocyanines when compared to porphyrins and due to the remarkable results obtained with ruthenium porphyrins as epoxidation catalysts, it was decided to investigate the possibility of utilizing non-peripherally alkyl substituted ruthenium phthalocyanines as catalysts in the epoxidation of alkenes. Since the best

results with the porphyrin systems were obtained with pyridine *N*-oxides as oxidant (the Hirobe method),¹⁴ the investigation was started with this oxidant and included a series of 1,4,8,11,15,18,22,25-octaalkyl ruthenium phthalocyanine catalysts that were evaluated for reactions with several alkene substrates.

1.3 References

1. Van Leeuwen, P. W. N. M. *Homogeneous Catalysis*; Kluwer Academic Publishers: Dordrecht, 2004, pp 299.
2. (a) Meunier, B. *Chem. Rev.* **1992**, *92*, 1411-1456. (b) Gert, A.; Sheldon, R.A. *J. Mol. Catal. A: Chem.* **1995**, *98*, 143-146.
3. Buranaprasertsuk, P.; Tangsakol, Y.; Chavasiri, W. *Catalysis Communications* **2007**, *8*, 310.
4. Neumann, R.; Dahan, M. *Nature* **1997**, *388*, 353.
5. Matar, S. and Hatch, L.F., *Chemistry of Petrochemical Processes*, Gulf Publishing Company, Houston, Texas, 1994, pp 1-10.
6. Jorgensen, K.A. *Chem. Rev.* **1989**, *89*, 431.
7. (a) Gorzynski, S. *J. Synthesis* **1984**, 629-656. (b) Bonini, C.; Righi, G. *Synthesis* **1994**, 225-238.
8. Che, C-M. and Huang, J-S. *Chem. Commun.* **2009**, 3996-4015.
9. Larsen, E. and Jorgensen, K.A. *Acta Chem. Scand.* **1989**, *43*, 259-263.
10. Mahtab, P.; Nasser, S.; Abbas Ali, S. Iran. *J. Chem. Chem. Eng.* **2006**, *25*(4), 85. (b) Ebadi, A.; Nasser, S.; Peyrovi, M.H. *Applied Catalysis A: General* **2007**, *321*, 135-139. (c) Sorokin, A.B.; Mangematin, S.; Pergale, C. *J. Mol. Cat. A: Chem.* **2002**, *182-183*, 267-281.
11. Capobianchi, A.; Paoletti, A.M.; Pennesi, G.; Rossi, G.; Caminiti, R. and Ercolani, C. *Inorg. Chem.* **1994**, *33*, 4635-4640.
12. Kenneth J. Balkus, Jr.; Eissa, M. and Levado, R. *J. Am. Chem. Soc.* **1995**, *117*, 10753-10754.

13. McKeown, N.B.; Chambrier, I. and Cook, M.J. *J. Chem. Soc., Perkin Trans. 1* **1990**, 1169
14. (a) Higuchi, T.; Ohtake, H.; Hirobe, Herobe, M. *Tetrahedron Lett.* **1989**, 30, 6545. (b) Higuchi, T.; Ohtake, H.; Herobe, M. *Tetrahedron Lett.* **1991**, 32, 7435. (c) Higuchi, T.; Ohtake, H.; Herobe, M. *Tetrahedron Lett.* **1992**, 33, 2521. (d) Higuchi, T.; Ohtake, H.; Herobe, M. *Tetrahedron Lett.* **1989**, 30, 6545.

Chapter Two

Metal-catalyzed (Ep)oxidation of Alkenes

2.1 Introduction

The study of transition metal catalyzed epoxidation stems from the rich and diverse chemistry of the naturally occurring heme containing protein, cytochrome P-450. These enzymes are known to be very active and selective in catalyzing the transfer of oxygen atoms to hydrocarbons *in vivo*.¹⁻³ Under mild conditions, using oxygen from air, these enzymes efficiently catalyze the conversion of hydrocarbons to alcohols.¹ Controlled and selective oxygenation reactions demonstrated by these enzymes is quite valuable both in biological systems and industries.⁴ Over the years, significant efforts have been directed at studying these enzymatic reactions and the development of their artificial mimics to effect similar oxidation reactions in organic systems. As a result, a variety of cytochrome P-450 models have been developed and applied as catalysts in oxidation reactions.

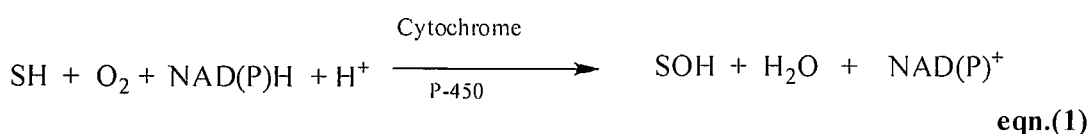
The use of dioxygen as oxidant posed a lot of difficulty for artificial monooxygenases. The discovery of the peroxide shunt route which allows for the use of mono-oxygen donors opened the way for several metal complexes including metalloporphyrins, metallophthalocyanines, manganese (III) Schiff base complexes, etc. to be studied as cytochrome P-450 models. Often, the objective is to mimic the activity, selectivity, and catalyst stability that are well known for the cytochrome P-450 enzymes. A number of effective catalytic systems for the epoxidation of unfunctionalized olefins based on metalloporphyrin catalysts with iron, manganese and ruthenium complexes have been developed.⁵⁻⁷ Another useful and well developed catalyst system in the field of epoxidation reactions is based on (salen)manganese complexes.⁸

Owing to the value of enantiopure epoxides, catalytic asymmetric epoxidation has also received considerable attention. Since the discovery of the Ti^{IV} -diethyl tartrate catalytic

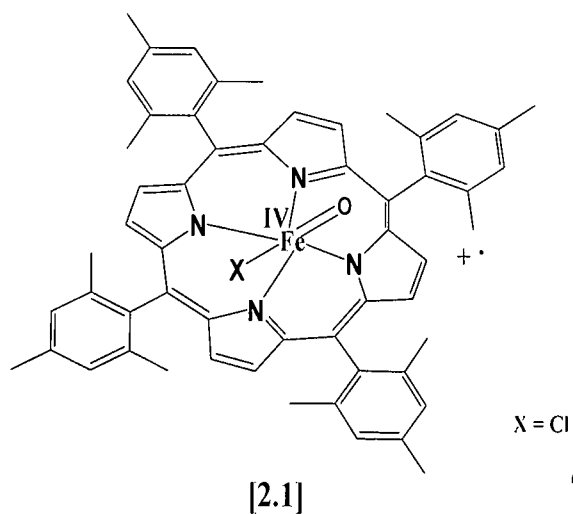
system by Sharpless⁹ for the stereoselective epoxidation of allylic alcohols, a number of transition metal chiral catalysts have been synthesized to perform asymmetric epoxidation of unfunctionalized olefins with moderate to high enantioselectivity.⁹⁻¹¹ For example, Berkessel *et al.*¹² reported the use of chiral ruthenium porphyrin complexes for the epoxidation of styrene in $\approx 80\%$ enantiomeric excess.

2.2 Cytochrome P-450 based oxidation systems

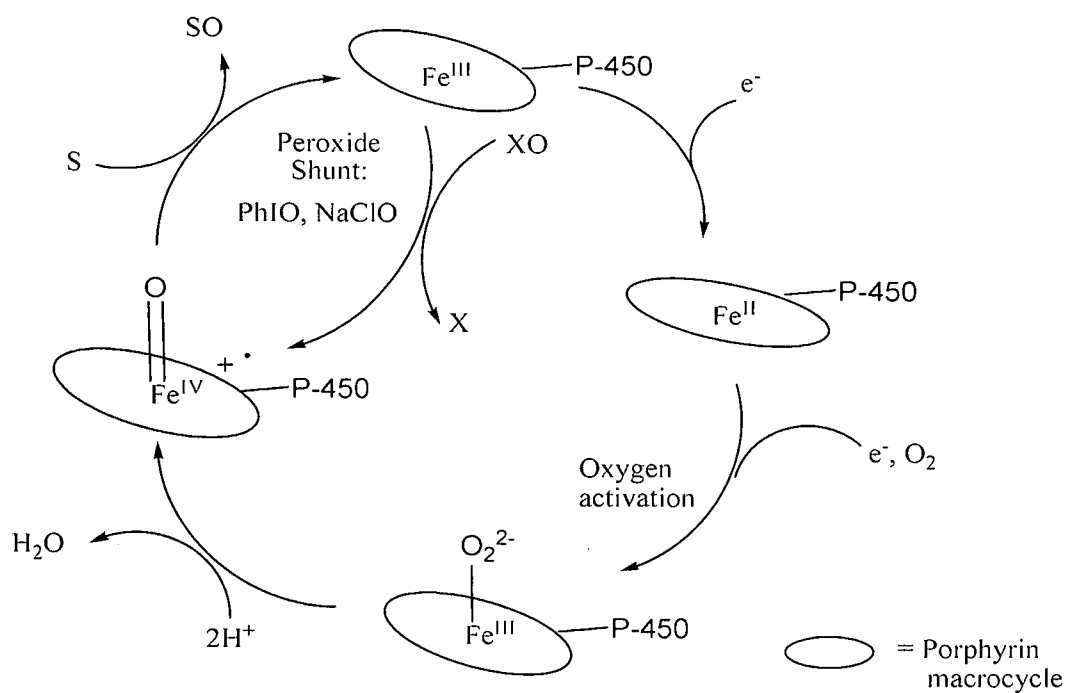
Cytochrome P-450 is the name given to a huge family of heme-containing monooxygenase enzymes engaged in the metabolism of a range of both exogenous and endogenous compounds.¹ This enzyme is part of the enzyme system referred to as the mixed function oxidase (MFO) system. During the process of oxygenation of a substrate (S) by cytochrome P450 using molecular oxygen, one atom of the molecular oxygen is incorporated into the substrate (oxygenation) and the other oxygen atom is reduced to water. The overall reaction is given in eqn (1) (S = substrate).¹ The P-450 enzymes are called monooxygenases because only one of the two oxygen atoms initially present in the O₂ molecule gets added into the oxidized substrate.



The cytochrome P-450 active site contains a high-valent iron atom enclosed in a porphyrin type macrocycle, [2.1],^{1,13,14} which catalyzes the epoxidation of alkenes.^{13,14} At the active site of cytochrome P-450, molecular oxygen is bound, reduced, activated, and then transferred to the substrate.



Through the peroxide shunt route (Scheme 2.1)^{2b} the oxygen binding and activation step in the cytochrome P-450 reaction cycle were circumvented, due to the direct release of the high-valent intermediate. Hence, it became possible to use other exogenous single oxygen transfer reagents such as iodosylbenzene (PhIO), peracids, peroxides, *N*-oxides, and hypochlorites and thereby eliminating the need for a co-reductant.¹⁵



Scheme 2.1: Cytochrome P-450 reaction cycle.^{2b}

In 1979, Groves *et al.*¹⁶ reported the first synthetic model of the peroxide shunt route for the oxidation of alkenes and alkanes based on iron porphyrin and PhIO. This system was later on extended to manganese porphyrin complexes. Over the past three decades, the peroxide shunt route has been extensively studied and efficient catalytic systems based on metalloporphyrin and manganese (III) Schiff base complexes with iron, manganese and ruthenium have been developed.¹⁷

2.3 Oxidants

The discovery of the peroxide shunt pathway opened the way for the utilization of exogenous single oxygen donors in metal catalyzed oxidation. A variety of exogenous single oxygen atom donors can in principle be used as terminal oxidants for transition metal-catalyzed oxidation reactions (Table 2.1).¹⁸ This circumvents the problem of dioxygen activation by artificial mono-oxygenases.

The choice of oxidant for a particular system is determined by:

- The active oxygen content of the oxidant.
- The cost of the oxidant.
- The nature of the post reaction effluents.
- Compatibility of oxidant with catalyst type.

Table 2.1: Oxidants used in transition metal-catalyzed epoxidation, and their active oxygen content.

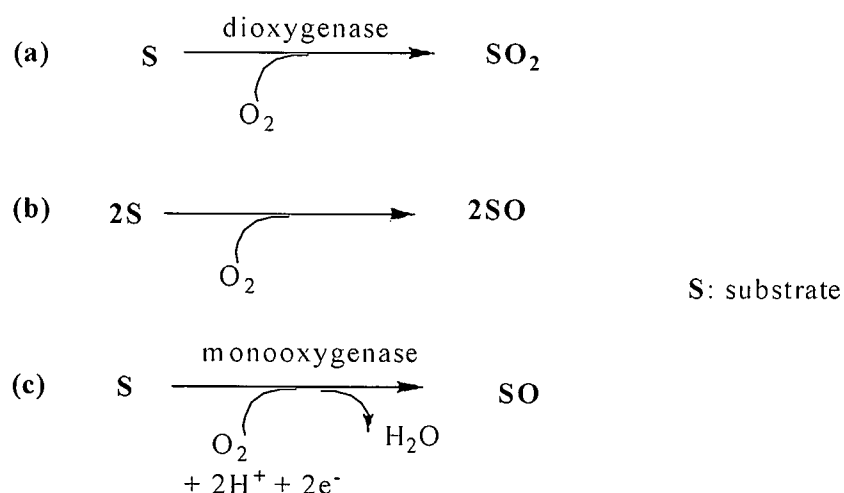
Oxidant	Active oxygen content (wt.%)	Waste product
Oxygen (O ₂)	100	Nothing or H ₂ O
Oxygen (O ₂)/reductor	50	H ₂ O
H ₂ O ₂	47	H ₂ O
NaOCl	21.6	NaCl
CH ₃ CO ₃ H	21.1	CH ₃ CO ₂ H
^t BuOOH(TBHP)	17.8	^t BuOH
KHSO ₅	10.5	KHSO ₄
BTSP ^a	9	hexamethyldisiloxane
PhIO	7.3	PhI
C ₅ H ₁₁ NO ₂ ^b	13.6	C ₅ H ₁₁ NO

^a Bistrimethylsilyl peroxide, ^b N-Methylmorphiline-*N*-oxide.

Despite low active oxygen contents (Table 2.1), alkyl hydroperoxides, or hypochlorite, or iodosylbenzene are utilized as oxidants in most catalytic systems.

2.3.1 Epoxidation with O₂

Since O₂ is the ideal oxidant, the objective and challenge in the development of epoxidation catalysts have always been to design one with the ability to transfer oxygen from O₂ in the air directly to the substrate. In nature, oxygenation of substrates is effected by either monooxygenases of cytochrome P-450 or methane monooxygenase and dioxygenases (see Scheme 2.2). **Monooxygenases (c)** work with a reducing agent in such a manner that only one O-atom is incorporated in the substrate, whilst the second atom is reduced to H₂O. The O=O bond is split by the two electrons from the reducing agent resulting in the formation of the high-valent metal-oxo (M=O) species that later transfers its oxygen to the substrate. Though many versions of synthetic monooxygenase models have been reported, these epoxidation reactions require stoichiometric amounts of a co-reductant to regenerate the oxidizing species, making this process undesirable for industrial application.



Scheme 2.2: Oxygen atom transfer to substrate.

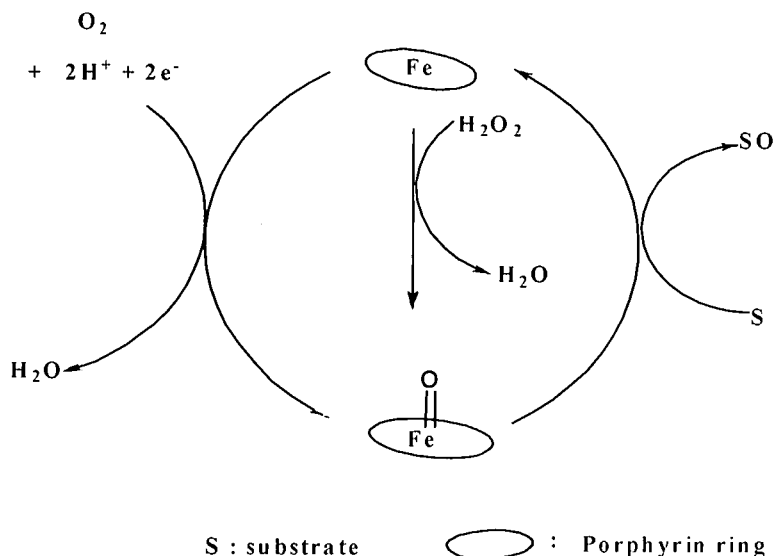
Dioxygenase-like epoxidation or sulfoxidation with air (b) entails the homolytic cleavage of the O=O bond by two metal centres to form two high valent metal-oxo species and each substrate molecule eventually receives one oxygen atom. This process is important especially to industry, because there is no generation of any by-products or waste that has to be separated from product as is the case when co-reductants are used.

Even though molecular oxygen is a neat and economical way of performing oxidation, molecular oxygen activation is a huge problem in most complexes, Groves and Quinn^{7b} noted, "for molecular oxygen to act as oxidant for epoxidation, the catalyst must be able to activate it without the help of a co-reductant". In practice, very few catalysts have until now been developed with the ability to carry out aerobic oxidation without the help of a co-reductant. These include, the Ru(TMP)(O)₂ (TMP = tetramesitylporphyrin) reported by Groves and Quinn,¹⁹ ruthenium polyoxometalate,²⁰ {[WZnRu₂(OH)(H₂O)](ZnW₉O₃₄)₂},¹¹ and the ruthenium-phenanthroline complex,²¹ [Ru(dmp)₂(CH₃CN)₂](PF₆) (dmp = 2,9-dimethyl-1,10-phenanthroline). TONs in these systems are still very low. Consequently, for most oxidations with molecular oxygen as oxidant, a sacrificial reductant is added. Examples include, O₂ and aldehyde or alcohols,²² O₂ and H₂,²³ and O₂ with Zn powder.^{24a}

2.3.2 Epoxidation with Hydrogen Peroxide.

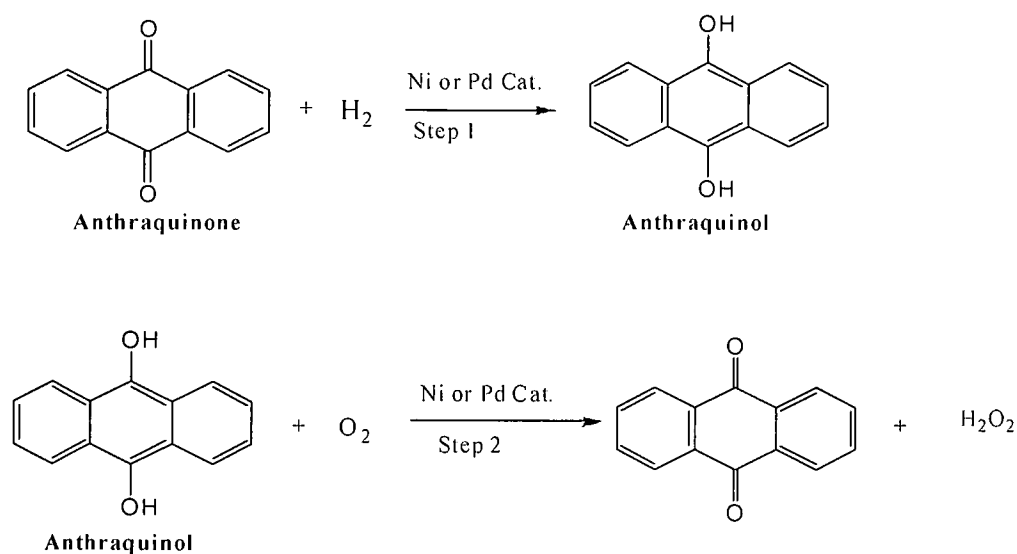
The oxidant, H₂O₂, has been used because it is considered environmentally clean. The main reason being the fact that water is the only side product of H₂O₂ oxidation. In addition, H₂O₂ contains a high proportion of active oxidant (48.5%). Furthermore, no chlorinated residues are formed as in bleaching methods, or with other chlorine-containing oxidants. Due to the benefits derived from performing epoxidation with hydrogen peroxide, coupled with the difficulties in activating molecular oxygen, the recent trend in this area of research has been towards the design of catalytic species for olefin epoxidation that are compatible with the environmentally friendly hydrogen peroxide. With hydrogen peroxide, some of the problems encountered with using

molecular oxygen as oxidant can be partly avoided as the reactive oxene-intermediate is generated without the help of a co-reductant (Scheme 2.3).^{24b}



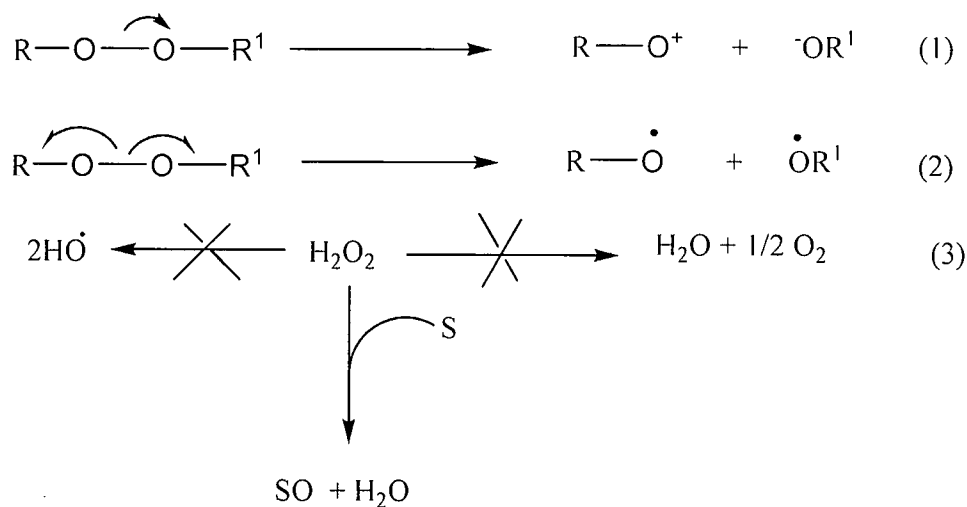
Scheme 2.3: H₂O₂ catalyzed cycle.^{24b}

Hydrogen peroxide is relatively cheap (< 0.6 € kg⁻¹ of 100% H₂O₂), readily available, and can be used safely without much precautions. In addition, the structural feature of hydrogen peroxide makes it more suitable for liquid-phase oxidations. Up to 2006, about 2.2 million tonnes of hydrogen peroxide were produced annually exclusively by the autooxidation of anthraquinol to anthraquinone and hydrogen peroxide using oxygen from the air (Scheme 2.4).^{24c} The anthraquinone serves as a hydrogen carrier as direct reaction of hydrogen with oxygen may lead to explosive mixtures.



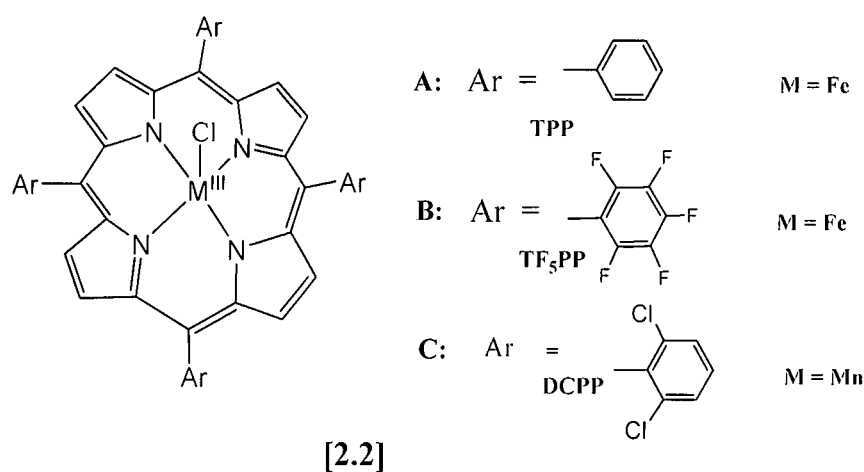
Scheme 2.4: Production of H₂O₂

In metal complex-catalyzed epoxidation with hydrogen peroxide and other alkylhydroperoxides, the O=O bond can either be cleaved homolytically or heterolytically (Scheme 2.5).



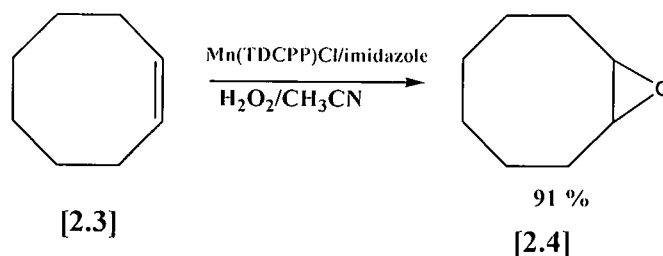
Scheme 2.5: Homolytic (2) and Heterolytic (1) bond cleavage
 (3) Disproportionation or a homolytic cleavage of H₂O₂-molecule.

With iron porphyrin complexes [2.2], heterolytic fission leads to the formation of the appropriate high-valent reactive intermediate $[\text{Fe}^{\text{IV}}\text{porp}^{\bullet+}(\text{O})]$ that oxidizes the substrate.²⁵ Homolytic cleavage of the H_2O_2 is an undesired pathway as it rather brings about a breakdown of the oxidant [Scheme 2.5 (3)], hampering the transfer of oxygen to the substrate.



So, in general, a catalyst is needed that will transfer oxygen from hydrogen peroxide to the substrate without its decomposition through disproportionation to water and oxygen. To overcome the problem of hydrogen peroxide decomposition during epoxidation, more than stoichiometric amounts of hydrogen peroxide are used.^{25e} Most metal catalysts tend to be unstable and experience rapid decay when subjected to such high amounts of hydrogen peroxide.²⁵ Hence, for hydrogen peroxide to be efficiently employed in alkene epoxidation, the choice of catalyst should be such that minimal decomposition of the hydrogen peroxide occurs. The catalyst should also be stable in the presence of high hydrogen peroxide concentrations.^{15b,25e} For example, the highly robust $\text{Mn}^{\text{III}}(\text{TDCPP})\text{Cl}$ TDCPP = tetrakis(dichlorophenyl)porphyrin][2.2C] efficiently catalyzes alkene epoxidation with hydrogen peroxide in the presence of imidazole.^{15b,25e} Cyclooctene [2.3] epoxidation (Scheme 2.6) under this condition afforded 91 % of the epoxide [2.4]. The

imidazole performs a dual role as a stabilizing axial ligand and as acid-base catalyst to favor the heterolytic cleavage of the O=O bond.



TDCPP = tetrakis(dichlorophenyl)porphyrin

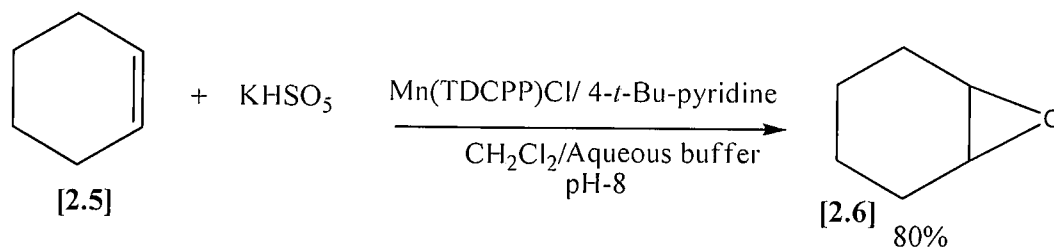
Scheme 2.6

2.3.3 Epoxidation with potassium hydrogen persulphate (Oxone)

Potassium hydrogen persulphate is a stable inorganic peroxide obtained by co-crystallization of a mixture of potassium sulphate and potassium monoperoxysulfate into a triple salt: 2KHSO₅·KHSO₄·K₂SO₄, which is commercially available under the name oxone.^{15b} While it is a safe and easy to handle oxygen donor, the utilization of oxone in epoxidation reactions has certain distinct disadvantages, i.e.

- Oxone has very low active oxygen content (10.5%)
- It is highly stable in water. Aqueous solutions of KHSO₅ only loses *ca.* 5 % of its active oxygen content in three days.
- 3 moles of SO₄²⁻ is produced for every mole of alkene epoxide formed.

An example of epoxidation with oxone is shown in Scheme 2.7A.^{15b} With 0.1 - 0.25 mol% of the catalyst in the presence of 4-*tert*-butylpyridine, cyclohexene [2.5] epoxidation afforded the epoxide [2.6] in 80 % yield.

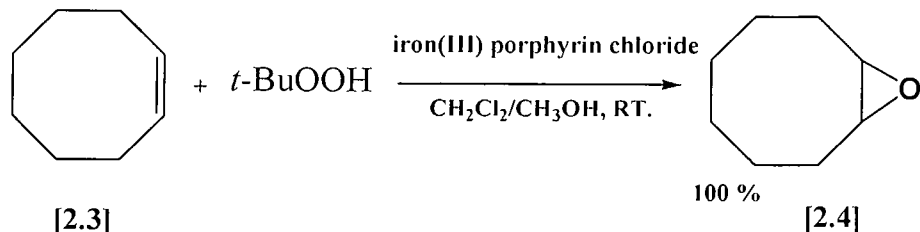


TDCPP = tetrakis-dichlorophenyl porphyrin

Scheme 2.7A: Epoxidation with oxone.

2.3.4 Epoxidation with alkyl hydroperoxides (ROOH)

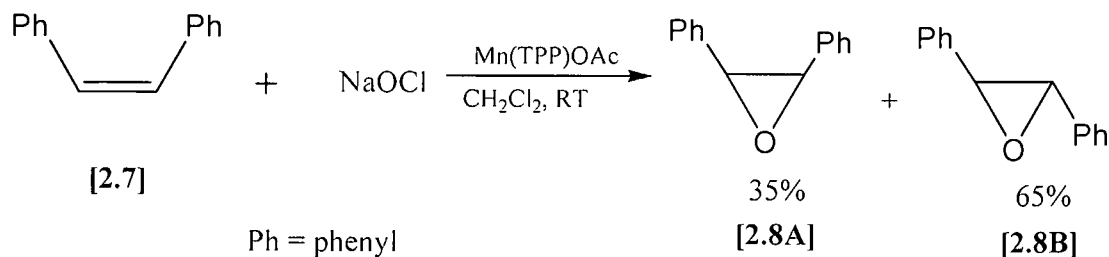
Alkyl hydroperoxides are easily produced by autoxidation of alkanes having one tertiary C-H bond, e.g. isobutane, and used as oxygen donors in olefin epoxidation catalysed by molybdenum, vanadium, or titanium complexes.^{15b} These compounds are the oxidants of choice for reactions like the Sharpless asymmetric epoxidation of allylic alcohols.^{25f} As with hydrogen peroxide, the major difficulty with alkyl hydroperoxides is to avoid the homolytic cleavage of the peroxide bond, which leads to the formation of the RO^\bullet radical that is able to abstract one hydrogen atom from alkenes without forming the epoxide. Only traces of the epoxide are formed when an alkyl hydroperoxide is used as the terminal oxidant, but in the presence of imidazole the epoxide yields increase.^{15b} The imidazole is thought to perform two roles; as a stabilizing axial ligand and as an acid-base catalyst which enhances the heterolytic cleavage of the RO-OH bond. Cyclooctene [2.3] epoxidation with *tert*-butyl hydroperoxide catalyzed by iron(III) porphyrin chloride afforded the epoxide [2.4] in 100 % yield (Scheme 2.7B).^{25g}



Scheme 2.7B: Epoxidation with *tert*-butyl hydroperoxide

2.3.5 Epoxidation with hypochlorites.

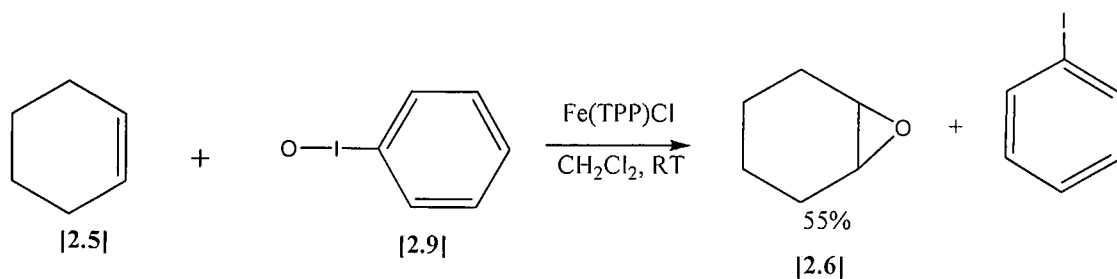
Sodium hypochlorite solutions (NaOCl) which are prepared by the chlorination of sodium hydroxide, are cheap, safe, readily available and can be used easily. The pH value of the aqueous solution greatly determines its chemical properties. Metalloporphyrin catalysed epoxidation of alkenes with hypochlorites was investigated by, amongst others, Meunier *et al.*,^{26a} and Montanari and co-workers.^{26b} Montanari and co-workers reported that highly efficient catalytic epoxidations can be performed by adjusting the pH of hypochlorite solutions to 9.5 with diluted HCl.^{26b} It was however also found that selectivity towards the product (epoxide) decreased at lower pH values (7, 8.5), while the addition of small amounts of pyridine and imidazole strongly increased the stereoselectivity, reaction rate and overall turnover numbers. An example of epoxidation with NaOCl is shown in Scheme 2.8.^{26a} *Cis*-stilbene [2.7] epoxidation yielded a mixture of the *cis*-epoxide [2.8A] and the *trans*-epoxide [2.8B]. The disadvantages of the oxidant include NaCl being formed as waste product and the low oxygen content of NaOCl (21.6 %).



Scheme 2.8^{26a}

2.3.6 Epoxidation with Iodosylbenzene.

Iodosylbenzene [2.9], another one-oxygen atom donor reagent for epoxidation reactions, showed high stereoselectivity when iron porphyrins were used with *cis*-olefins giving only *cis*-epoxides. A large loss in stereoselectivity is, however, observed when manganese porphyrins are used.^{15b}



Scheme 2.9

The use of iodosylbenzene has been limited due to the following aspects²⁷:

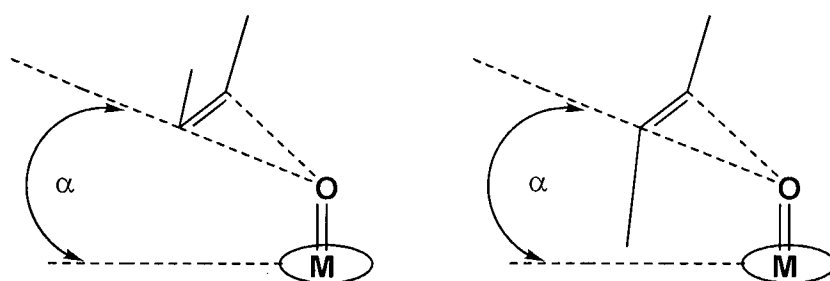
- It is insoluble in common organic solvents
- It has low oxygen content (7.3 %)
- It produces C₆H₅I

An example of epoxidation with PhIO is shown in Scheme 2.9.^{2a}

2.4 Porphyrin - catalyzed Epoxidations.

2.4.1 Iron Porphyrin

Synthetic iron complexes of both heme and non-heme ligands, because of their relationship to biological systems, have been extensively studied as epoxidation catalysts together with a variety of oxidants to mimic cytochrome P-450 type reactions. With iodosylbenzene (PhIO) as exogenous oxygen source, Groves *et al.*¹⁶ showed that (FeTPP)Cl [2.2 A] catalyzed the epoxidation of alkenes giving high epoxide yields. The epoxidation was stereospecific with *cis*-alkenes generating *cis*-epoxides. The (FeTPP)Cl/PhIO system was found to be particularly selective for the *cis*-olefins. Unlike the epoxidation with *m*-CPBA where the *cis*- and *trans*-olefins epoxidize at equal rates at room temperature, the *cis*-epoxide formed 15 times faster than the *trans*-epoxide. With the (FeTPP)Cl/PhIO system, preference for the *cis*-alkene apparently originates from the steric hindrance by the substituents on the porphyrin ring,² as bulky TMP ligands show enhanced *cis* selectivity. To explain the *cis*- vs. *trans*-alkene selectivity, Groves *et al.*^{2a} proposed the renowned 'side on approach model' (Scheme 2.10).

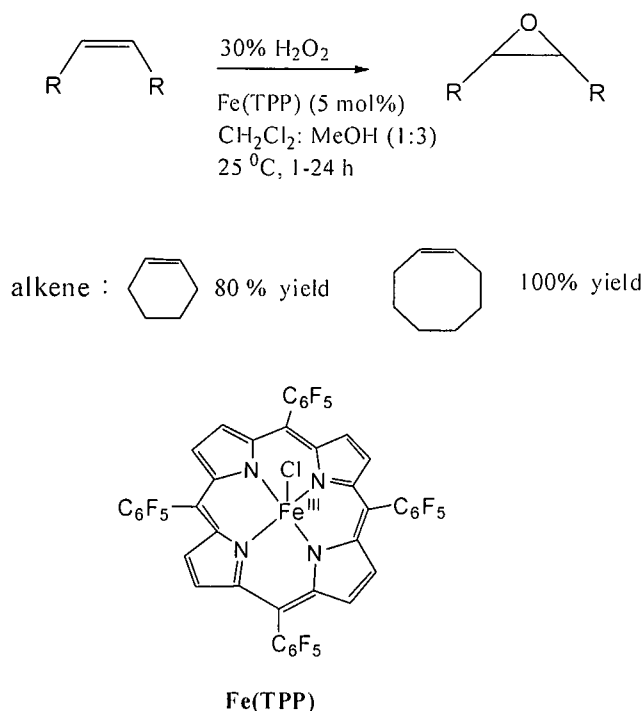


Scheme 2.10: The "side-on approach" model for oxygen transfer showing the less hindered approach for *cis*-alkenes compared to *trans*-alkenes.

In this model, it is postulated that the olefin approaches the metal oxygen ($M=O$) sideways at an angle (α). For the *cis*-alkenes, there is maximum overlap of the filled π -orbital of the alkene with the $d_{\pi-p\pi}$ M-O antibonding orbital, resulting in high epoxide yields. On the other hand, less overlap of these orbitals due to an unfavorable interaction caused by the geometric constraints/demands imposed by one of the *trans*-substituents and the porphyrin plane results in low or zero epoxide yields in the case of *trans*-alkenes.

Though the mechanism for this reaction has been the subject of debate, the active species is however thought to be the oxo-iron (IV) porphyrin species formed from the oxidation of the porphyrin by PhIO. These results led to the synthesis of many chiral versions of iron porphyrins for asymmetric epoxidation.

Iron porphyrin catalyzed epoxidation has also been extensively studied with alkyl and hydrogen peroxides.^{15,27,28} Traylor and coworkers²⁹ first reported an efficient polyfluorinated Fe(TPP) system for the epoxidation of cyclooctene with H_2O_2 (Scheme 2.11). These workers further showed that, by avoiding competitive side reactions of the oxo-perferryl species, a high epoxide yield could be achieved. This system was however limited by the fact that a catalyst loading of 5 mol % and a slow addition of the oxidant were required.



Scheme 2.11¹⁸: Epoxidation with Fe(TPP) catalyst.

2.4.2 Manganese Porphyrin

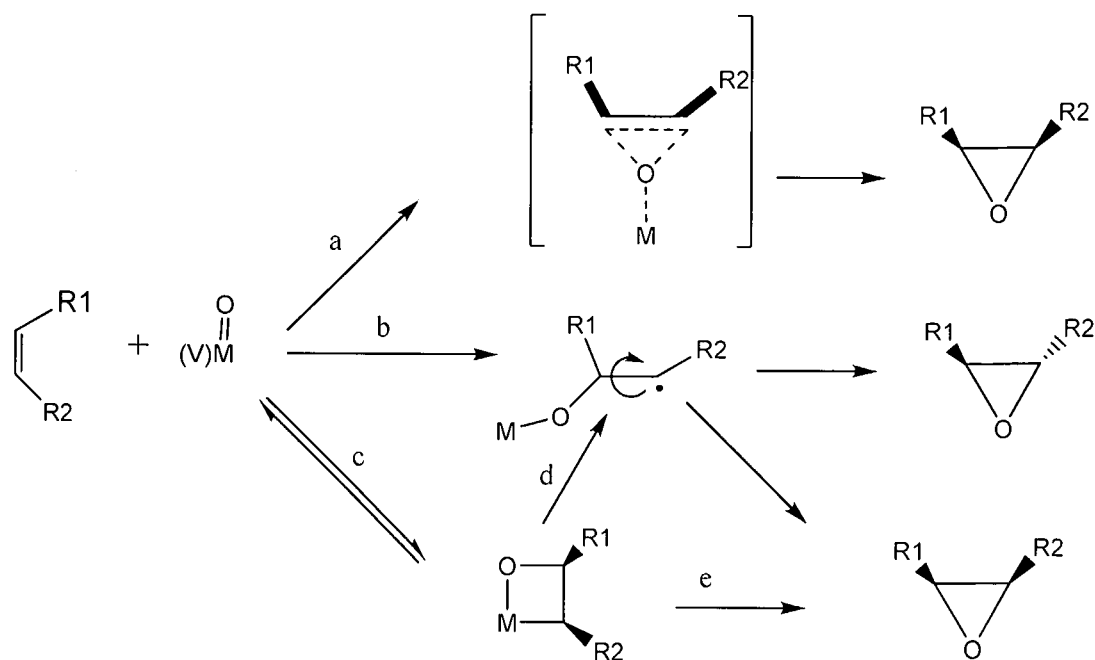
Synthetic manganese(III)porphyrins are efficient catalysts for the epoxidation of olefins and the hydroxylation of alkanes with a variety of oxidants, and have been developed for both chiral and non-chiral epoxidations. In biological systems manganese complexes show cytochrome P-450 type reactions and this led to interest in the development of synthetic systems. Earlier reports on manganese catalyzed epoxidation mainly describe the use of manganese porphyrins with iodobenzene as oxygen source. The presence of the ligand around the metal center is, however not necessary to achieve the catalytic properties of manganese, since it was shown that manganese(II) triflate also catalyzed

alkene epoxidation with iodosylbenzene (PhIO) in acetonitrile.^{28b} The ligand mainly enhance the selectivity of this system.

Catalytic epoxidation with manganese porphyrin and PhIO as the oxygen source was first reported by Groves *et al.* in 1980.^{28b,30} The electron-deficient porphyrins, Mn(TPP)Cl [TPP = tetrakis(phenylporphyrin)] efficiently catalyses the epoxidation of alkenes. Electron-rich alkenes were found to be more reactive than electron deficient ones. In contrast to the Fe(TPP)Cl/PhIO system earlier reported, the Mn(TPP)Cl/PhIO system yielded products with loss of stereoselectivity. For example, the epoxidation of *cis*-stilbene gave mostly the *trans*-epoxide (65%).^{28b,31}

Mechanistic studies based on the isolation of the high-valent intermediate, conducted by Castellino and Bruice³² and by Groves,³³ revealed that the oxomanganese(V) ($Mn^V=O$) porphyrin intermediate, generated from the reaction between Mn(TPP)Cl and PhIO, actually transfers its oxygen to the alkene forming the products. To explain oxygen transfer in the manganese and other metal catalyzed epoxidations, three debatable pathways have been proposed. In the first path (path **a**, Scheme 2.12), the metal-oxo species reacts with the alkene *via* a concerted mechanism. This pathway fails to account for the formation of *trans*-epoxide from *cis*-olefins. In pathway (**b**) (Scheme 2.12), a stepwise C-O bond formation involving a free radical intermediate is proposed. Free rotation about the C-C bond in the radical intermediate accounts for the isomerization observed. According to this mechanism, retention of configuration happens when the oxygen transfer step is faster than the rotation of the free radical intermediate. For cases with more than one product, the product distribution is seen to be sensitive to the type of metal centre on the porphyrin ligand. As indicated in the third pathway (path **c**, Scheme 2.12), the initially formed metallaoxetane can either convert to the radical intermediate (path **d**, Scheme 2.12), forming non-stereospecific products, or decompose to stereospecific products (path **e**, Scheme 2.12). For the Mn(TPP)Cl/PhIO system, a stepwise addition of the oxo-manganese(V) species to the double bond resulting in a freely rotating free radical intermediate with a long life-time, was suggested (path **b**,

Scheme 2.12).³¹ Compared to the Fe(TPP)Cl/PhIO systems, the manganese(III)porphyrin catalyzed reaction of norbornene give large exo/endo epoxynorbornanes.



Scheme 2.12³¹

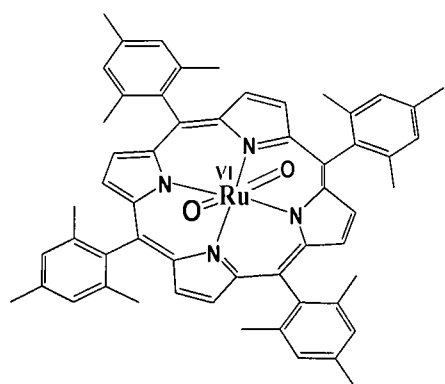
Mansuy and co-workers were the first to report that oxygenation of unsaturated hydrocarbons can be carried out with 30% H_2O_2 and Mn-porphyrin catalysts.³⁵ The reduced activity of the Mn(porp)/ H_2O_2 system for alkene epoxidation necessitated the addition of large amounts of imidazole or benzoic acid to improve reaction rates and yields. It is thought that the imidazole or benzoic acid help to stabilize the active oxo-metal complex ($M=O$) by forming a hexadentate Mn-oxo complex. *Trans*-alkenes were found to be almost unreactive in this system. Contrary to the Mn(TPP)Cl / PhIO system, epoxidation by the Mn(porp)/ H_2O_2 system is stereospecific for *cis*-alkenes, the *cis*-stilbene giving only the *cis*-epoxide.

Sodium hypochlorite (NaOCl) has also been used as oxygen source in manganese porphyrins catalyzed epoxidations.^{15b,28b} Slow epoxidation rates and poor yields were observed. The reaction rates and product selectivity could be increased by the addition of small amounts of pyridine or imidazole.

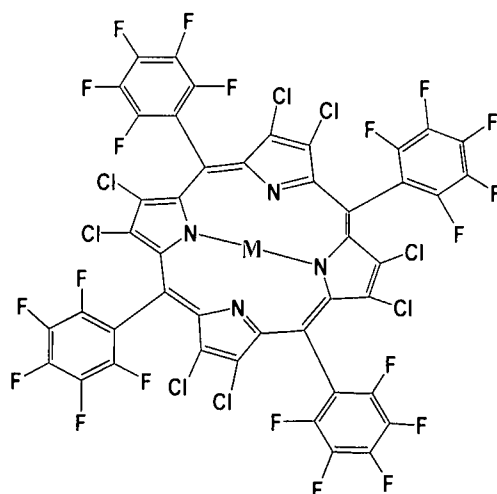
2.5 Ruthenium Porphyrins

2.5.1 Introduction

Since it was discovered that the active site of the Cytochrome P450, where biological oxidative transformations take place, has a high valent iron-oxo species, early studies aimed at understanding the redox chemistry of cytochrome P450 utilized mainly iron based synthetic models of these enzymes. Although synthetic iron complexes are the most reactive in oxo-transfer reactions, these high-valent iron-oxo species are very labile and could not be isolated for comprehensive studies.³⁷ Failure to obtain pure solids of high-valent iron-oxo complexes for cytochrome P450 related studies opened the way for such studies to be conducted with higher valent oxoruthenium(IV, V, VI) complexes [2.10],^{38,39,40} which are reportedly more stable.

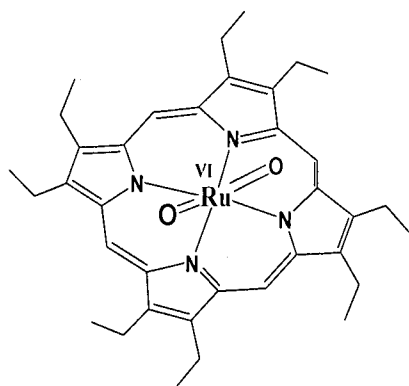


[2.10]



[2.10b], M = Ru-CO

[2.10c], M = O=Ru=O



[2.10a]

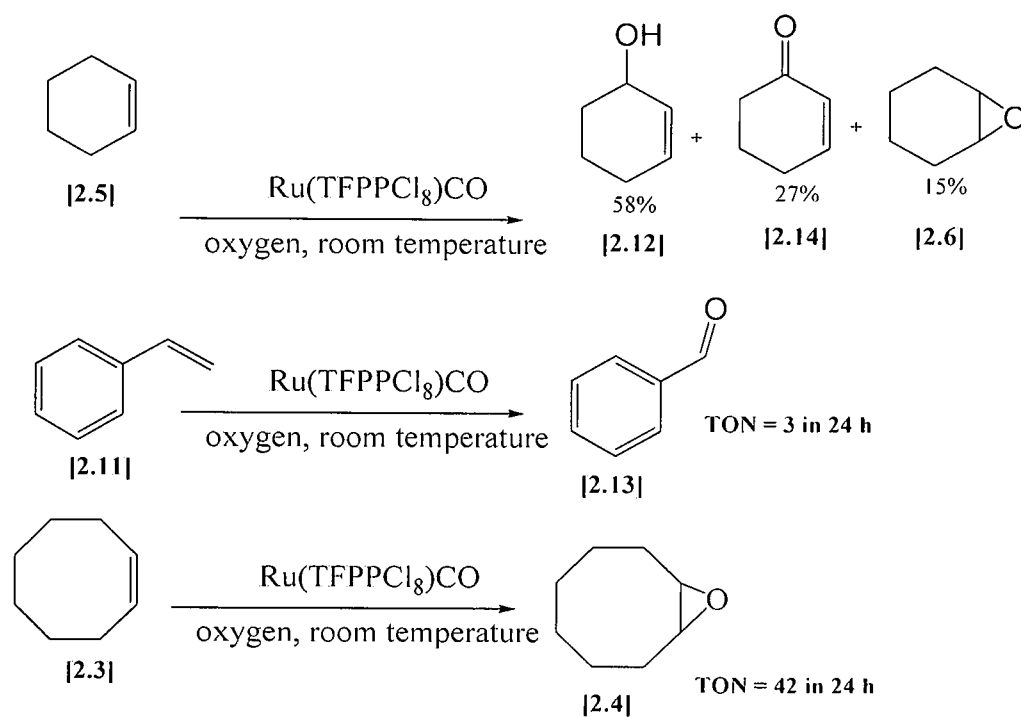
Although initial studies were aimed at mimicking biological enzymes, there have been intense efforts towards the development of efficient oxo-transfer catalytic systems based on ruthenium complexes during the past twenty five years.⁴¹ Many transition-metal catalysts are capable of giving oxidation together with epoxidation. Furthermore, the reaction conditions and type of oxidant may change the outcome of the reaction with the same catalyst.

2.5.2 Ruthenium Metal Complexes as oxidation catalysts.

Going back to the periodic table, ruthenium sits on a central position; close to both iron and manganese with rich redox chemistries. By virtue of its position (in the second row), ruthenium tends to display a combination of some of the properties of both the early and late transition metals that are desirable for catalysis.⁴⁴ Added to ruthenium's ability to form coordinated compounds in eleven different oxidation states (-2 to +8), oxo-ruthenium(IV, V, VI) intermediates are known to be stable solids that could be isolated for oxidative studies.³⁸ By varying the ligands around the **Ru=O** moiety and consequently the oxidation state, ruthenium complexes have been widely utilized in different oxidative catalytic processes.⁴²⁻⁴⁶ For example, RuO₄ has been used in the dihydroxylation of olefins and Ru(OH)₃nH₂O/Al₂O₃ in the oxidation of alcohols.⁴⁴ Of all the ligands studied, ruthenium porphyrin based complexes have received most attention. A variety of ruthenium porphyrin complexes, and mainly the halogenated ones, have shown good activity in the transfer of oxygen to olefins with high regioselectivity.

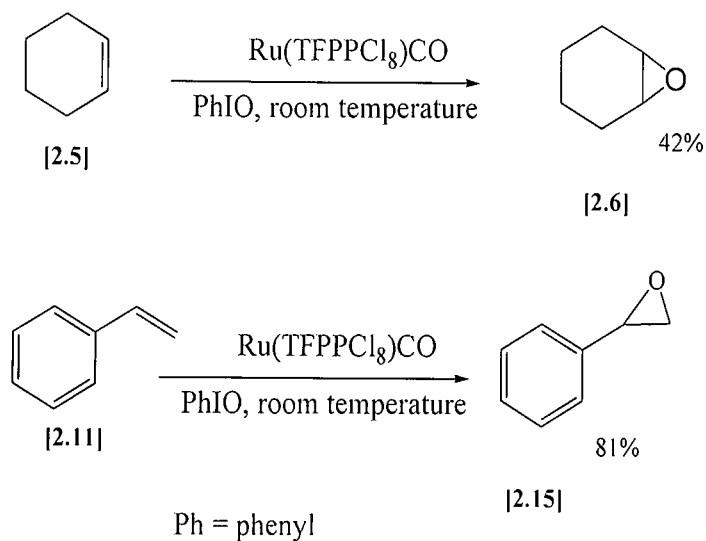
Catalyst deactivation was identified as the main drawback in the application of ruthenium complexes in olefin oxidation/epoxidation, especially with molecular oxygen as oxidant. The introduction of the electron withdrawing halogen substituent at the pyrole or mesopositions improved both catalyst activity and stability substantially.⁴⁷ Birnbaum and co-workers⁴⁸ used the perhalogenated ruthenium porphyrin (TFPPCl₈)RuCO {TFPPCl₈ = octachlorotetrakis(pentafluorophenyl) porphyrin} **[2.10b]** and (TFPPCl₈)Ru(O)₂ **[2.10c]** to catalyze the oxidation of olefins with molecular O₂ and iodosylbenzene (PhIO). Aerobic oxidation was performed at conditions similar to that of Groves and Quinn¹⁹ (room temperature and 1 atm. of O₂). The improved activity and stability of this complex is reflected by the high TONs (up to 300 in 24 h), with 90 % of the catalyst being recovered at the end of reaction. The product distribution and catalyst activity was heavily influenced by the oxidant. With molecular oxygen, cyclohexene **[2.5]** was oxidized to give more of the allylic oxidation product cyclohex-2-en-1-ol **[2.12]** (58%), 2-cyclohexen-1-one **[2.14]** (27%) and only 15% cyclohexene oxide **[2.6]**. Styrene **[2.11]** was oxidized to give benzaldehyde **[2.13]** (TON = 3 in 24 h) (Scheme 2.13) as the sole

product while cyclooctene [2.3] oxygenation yielded only cyclooctene oxide [2.4] (TON = 42 in 24 h).



Scheme 2.13

Contrary to oxygenation with molecular oxygen, the epoxidation with iodosylbenzene proceeded at a slower rate yielding mainly the epoxides. For example styrene [2.11] was selectively oxidized to styrene oxide [2.15] (81%) and cyclohexene [2.5] to cyclohexene oxide [2.6] (42 %) (based on total amount of oxidation products) (Scheme 2.14).



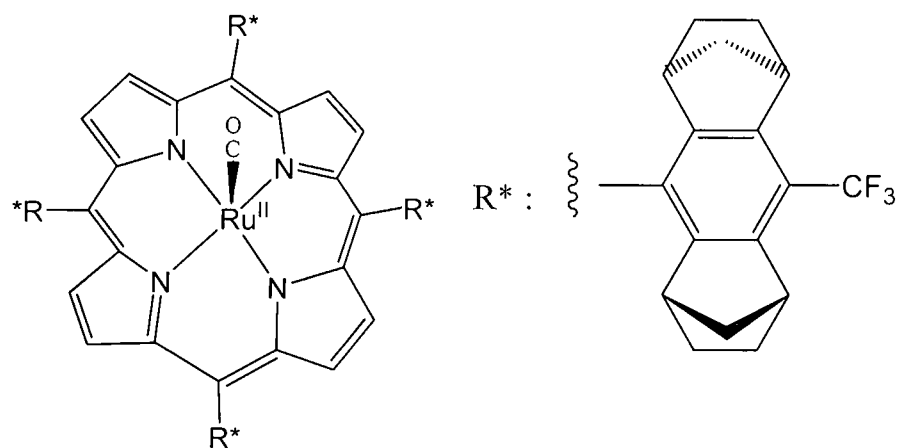
Scheme 2.14

2.5.3 Ruthenium porphyrin epoxidation.

The potential of ruthenium complexes in oxo-transfer reactions were first revealed when Groves and co-worker showed that dioxo(tetramesitylporphyrinato)ruthenium(VI) $[\text{Ru(TMP)(O)}_2]$ [2.10] could transfer dioxygen from air to alkenes under mild conditions without a co-reductant.¹⁹ Since then, a variety of ruthenium complexes with ligands like schiff-bases, polyoxometalates, etc. have been synthesized and applied extensively in the epoxidation of a wide variety of substrates with oxidants such as O_2 , H_2O_2 , pyridine *N*-oxide, iodosylbenzene, oxone, etc.¹⁸ The high interest in ruthenium catalyzed epoxidation, especially asymmetric epoxidation with ruthenium porphyrin-like complexes is evident by the numerous publications that have emerged over the past twenty years.

A notable oxidation system with wide applicability is that developed by Hirobe and co-workers in 1989.⁴¹ In this system, which thus far utilizes mainly ruthenium porphyrin

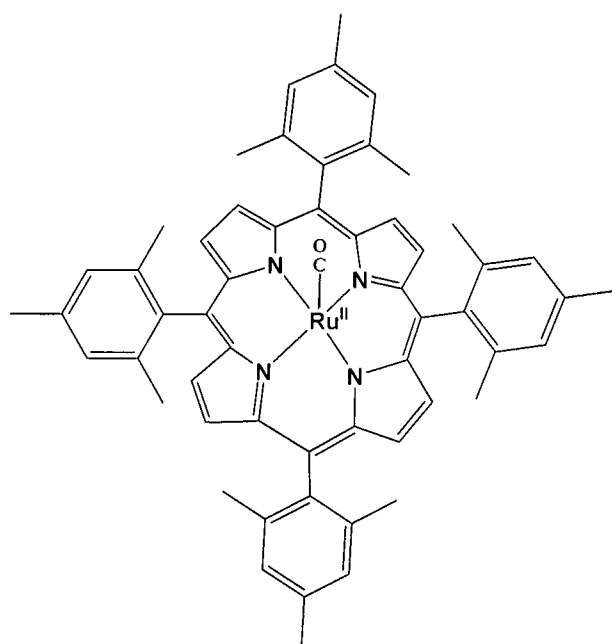
complexes, efficient oxygen transfer to olefins, sulfides and alkanes to form epoxides, sulfoxides and alcohols respectively, have been realized. In most of these studies, sterically encumbered ruthenium porphyrins with strongly electron withdrawing groups are used. For example, in 2003 Berkessel *et al.*⁴² obtained up to 14 200 turnovers in the epoxidation of styrene with the highly electron deficient ruthenium carbonyl porphyrin catalyst [2.16]. Available evidence for alkene epoxidation point to a mechanism with either a mono-oxoruthenium (IV) or di-oxoruthenium (VI) species as the intermediate.⁴³ The catalyst deactivation, thermal instability of the porphyrin nucleus under oxidative conditions, and poor or no catalytic activity towards some substrates are the main limitations of this system.



[2.16]

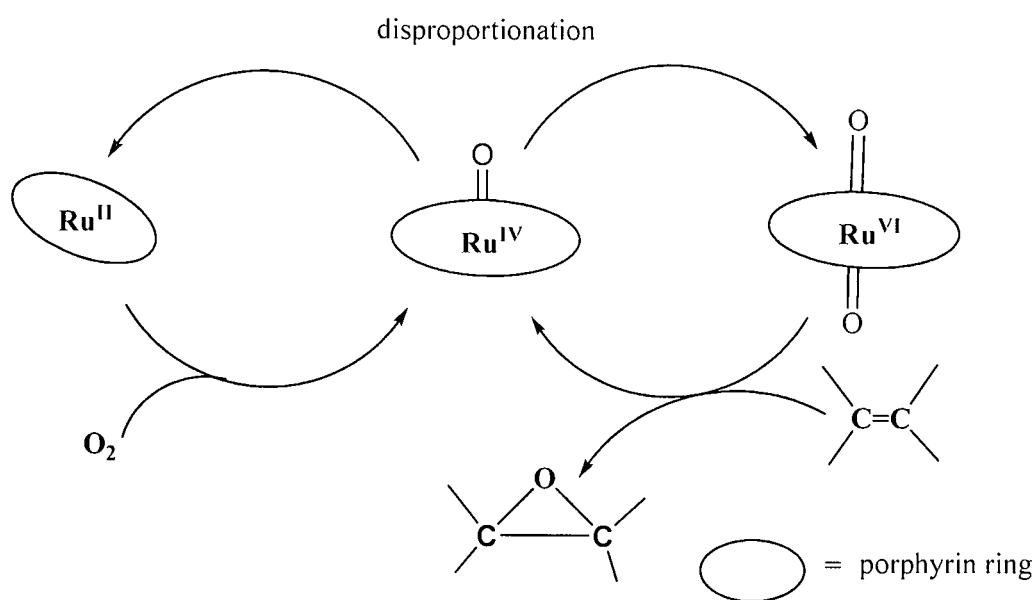
The successful application of ruthenium porphyrins in epoxidation with dioxygen was first reported by Groves and Quinn.¹⁹ The main problem with the application of ruthenium porphyrins as well as other metal porphyrins in dioxygen reactions, is the formation of LRu(III)-O-O-Ru(III)L dimers (Ru stands for ruthenium porphyrin). Such species are unreactive and cannot transfer their oxygen to olefinic substrates. Groves and Quinn¹⁹ circumvented this by using sterically hindered tetramesityl ruthenium porphyrins, the bulky tetramesityl group helping to prevent the formation of μ -oxo dimers that will stop the reaction from proceeding. Dioxo(tetramesitylporphyrinato)ruthenium(VI) [Ru(TMP)(O)₂] [2.10] was prepared by oxidation of [Ru(TMP)CO] [2.17] with *m*-CPBA, periodate or iodosybenzene. The

aerobic epoxidation of cyclooctene, *cis*- and *trans*- β -methyl styrenes and norbornene was carried out by [2.10] in benzene at room temperature and 1 atmosphere of dioxygen over a 24-hr period. The epoxidation was almost completely stereoselective since epoxidation of *cis*- β -methylstyrene gave a *cis/trans* epoxide (32.7/1.5). Competitive reaction of *cis/trans* alkenes showed that the *cis*-alkenes were more reactive (14.5 times) than the *trans*-alkenes. The highest catalyst activity was observed with norbornene (45 TON in 24 hr). The main problem with this system is the low turnovers realized (16-45 TONs in 24 hr).



[2.17]

Grove proposed the mechanism shown in Scheme 2.15¹⁹; the transfer of an oxygen atom from [2.10] to the substrate forms Ru(TMP)(O) which through disproportionation forms Ru(TMP)(O)₂ and Ru^{II}(TMP). Ru^{II}(TMP), upon reacting with the molecular oxygen replenishes the Ru(TMP)(O). Catalyst deactivation is thought to be a result of the formation of inactive Ru(TMP)CO [2.17].



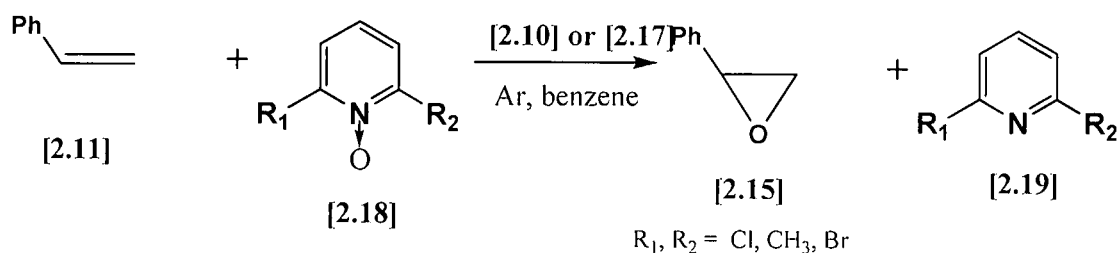
Scheme 2.15⁴⁵

Leung and Che,⁴⁶ following Groves' work to some extent, synthesized and isolated the first version of non-sterically encumbered ruthenium porphyrin $\text{Ru}^{\text{VI}}(\text{OEP})\text{O}_2$ [OEP = octaethylporphyrin] **[2.10a]**. $\text{Ru}^{\text{VI}}(\text{OEP})\text{O}_2$ **[2.10a]** was synthesized by the *m*-CPBA oxidation of $[\text{Ru}^{\text{IV}}(\text{OEP})(\text{CO})]$ in alcohol (methanol or ethanol), which prevented dimer $[\text{Ru}^{\text{VI}}(\text{OEP})(\text{OH})]_2\text{O}$ formation. It is thought that the alcohol molecules stop dimerization by filling the vacant coordination sites on the $\text{Ru}^{\text{VI}}(\text{OEP})\text{O}$ intermediate. This $(\text{Ru}^{\text{VI}}(\text{OEP})\text{O}_2)$ **[2.10a]** complex can effect both the stoichiometric and the catalytic aerobic epoxidation of olefins in ethanol solution. In dichloromethane, dimerization of the $\text{Ru}^{\text{VI}}(\text{OEP})\text{O}$ prevents catalytic aerobic epoxidation even at 10 atm O_2 pressure. Even though some aerobic epoxidation was realized in ethanol, the yields and turnovers were by far inferior to those obtained by Groves and Quinn¹⁹ with a sterically encumbered porphyrin. For example, only 3 TONs were obtained with norbornene compared to the 45 TONs obtained with Groves' sterically encumbered porphyrin under the same reaction conditions after 24 h.

$\text{Ru}^{\text{VI}}(\text{OEP})\text{O}_2$ **[2.10a]** did however prove to be an efficient oxidant in the stoichiometric epoxidation of norbornene, styrene, *cis*- and *trans*-stilbene in dichloromethane. Epoxides

were the main products (in quantitative amounts), though some benzaldehyde (oxidative cleavage product) also formed in the epoxidation of the stilbenes. Conservation of stereoselectivity in this system was very poor as *cis*-stilbene gave mainly the *trans*-epoxide.

In 1989, Hirobe and coworkers⁴¹ showed for the first time that the Ru^{II} TMP(O)₂ [2.10] / 2,6-dichloropyridine *N*-oxide or Ru^{II}(TMP)(CO) [2.17] / 2,6-dichloropyridine *N*-oxide [2.18] systems could effect olefin epoxidation (Scheme 2.16), hydroxylation of alkanes, and oxidation of alcohols and sulfides. In fact most of the studies on ruthenium catalyzed oxidations have been an expansion of the so called 'Hirobe system'.



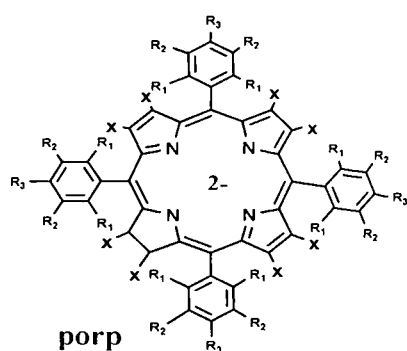
Scheme 2.16⁴⁹

Alkene epoxidation catalyzed by the ruthenium porphyrin complexes using the oxidant 2,6-dichloropyridine *N*-oxide (2,6-DCPNO)[2.18] were performed at 30 °C in benzene under argon. Styrene and substituted styrenes, stilbenes and some conjugated *cis*-disubstituted alkenes are efficiently and selectively epoxidized to the epoxides in the presence of [2.10] and [2.17] as catalyst. The epoxidation was stereospecific; the *cis*-alkenes giving the *cis*-epoxides. Epoxidation was faster when [2.10] was employed as catalyst. Up to 17,000 turnovers were achieved with styrene in 24 h. The presence of substituents on the 2 and 6 position of the pyridine *N*-oxide is critical to achieve high catalytic properties of the ruthenium complexes because their deoxygenated compounds do not coordinate strongly to the ruthenium atom due to steric hindrance. The post reaction pyridine released by 2-mono-substituted pyridine *N*-oxides and those with no

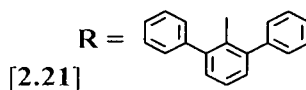
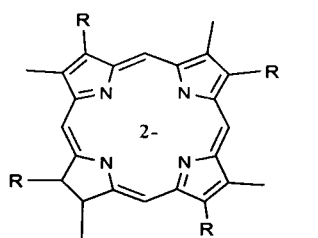
substituents at the 2,6-positions coordinates strongly to the ruthenium atom on the metal complex, inhibiting its reactivity. No epoxidation reaction was observed when porphyrin complexes with metals such as Mn, Fe, Co and Rh were used with the pyridine *N*-oxides. The high *cis*-selectivity of this system was demonstrated through competitive studies using a 1:1 mixture of *cis*- and *trans*-stilbene which gave the *cis*-stilbene oxide in (87% yield) and *trans*-stilbene oxide in (1% yield).

Since the earlier reports by Hirobe *et al.*⁴¹ recent trends (apart from the asymmetric version) have been towards the development of more robust complexes that can epoxidize a wider range of substrates.⁵⁰

Che *et al.*⁵⁰ developed a series of ruthenium porphyrin catalysts (Scheme 2.17) for the homogeneous and heterogeneous epoxidation of a variety of organic substrates such as styrenes, cycloalkenes, α,β -unsaturated ketones, steroids, benzylic hydrocarbons and arenes with pyridine *N*-oxide or air. Only 0.1 mol% of catalyst was required to efficiently epoxidize most of these organic substrates. Up to > 99 % yields and product TONs of up to 3.0×10^4 after 48 h were achieved. The epoxidation of styrenes to the corresponding epoxide was achieved with most of these complexes with 2,6-DCPNO [2.18]. For example, epoxidation of styrene with 2,6-DCPNO catalyzed by $[\text{Ru}^{\text{IV}}(2,6\text{-Cl}_2\text{tpp})\text{Cl}_2]$ gave the epoxide in 89 % yield, with product turnovers of up to 8.8×10^2 .^{50a} While most of these complexes efficiently catalyze the epoxidation of *cis*-alkenes to *cis*-epoxides, the *trans*-alkenes such as *trans*-stilbene are poor substrates with these catalysts.



[2.20]



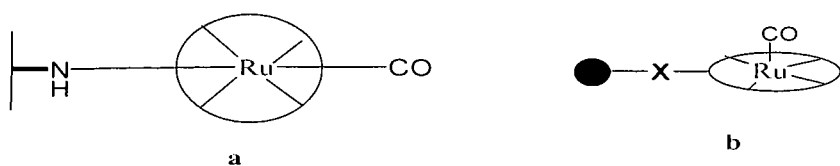
[2.21]

	Porp	x	R1	R2	R3
a	tpp	H	H	H	H
b	ttp	H	Me	H	H
c	4-Cl-tpp	H	OMe	H	H
d	4-OMe-tpp	H	OH	H	H
e	4-OH-tpp	H	H	OH	H
f	3,5-(OH) ₂ tpp	H	H	OH	H
g	F ₂₀ -tpp	H	F	F	F
h	tmp	H	Me	H	Me
i	2,6-Cl ₂ tpp	H	H	H	Cl
j	β-Br ₈ -tmp	Br	Me	H	Me
k	F ₂₈ -tpp	F	F	F	F
l	β-Ph ₈ -tpp	Ph	H	H	H

Porp = Porphyrin
tpp = tetrakis(triphenyl) porphyrin
ttp = *meso*-tetrakis(*p*-tolyl) porphyrin
tmp = tetramesityl porphyrin
Cl₂tpp = tetrakis(2,6-dichlorophenyl) porphyrin

Scheme 2.17: Structures of porphyrin ligands in the Che *et al.*^{50a} study.

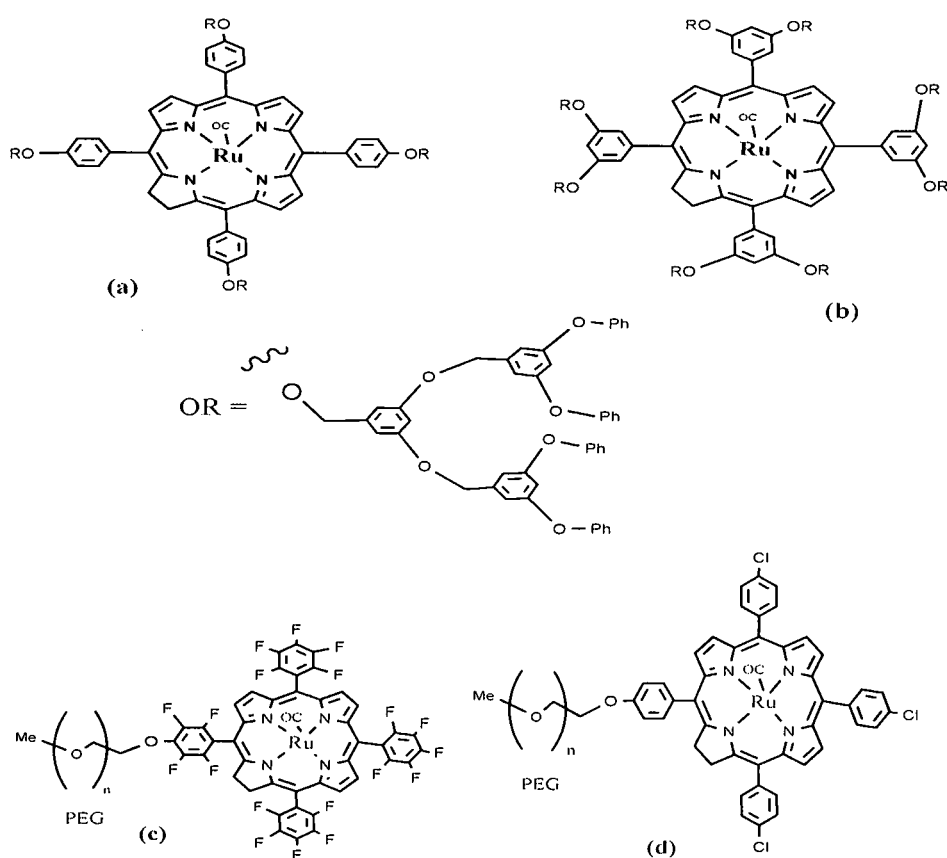
In an attempt to increase efficiency and substrate scope, some of these catalysts have been immobilized onto insoluble supports such as modified mesoporous molecular sieves (MCM-41) (Scheme 2.18), and others covalently attached to soluble supports such as dendrimers [Scheme 2.19, (a) and (b)] and polyethylene glycol(PEG) [Scheme 2.19, (c) and (d)].^{50a}



1. MCM-41 : Por = 4-Cl-TPP
2. MCM-41 : Por = 2,6-Cl-TPP

[2.22]

Scheme 2.18: Structures of ruthenium porphyrins (a) coordinatively grafted onto surface modified MCM-41 and (b) covalently attached to a solid support.

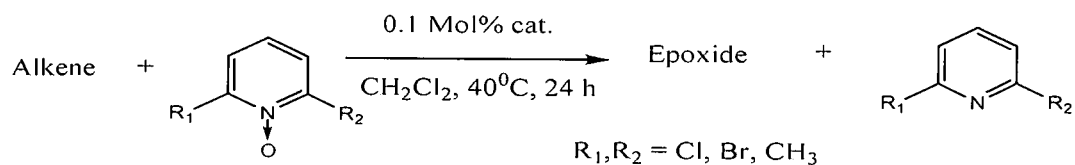


[2.23]

Scheme 2.19

Enhanced catalytic activity, stability and selectivity were observed with heterogenized ruthenium porphyrin catalysts towards alkene epoxidations. Using the heterogenized ruthenium porphyrin catalysts (some represented in Scheme 2.19), a wide range of

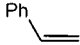
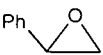
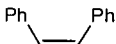
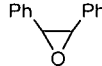
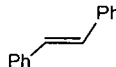
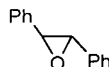
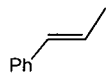
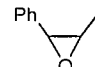
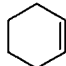
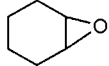
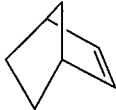
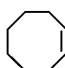
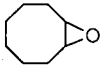


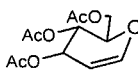
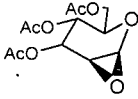
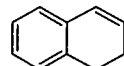
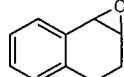
aromatic and aliphatic alkenes were selectively converted to their corresponding epoxides with 2,6-DCPNO as terminal oxidant (Scheme 2.20).



Scheme 2.20

Enhanced catalyst stability is reflected by the high turnovers reported for the heterogeneous ruthenium porphyrin/*N*-oxide systems (Table 2.2).^{50b} While catalyst (2.22a, Scheme 2.18) was found to be completely ineffective in the epoxidation of *trans*-alkenes, catalysts [2.22b] and [2.23a, b, c, d]; (Scheme 2.19) efficiently catalyzed the epoxidation of both *cis* and *trans*-alkenes.

Table 2.2^{50b}: Epoxidation of alkenes with 2,6-DCPNO catalyzed by [2.23d].

Entry	alkene	conv. %	yield % ^a	TON ^b	Products
1		96	98	940	
2		94	99	930	
3		88	99	870	
4		90	99	890	
5		76	48 ^c	360	
6		96	99	950	
7		99	99	980	
8		88	99	870	
9		90	67	670	
10		88	99	870	

^a based on amount of olefin consumed, ^bTON = turnover number in 24 h,

^cother products.

With the heterogenized catalyst [Ru^{II}(2,6-Cl₂tpp)]-MCM-41 (**2.22b**, Scheme 2.18), up to 4.6 x 10³ TON in 24 h were achieved for styrene epoxidation.^{50a} Moderate conversion (49%) was also realized by using [Ru^{II}(4-Cl-tpp)(CO)]-PEG [**2.23d**] in *trans*-stilbene epoxidation with 2,6-DCPNO. Linear alkenes e.g. 1-octene, which are usually the most difficult to oxidize, were efficiently oxidized giving the epoxides in high yields (91-99%)

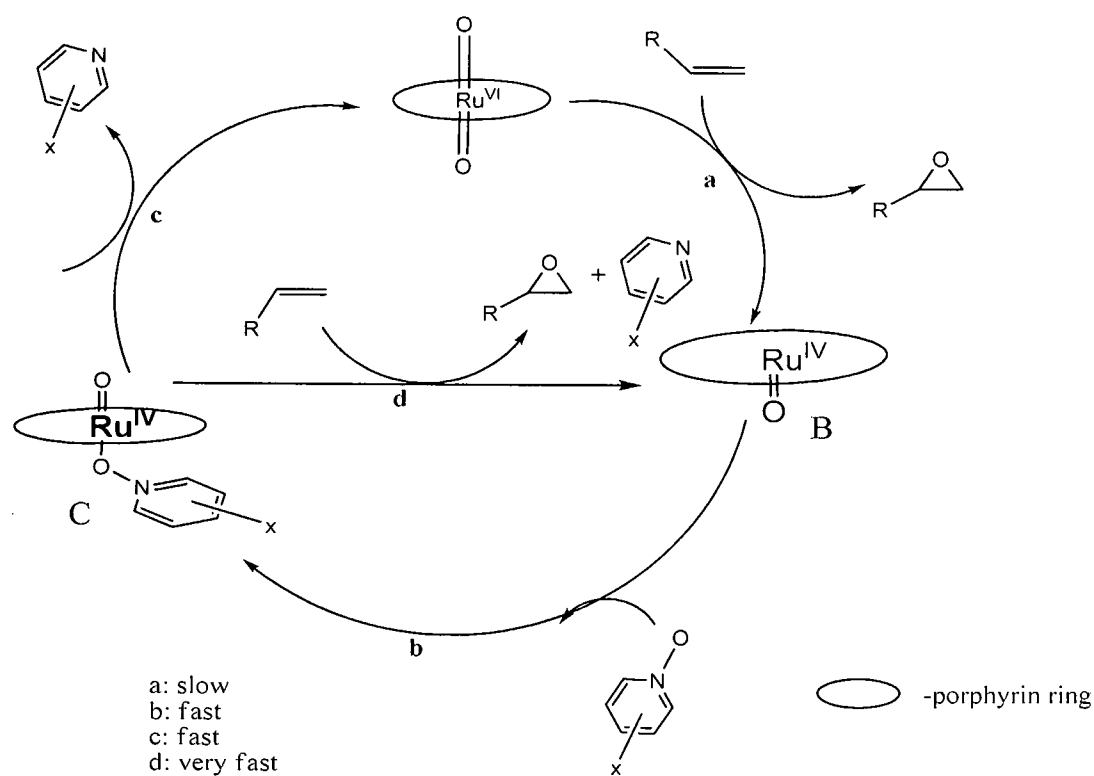
and TONs (3,800 within 24-30 h) by using catalyst $[\text{Ru}^{\text{II}}(2,6\text{-Cl}_2\text{tp})]\text{-MCM-41}$ (**2.22b**, Scheme 2.18).^{50c}

2.5.4 Mechanism of ruthenium porphyrin oxidative catalysis.

A couple of mechanisms have been postulated for the epoxidation of olefins by ruthenium porphyrins and 2,6-disubstituted pyridine-*N*-oxides. Ohtake, Higuchi and Hirobe^{41c} suggested that the active intermediate is possibly a regenerated $\text{Ru}(\text{TMP})(\text{O}_2)$ [**2.10**] or an *N*-oxide-coordinated-monooxoruthenium(IV) complex, such as $\text{Ru}(\text{TMP})(\text{O})(\text{lutidine } N\text{-oxide})$, that transfers the oxygen atom to the alkene.

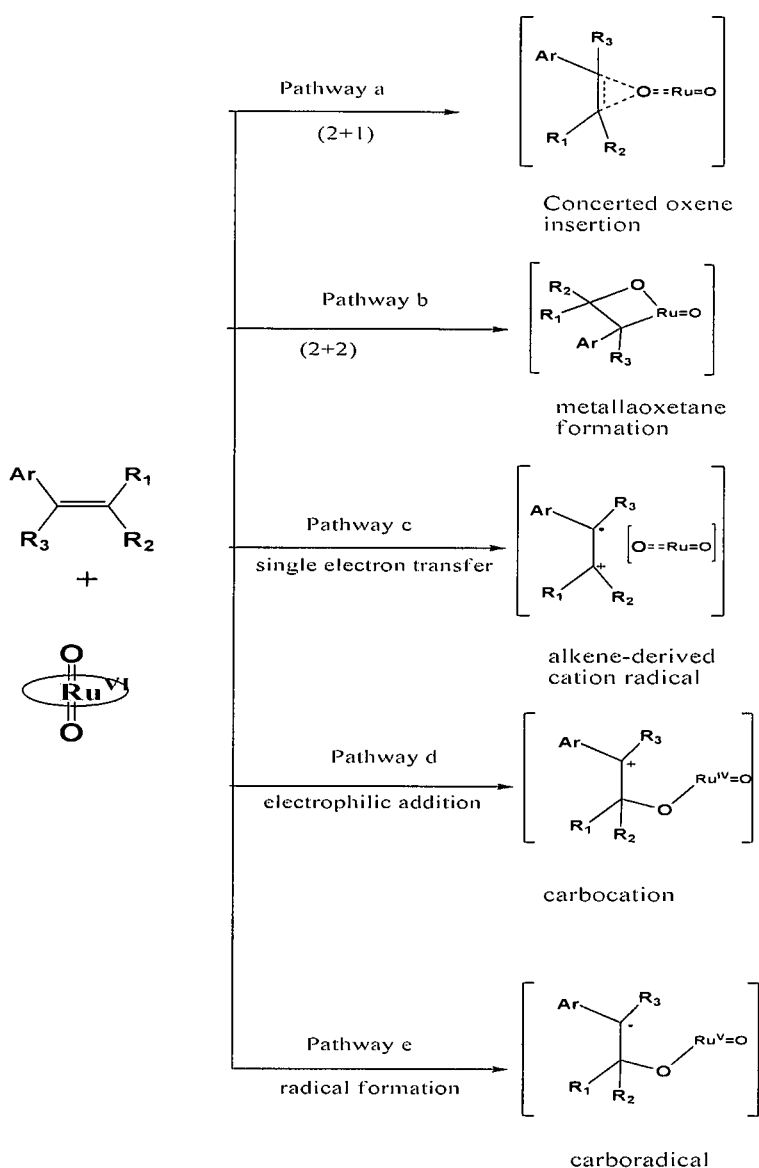
Gross and Ini⁵¹ investigated chiral $[\text{Ru}(\text{Por})^*(\text{O}_2)]/N\text{-oxide}$ systems and postulated the catalytic cycle shown in Scheme 2.21. On the basis of the following two observations, $\text{Por}^*\text{Ru}(\text{O}_2)$ was ruled out as a possible active species, while the *N*-oxide-coordinated – monooxoruthenium (IV) complex ($\text{Ru}(\text{TMP})(\text{O})(N\text{-Oxide})$) (**C**, Scheme 2.21) was proposed to be the best candidate.

- The reaction of isolated $\text{Por}^*\text{Ru}(\text{O}_2)$ (route **a**, Scheme 2.21) and olefins was too slow to account for the fast reaction of the olefin with a combination of $(\text{TMP})\text{-Ru}(\text{O})$ and *N*-oxide (route **b**, Scheme 2.21).
- $(\text{TMP})\text{Ru}(\text{O})_2$ -catalyzed epoxidation of styrene with enantiopure *N*-oxides gave a racemate, which suggests that the olefin approach the intermediate **C** toward the oxometal bond and not toward the *N*-oxide coordination site.



Scheme 2.21⁵¹

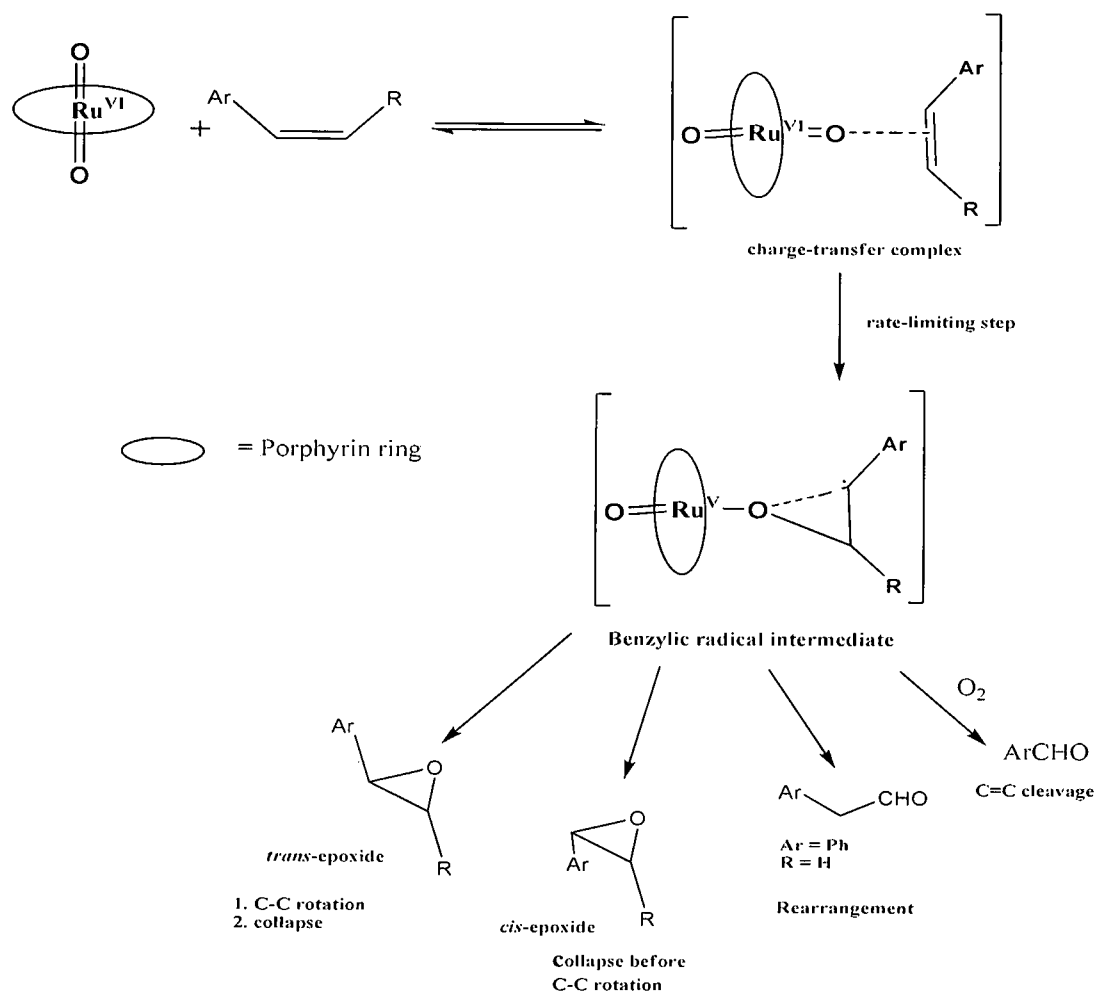
Contrary to previous reports where the focus was on the active Ru-species involved in the reaction, Liu *et al.*^{50f} investigated the mechanism of oxygen transfer during stoichiometric epoxidation of alkenes using $\text{Ru}(\text{O})_2$ (Scheme 2.22).



Scheme 2.22^{50f} $R_1, R_2, R_3 = H$

Stereospecificity of *cis*-alkene epoxidation depended on the alkene as well as the ruthenium porphyrin, with certain reactions being highly stereoretentive and others giving the *trans*-epoxide as the major product. The loss of stereospecificity ruled out the concerted reaction pathway (pathway a, Scheme 2.22). Also, evidence from inverse secondary kinetic isotope effects ruled out both a concerted oxene insertion mechanism and the formation of a metallaoxetane. It instead rather pointed towards the formation of

an acyclic intermediate in the rate-limiting step, whereas Hammett correlations ruled out carbocation as well as cation radical formation and rather were consistent with the formation of a benzylic radical in the rate limiting step (pathways b-e, Scheme 2.22). Ultimately, the authors thus proposed a mechanism involving the rate limiting formation of a benzylic radical (Scheme 2.23).

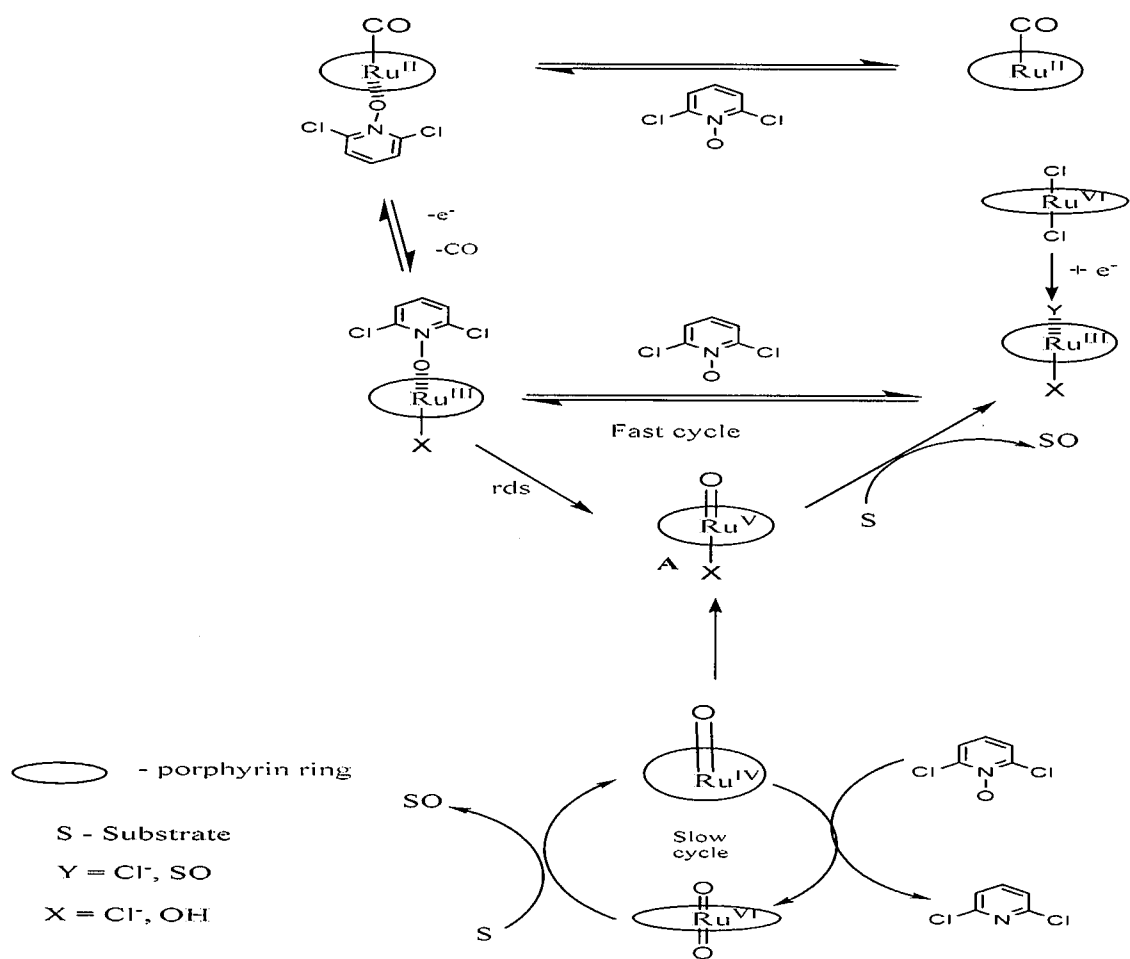


Scheme 2.23^{50f}

The benzylic radical intermediate formed resort to, amongst others, ring closure, thereby forming the *cis*-epoxide, or a C-C bond rotation/ collapse to form the *trans*-epoxide. Phenylacetaldehydes and benzaldehyde are formed by rearrangement and C=C bond

cleavage (in the presence of dissolved oxygen), respectively. When bulky groups are present, the C-C bond rotation of the benzylic radical intermediate may be hindered.

Wang *et al.*⁴³ investigated the mechanism of alkane hydroxylation with several Ru species. Evidence is in favor of a Ru^V species as the active catalyst (A, Scheme 2.24). The authors argue for this Ru^V to be the active catalyst in epoxidation as well, although there was no evidence to prove this claim.

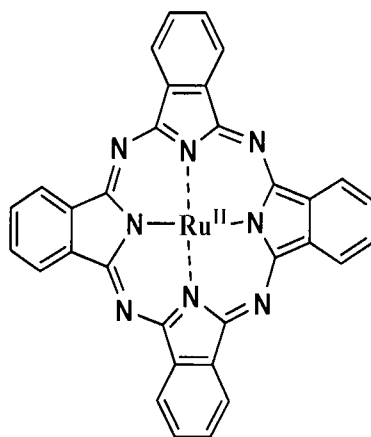


Scheme 2.24

2.6 Metallo-phthalocyanine - catalyzed (Ep)oxidations.

Oxidative catalysis is one of the many fields in which metallo-phthalocyanines have gained importance within the past two decades or so.⁵³ The interest in using Metallo-phthalocyanines in cytochrome P450 type reactions and as catalysts in oxidation reactions stem from their structural similarity to the porphyrins. In addition, metal phthalocyanines (MPc) are cheaper and more stable to oxidative degradation than their porphyrin counterparts. The main limitation in using MPcs is their poor solubility in hydrocarbons solvents. The natural trend in the development of phthalocyanine oxidative chemistry has been by comparing it with their porphyrin counterpart.

In 1994, Capobianchi *et al.*⁵⁴ reported that the unsubstituted ruthenium phthalocyanine [2.24], which exist as a dimer, catalyze the aerobic oxidation of 1-octene to 2-octanone. The reactions were performed in THF at room temperature and O₂ pressure of 50 atm in the presence of an olefin activator (C₆H₅CN)₂PdCl₂. Low turnover numbers (up to 10-12) were obtained in 22 h, while 2-octanone (98-100%) was almost exclusively formed.



[2.24]

The highly efficient oxidation of alkanes by zeolite-encapsulated perfluorinated ruthenium phthalocyanine (RuF_{16}Pc) was also reported by Balkus and coworkers.⁵⁵ Cyclohexane was converted to cyclohexanone and cyclohexanol with *tert*-butyl hydroperoxide (*t*-BOOH) as oxidant, (TON = 20,000 at a rate of 3000/day).

2.7 Ruthenium-Schiff-base complexes catalyzed epoxidation.

Ruthenium, in a variety of ligand environments has been found to be active as epoxidation catalyst with a variety of oxidants. In general, the ruthenium oxo species ($\text{Ru}=\text{O}$), irrespective of its ligand environment, has the ability to transfer its oxygen to an alkene substrate.

In this regard, salen based ruthenium complexes have also been utilized as catalysts in the alkene epoxidation alongside with metalloporphyrins. Although these compounds are structurally different from the porphyrins, they are iso-electronic in nature. Ruthenium (III)-salen complexes {[Ru(III)(salen)(PPh₃)(Cl)], Ru(III)(salen)(PPh₃)(py)⁺], [Ru(III)(salen)(py)]ClO₄], [Ru(III)(salen)(PPh₃)(N₃)], [Ru(III)(salen)(PBu₃)]ClO₄], and [(NBu₄)Ru(III)(salen)(TsO)]} have been described to function as efficient catalysts in the epoxidation of alkenes using iodosylbenzene as terminal oxidant (Table 2.4).⁵⁶ The epoxidation was performed in DCM with a catalyst/substrate/oxidant molar ratio of 1: 5000 : 200.

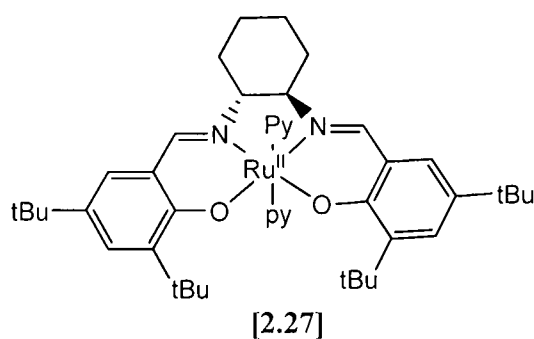
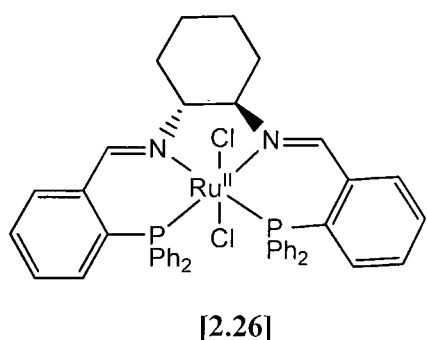
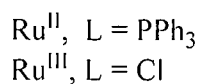
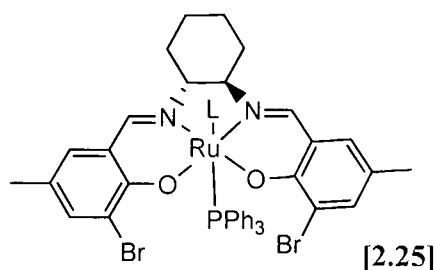
Low levels of conversion and poor epoxide selectivities were observed for all of the complexes studied in this system. *Cis*- and *trans* stilbene oxide (in a 4:1 ratio) was detected in the epoxidation of the *cis*-stilbene.

Table 2.4: Catalytic Oxidation by PhIO with the [Ru(III)(salen)(PPh₃)(py)]⁺ complex

Substrate	Product (% yield) ^a
Styrene	Styrene oxide (6), Benzaldehyde (22)
Cyclohexene	Cyclohexene oxide (9) ^b
Cyclooctene	Cyclooctene oxide (29)
<i>Trans</i> -stilbene	Benzaldehyde (35), <i>Trans</i> -stilbene oxide (12)
<i>Cis</i> -stilbene	Benzaldehyde (30), <i>Cis</i> -stilbene oxide (9) <i>Trans</i> -stilbene oxide (2.4)
Norbornene	<i>exo</i> -norbornene oxide (13)

^aYields based on PhI generated. ^bSmall amounts of cyclohexanone and cyclohexenol were detected (< 3%).

Recently, Che and Zhang^{50d} examined the ruthenium Schiff base complexes [2.25], [2.26] and [2.27] in the catalytic epoxidation of styrene with 2,6-dichloropyridine *N*-oxide. Less than 15 % conversion of styrene was recorded and the C=C cleavage pathway prevailed with high yields of benzaldehyde being formed.

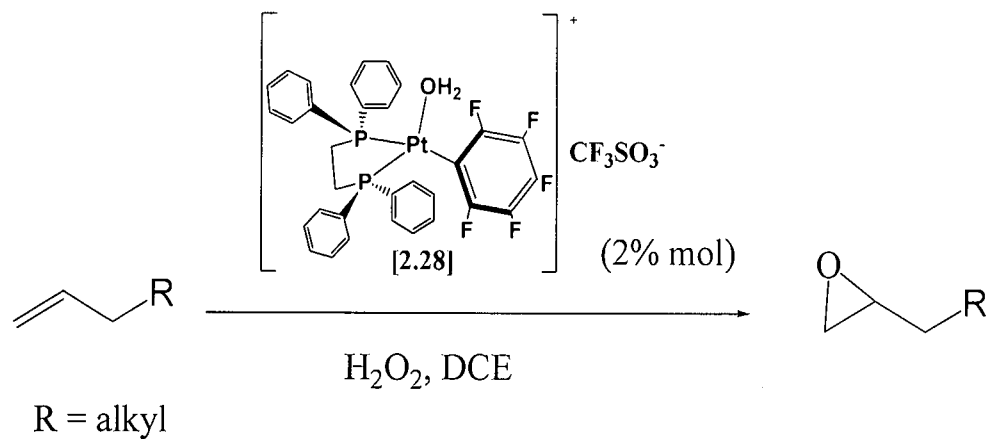


2.8 Electron-Poor Platinum (II) Complexes as efficient Epoxidation catalysts.

With most of the reported epoxidation systems discussed so far, acceptable catalyst activities have been realized in the epoxidation of electron-rich olefins ($\text{C}=\text{C}$) like stilbene and styrene derivatives, because of the high electron density associated with the conjugated aromatic system. Terminal mono-substituted alkenes like propene and 1-octene, which are of high industrial value, are generally unreactive towards these electrophilic oxidation systems. Hence the development of a catalytic system of high activity and selectivity towards this type of substrate is of prime importance to industry.

Pizzo *et al.*⁵⁷ and Collado *et al.*⁵⁸ recently developed a catalytic epoxidation system that is highly active and selective for terminal olefins. The catalytic system comprise of a highly

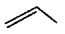
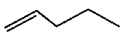


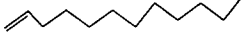
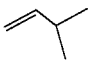
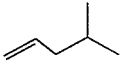
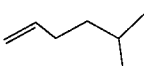
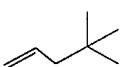
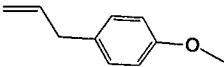
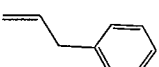
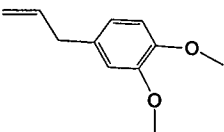
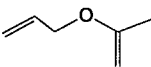
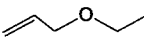
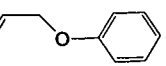
electron-poor Pt(II) catalyst [2.28] (2-3.5 mol %) (Scheme 2.25) which reacts with the olefin in DCM with H_2O_2 as oxidant (Scheme 2.25).



Scheme 2.25

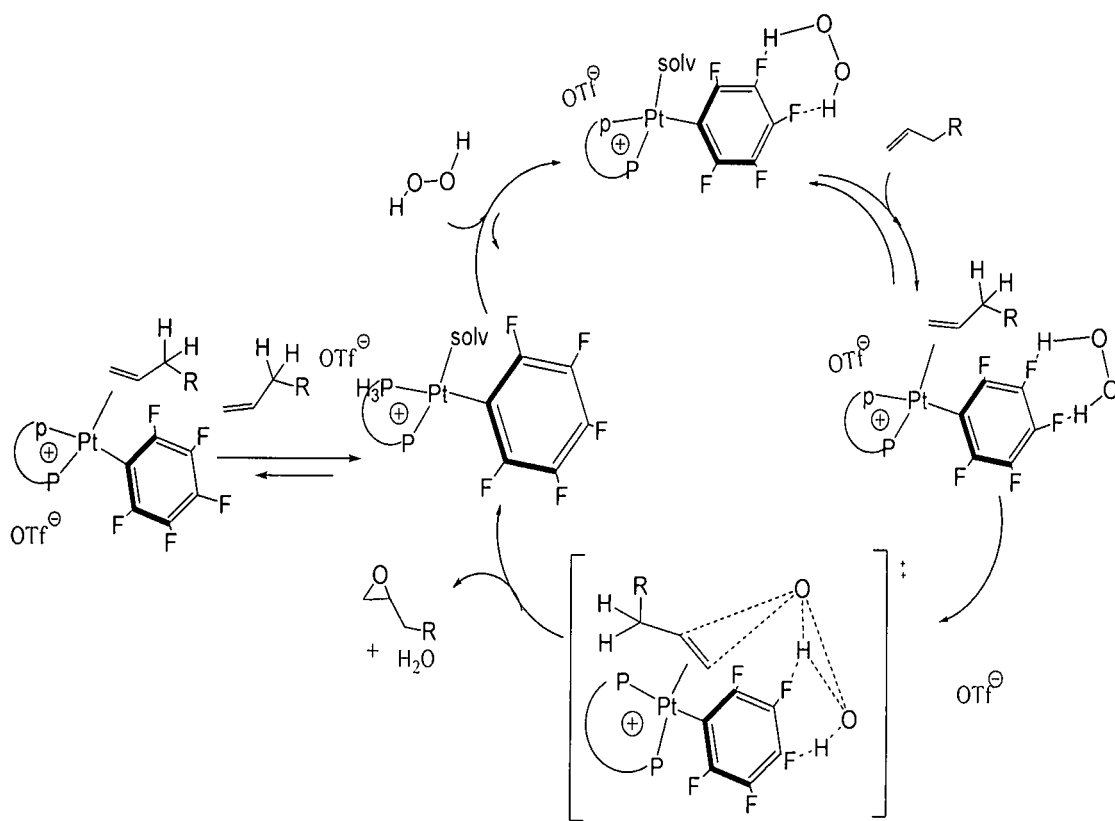
As indicated in Table 2.5, the monofunctionalized terminal linear alkenes were smoothly epoxidized in high yields within 5 hours (entries 1 – 5), while allyl benzene derivatives (entries 10 - 12) gave only moderate yields. Sterically hindered substrates (entries 6 and 9) and vinyl ethers (entries 13 - 15) were found to be almost unreactive.

Table 2.5: Catalytic Epoxidation of Various Alkenes with Hydrogen Peroxide Mediated by Pt(II) catalyst [2.28].^a

Entry	Substrate	Time (h)	Yield (%) ^b
1		20	78 ^c
2		3.5	96
3		5	89
4		4	81
5		4	81
6		24	0
7		3	59
8		4	82
9		24	4
10		6	55
11		6	38
12		6	34
13		5	4
14		6	0
15		24	5

^aExperimental conditions: Substrate = 0.83 mmol, H₂O₂ = 0.83 mmol, cat = 2% mol, solvent = 1 ml of dichloroethane at RT. ^bYield determined by GC analysis. ^cReaction performed at 0 °C, cat = 3.5% mol; yield determined by ¹H NMR integration.

In contrast to the generally accepted mechanism for metal catalyzed epoxidation reactions where a nucleophilic alkene is involved in the reaction, these workers proposed this epoxidation to proceed *via* an electrophilic alkene and nucleophilic oxidant (Scheme 2.26).



Scheme 2.26⁵⁸

2.9 References

1. Groves, J. T.; Han, Y. Z. In *Cytochrome P-450, Structure, Mechanism and Biochemistry*; Ortiz de Montellano, P. R., Ed.; Plenum Press, New York, 1995. pp 3-48.
2. (a) Groves, J. T.; Nemo, T.E. *J. Am. Chem. Soc.* **1983**, *105*, 5786-5791. (b) Katsuki, T. *Coord. Chem. Rev.* **1995**, *140*, 189-214.
3. Groves, J. T. *J. Porphyrins Phthalocyanines* **4**, **2000**, 350-352.
4. Sheldon, R. A.; Kochi, J. K. *Metal-Catalyzed Oxidations of organic compounds*; Academic Press: New York, 1981. pp 216-268.
5. Wang, C.; Shalyaev, K. V.; Bonchio, M.; Carofiglio, T.; Groves, J. T. *Inorg. Chem.* **2006**, *45*, 4769-4782.
6. Adam, W.; Stegmann, V. R.; Saha-Möllner, C. R. *J. Am. Chem. Soc.* **1999**, *121*, 1879-1882.
7. (a) Battioni, P.; Renaud, J.-P.; Bartoli, J. F.; Reina-Artiles, M.; Fort, M.; Mansuy, D. *J. Am. Chem. Soc.* **1988**, *110*, 8462. (b) Groves, J. T.; Quinn, R. *J. Am. Chem. Soc.* **1985**, *107*, 5790-5792.
8. (a) Irie, R.; Noda, K.; Ito, Y.; Matsumoto, N.; Katsuki, T. *Tetrahedron Lett.* **1990**, *31*, 7345. (b) Zhang, W.; Loebach, J. L.; Wilson, S. R.; Jacobsen, E. N. *J. Am. Chem. Soc.* **1990**, *112*, 2801.
9. Michaelson, R. C.; Palermo, R. E.; Sharpless, K. B. *J. Am. Chem. Soc.* **1977**, *99*, 1990-92.
10. Gross, Z.; Ini, S. *J. Org. Chem.* **1997**, *62*, 5514-5521
11. Zhang, R.; Yu, W.-Y.; Wong, K.-Y.; Che, C.-M. *J. Org. Chem.* **2001**, *66*, 8145-8153.
12. Berkessel, A.; Kaiser, P.; Lex, J. *Chem. Eur. J.* **2003**, *9*, 4746-4756.
13. Suslick, K.S. In *The Porphyrin Handbook*; Kadish, K. M., Smith, K., Guilard, R., Eds.; Academic Press: San Diego, 2000; Vol. 4, pp 41-62.
14. Meunier, B.; de Visser, S. P.; Shaik, S. *Chem. Rev.* **2004**, *104*, 3947-3980.

15. (a) Groves, J.T.; Han, Y.Z. In *Cytochrome P450: Structure Mechanism and Biochemistry*; Ortiz de Montellano, P. R., Ed.: Plenum: New York, 1995; pp 3-48. (b) Meunier, B. *Chem. Rev.* **1992**, *92*, 1411. (c) Dolphin, D.; Traylor, T.G.; Xie, L. Y. *Acc. Chem. Res.* **1997**, *30*, 259.
16. Groves, J. T.; Nemo, T E.; Myers, R. S. *J. Am. Chem. Soc.* **1979**, *101*, 1032-3.
17. Groves, J. T. *J. Porphyrins Phthalocyanines*, **2000**, *4*, 350-352.
18. Adolffson, H. In *Modern Oxidation Methods*; Bäckvall, J.-E Ed.; Wiley-VCH: Weinheim, 2004, pp 21-49.
19. Groves, J. T.; Quinn, R. *J. Am. Chem. Soc.* **1985**, *107*, 5790-5792.
20. Neumann, R.; Dahan, M. *Nature* **1997**, *388*, 353-355.
21. (a) Goldstein, A. S.; Beer, R. H.; Drago, R. S. *J. Am. Chem. Soc.* **1994**, *116*, 2424-2429. (b) Robbins, M. H.; Drago, R. S. *J. Chem. Soc., Dalton Trans.* **1996**, 105-110.
22. Clerici, M. G.; Inagallina, P. *Catal. Today* **1998**, *41*, 351.
23. Uphade, B. S.; Akita, T.; Nakamura, T.; Haruta; M. *J. Catal.* **2002**, *209*, 331.
24. (a) Yamanaka, I.; Nakagaki, K.; Otsuka, K. *J. Chem. Soc. Chem. Commun.* **1995**, 1185. (b) Berkessel, A. Biomimetic Oxidation of Organic Substrates with Hydrogen Peroxide. Available: <http://www.tokyokasei.co.jp>. (c) Hage, R.; Lienke, A. *Angew. Chem. Int. Ed.* **2005**, *45*, 206-222. (d) Traylor, T. G.; Tsuchiya, S.; Byun, Y.-S.; Kim, C. *J. Am. Chem. Soc.* **1993**, *115*, 2775.
25. (a) Traylor, T.G.; Kim, C.; Richards, J.L.; Xu, F.; Perrin, C.L. *J. Am Chem. Soc.* **1995**, *117*, 3468. (b) Traylor, T.G.; Kim, C.; Fann, W.P.; Perrin, C.L. *Tetrahedron* **1998**, *54*, 7977. (c) Mansuy, D.; Battioni, P. and Prenaude, P. *Chem. Commun.* **1984**, 1255. (d) Cunningham, I.D.; Danks, T.N., Hay, J.N.; Hamerton, I. Gunathilagan, *Tetrahedron* **2001**, *57*, 6847. (e) Battioni, P.; Renaud, J.P.; Bartoli, J.F.; Reina-Artiles, M.; Fort, M. and Mansuy, D. *J. Am. Chem. Soc.* **1988**, *110* (25), 8462-8470. (f) Katsuki, T.; Sharpless, K.B. *J Am. Chem. Soc.* **1980**, *102*, 5974-5976. (g) Traylor, T.G.; Tsuchiya, S.; Byun, Y.-S. and Kim, C. *J Am. Chem. Soc.* **1993**, *115*, 2775-2781.

26. (a) Meunier, B.; Guilmet, E.; De Carvalho, M.-E. Poilblanc, R. *J Am. Chem. Soc.* **1984**, *106*, 6668-6676. (b) Montanari, F.; Penso, M.; Quinci, S and Vigano, P. *J. Org. Chem.* **1995**, *50*, 4889.
27. Quici, S.; Banzi, S.; Pozzi, G. *Gazzetta chim. Italiana* **1993**, *123*, 597.
28. (a) Meunier, B. *Bull. Soc. Chim. Fr.* **1986**, 578. (b) Jorgensen, K. A. *Chem. Rev.* **1989**, *89*, 431
29. Traylor, T. G.; Tsuchiya, S.; Byun, Y.-S.; Kim, C. *J. Am. Chem. Soc.* **1993**, *115*, 2775.
30. Groves, J. T.; Kruper, W. J.; Haushalter, R. C. *J. Am. Chem. Soc.* **1980**, *102*, 6375.
31. Dalton, C. T.; Ryan, K. M.; Wall, V. M.; Bousquet, C. and Gilheany, D. G. *Topics in catalysis* **1998**, *5*, 75-91.
32. Castellino, A. J. and Bruce, T. C. *J. Am. Chem. Soc.* **1988**, *110*, 158-162.
33. Groves, J. T.; Kruper Jr., W. J. and Haushalter, R. C. *J. Am. Chem. Soc.* **1980**, *102*, 6375-6377.
34. Battioni, p.; Renaud, J.-P.; Bartoli, J. F.; Reina-Artiles, M.; Fort, M.; Mansuy, D. *J. Am. Chem. Soc.* **1988**, *110*, 8462.
35. Mansuy, D.; Battioni, P. and Prenaud, J. *Chem. Com.*, **1984**, 1255.
36. Dolphin, D.; Traylor, T. G.; Xie, L. Y. *Acc. Chem. Res.* **1997**, *30*, 251.
37. Leung, W-H.; Che, C-M. *J. Am. Chem. Soc.* **1989**, *111*, 8812-8818.
38. Groves, J.T.; Quinn, R. *Inorg. Chem.* **1984**, *23*(24), 3844-3846.
39. Groves, J.T, Quinn, R. *J. Am. Chem. Soc.* **1985**, *107*, 5790-5792.
40. Chatterjee, D. *Coord. Chem. Rev.* **2008**, *252*, 176-198.
41. (a) Higuchi, T.; Hirobe, M. *J. Mol. Catal. A: Chem.* **1996**, *113*, 403-422, (b) Higuchi, T.; Ohtake, H.; Hirobe, M. *Tetrahedron Lett.* **1989**, *30*, 6545. (c) Ohtake, H.; Higuchi, T. and Hirobe, M. *Tetrahedron Lett.* **1992**, *33*, 2521. (d) Higuchi, T.; Ohtake, H.; Hirobe, M. *Tetrahedron Lett.* **1991**, *32*, 7435.
42. Berkessel, A.; Kaiser, P.; Lex, J. *Chem. Eur. J.* **2003**, *9*, 4746-4756.
43. Wang, C.; Shalyaev, K. V.; Bonchio, M.; Carofiglio, T.; Groves, J. T. *Inorg. Chem.* **2006**, *45*, 4769-4782.
44. Pagliaro, M.; Campestrini, S.; Ciriminna, R. *Chem. Soc. Rev.* **2005**, *34*, 837-845
45. Barf, G. A.; Sheldon, R. A. *J. Mol. Catal. A: Chem.* **1995**, *102*, 23-39.

46. Leung, W.-H.; Che, C.-M. *J. Am. Chem. Soc.* **1989**, *111*, 8812-8818
47. Masuda, H.; Taga, T.; Osaki, K.; Sugimoto, H.; Mori, M.; Ogoshi, H. *J. Am. Chem. Soc.* **1981**, *103*, 2199.
48. Birnbaum, E.R.; Labinger, J.A.; Bercaw, J.E. and Gray, H.B. *Inorg. Chim. Acta.* **1998**, *270*, 433-439.
49. Groves, J.T. In *Cytochrome P-450, Structure, Mechanism and Biochemistry*, Ortiz de Montellano, P. R., Ed.; Kluwer Academic / Plenum Publishers: New York, 2005. pp 1-43.
50. (a) Che, C.-M. and Huang, J.-S. *Chem. Commun.* **2009**, 3996-4015. (b) Zhang, J.-L. and Che, C.-M. *Org. Lett.* **2002**, *4* (11), 1911-1914. (c) Liu, C.-J.; Yu, W.-Y.; Li, S.-G. and Che, C.-M. *J. Org. Chem.* **1998**, *63*, 7364-7369. (d) Zhang, J.-L. and Che, C.-M. *Chem. Eur. J.* **2005**, *11*, 3899-3914. (e) Zhang, R.; Yu, W.-Y.; Sun, H.-Z.; Liu, W.-S. and Che, C.-M. *Chem. Eur. J.* **2002**, *8* (11), 2495-2507. (f) Liu, C.-J.; Yu, W.-Y. Che, C.-M. and Yeung, C.-H. *J. Org. Chem.* **1999**, *64* (20), 7365-7374. (g) Zhang, R.; Yu, W.-Y.; Wong, K.-Y. and Che, C.-M. *J. Org. Chem.* **2001**, *66* (24), 8145-8153. (h) Che, C.-M. and Yu, W.-Y. *Pure & Appl. Chem.* **1999**, *71* (2), 281-288.
51. Gross, Z.; Ini, S. *Inorg. Chem.* **1999**, *38*, 1446-1449.
52. Larsen, E.; Jorgensen, K. A. *Acta Chem. Scan.* **1989**, *43*, 259.
53. (a) Ebadi, A.; Safari, N.; Peyrovi, M. N. *Applied Catalysis A: General* **2007**, *321*, 135-139. (b) Gonzalez, L. M.; Villa de P. A. L.; Montes de C., C. and Sorokin, A. *Tetrahedron Lett.* **2006**, *47*, 6465-6468.
54. Capobianchi, A.; Paoletti, A. M.; Pennesi, G.; Caminiti, R. and Ercolani, C. *Inorg. Chem.* **1994**, *33*, 4635-4640.
55. Balkus, Jr.K. J.; Eissa, M.; Levado, R. *J. Am. Chem. Soc.* **1995**, *117*, 10753-10754.
56. Leung, W.-H.; Che, C.-M. *Inorg. Chem.* **1989**, *28*, 4620.
57. Pizzo, M. Sgarbossa, P.; Scarso, A.; Michelin, R. A. and Strukul, G. *Organometallics* **2006**, *25* (12), 3056-3062.
58. Colladon, M; Scarso, A.; Sgarbossa, P.; Michelin, R. A. and Strukul, G. *J. Am. Chem. Soc.* **2007**, *129*, 7680-7689.

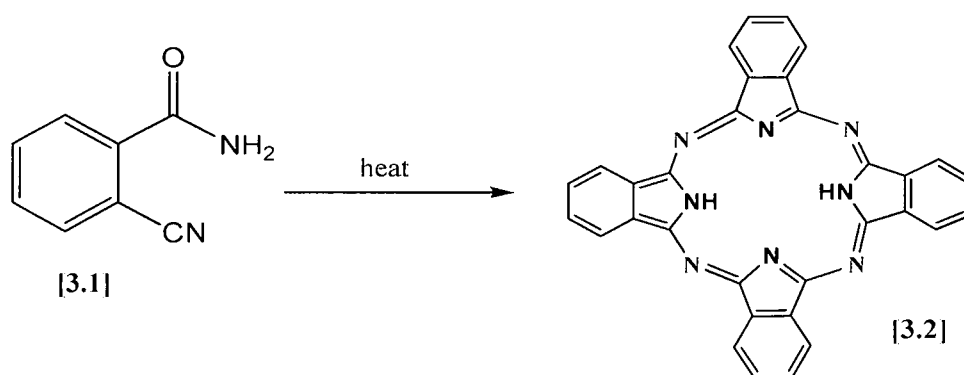
Chapter 3

Phthalocyanines

3.1 Introduction

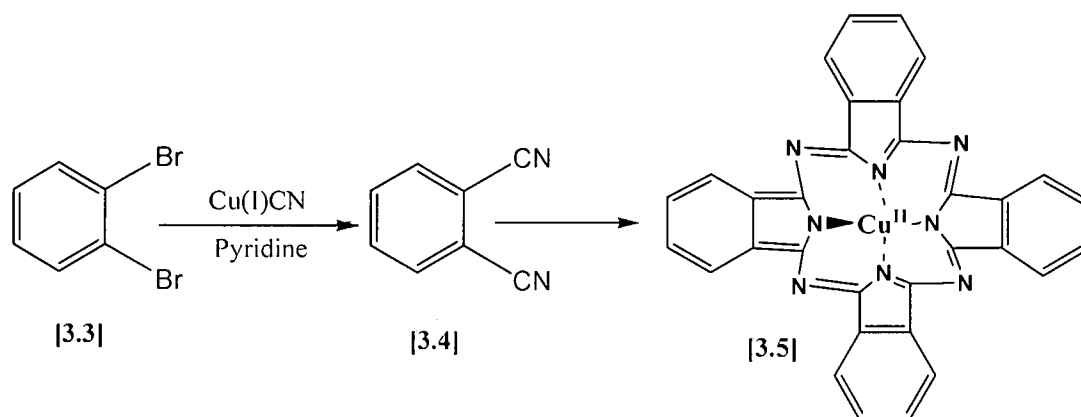
3.1.1 History and structure

Phthalocyanine was accidentally found in 1907 when Braun and Tcherniac¹ noticed a highly colored impurity during preparation of *o*-cyanobenzamide [3.1] (scheme.3.1) from phthalimide and acetic anhydride. At that time, very little significance was given to this discovery. It is likely that those authors produced metal-free phthalocyanine [3.2] as a by-product of their reaction, but they were unable to assign a structure to the colored impurity.



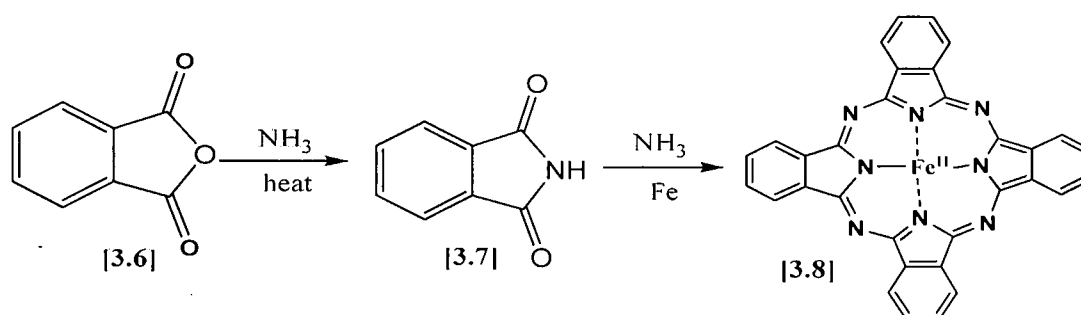
Scheme 3.1: First synthesis of phthalocyanine

De Diesbach and Von der Weid² next reported the preparation of phthalocyanine (Pc) in 1927. While attempting the synthesis of phthalonitrile [3.4] from 1,2-dibromobenzene [3.3] in pyridine, they obtained a blue product (23% yield) now considered to be copper (II) Pc [3.5] (Scheme 3.2). This compound was particularly stable to heat, sulfuric acid and alkali.



Scheme 3.2: First synthesis of copper phthalocyanine [3.5]

The third observation of Pc was in 1928 at Scottish Dyes Limited in Grangemouth, Scotland, during the reaction of phthalic anhydride [3.6] with ammonia to prepare phthalimide [3.7].³ A cracked glass reaction vessel contained in a steel casing allowed vapours to come into contact with a source of iron resulting in the synthesis of blue, insoluble, stable pigments which turned out to be iron(II) Pc [3.8] (Scheme 3.3).



Scheme 3.3: Accidental preparation of iron(II) Pc [3.8]

Subsequent more comprehensive studies by Linstead⁴ and Robertson⁵ established the ring structure of this new class of compounds for both the metal free (H_2Pc) analogues as well as derivatives metallated with first row transition elements (MPc). The name phthalocyanine was derived by Linstead from the Greek words for rock oil (*naphtha*) and blue (*cyanine*).

Nowadays, the phthalocyanines are considered as a family of intensely coloured compounds (blue, green) that are structurally similar to porphyrins. Porphyrins [3.10] consist of 4-pyrrole type residues linked together by four methine-bridging groups. However, in Pcs (e.g. [3.9]) the methine groups are replaced by imine functionalities and the pyrrole type residues are benzo-fused. The relationship between the Pc and porphyrin ring system is shown in Figure 3.0. The basic structure of phthalocyanine consist of a planar macrocycle of four identical isoindole units linked together through their 1,3-positions by four aza bridges with a central cavity of perfect size to bind various metal ions. Phthalocyanine (Pc) has an 18π electron aromatic system. Although structurally similar to naturally occurring porphyrins such as haemoglobin, vitamin B_{12} or chlorophyll, phthalocyanines do not occur in nature.

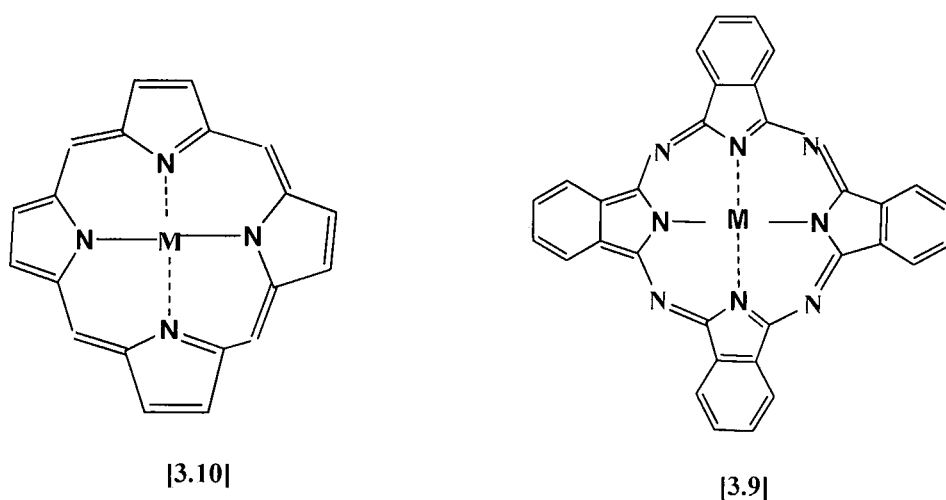


Fig. 3.0: The porphyrin [3.10] and phthalocyanine [3.9] macrocycle ($M=H_2$ or metal).

The aromaticity of the Pc ring system is the basis of the Pc high stability. Thus, Pcs are chemically and thermally stable compounds with exceptional optical and electrical behaviour. Furthermore, several chemical modifications can be made to the Pc ring, thereby allowing a fine-tuning of their physical properties.⁶ Any Pc derivative in which at least one of the central nitrogen atoms of the Pc, i.e. [(H₂)Pc], forms a bond to a metal atom is called metal phthalocyanine (MPc). During the process of coordination, protons on the pyrole nitrogen atoms are lost, leaving two negative charges that are distributed equally about the whole inner ring. The flexibility of the Pc structure accounts for its numerous applications.⁶ The Pc's role is largely determined by both the type of metal ion in the ring and the benzo-substituents as these tend to modify their chemical and physical properties. The macrocycle of Pc has sixteen ring sites for possible substitution and the range and applications of Pcs can be extended by incorporating different substituents at some or all of these sites. The sixteen sites available for such substituents fall into two categories: peripheral sites (2, 3, 9, 10, 16, 17, 23, 24) and non-peripheral sites (1, 4, 8, 11, 15, 18, 22, 25). (Figure 3.1). Although the coordination number of the square planar Pc is four, most of the incorporated metals have higher coordination numbers and as such are capable of accommodating a variety of axial ligands together with the Pc.^{6,7}

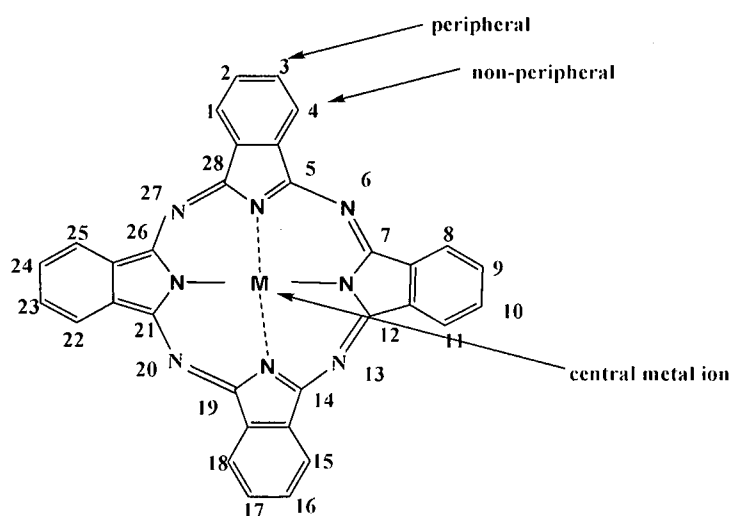


Fig. 3.1: Peripheral and non-peripheral Pc positions.⁶

3.1.2 Electronic absorption spectra.

Due to their extended π -electron system (fused benzene rings), phthalocyanines are highly coloured compounds which generally appear blue or green in solutions compared to porphyrins that tend to be red or purple. These color differences are explicable in terms of the UV-vis absorption spectra⁸ where the UV-vis spectrum for Pcs originate from the molecular orbitals within the highly conjugated 18π -electron system and overlapping of that with the central metal atom.⁹ Pcs absorb light in the near UV and visible regions where several sets of absorption bands have been observed. The most studied and characteristic of these bands are the B- or Soret band between 320-370 nm and the Q-band between 620-720 nm (Fig. 3.2).⁸

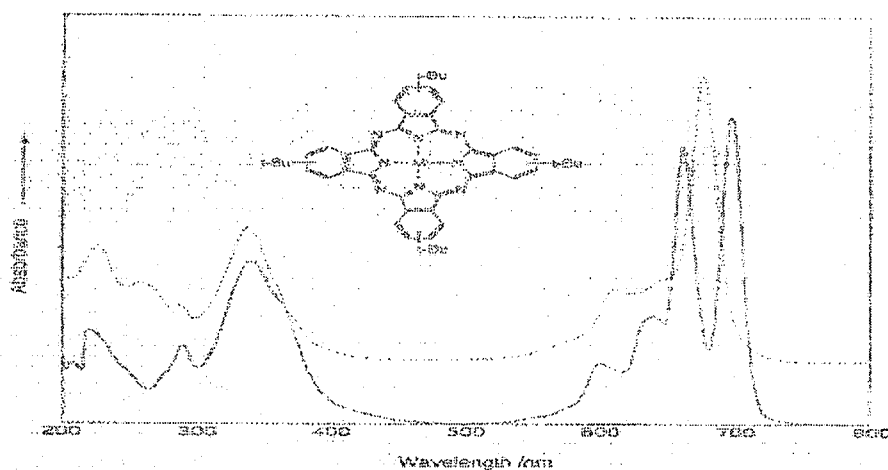


Fig. 3.2: Absorption spectrum of tetra-*tert*-butylphthalocyanine, solid line M = H₂ and, dashed line, M = Cu analogue.

Unlike porphyrins, Pc spectra appear with the Q-band having the highest intensity and thus being responsible for the blue or green colour of the Pc. This intense absorption in the visible region results from a $\pi \rightarrow \pi^*$ electronic transition from the HOMO (highest occupied molecular orbital) to the LUMO orbital (lowest unoccupied molecular orbital) within the macrocycle.¹⁰ The less intense Soret band can be attributed to a deeper $\pi \rightarrow \pi^*$ electronic transition in the macrocycle (Figure 3.3).^{11,12} According to Gouterman's more detailed four orbital model for MPcs,^{7,13} the Q-band results from an $a_{1u} \rightarrow e_g$ ($n \rightarrow$

π^*) transition and the B-band from an $a_{2u} \rightarrow e_g(\pi \rightarrow \pi^*)$ transition (Figure 3.3). The shift in the Q-band to longer wavelength was attributed to a lowering of the LUMO energy by interaction with the metal.

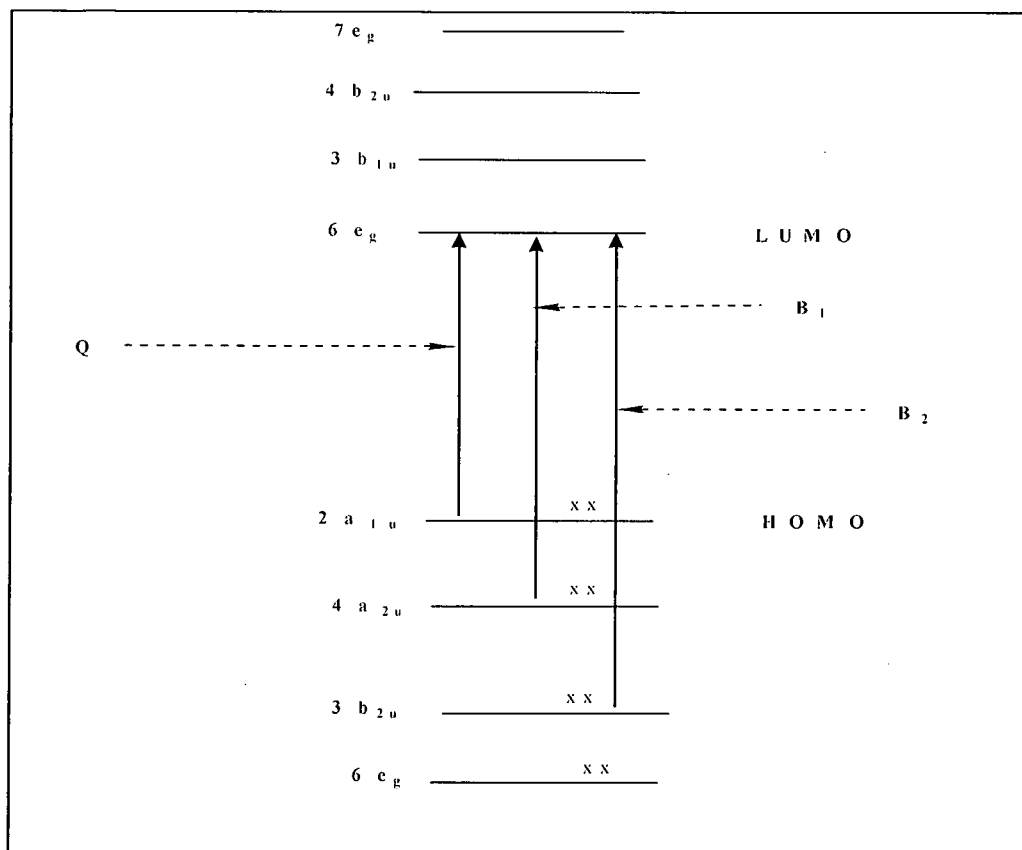


Fig. 3.3: Electronic transitions showing the derivation of the Q and B bands in phthalocyanine complexes. 'x' represents an electron.

Metal-free Pcs, being of lower symmetry, exhibit an absorption band which is split into two principal components usually termed Q_x and Q_y in the 620-720 nm region. Metallated Pcs on the other hand are characterized by a single intense Q-band. The sharpness of the peak can therefore be used as an indication of the level of product purity and thus an indication as to the degree of metal insertion into the Pc cavity. Charge transfer (CT) transitions due to electron excitations from the atomic orbitals of the metal ion to the ligand's molecular orbitals, or vice versa, may also appear as a shoulder on the Soret band in the region 340-385 nm and the Q-band in the region 560-595 nm^{14, 15}.

Furthermore, the position of the Q-band in the UV-vis spectra of Pcs is influenced by the kind of central metal ion and the nature of the substituent(s) on the Pc ring itself.¹⁶ Peripheral substituents tend to have little influence on the position of the Q-band except for naphthalocyanines and anthracocyanines where the Q-band experience a slight red shift of about 90 and 170 nm, respectively, with the expansion of the π -system.¹⁷ The Soret band in this instance remained unchanged.¹⁷ For non-peripherally substituted compounds, the Q- and B-bands exhibit a shift to higher wavelengths due to contraction of the gap between the HOMO and LUMO orbitals.^{16,18} In addition to this, electron donating substituents in the non-peripheral positions cause a 70 nm red shift in the position of the Q-band.¹⁶

3.1.3 Aggregation phenomena in phthalocyanine chemistry

Aggregation, described as the association of molecules leading to dimers, oligomers or mixtures of both and one of the profound properties of phthalocyanines, decrease the solubility of Pcs in common organic solvents and brings about numerous problems during purification and characterization of these compounds. One or more of the following processes may account for aggregation between Pc molecules:¹¹ (i) Intramolecular interaction due to direct linkage of one phthalocyanine ring to another,¹⁹ (ii) In the case of MPc, covalent bonding between metals as μ -oxo-links may exist, (iii) Two phthalocyanine rings may share the same central metal in what is known as a sandwich-type complex,^{20,21} and finally (iv) Peripheral substituents may hold two rings in space through weak bonding associations.²²

In solution, the degree of aggregation depends on the level of π - π interaction (the π - π interactions between adjacent molecules resulting in the stacking of the molecules like a pack of cards which turn to render inner molecules inaccessible), Van der Waal forces and hydrogen bonding between the Pc molecules themselves and the solvent molecules. Aggregation of a Pc in solution is more profound at high concentrations, as more Pc

molecules are brought into close contact with each other. Unsubstituted Pcs hence are practically insoluble in common organic solvents,⁶ compared to the substituted ones.

Since aggregation has to a large extent limited the utilization of Pcs during chemical reactions, most researchers have focussed on synthesizing phthalocyanine molecules that are soluble in common organic solvents and even water. The main method for reducing Pc aggregation is by introducing substituents at the peripheral and non-peripheral positions of the benzo group. Since bulkier groups reduce the closeness of the Pc rings to each other, bulky substituents attached to the Pc ring system was found to suppress aggregation. In general, the degree of aggregation depends to a large extent on the nature and position of the benzo-substituents as well as the metal ion in the macrocycle and the solvent in question. Piechocki *et al.* found that molecules containing substituents with long aliphatic chains (carbon atoms ≥ 8) attached to the peripheral positions exhibit greater solubility in common organic solvents than their unsubstituted counterparts.²³ Cook *et al.*^{24a} reported the synthesis of Pcs bearing alkyl substituents at all eight non-peripheral positions. These workers also found that these compounds tend to adopt a saddle or saucer like shape so their tendency to aggregate in solution is much less than that of their peripherally substituted counterparts.^{24b}

Aggregation has a profound influence on the appearance of the characteristic Q-band of Pcs in solution and is easily detected by UV-visible spectroscopy where two absorption bands are visible at *ca.* 650 to 750 nm.^{24c} It has however to be taken into account that the solvent plays an important role in the degree of aggregation observed during UV-Vis measurements. For example, aggregation seems not important in chloroform and chloronaphthalene, but it does become important in mixtures of chloroform and methanol,²³ which is attributed to the increase in solvent polarity. With increasing methanol concentration in chloroform, there is a strong solvent-solvent interaction between the methanol and the chloroform isolating the Pc molecules from solution and causing them to aggregate. In pure methanol and related solvents, Pcs are insoluble due to high levels of aggregation.

3.2 Synthesis

3.2.1 Synthesis of unsubstituted Pcs

3.2.1.1 Metal-free Pc (H_2Pc)

The Pc macrocycle can be broken down into four identical subunits (Fig 3.4), hence most synthetic methods towards the preparation of unsubstituted Pcs begin with the condensing of suitable corner units.^{6,25} Preparative methods are therefore based on a range of *ortho*-disubstituted benzene derivatives like phthalic anhydride [3.6], phthalimide [3.7], phthalic acid [3.11], phthalonitrile [3.4], and 1,3-diiminoisoindoline [3.8a].

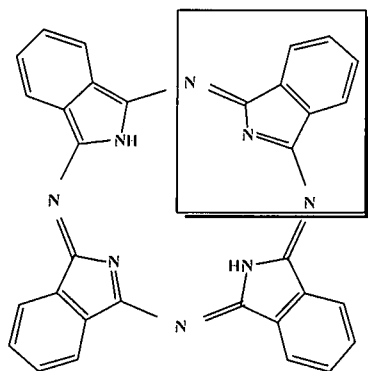
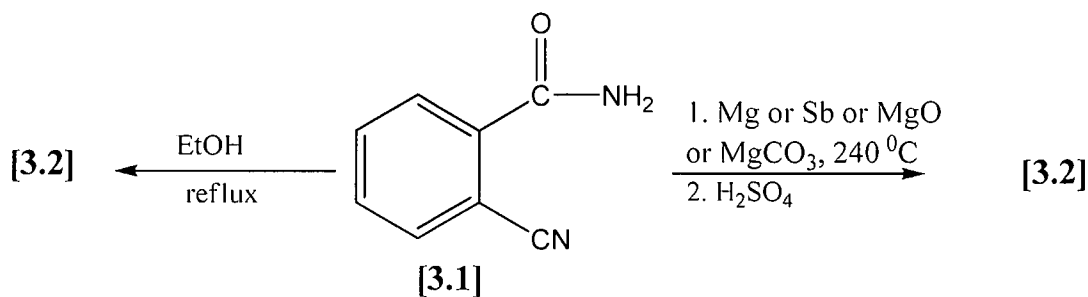


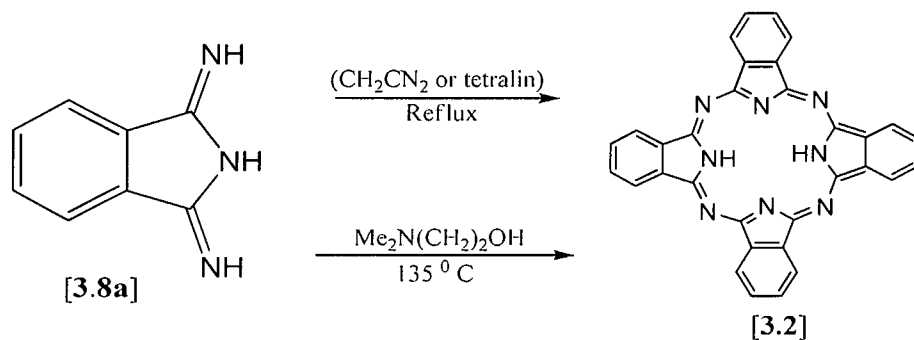
Fig 3.4: Metal free phthalocyanine

The first deliberate attempt at the synthesis of a Pc molecule entailed refluxing *o*-cyanobenzamide [3.1] in ethanol, which led to the Pc being isolated in low yield.⁴ Through the utilization of metals like Mg or Sb or magnesium salts, Linstead and coworkers²⁷ were able to increase Pc yields with the same starting material to *ca.* 40% (Scheme 3.4).



Scheme 3.4

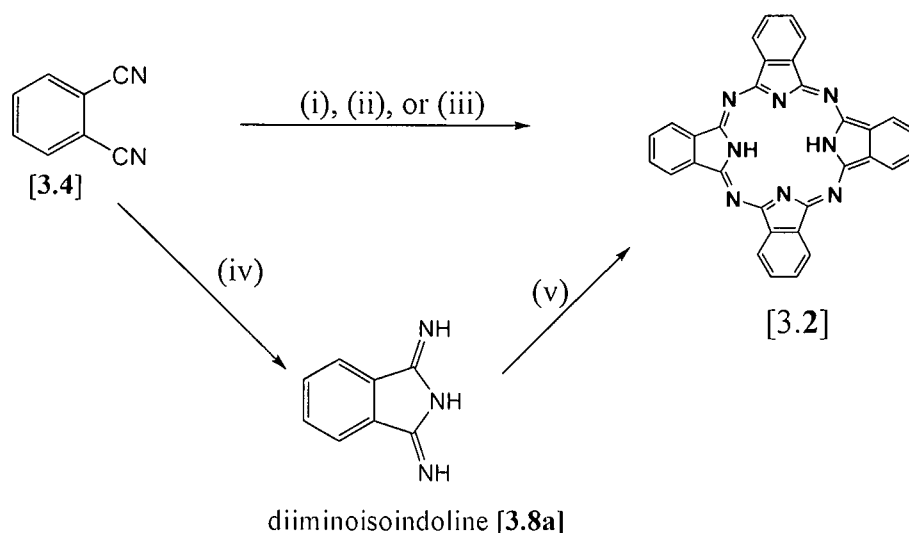
Elvidge and Linstead²⁸ showed that H₂Pc [3.2] could also be formed by boiling 1,3-diiminoisoindoline [3.8a] in succinonitrile or tetralin (34 and 45 % yield, respectively), while the yield of [3.2] could be increased to 85 % by refluxing [3.8a] in 2-N,N-dimethylaminoethanol.(Scheme 3.5).²⁹



Scheme 3.5

Cyclotetramerization of phthalonitrile [3.4] currently is the most common method for the laboratory synthesis of Pc [3.2]⁶ and may take one of the two pathways (Scheme 3.6). The phthalonitrile [3.4] can either be converted to the Pc directly or formed *via* the diiminoisoindoline [3.8a] intermediate. Leznoff and Hall,³⁰ during their synthesis of unsymmetrical phthalocyanine, found that phthalonitrile could be converted to the diiminoisoindoline [3.8a] through reaction with ammonia. Subsequent self-condensation

of [3.8a] under relatively mild conditions led to the formation of [3.2].³¹ McKeown *et al.*³⁴ reported the reaction of phthalonitrile with lithium metal in refluxing pentanol as a new method for synthesising Pcs. During this reaction the initially formed Li₂Pc is converted to the desired metal free compound through an acid work-up process.

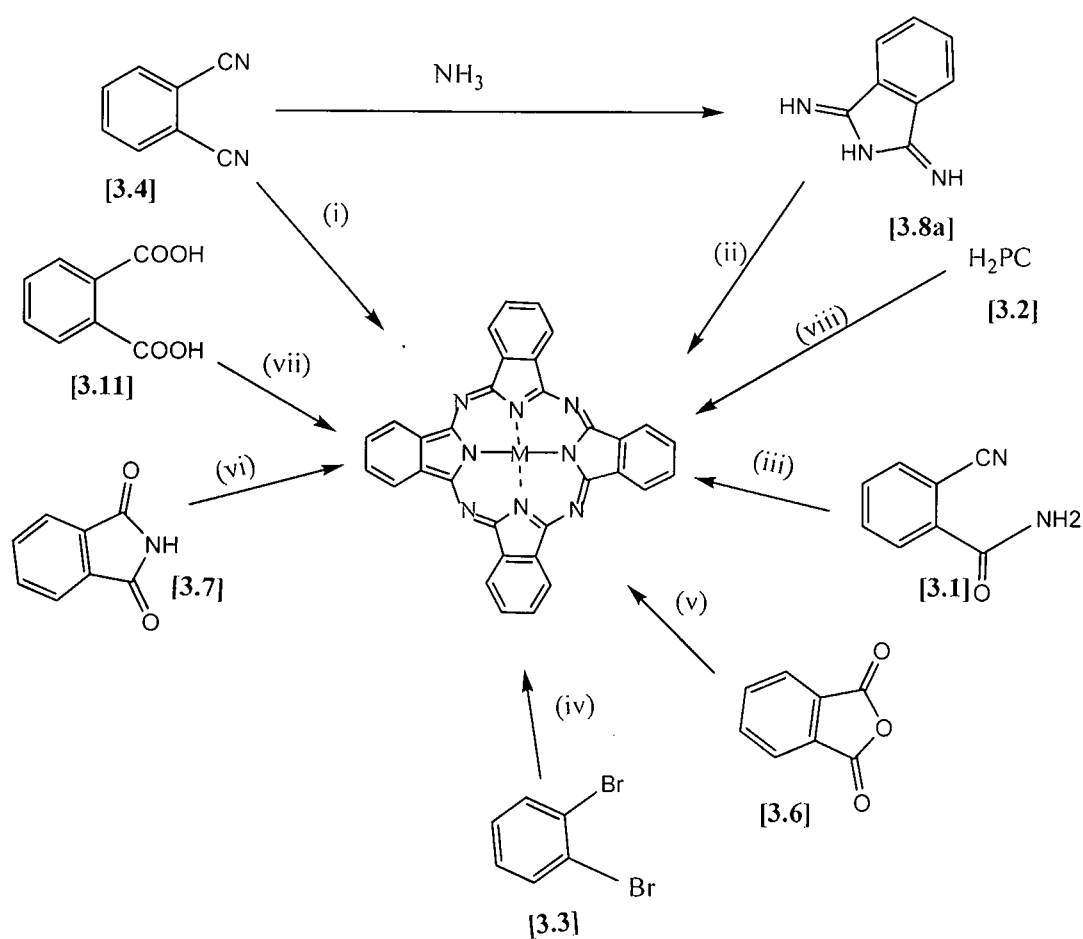


Scheme 3.6: Synthetic routes to [3.2] from phthalonitrile [3.4]. (i) Lithium, refluxing pentanol, followed by aqueous hydrolysis. (ii) Fuse with hydroquinone.³² (iii) Heat with 1,8-diazabicyclo[4.3.0]non-5-ene (DBN) in a melt or in pentanol solution.³³ (iv) NH₃, refluxing methanol, sodium methoxide.³⁰ (v) Reflux in a high boiling alcohol.³¹

A new cyclotetramerisation route called the cerium-promoted formation of metal-free phthalocyanine have recently been put forward by Ng and Lee.⁴⁹ This involves the treatment of phthalonitriles with 6 mol% of anhydrous CeCl₃ in 1-pentanol at 160 °C for 24-72 h. A range of phthalonitriles with nitro, alkoxy, thioalkoxy, and amino groups were converted into the corresponding metal-free phthalocyanines in 20-60% yield. The addition of 1,8-diazabicyclo[5.4.0]undec-7-ene (DBU) greatly shortens the reaction time and increase the yield of these reactions.

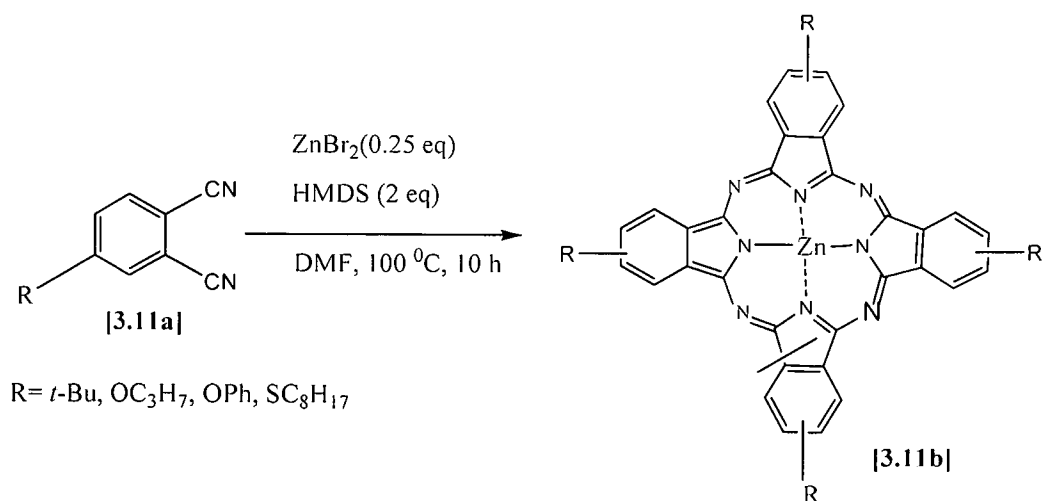
3.2.1.2 Metal containing unsubstituted Pcs (MPcs)

Over seventy different metals have been incorporated into the macrocyclic cavity of Pcs. Yields generally depend on the metal salts used and the reaction conditions. Metallated phthalocyanines have been prepared by either cyclotetramerisation of the phthalic acid derivative (such as phthalonitrile or diiminoisoindolene) in the presence of the metal salt, or by insertion of the metal ion into a preformed phthalocyanine ring either as its metal-free (H_2Pc) or dilithiated derivative.⁶ Although many precursors for synthesizing MPcs exist, those often used are phthalonitriles [3.4], phthalic anhydride [3.6], phthalimide [3.7] and phthalic acid [3.11]. Most of the metals incorporated are in the +2 or +3 oxidation states. Scheme 3.7 shows some general routes towards the synthesis of metallated phthalocyanine. During the laboratory synthesis, most MPcs have been prepared through cyclotetramerization of phthalonitrile [3.4] or phthalic anhydride [3.6]. From phthalonitrile [3.4], MPcs are prepared by reaction with a base such as DBU (to decrease the temperature required for the synthesis), a metal salt and a high boiling point solvent such as pentanol, quinoline or DMF.⁶ For the phthalic anhydride [3.6] and phthalimide [3.7] routes, cyclotetramerization is done in the presence of a nitrogen source (urea) and a metal salt (e.g. copper(II)acetate or nickel(II)chloride).



Scheme 3.7: Synthetic routes to MPcs. i) LiOR/ROH; M^{2+} /DBU; M^0 . ii) heat; M^{2+} . iii) heat; M^{2+} /EtOH. iv) CuCN/DMF. v) Cu(I)Cl/Urea/Cat. (vi) M^{2+} /Formamide. vii) Metal ion, urea, heat. viii) Metal or metal salt, heat.

A more convenient modification of the standard preparation of metallated phthalocyanines [3.11b] from phthalonitriles [3.11a] has been accomplished by the treatment of the latter with metal salts and hexamethyldisilazane (HMDS) in DMF at 100 °C (Scheme 3.8).³⁶ This procedure provides a preparative method using mild conditions and can be applied to phthalocyanines having a variety of metals and substituents. A variety of metal salts such as $ZnCl_2$, $Zn(OAc)_2$, $MgBr_2$ etc. can be used.



Scheme 3.8: Synthesis of MPc [3.11b] under mild conditions.

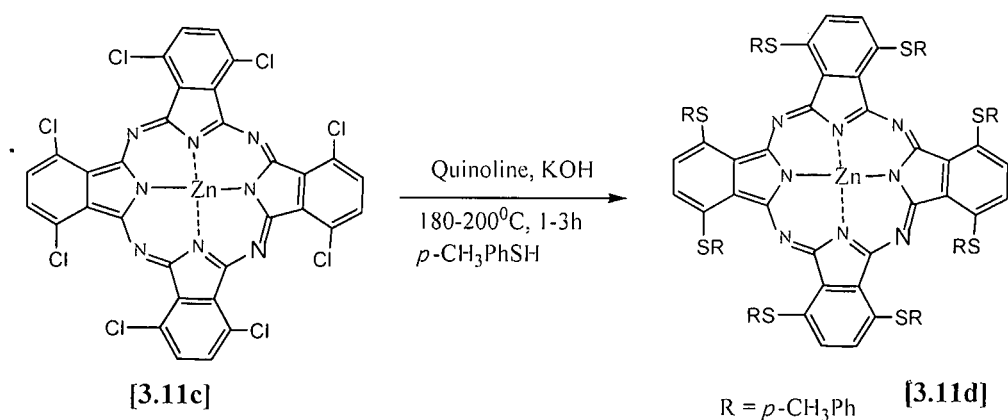
In addition, phthalocyanines have been synthesized using microwave irradiation.³⁷ In particular Cu, Co, Ni, Zn and Fe MPcs have been synthesized by this method. The advantages include shorter reaction times (from several hours to minutes) and absence of solvents.

Synthesis of MPc by means of metal ion insertion is accomplished by heating the metal free Pc or the lithiated Pc (Li_2Pc) with the appropriate metal or metal salt. In the case of the unsubstituted metal free Pc, a high boiling solvent such as 1-chloronaphthalene and quinoline is required for complete metallation to take place.^{6,35}

3.2.2 Synthesis of substituted Pcs

Since unsubstituted phthalocyanines show poor solubility in common organic solvents, the introduction of substituents at the peripheral or non-peripheral positions assist in increasing the solubility of these compounds. Hence, substituents have been incorporated into the Pc ring system either through substitution reactions on the preformed macrocycle

(a rather difficult process) or by the introduction of the substituent into the appropriate precursors prior to cyclization. Because of poor regioselectivity and limited scope, the former method is, however, rarely used during the synthesis of substituted Pcs. Despite these draw-backs, some examples like the high temperature thiolation of non-peripherally octachloro substituted phthalocyanine **[3.11c]** have been reported (Scheme 3.9).³⁸ Electrophilic aromatic substitution reactions, such as halogenation,³⁹ and nitration⁴⁰ have been described for producing Pc based dyes and pigments.



Scheme 3.9.

3.2.2.1 Synthesis of substituted phthalonitriles.

Although the synthesis of several substituted phthalocyanines have been reported, synthetic routes towards these compounds almost exclusively utilize phthalonitrile derivatives as starting material and entail the introduction of the appropriate substituents onto the precursor phthalonitrile **[3.4]** or phthalic acid **[3.11]**.^{41,42} The challenge in the synthesis of substituted phthalocyanines therefore lies in the preparation of the appropriately substituted phthalonitrile and, apart from low yields, not in the cyclisation to the Pc. From the appropriate phthalonitriles, three main series of phthalocyanines, *i.e.*

tetra-substituted Pcs [3.12] and peripherally [3.13] and non-peripherally [3.14] octa-substituted Pcs, can be obtained (Figure 3.5).⁴²

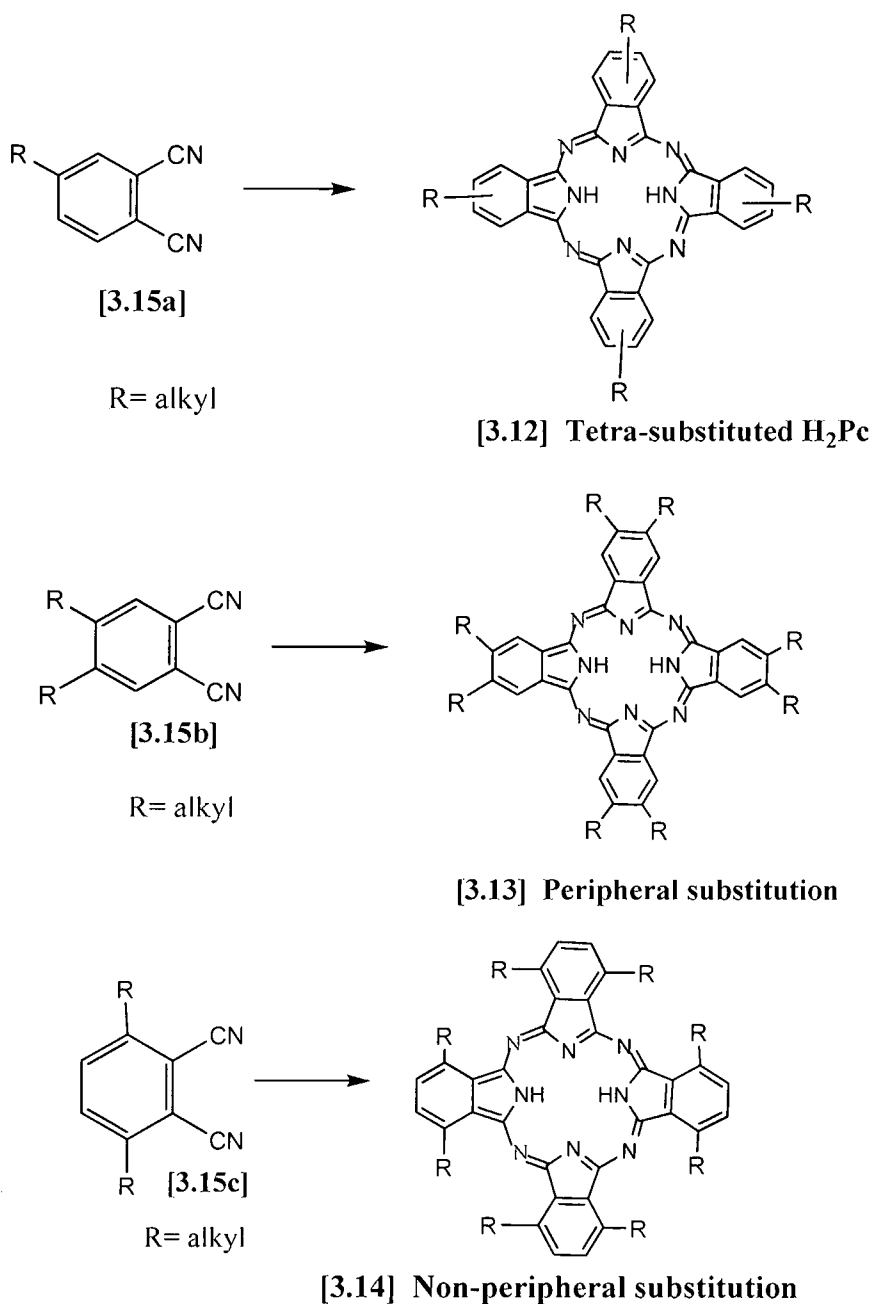
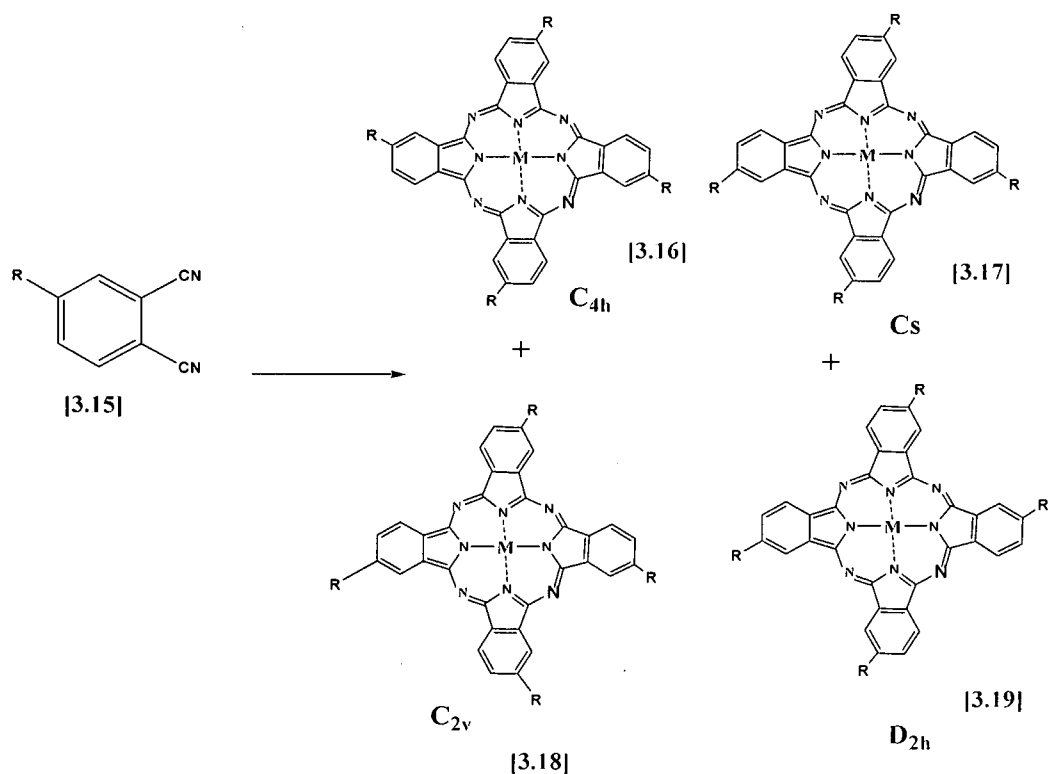


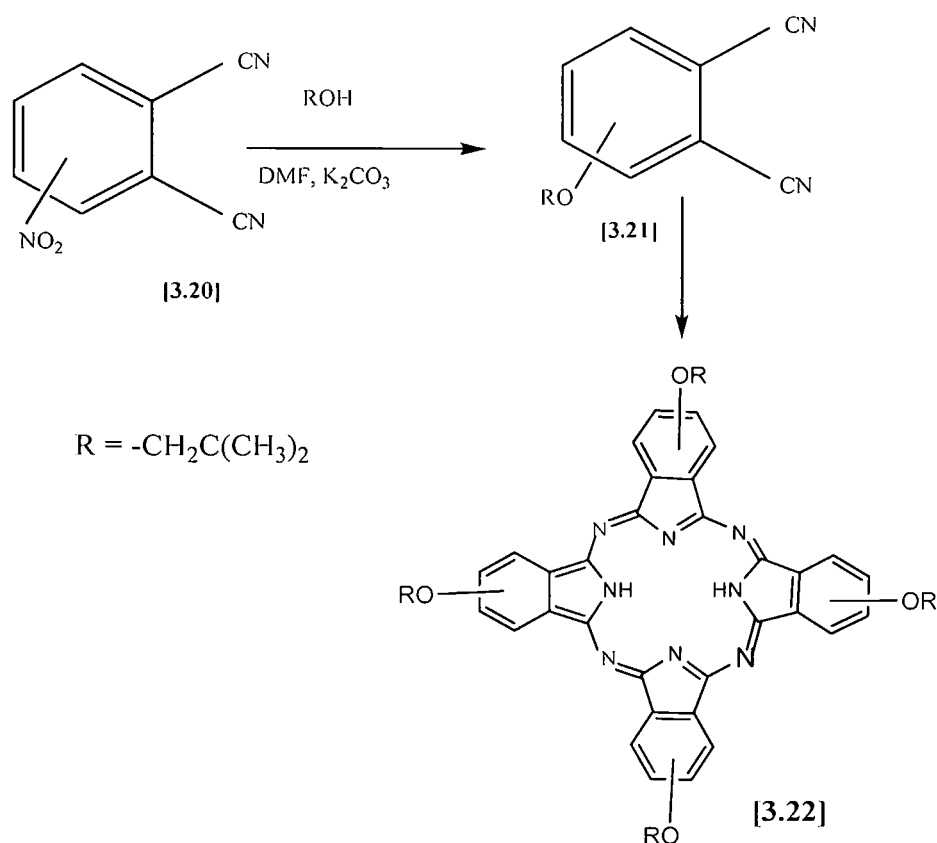
Fig 3.5

Mono-substituted phthalonitriles [3.15] are the precursors to tetra-substituted phthalocyanines. Cyclisation of these phthalonitriles [3.15] may result in the formation of phthalocyanines with a mixture of up to four regioisomers being possible^{41,42} (Scheme 3.10).



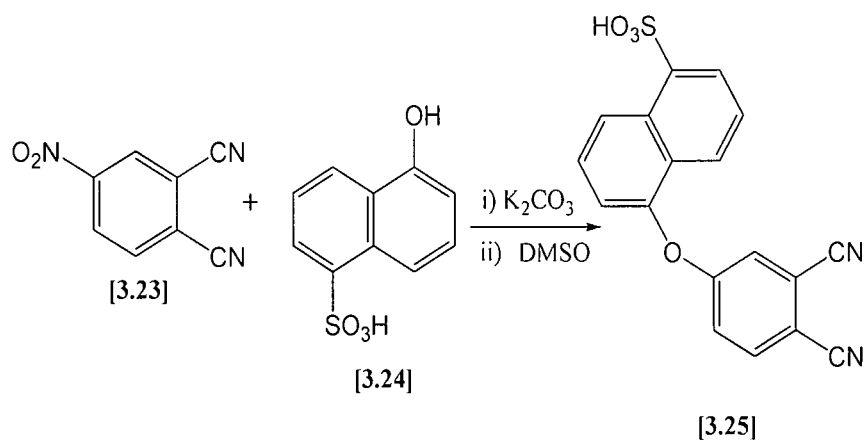
Scheme 3.10: Four structural isomers of tetra-substituted MPc obtained by condensation of a mono-substituted phthalonitrile

Since nitro groups can easily be displaced by nucleophiles in S_NAr reactions, 3- and/or 4-nitrophthalonitriles have been critical intermediates in the synthesis of various tetra-substituted Pcs. If the substitution is executed before cyclization, the two strongly electron withdrawing cyano groups enhance the reaction by draining electron density away from the aromatic ring. For example, nucleophilic substitution of the nitro group by an alcohol gave the mono-alkoxyphthalonitrile [3.21], which could be cyclized to the tetra-substituted Pc [3.22] (Scheme 3.11).⁴³



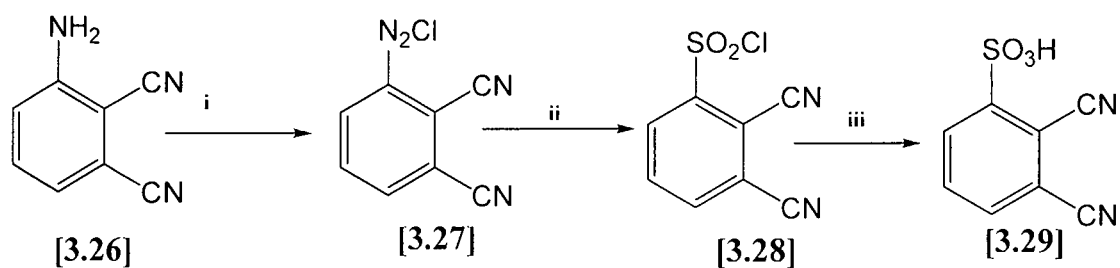
Scheme 3.11: Synthesis of tetra-alkoxysubstituted H_2Pc

Various 1,2-dicyanobenzenes bearing sulfur containing substituents have been prepared in this way by displacing the nitro functionality. In an effort to obtain a water soluble Pc, 4-(5-sulfo-1-naphthoxy)phthalonitrile [3.25] was prepared by a nitro displacement reaction⁴⁴ on 4-nitrophthalonitrile [3.23] with 5-hydroxy-1-naphthalene sulfonic acid [3.24] in the presence of potassium carbonate (Scheme 3.12).



Scheme 3.12: Preparation of sulfonaphthoxy-substituted phthalonitrile (**3.25**).

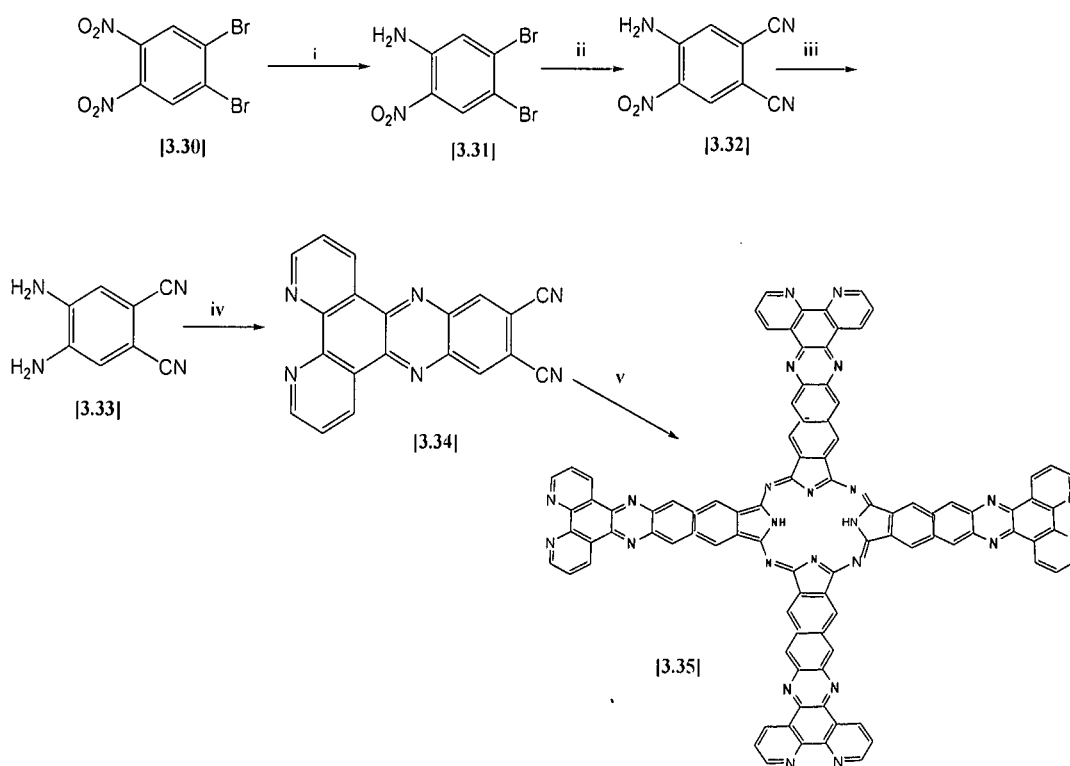
Reduction of the nitro group into an amino group in [3.26] opens the way towards further structural manipulation during the synthesis of Pcs. Thus a sulfonic acid group can be introduced into the non-peripheral position of the phthalonitrile by diazotization of the 3-amino-1,2-dicyanobenzene [3.27] followed by reaction with sulfur dioxide⁴⁵ (Scheme 3.13).



Scheme 3.13: Synthesis of 2,3-dicyanobenzenesulfonic acid [3.29].

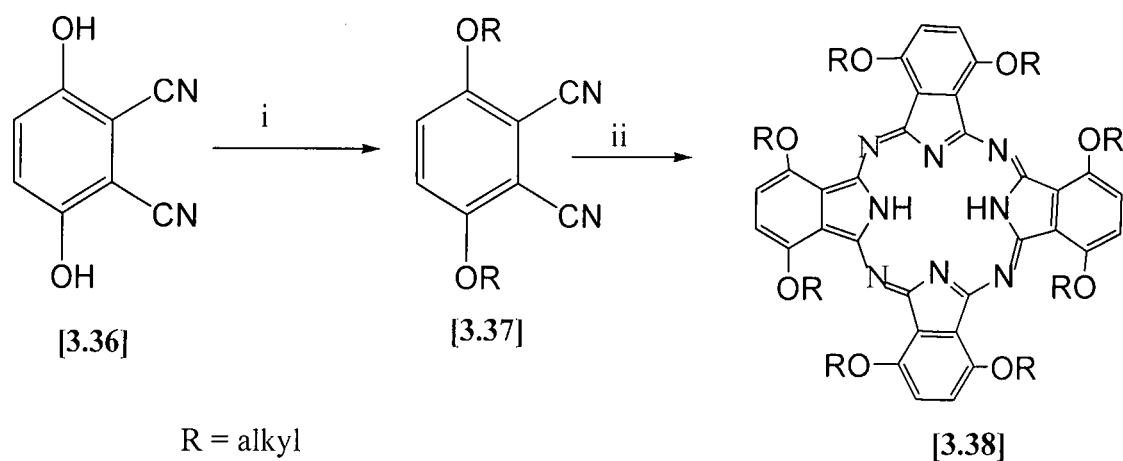
i) $NaNO_2$, HCl. ii) SO_2 , HOAc, CuCl. iii) H_2O .

The 2,3,9,10,16,17,23,24-octa-substituted (peripheral) and the 1,4,8,11,15,18,22,25-octa-substituted (non-peripheral) phthalocyanines can be synthesized from the 4,5-disubstituted phthalonitrile [3.34] and 3,6-disubstituted phthalonitrile [3.37] in the same way (Scheme 3.14 and Scheme 3.15).⁴⁶

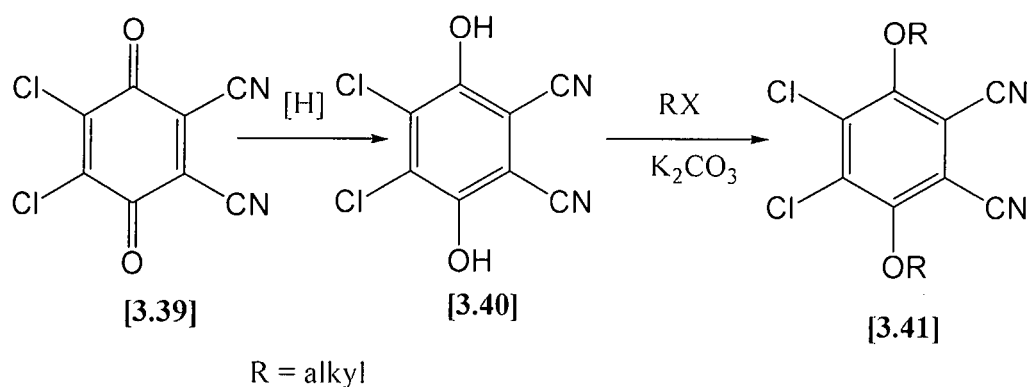


Scheme 3.14: Synthesis of conjugated phenanthroline appended Pc [3.35]. (i). NH_3/EtOH , (ii). CuCN , $\text{DMF}/\text{nitrobenzene}$, 180°C , 4.5 h. (iii). SnCl_2 , 70°C , 20 min. (iv) 1,10-phenanthroline-5,6-dione, EtOH , reflux. (v) Li metal, 1-Pentanol.

Since some 3,6-dioxygenated 1,2-dicyanobenzenes, e.g. [3.36] and [3.37] are commercially available, these compounds have been utilized in the synthesis of non-peripherally substituted alkoxy phthalocyanines like [3.38] in 60 % yield. (Scheme 3.15).⁴⁷ The same alkylation type approach can be utilized with DDQ (dichlorodicyanoquinone) [3.39] as starting material in the synthesis of highly substituted phthalocyanines (Scheme 3.16).⁴⁸



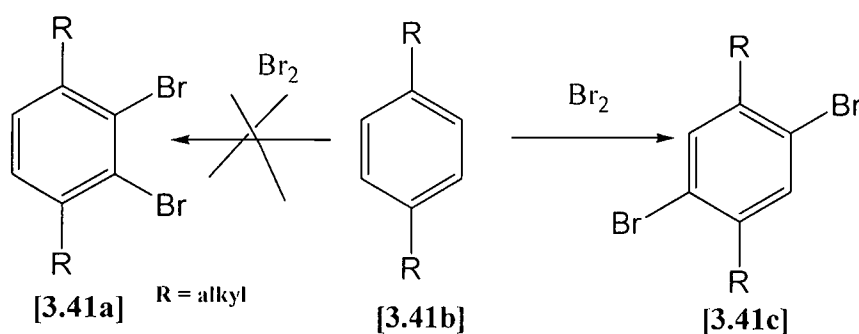
Scheme 3.15: Preparation of octa-alkoxy substituted phthalocyanines [3.38]. (i) RX, K₂CO₃, DMF (ii) Li, 1-Pentanol



Scheme 3.16: Preparation of dialkoxydichlorophthalonitriles

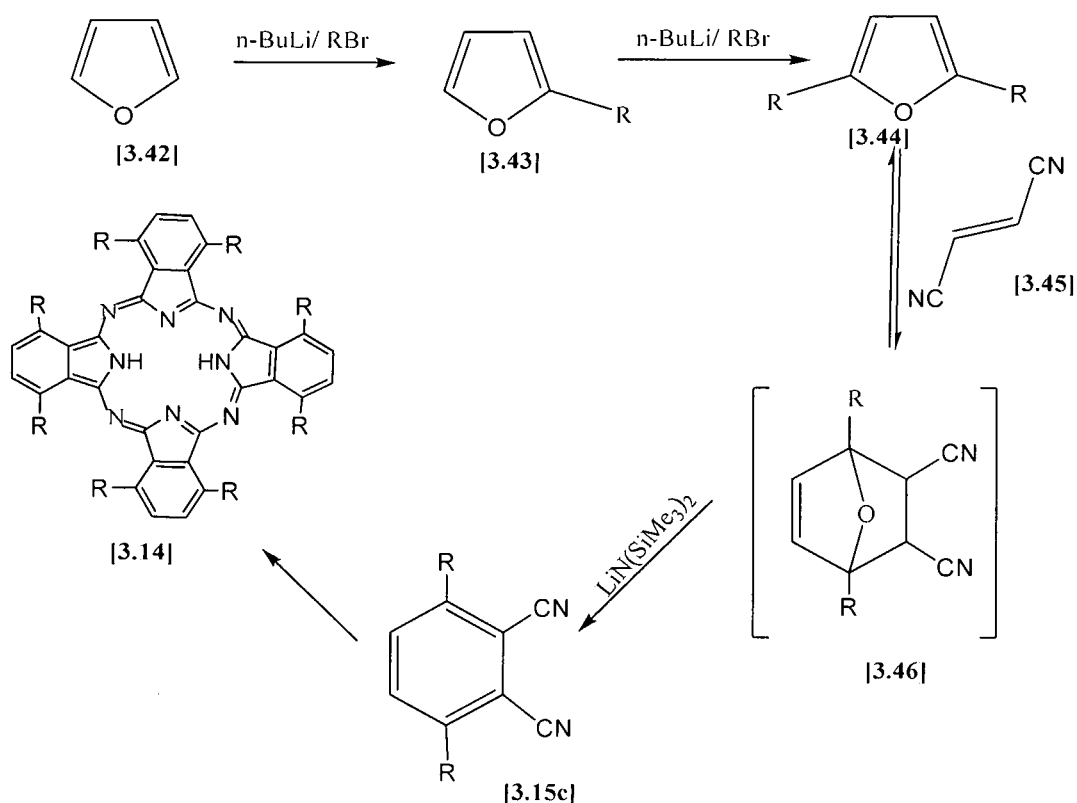
3.2.2.2 Synthesis of non-peripheral octa-alkylphthalocyanines

The synthesis of non-peripherally alkylsubstituted phthalocyanines are generally much more difficult and yields lower than those with substituents at the outer less crowded peripheral positions of the benzoid ring system. Furthermore, phthalonitriles substituted at the 3 and 6-positions [3.41a] are not available *via* direct bromination of the 1,4-disubstituted benzene rings [3.41b], since steric factors favour bromination in the 2 and 5 rather than the 2- and 3-positions (Scheme 3.17).



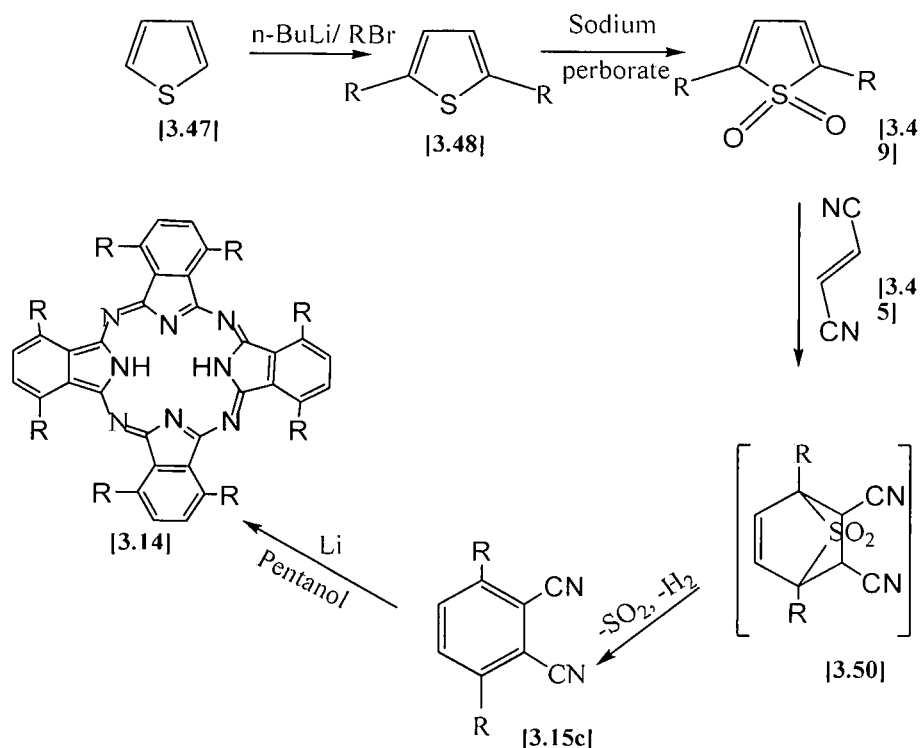
Scheme 3.17: Bromination of 1,4-dialkylbenzene[3.41b].

Since Diels-Alder reactions are well suited for synthesizing substituted six membered rings, Cook *et al.*⁵¹ described the utilization of this methodology in the synthesis of non-peripheral octaalkyl substituted phthalocyanines [3.14] through either the furan route (Scheme 3.18) or thiophene route (Scheme 3.19). The furan route is however disfavoured due to the fact that the Diels-Alder reaction with fumaronitrile [3.45] is reversible.



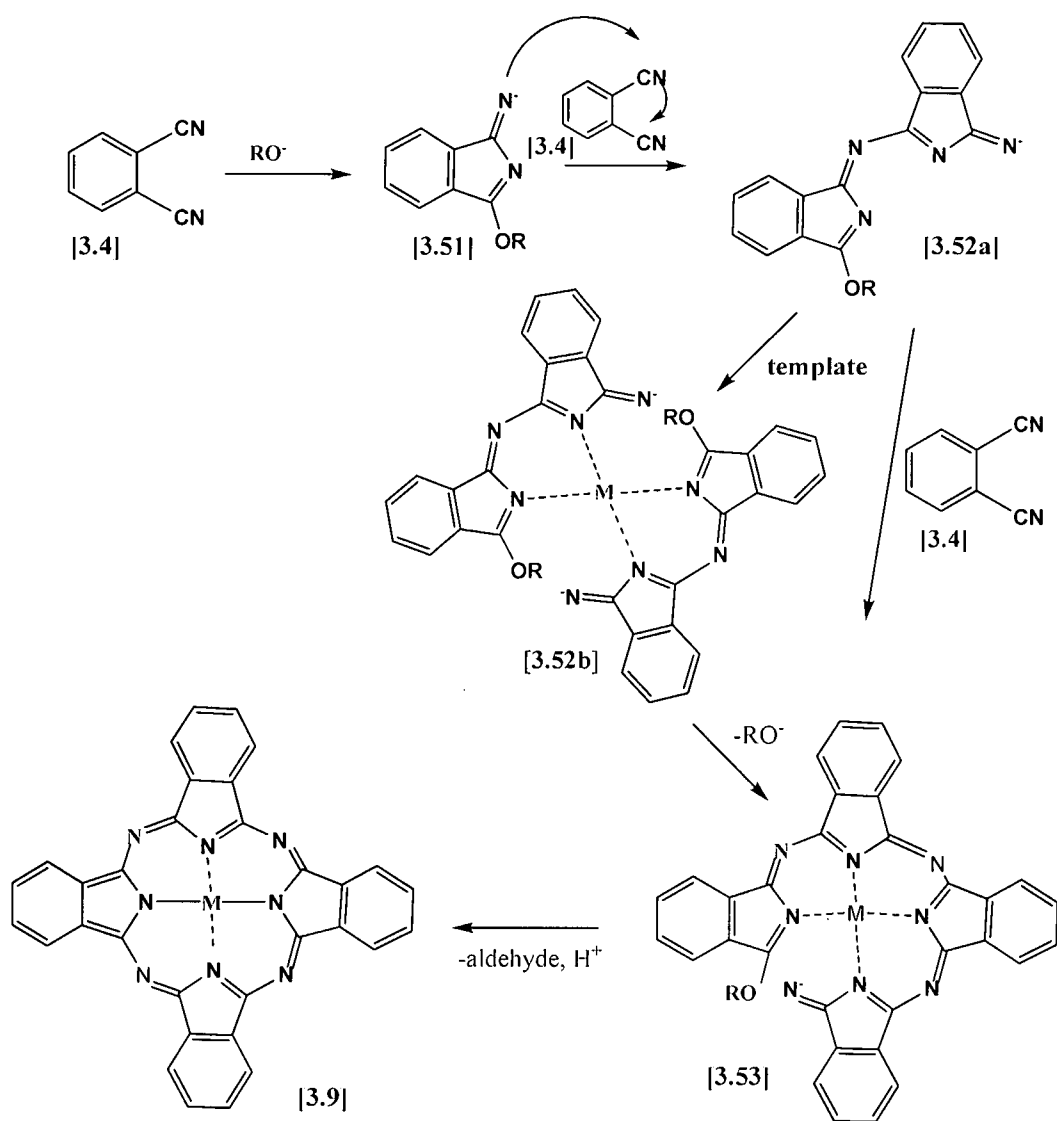
Scheme 3.18: Preparation of 1,4-dialkylphthalonitrile [3.15c] via the furan route (R = alkyl).

Alternatively, thiophene [3.47] (Scheme 3.19) can be alkylated in a single step using two equivalents of *n*-BuLi and an alkylating agent. The resulting thiophene [3.48] does not react with furaronitrile [3.45], but once oxidized to the non-aromatic thiophen-1,1-dioxide [3.49], reaction occurs at 150 °C in a sealed tube. The Diels-Alder intermediate [3.50] subsequently aromatises spontaneously with the loss of SO₂ and dehydrogenation. Cyclotetramerization of [3.15c] in a lithium pentanol solution eventually afford the Pc [3.14] in 12-20% yield.



Scheme 3.19: Preparation of 1,4-dialkylphthalonitrile [3.15c] via the thiophene route (R = alkyl).

The mechanism for the formation of the phthalocyanine macrocycle is not clearly understood, but Oliver and co-worker⁵² described the role of the alkoxide anion as indicated in Scheme 3.20. In the presence of a metal ion, which can act as a template, two moles of the initially formed dimeric species [3.52a] may react to form the product [3.53] in a single step or stepwise reaction of 1-imido-3-methoxyisoindoline [3.51] with three more phthalonitriles may also lead to the formation of [3.53] which after ring closure forms the Pc [3.9].

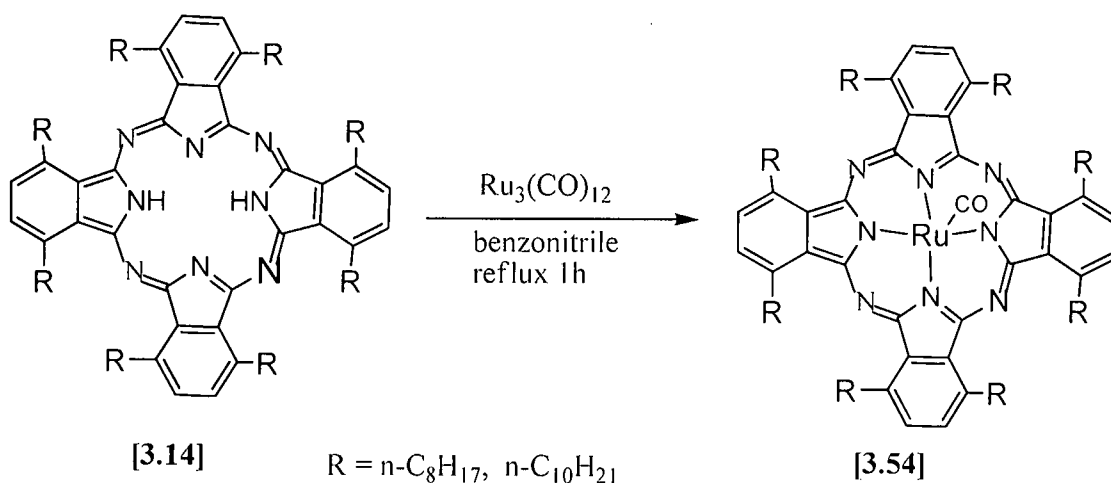


Scheme 3.20⁵²: Mechanism of formation of phthalocyanines. (R = CH₃)

3.2.2.3 Synthesis of Nonperipheral Octa-alkyl ruthenium phthalocyanine complexes

As for other metallated phthalocyanines (MPc), substituted ruthenium phthalocyanines [3.54] have been synthesized either through cyclotetramerization of the appropriate phthalonitrile in the presence of the metal salt⁵³ or the insertion of ruthenium into the metal free phthalocyanine.⁵⁴

Metal insertion into the preformed metal free phthalocyanine macrocycle has been the main method for synthesizing ruthenium phthalocyanines like 1,4,8,11,15,18,22,25-ruthenium carbonyl phthalocyanines [3.54] (Scheme 3.21). Metal insertion was achieved by simply reacting the metal free Pc [3.14] and $\text{Ru}_3(\text{CO})_{12}$ in benzonitrile.⁵⁴ The authors noted that the complexation of axial ligands are dependent on reaction time. Short reactions (< 1 h) resulted in the axially unsymmetrical mono-carbonyl species [3.54], while extended reaction times yielded the axially symmetrical dibenzonitrile ligated compounds.



Scheme 3.21: Synthesis of ruthenium phthalocyanine [3.54].

3.3 References

1. Braun, A; Tcherniac, J; *Ann. Ber.* **1907**, *40*, 2709.
2. De Diesbach, E.; Von der weid, E. *Helv. Chim. Acta* **1927**, *10*, 886.
3. Dandrige, A.G.; Drescher, H.A.; Thomas, J., (to Scottish Dyes Ltd), British Patent 332, 169, November 18, **1929**.
4. (a) Linstead, R.P.; *J. Chem. Soc.* **1934**, 1016. (b) Linstead, R.P.; and Lowe A.R.; *J. Chem. Soc.* **1936**, 1136.
5. (a) Robertson, J.M.; *J. Chem. Soc.* **1935**, 615. (b) Robertson, J.M.; *J. Chem. Soc.* **1936**, 1136.
6. McKeown, N.B. *Phthalocyanine Materials: Structure, Synthesis and Function*; Cambridge University Press: Cambridge; 1998. Pp. 1-167.
7. Leznoff, C.C.; Lever, A.B.P. *Phthalocyanines: Properties and Applications*; VCH: New York, 1989 (Vol. 1), 1993 (Vol. 2), 1993 (Vol. 3), 1996 (Vol. 4).
8. Cook, M.J.; *Spectroscopy of New Materials – Advances in Spectroscopy*, Eds. Clark, R.J.; Hester, R.E.; Wiley, Chichester; 1993, p. 87.
9. Sastre, A.; Gouloumous, A.; Vazqyez, P.; *Org. Lett.* **1999**, *1*, 1807.
10. Boucher, L. *Coordination Chemistry in Macrocyclic Compounds*, Melson, G.A. (ed.) Planium Press: New York; **1971**, p. 461.
11. Stilman, M.J. and Nyokong, T. *In Phthalocyanines, Properties and Applications*, Leznoff, C.C. and Lever, A.B.P. (eds.); VCH Publishers: New York; **1989**, Vol. 1, Chapter 3.
12. Lever, A.B.P. *Adv. Inorg. Radiochem* **1965**, *7*, 28.
13. Gouterman, M. *In The Porphyrin, Physical Chemistry*; Dolphin, D. (ed.); Academic Press: New York; 1978, Vol III, Part A. pp 1-10.
14. Fan, F.R. and Faulkner, L.R. *J. Am. Chem. Soc.* **1979**, *101*, 4779.
15. Nyokong, T.; Gasyna, Z. and Stilman, M.J. *Inorg. Chem.* **1987**, *26*, 548.
16. Cook M.J.; Dunn, A.J.; Howe, S.D.; Thomson, A.J. and Harrison, K.J. *J. Chem. Soc. Perkin Trans. 1* **1988**, 2453.

17. (a) Kobayashi, T. and Isoda, S. *J. Mater. Chem.* **1993**, 72, 3230. (b) Kobayashi, N.; Nakajima, S. and Osa, T. *Inorg. Chim. Acta* **1993**, 210, 131.
18. Li, R.; Zhang, X.; Zhu, P.; Ng, D.K.P.; Kobayashi, N. and Jiang, *J. Inorg. Chem.* **2006**, 45, 2327-2334.
19. Nevin, W.A.; Liu, W.; Greenberg, S.; Hempstead, M.R.; Maruccio, S.M.; Melnik, M.M.; Leznoff, C.C. and Lever, A.B.P. *Inorg. Chem.* **1987**, 26, 291.
20. Kasuga, K.; Tsutsui, M. *Coord. Chem. Rev.* **1980**, 32, 67.
21. Nensala, N.; Nyokong, T. *Polyhedron* **1996**, 15, 867.
22. Sielcken, O.T.E.; van Tilborg, M.M.; Rocks, M.F.M.; Hendricks, R.; Drenth, W. and Nolte, R.J.M. *J. Am. Chem. Soc.* **1987**, 109, 4261.
23. Piechocki, C.; Simon, J.; Skoulios, A.; Guillon, D.; Weber, P. *J. Am. Chem. Soc.* **1982**, 104, 5245.
24. (a) McKeown, N.B.; Chambrier, I. and Cook, M.J. *J. Chem. Soc. Perkin Trans 1*, **1990**, 1169. (b) Chambrier, I., Cook, M.J., and Wood, P.T., *Chem. Commun.* **2000**, 2133. (c) Hu, Y.; Shen, Y.; *J. Heterocyclic Chem.* **2002**, 39, 1071.
25. (a) Wohrle, D.; Schnurpfeil, G. and Knothe, G. *Dyes and pigments* **1992**, 18, 91 (b) Lutzen, A.; Starnes, S.D.; Rudkevich, D.M. and Rebeck Jr, J. *Tetrahedron Lett.* **2000**, 41, 3777.
26. Yiru, P.; Fenghua, H.; Zhipeng, L.; Naisheng, C. and Jinling, H. *Inorg. Chem. Commun.* **2004**, 7, 813.
27. Byrne, G.T.; Linstead, R.P. and Lowe, A.R. *J. Chem. Soc.* **1934**, 1017.
28. Elvidge, J.A. and Linstead, R.P. *J. Chem. Soc.* **1955**, 3536.
29. Brach, P.J.; Grammatica, S.J.; Ossanna, O.A. and Weinberger, L. *J. Heterocyclic Chem.* **1970**, 7, 1403.
30. Leznoff, C.C. and Hall, T.W. *Tetrahedron Lett.* **1982**, 23, 3023.
31. Maya, E.V.; Haisch, P.; Vazquez, P. and Torres, T. *Tetrahedron* **1998**, 54, 4397.
32. Thompson, J.A.; Murata, K.; Miller, D.C.; Stanton, J.L.; Broderick, W.E.; Hoffman, B.M. and Ibers, J.A. *Inorg. Chem.* **1993**, 32, 3546.
33. Wöhrle, D.; Eskes, M.; Shigehara, K. and Yamada, A. *Synthesis*, **1993**, 194.
34. McKeown, N.B.; Chambrier, I.; Cook, M.J. *J. Chem. Soc. Perkin Trans. 1* **1990**, 1169.

35. Vollman, H. In *Chemistry of Synthetic Dyes*; Venkataraman, K. (ed.); Academic Press: New York; 1971; pp. 283-311.
36. Uchida, H.; Tanaka, H.; Yoshima, H.; Reddy, P. Y.; Nakamura, S.; Toru, T. *Synlett* **2002**, 10, 1649.
37. Biyiklioglu, Z.; Kantekin, H.; Özil, M. *Journal of Organometallic Chemistry* **2007**, 692, 2436-2440.
38. Duggan, P.J.; Gordon, P.F. Eur. Pat. Appl. Ep 155780 (1985); *Chem. Abstr.* **1987**, 105, 70242r
39. Barret, P.A.; Bradbrook, E.F.; Dent, C.E.; Linstead, R.P.; *J. Chem. Soc.* **1939**, 1820.
40. Hedayatullah, M., *Compt. Rend. Acad. Sci. Ser. II Mec. Phys.* **1983**, 296, 621.
41. Leznoff, C.C.; Lever, A.B.P. *Phthalocyanines: Properties and Applications*; VCH: New York, 1989, Vol. 1, pp. 1-23.
42. Cook, M.J. *The Chemical Record* **2002**, 2, 225-236.
43. Marcuccio, S.M.; Svirskaya, P.I.; Greenberg, S.; Lever, A.B.P.; Leznoff, C.C. and Tomer, K.B. *Can. J. Chem.* **1985**, 63, 3057.
44. Wei, S.; Zhou, J.; Huang, D.; Wang, X.; Zhang, B.; Shen, J. *Dyes and Pigments* **2006**, 71, 61-67.
45. Negrinmovsky, V. M.; Derkacheva, V.M.; Luk'yanets, E.A.; Weitemeyer, A.; Wöhrle, D.; Schneider, G. *Phosphorus, Sulfur, Silicon* **1995**, 104, 161.
46. (a) Rusanova, J.; Pilkington, M. and Decurtins, S. *Chem. Commun.* **2002**, 2236-2237. (b) Mikhalenko, S.A.; Derkacheva, V.M. and Luk'yanets, E.A. *Russ. J. Gen. Chem.* **1981**, 51, 1405.
47. Cook M.J.; Dunn, A.J.; Howe, S.D.; Thomson, A.J. and Harrison, K.J. *J. Chem. Soc., Perkin Trans. 1* **1988**, 2453-2458.
48. Wallenfels, K.; Bachmann, G.; Hofmann, D. and Kern, R. *Tetrahedron* **1965**, 21, 2239.
49. Lee, C.; Ng, D.K.P.; *Tetrahedron Lett.* **2002**, 43, 4211.
50. Swart, J.C.; Langner, E.H.G.; Krokeide-Hove, N.; Cook, M.J. *J. Mater. Chem.* **2001**, 11, 434.

51. (a) McKeown, N.B.; Chambrier, I.; Cook, M.J. *J. Chem. Soc., Perkin Trans. I* **1990**, 1169. (b) Chambrier, I.; Cook, M.J.; Cracknell, S. T. and McMurdo, J. *J. Mater. Chem.* **1993**, *3*, 841-849
52. Oliver, S. W.; Smith, T.D.; *J. Chem. Soc., Perkin Trans. II* **1987**, 1579.
53. Gorbunova, Y.G.; Enakieva, Y.Y.; Sakharov, S.G. and Tsivadze, A.Y. *Russian Chemical Bulletin, International Edition, Vol. 53*, No. 1, pp. 74-79, January, **2004**
54. (a) Cammidge, A.N.; Berber, G.; Chambrier, I.; Hough, P.W. and Cook, M.J. *Tetrahedron* **2005**, *61*, 4067-4074. (b) Berber, G.; Cammidge, A.N.; Chambrier, I.; Cook, M.J.; Hough, P.W. *Tetrahedron Lett.* **2003**, *44*, 5527-5529.

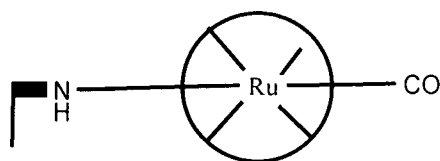
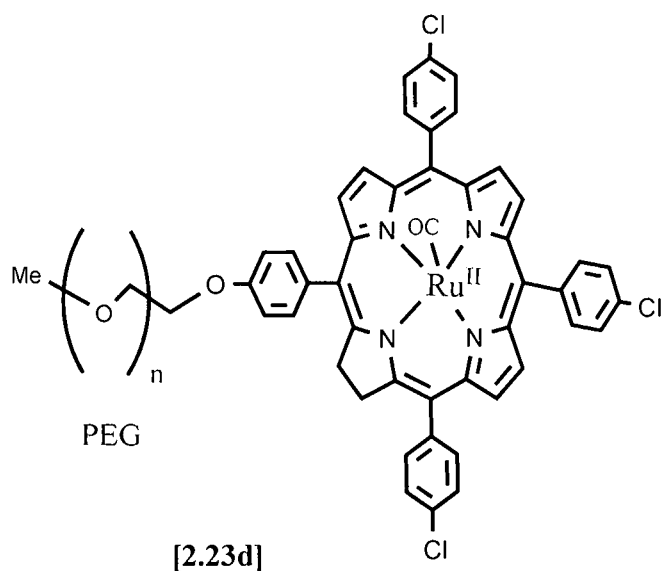
Chapter 4

Synthesis of alkyl-substituted ruthenium(II) phthalocyanine complexes

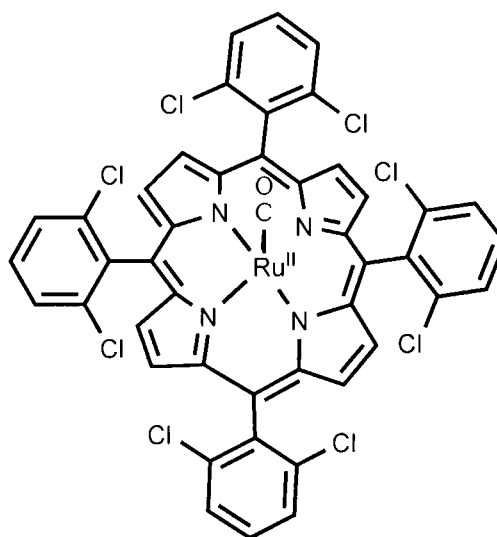
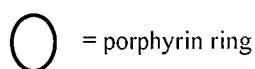
4.1 Introduction

Homogeneous epoxidation of alkenes with the ruthenium porphyrin-*N*-oxide system developed by Hirobe,¹ has received considerable attention from several groups like those of Berkessel,² Che³ and Gross⁴ during the past three decades. In most of these studies the objective has been to extend the scope of oxidizable substrate by catalyst variation and to obtain high turnover numbers and frequencies. Catalyst stability, the other main issue with porphyrin systems, has been enhanced by either synthesizing complexes with a range of halogenated substituents e.g. [4.1] or heterogenizing the complexes (e.g. [2.23d] and [2.22a]) through encapsulation or placing them on supports.³

While some Fe, Mn, and Co containing phthalocyanines have been studied as epoxidation catalysts,⁵ the poor solubility of these complexes in common organic solvents due to aggregation has limited success in the application of phthalocyanine catalysts in epoxidation reactions. Attachment of alkyl substituents to the non-peripheral positions of Pc complexes, however, result in those molecules adapting a 'saddle shaped' structure with the consequence of reduced aggregation and enhanced solubility in organic solvents.⁶⁻⁹ The improved solubility and associated reduced deactivation through aggregation served as impetus towards an investigation as to the application of ruthenium carbonyl phthalocyanine complexes as catalysts in the epoxidation of alkenes.

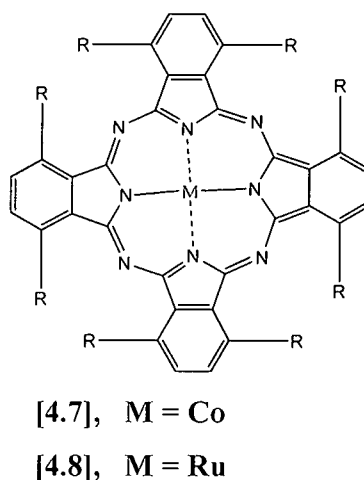
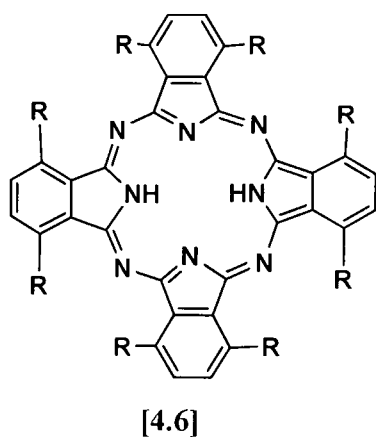


1. MCM-41: Por = 4-Cl-TPP
2. MCM-41 : Por = 2,6-Cl-TPP

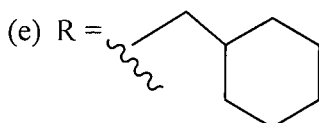


Since catalytic activity and selectivity for oxidation would largely depend on how the structure and electronics of the catalyst is influenced by the non-peripheral substituents, Pcs with a variety of alkyl substituents, i.e. hexyl, octyl, dodecyl, isopentyl, and 2-cyclohexylethyl, around the ring, were synthesized to be tested in epoxidation reactions (Scheme 4.1). Although the main focus of the study was directed at the evaluation of and thus synthesis of ruthenium phthalocyanines [4.8a-4.8e], one cobalt phthalocyanine [4.7b] was also synthesized. In order to be in a position to insert a metal of choice into

the Pc ring, all of the Pcs were prepared in the metal free form and the ruthenium inserted through reaction with $\text{Ru}_3(\text{CO})_{12}$ after formation of the ring system.



- (a) $\text{R} = \text{C}_6\text{H}_{13}$,
- (b) $\text{R} = \text{C}_8\text{H}_{17}$,
- (c) $\text{R} = \text{C}_{12}\text{H}_{25}$,
- (d) $\text{R} = \text{CH}_2\text{CH}_2\text{CH}(\text{CH}_3)_2$,



- (f) $\text{R} = \text{H}$

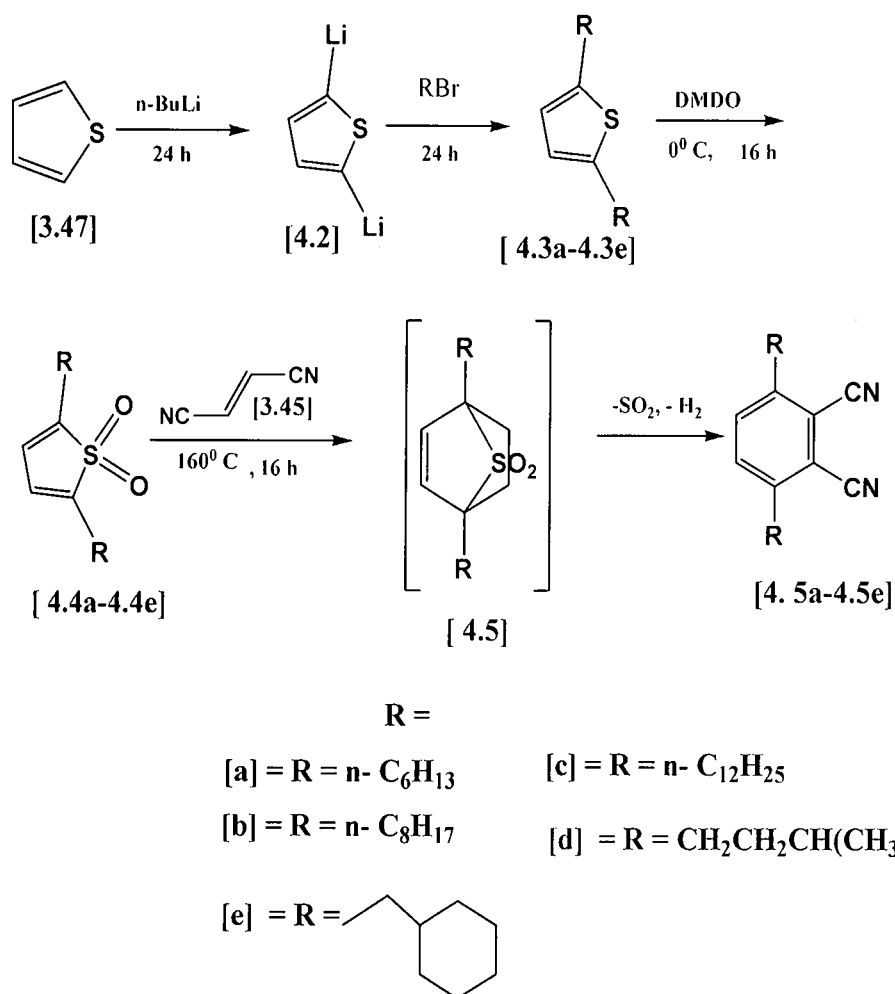
Scheme 4.1: Metallated phthalocyanine complexes.

4.2 Results and discussions

4.2.1 Synthesis and characterization

The metal free phthalocyanines [4.6a-4.6e] (*cf.* p 94) and metallated phthalocyanines [4.8a-4.8f] and [4.7b] for testing in epoxidation reactions were prepared according to the method described by Cook *et al.*⁶⁻⁸ The required 3,6-dialkylphthalonitriles [4.5a – 4.5e]

were therefore prepared by reaction of the thiophene dianion [4.2] with the appropriate alkylbromides [4.2a-4.2e] as shown in Scheme 4.2. Thus double deprotonation of thiophene [3.47] followed by reaction with 1-bromohexane [4.2a], 1-bromooctane [4.2b], 1-bromododecane [4.2c], 1-bromo-3-methylbutane [4.2d], and 1-bromo-2-cyclohexylethane [4.2e] respectively led to the formation of the dialkylthiophenes [4.3a-4.3e] in 70%, 60%, 76%, 84% and 69% yields, respectively after removal of unreacted 1-bromoalkanes by vacuum distillation. The ¹H-NMR spectra (Spectra 1, 3, 5, 7, 9) of compounds [4.3a-4.3e] clearly showed the presence of the thiophene ring protons as a singlet at δ 6.66, 6.59, 6.62, 5.59, 6.69 ppm, respectively, together with resonances for the expected aliphatic hydrogens at δ 0.88 – 2.81 ppm.



Scheme 4.2¹⁻⁴: Synthesis of 3,6-(dialkyl) phthalonitrile, [4.5a-4.5e].

^{13}C -NMR spectra (**Spectra** 2, 4, 6, 8, 10) of [4.3a-3e] further confirmed the presence of the alkyl groups by resonances at δ 31.94-14.22 ppm. A total of 6 signals for [4.3a], 8 signals for [4.3b], 12 signals for [4.3c], 4 signals for [4.3d] and 8 signals for [4.3e] were observed in the aliphatic region (δ 31.94-14.22 ppm) for the alkyl carbons, which are in agreement with the respective expected alkyl groups. Final confirmation of the structures of [4.3a – 3e] for the respective dialkylthiophenes came from IR spectra (**Plates** 1, 2, 3, 4, 5) where the stretching vibrations for the C-H and CH_3 are observed at $2955\text{-}2850\text{ cm}^{-1}$ (C-H) and $1447\text{-}597\text{ cm}^{-1}$ (CH_3).

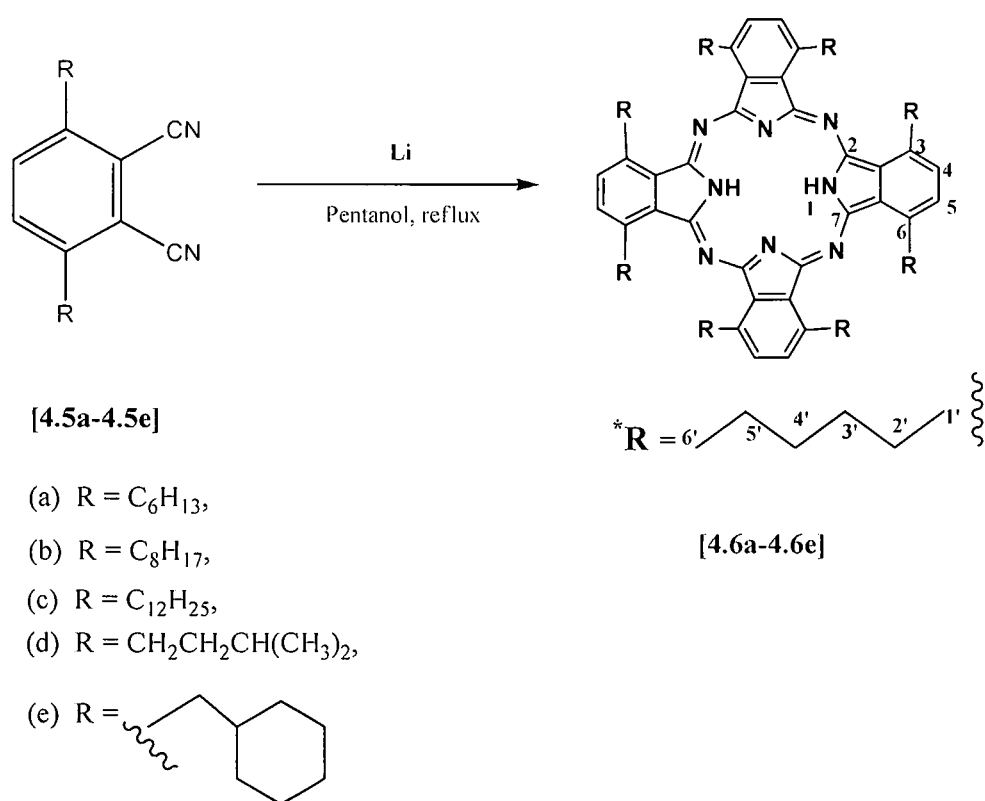
Since it was found by Chambrier and Cook⁶ that dialkylthiophenes are not suitable substrates for application of the Diels-Alder reaction for preparing the required 3,6-dialkyldinitriles (*cf.* paragraph 3.2.2.2), the heterocyclic sulphur of the thiophenes [4.3a-4.3e] were subjected to oxidation to the dialkylsulphones [4.4a-4.4e] by treatment with sodium perborate. Yields with this oxidant were, however, unacceptably low (17-12 %), which could be due to poor substrate solubility in the acetic acid solvent at low temperatures ($< 50\text{ }^\circ\text{C}$) and/or formation of polymeric products at reaction temperatures above $50\text{ }^\circ\text{C}$. In an effort to obtain better yields, it was decided to evaluate *m*-chloroperoxybenzoic acid (*m*-CPBA) as oxidant for this reaction. When dialkylthiophene [4.3b] was, however, subjected to oxidation with *m*-CPBA, only a marginal improvement in yield (to 22 %) could be achieved. In the end *in situ* prepared dimethyldioxirane (DMDO) proved to be the reagent of choice for this type of oxidation leading to sulphones [4.4a – 4.4e] being obtained in 48 to 70% yields.

The ^1H -NMR spectra (**Spectra** 11, 13, 15, 17 and 19) of all products [4.4a-4.4e] displayed an upfield shift in the resonances of the thiophenyl ring from δ 6.59 – 6.69 ppm (for the dialkylthiophene) to δ 5.57 – 5.62, thus confirming the presence of an oxidized S-atom in all of the structures. Additional confirmation of the presence of an SO_2 -group in all of the products [4.4a-4.4e] came from the IR spectra (**Plates** 6, 7, 8, 9, 10) where asymmetric and symmetric stretching frequencies for the SO_2 -groups were evident at $1291\text{-}1277\text{ cm}^{-1}$ and 1141 cm^{-1} respectively. Mass spectrometry of [4.4e] confirmed the

presence of the $[M+Na]^+$ ion at m/z 359.2196. The spectroscopic data for **[4.4a-4.4d]** are identical to those published.^{6,7}

Finally, the 3,6-dialkylphthalonitriles **[4.5a-4.5e]** were obtained by Diels-Alder reaction of the respective sulphones **[4.4a-4.4e]** with fumaronitrile **[3.45]** in a sealed tube at 150 °C leading to the desired products in 30.7-52% yields. The ¹H-NMR spectra (**Spectra** 21, 23, 25, 27 and 29) of **[4.5a-4.5e]** showed the aromatic protons as a single two-proton singlet resonance at δ 6.75-7.48 ppm due to the plane of symmetry present in the molecule, as well as the expected peaks from the different alkyl groups in the aliphatic region of the spectra. In the ¹³C-NMR spectra (**Spectra** 22, 24, 26, 28 and 30) of **[4.5a-4.5e]**, three aromatic resonances [δ 115.16(C-1), 133.47(C-2), 146.22(C-3); 115.16(C-1), 133.47(C-2), 146.22(C-3); 115.14(C-1), 133.42(C-2), 146.20(C-3); 115.08(C-1), 133.37(C-2), 146.43(C-3) 115.09(C-1), 133.37(C-2), 146.56(C-3) ppm] as well as one from the CN-groups in each molecule (δ 115.59, 115.59, 115.63, 115.64, and 115.59 ppm, respectively) were clearly visible in the aromatic region. These were accompanied by the expected carbon peaks from each alkyl group present in the molecule. The IR spectra (**Plates** 11, 12, 13, 14, 15) of **[4.5a-4.5e]** showed the distinctive aromatic nitrile absorption band at 2228-2225 cm^{-1} . Mass spectrometry of **[4.5e]** confirmed the presence of the $[M + Na]^+$ ion at m/z 371.2455. Spectroscopic data for **[4.5a-4.5d]** are consistent with those reported before.^{6,7}

The synthesis of the different metal-free phthalocyanines **[4.6a-4.6e]** were completed by cyclotramerisation of the 3,6-dialkylphthalonitrile precursors **[4.5a-4.5e]**, through treatment with lithium (metal) in refluxing pentanol or 1-butanol for 16 h (Scheme 4.3). After conventional work up, the green slurries were separated by column chromatography (silica gel, THF) and recrystallised from THF/methanol to afford green solids in low yields (10-14%). Although low, these yields are in the typical range for the preparation of non-peripherally alkyl substituted H₂Pcs.^{6,7}



Scheme 4.3: Synthesis of the metal-free Pcs [4.6a-4.6e]. *Numbering system for the Pc ring to be used throughout the discussion.

The ¹H-NMR spectra (Spectra 31, 32, 33, 35, 37, 39) of compounds [4.6a-4.6e] clearly indicated the formation of the envisaged Pcs by a dramatic downfield shift in the position of the benzylic protons^{6,7,8} (table 4.1), thus confirming products [4.6a-4.6e] to be the Pcs. This is attributed to the larger deshielding effect of the large Pc vs the benzene ring. The aromatic protons in all of these compounds appeared as a singlet [δ 7.89, 7.91, 7.77, 7.88, and 7.88] and were also deshielded relative to those in the phthalonitrile precursors [δ 7.48, 7.47, 6.77, 7.48, and 6.75]. The spectra of all of the Pcs also displayed the appropriate alkyl resonances in the aliphatic region of the spectra. Interestingly, the signals from the inner core NH-protons of compounds [4.6a-4.6c] appeared at δ -0.32, -0.29, and -0.32 ppm [each 2H, s, H-1(x2)] respectively, while those for compounds [4.6d-4.6e] could not be identified.

Table 4.1: Chemical shifts of benzylic protons in Pcs [4.6a-4.6e] vs those in phthalonitriles [4.5a-4.5e].

Phthalonitriles (1'-CH ₂)		Phthalocyanines (1'-CH ₂)	
Compound	Chemical shift (δ)	Compound	Chemical shift (δ)
[4.5a]	2.86 (4H, m)	[4.6a]	4.70 (16H, t)
[4.5b]	2.86 (4H, m)	[4.6b]	4.72 (16H, t)
[4.5c]	2.86 (4H, m)	[4.6c]	4.34 (16H, t)
[4.5d]	2.86 (4H, m)	[4.6d]	4.49 (16H, t)
[4.5e]	2.60 (4H, m)	[4.6e]	4.48 (16H, t)

In the aliphatic region of the ¹³C-NMR spectra (Spectra 32, 34, 36, 38, 40) of phthalocyanines [4.6a-4.6e], signals corresponding to the respective alkyl groups were identical to those of the phthalonitrile starting materials [4.5a-4.5e] and, if the symmetry properties of the compounds are taken into account, is in agreement with the proposed structures for the different Pcs. The aromatic region of the spectra, however, showed only two resonances [δ 138.60 and 130.39; 138.68 and 130.50; 138.56 and 130.34; 139.70 and 130.77; 139.14 and 130.57 ppm]. Such overlap of peaks in the aromatic region of the ¹³C-NMR spectra of non-peripherally high carbon number alkyl substituted Pcs was also observed by Liu *et al.*¹³

In the IR spectra (Plates 16, 17, 18, 19, 20) of compounds [4.6a-4.6e], the strong CN absorption bands at ~ 2225 cm⁻¹ in the spectra of the phthalonitriles [4.5a-4.5e], were replaced by a NH absorption band at *ca.* 3300 cm⁻¹. MALDI-TOF MS of [4.6a-4.6e] showed the expected peaks associated with the molecular ion at *m/z* 1186.91(M-H), 1411.16(M-H), 1860.67(M-H), 1074.791(M), 1396.04(M), thus confirming the structures of the prepared Pcs. UV/Vis spectra of phthalocyanines in solution are key indicators of their structure. Generally the UV/Vis spectrum of phthalocyanines is characterized by a strong absorption band at about 300-400 nm (UV region, B-band) and two very intense absorption bands at about 600-700 nm (visible region), the Q band.^{8,9} The UV/Vis spectra (Figure 4.1) of compounds [4.6a-4.6e] all exhibited the splitting of the absorption

Q-band into two components, typical of a non-metalated Pcs. The red shifts of the Q-band absorption peak maxima for the phthalocyanines are typical of non-peripheral octa-substituted metal free phthalocyanines.^{6,8,9}

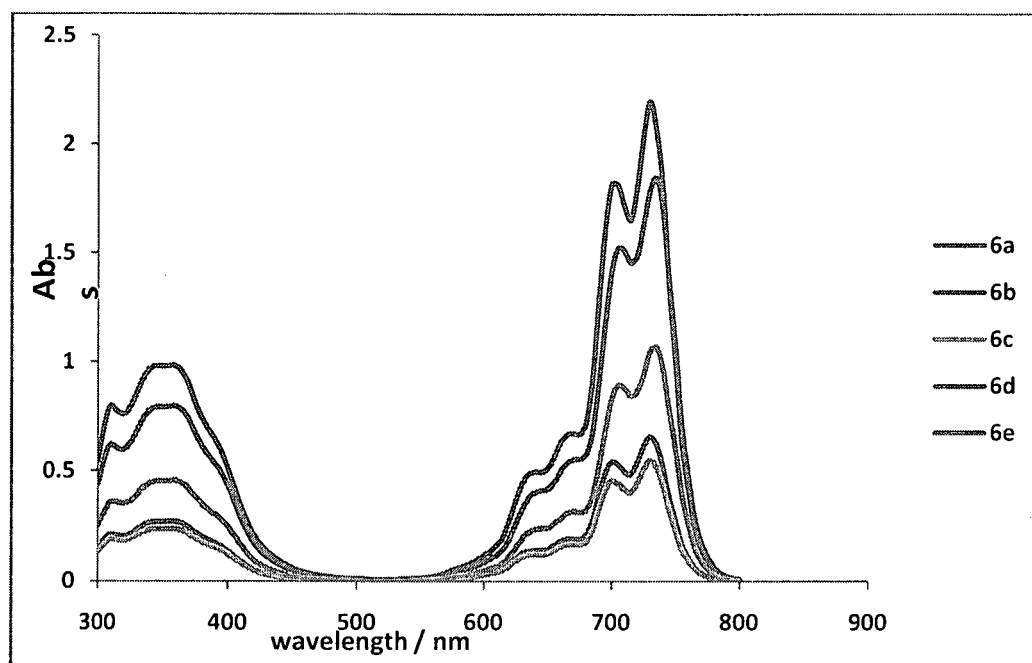
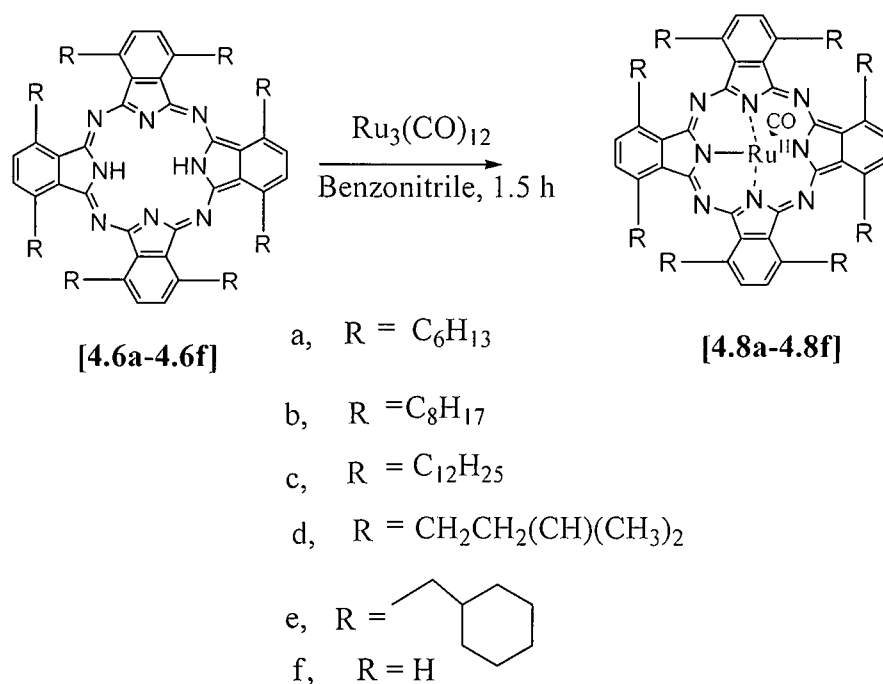


Figure 4.1: UV/Vis absorbance spectra of metal-free Pc [4.6a-4.6e] (Chloroform/r.t)

Since ruthenium porphyrin complexes were reported to be good catalysts in the epoxidation of alkenes (*cf.* paragraph 2.5.3), it was decided to insert ruthenium into the synthesized metal-free Pcs [4.6a-4.6e], as well as the commercially available unsubstituted Pc [4.6f], and start the investigation into the epoxidation properties of these metal phthalocyanine complexes.⁶⁻⁸

The synthesis of complexes [4.8a] and [4.8b] were initially attempted by metal insertion starting from [4.6a] and [4.6b], by reaction with $\text{RuCl}_3 \cdot 3\text{H}_2\text{O}$ in benzonitrile. Although these reaction mixtures were refluxed for a considerable time (~12 h), no product formation was observed after the addition of a large amount of cold methanol. Further attempts to obtain compounds [4.8a] and [4.8b] by the cyclotetramerization of [4.5a] and [4.5b] in the presence of the metal salt $\text{RuCl}_3 \cdot 3\text{H}_2\text{O}$ in quinoline according to the procedure of Gorbunova *et al.*^{14a} and Dudnik *et al.*,^{14b} gave traces of a blue compound

which could not be isolated. Utilization of the methodology developed by Cammidge *et al.*,¹⁰ i.e. refluxing the metal free Pc together with $\text{Ru}_3(\text{CO})_{12}$ in benzonitrile, eventually led to the formation of the desired ruthenium phthalocyanines **[4.8a-4.8f]** (Scheme 4.4). The reaction was stopped after 90 minutes to ensure that the diligated ruthenium species are not formed. Precipitating the products out of the benzonitrile solution by adding methanol proved to be a rather tedious process, even when large amounts of the methanol was added. So the pure products were obtained in 65-86 % yields by flash column chromatography followed by crystallization from methanol/petroleum ether.



Scheme 4.4: Preparation of ruthenium Pcs **[4.8a-4.8f]**.

Since the Q band in the UV-visible spectra of metal substituted phthalocyanines represent one of the characteristic properties of these compounds,¹⁻³ the prepared RuPcs **[4.8a-4.8f]** were analyzed with this technique first. The UV/Vis spectra (Figure 4.2) of compounds **[4.8a-4.8f]** exhibited a single Q-band [[**4.8a**] = 659 (0.51), [**4.8b**] = 675 (0.18), [**4.8c**] = 664.9 (0.38), [**4.8d**] = 665 (10), [**4.8e**] = 664 (0.5), [**4.8f**] = 635 (0.26)] of high intensity together with a blue shift (from *ca.* ~725 nm to 635-675 nm) indicative of a metal complex having been formed.¹⁰ The presence of the shoulder at the slightly lower

energy side of the Q-band is probably explicable in terms of some level of aggregation in the solution while the spectra were being recorded. The fact that the intensity of the shoulder increased at higher concentrations gave additional credence to this suggestion.

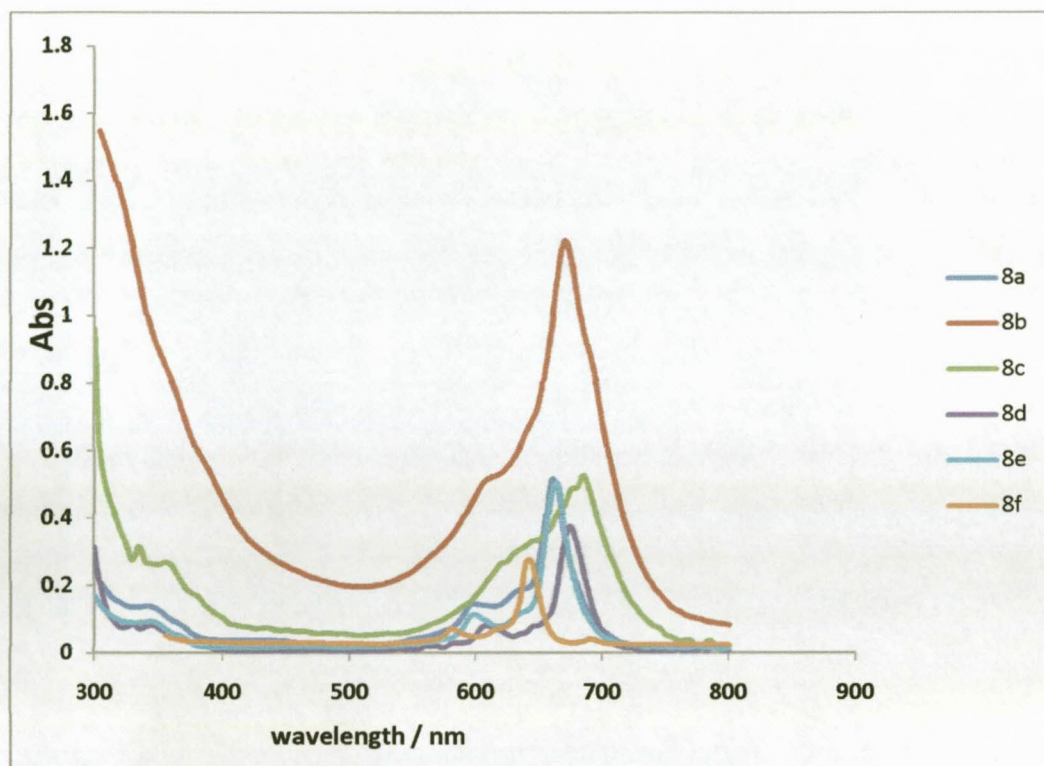


Figure 4.2: UV-Vis spectrum of compound [4.8a-4.8f].

The presence of an axial CO ligand in all of the prepared RuPc complexes [4.8a-4.8f] were confirmed by a strong absorption band at $1952-1965\text{ cm}^{-1}$ in the IR spectra (Plates 21, 22, 23, 24, 25, 26) of these compounds. Further evidence as to the presence of a metal inside the cavity of the phthalocyanine came from the absence of any N-H stretching vibrations at *ca.* 3300 in the IR spectra of all of the metal complexes.

The $^1\text{H-NMR}$ spectra (Spectra 41, 43, 45, 47, 49) of complexes [4.8a-4.8e] displayed all the expected proton signals and were almost identical to those of the metal-free Pcs [4.6a-4.6e], the only differences being the disappearance of the inner NH resonances (at δ -0.29 to -0.32 ppm in the spectra of the metal-free compounds) and a splitting of the

benzylic signals into two multiplets [δ 4.65-4.62 and 4.59-4.55 for **[4.8a]**; 4.65-4.60 and 4.57-4.52 for **[4.8b]**; 4.67-4.61 and 4.60-4.55 for **[4.8d]**; 4.65-4.61 and 4.60-4.56 for **[4.8e]**], except in the case of **[4.8c]**, indicating non-equivalence of these protons and thus two possible orientations for the alkyl substituents. The $^1\text{H-NMR}$ and $^{13}\text{C-NMR}$ spectra of complex **[4.8f]** could not be obtained because of its insolubility in common organic solvents. The spectroscopic data for **[4.8b]** are identical to that reported by Cammidge.¹⁰ The $^1\text{H-NMR}$ spectrum of **[4.8c]** is similar to those obtained by Buitendach¹⁸ for the equivalent Mn and Zn Pc complexes.

The presence of the CO ligand in the complexes was further confirmed by a CO resonance at δ 183.34, 180.25, 181.24, 174.77 and 183.32 for **[4.8a]**, **[4.8b]**, **[4.8c]**, **[4.8d]** and **[4.8e]**, respectively in the $^{13}\text{C-NMR}$ spectra. Contrary to the $^{13}\text{C-NMR}$ spectra of the metal free Pcs **[4.6a-4.6e]** where all the aromatic carbons were equivalent, these carbons in the ruthenium complexes **[4.8a-4.8e]** were visible as four separate signals at *ca.* δ 129-145 ppm.

The presence of ruthenium in the structures of complexes **[4.8a-4.8e]** were also confirmed by the isotope pattern found in the MALDI-TOF mass spectra (Plates 28, 29, 30, 31, 32, 33) where the spectra of **[4.8a]**, **[4.8b]** and **[4.8c]** showed a signal cluster for both the $[\text{M}]$ and $[\text{M} - \text{CO}]$ isotopes, whereas those of **[4.8d]** (Figure 4.3) **[4.8e]** and **[4.8f]** were represented by a cluster of isotope peaks at $[\text{M} - \text{CO}]$.

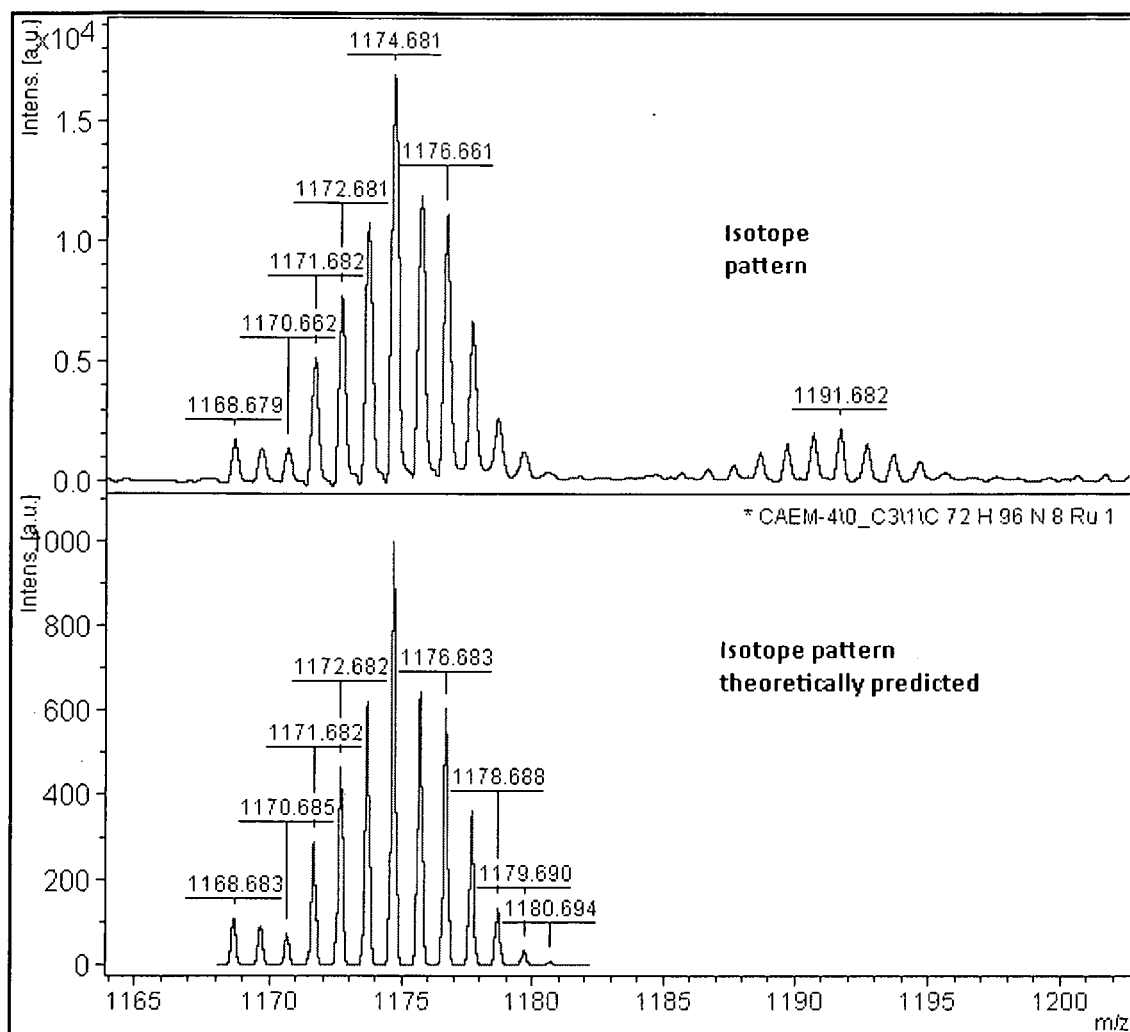


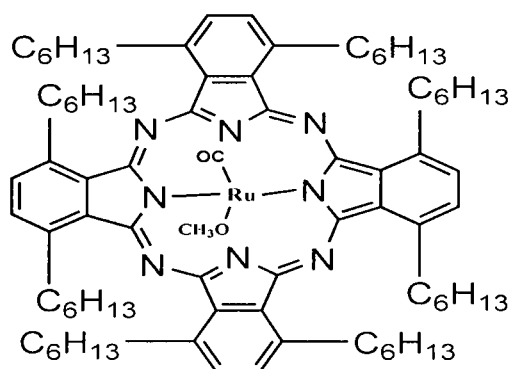
Figure 4.3: MALDI-TOF mass spectrum of [4.8d].

To further verify the composition and purity of compounds [4.8a], [4.8d], and [4.8e], elemental analysis were performed (Table 4.2). Generally a compound is considered to be pure if the determined composition of each element remains within a 0.5 % deviation of the calculated value. Compounds [4.8a] and [4.8e] are within this limit for hydrogen and nitrogen. The carbon content was found to be consistently lower than expected for compounds [4.8a], [4.8d] and [4.8e].

Table 4.2: Elemental analysis data for [4.8a], [4.8d] and [4.8e].

Comp.	Formula	Mol wt (g/mol)	Theoretical			Found			Difference		
			C (%)	H (%)	N (%)	C (%)	H (%)	N (%)	C (%)	H (%)	N (%)
[4.8a]	C ₈₁ H ₁₁₂ N ₈ ORu.	1314.87	73.99	8.59	8.52	71.84	8.72	8.16	2.15	0.2	0.36
[4.8d]	C ₇₃ H ₉₆ N ₈ ORu	1202.66	72.90	8.05	9.32	70.35	7.97	8.56	2.55	0.08	0.76
[4.8c]	C ₉₇ H ₁₂₈ N ₈ ORu	1523.18	76.49	8.47	7.36	74.07	8.26	7.10	2.42	0.21	0.26

Many phthalocyanines are difficult to combust and incomplete combustion may lead to erroneous determination of their elemental composition.¹⁵ Elemental compositions can furthermore be affected in several ways: the compound could contain foreign substances, unreacted material or solvent molecules being trapped within the crystal structure of the compound. Since our work-up involved methanol to precipitate the ruthenium complexes, it is possible that, as frequently observed, CH₃OH molecules could coordinate to the ruthenium vacant sites or get trapped within the complex [4.8g].^{16,8}

**[4.8g]**

Recalculating the composition together with 3 moles of CH₃OH (Table 4.3) explained the observed results with deviations within the allowed 0.5 % range.

Table 4.3: Elemental analysis data for [4.8a], [4.8d] and [4.8e].

Comp.	Formula	Mol wt (g/mol)	Theoretical			Found			Difference		
			C (%)	H (%)	N (%)	C (%)	H (%)	N (%)	C (%)	H (%)	N (%)
[4.8a]	C ₈₁ H ₁₁₂ N ₈ ORu 3CH ₃ OH	1410.04	71.49	8.86	7.94	71.84	8.72	8.16	0.35	0.14	0.22
[4.8d]	C ₇₃ H ₉₆ N ₈ ORu 3CH ₃ OH	1297.92	70.27	8.39	8.63	70.35	7.97	8.56	0.08	0.42	0.07
[4.8c]	C ₉₇ H ₁₂₈ N ₈ ORu 3CH ₃ OH	1618.17	74.16	8.72	6.92	74.07	8.26	7.10	0.09	0.46	0.18

Final proof of the structures of [4.8a], [4.8b], [4.8c] and [4.8d] came from the high resolution mass spectra (HRMS) (Plate 35, 36, 37, 38) of these compounds where [M⁺] (except in the case of [4.8c]) and [M⁺ + CH₃OH] (except in the case of [4.8d]) ions were found at *m/z* 1314.8062 and 1346.7935 for [4.8a], 1539.0474 and 1572.0377 for [4.8b], 2020.5658 for [4.8c] and 1202.6756 for [4.8d].

The cobalt Pc [4.7b] was prepared by the well established metal insertion of Co(II) into the metal free Pc macrocycle through reaction with cobalt chloride in refluxing pentanol (Scheme 4.5). After conventional work-up involving methanol, the compound was recrystallised from THF/methanol and obtained as a green amorphous solid in 12 % yield. The UV/Vis spectrum (Figure 4.4) showed intense Q and B bands at 705 nm and 329 nm respectively, typical of metallated phthalocyanines, thus indicating the presence of the cobalt. MALDI-TOF MS spectrum (Plate 34) exhibited the expected molecular peak of [M - CO] at *m/z* 614.338 with an isotopic pattern similar to the simulated one.

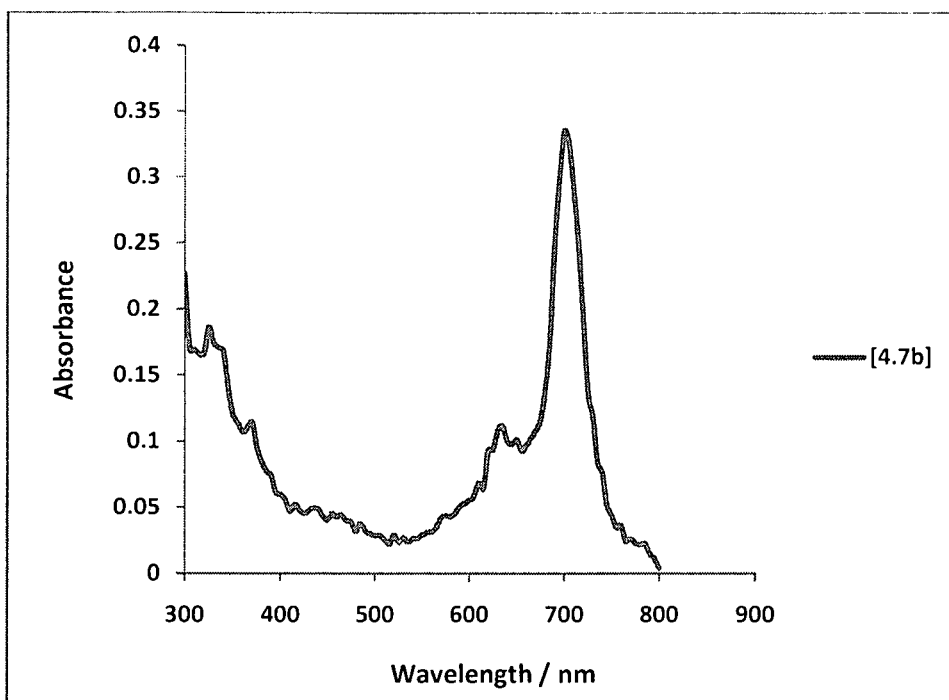
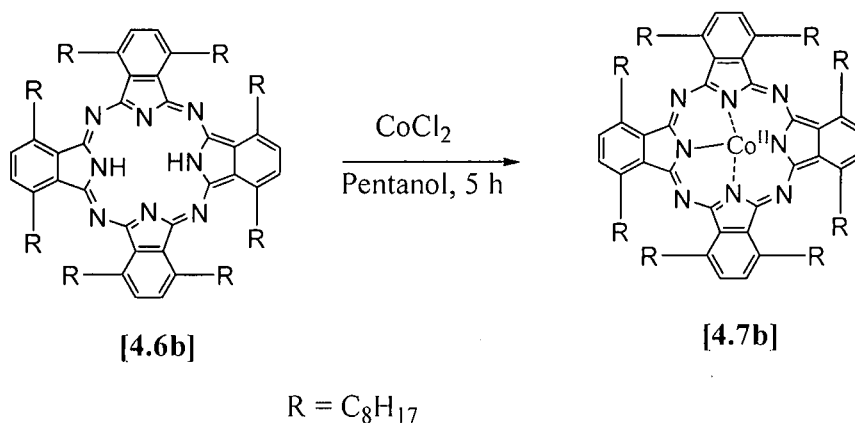


Figure 4.4: UV-Vis spectrum of compound [4.7b] in chloroform.

The $^1\text{H-NMR}$ spectrum (**Spectrum 51**) and $^{13}\text{C-NMR}$ spectrum (**spectrum 52**) of complex [4.7b] displayed all the expected proton and carbon signals, respectively, and was almost identical to those of the metal-free Pc [4.6b], the only differences being the disappearance of the inner NH resonances (at δ -0.29 ppm in the spectrum of [4.6b]). The IR spectrum (**Plate 27**) further confirmed that metallation had occurred as the NH absorption band at *ca.* 3300 cm^{-1} in [4.6b] is absent.



Scheme 4.5: Preparation of cobalt Pc [4.7b].

4.2.2 Conclusion

Sterically hindered RuPc complexes with non-peripheral hexyl- [4.8a], octyl- [4.8b], dodecyl- [4.8c], isopentyl [4.8d] and 2-cyclohexylethyl substituents [4.8e], the nonsubstituted MPc [4.8f] as well as the cobalt Pc, (1,4,8,11,15,18,22,25-octaoctylphthalocyaninato) cobalt(II) [4.7b] have been synthesized, albeit in low yields, and characterized by NMR, IR, UV, MS and elemental analysis. Compounds [4.8b] and [4.8f] had been previously reported in literature, while compounds [4.8a], [4.8c], [4.8d], [4.8e] and [4.7b], prepared by extending the procedure for [4.8b] to a range of ligands, are new compounds. For the first time, the MS isotope patterns of ruthenium phthalocyanines have been recorded. The formation of a huge amount of by-product alongside the metal-free Pcs [4.6a-4.6e] during cyclisation of the phthalonitriles [4.5a-4.5e] in refluxing pentanol largely account for the poor yields observed in this step. Improving on the yield of this step would be critical if these compounds are to be used as catalysts and this aspect will receive attention in a follow-up study.

Experimental Section

4.3 STANDARD EXPERIMENTAL TECHNIQUES

Unless otherwise stated, the following techniques were applied through the course of this study.

4.3.1 CHROMATOGRAPHIC TECHNIQUES

4.3.1.1 Thin layer chromatography (TLC)

TLC was performed on "Merck TLC-Aluminium plates (Silica Gel F₂₅₄, 0.2 mm layer)" divided into strips of *ca.* 2.5 x 5 cm. After development, the plates were dipped in a solution of permanganate and heated with a heat gun. *R_f* values are those observed in these qualitative TLC assessments.

4.3.1.2 Preparative scale thin layer chromatography (PLC)

PLC was conducted on glass plates (20 x 20 cm) coated with Kieselgel PF254 (1.0 mm), which were air-dried overnight at room temperature. Loaded with 10 - 15 mg of material per plate, the plates were developed in an appropriate eluent and dried in a stream of air. The bands were distinguished by UV (254nm) light and scraped off. Compounds were eluted from the adsorbent with acetone, which was then removed *in vacuo* at *ca.* 40 °C.

4.3.1.3 Flash column chromatography (FCC)

Flash column chromatography was performed in a glass column (3 cm diameter) charged with 100 g of Merck Kieselgel 60 (230-400 mesh) for every 1 g of the crude material. Air was displaced by elution with the appropriate solvent under N₂-pressure (*ca.* 40 kPa). The crude product was dissolved in a minimum of the appropriate solvent and applied to the column. The purified products were recovered by elution of 2 mL fractions under N₂-pressure with the appropriate solvent system. Clean fractions were then combined and evaporated under reduced pressure at 40 °C.

4.3.2 SPECTROSCOPICAL METHODS

4.3.2.1 Nuclear Magnetic Resonance spectroscopy (NMR)

NMR spectra were recorded on a Bruker AM 300 or a Bruker 600 FT-spectrometer at 296 K with tetramethylsilane (TMS) as internal standard. Unless specified to the contrary, deuteriochloroform (CDCl_3) was used as solvent. Chemical shifts are reported in parts per million (ppm) with the solvent residual peak at 7.26 ppm for proton spectra and 77.16 ppm for carbon spectra on the δ -scale, while coupling constants are measured in Hz. In the proton spectra, a chemical impurity resonating as a singlet at 1.56 ppm was identified in accordance to Gottlieb *et al.*¹⁹ as moisture. Extra peaks which can be ascribed to plate impurities were noticed in some cases between 1.5 and 0 ppm.

4.3.2.2 Infrared (IR)

IR-spectra were recorded neat with a Hitachi model 270-50 spectrophotometer.

4.3.2.3 Mass spectrometry (MS) and Microanalyses

Mass spectrometry was performed by means of electron impact (EI) ionization through direct injection onto the mass spectrometer of a Shimadzu GC-MS Qp-2010 gas chromatograph-mass spectrometer.

MALDI-TOF spectra were collected by a Bruker Microflex LRF20 in the positive mode with the minimum laser power required to observe signals.

High resolution MS were performed by Cambridge University Chemical Laboratory. Elemental analyses were performed by the Canadian Microanalytical Service.

4.3.2.4 UV-Vis

UV-visible spectra were obtained on a Varian 50 Conc UV-Visible Spectrophotometer.

4.3.3 MELTING POINTS

Melting points were recorded on a Barloworld Scientific Stuart Melting Point (SMP3) apparatus.

4.3.4 ANHYDROUS SOLVENTS AND REAGENTS

THF and toluene were predried with sodium metal, refluxed over sodium/ benzophenone under Ar until a dark blue colour persisted and freshly distilled under Ar prior to use.

Acetonitrile was left over 4 Å molecular sieves and was refluxed under Ar for 48 hours with subsequent distillation under Ar prior to use.

DCM was dried by refluxing over CaH_2 for 12 hours under Ar with subsequent fresh distillation prior to use.

All chemical reagents were obtained from Aldrich, Fluka or Merck and used without further purification. Solvents were HPLC grade or better and not specifically dried unless stated. Room temperature refers to *ca.* 20-25 °C.

4.4 ABBREVIATIONS

The following abbreviations were used throughout the experimental section:

4.4.1 Abbreviations for ^1H NMR signal multiplicities

s = singlet

dd = doublet of doublet

d = doublet

br = broadened

t = triplet

m = multiplet

4.4.2 Solvent abbreviations

Et_2O = diethyl ether

THF = tetrahydrofuran

DCM = dichloromethane

EtOH = ethanol

EtOAc = ethyl acetate

H = hexane

A = acetone

DMF = Dimethylformamide

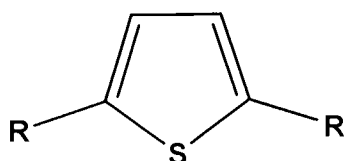
4.4.3 Chemical abbreviations

NaHCO_3 = sodium bicarbonate	KOH = potassium hydroxide
Na_2SO_4 = sodium sulphate	HCl = hydrochloric acid
n-BuLi = <i>n</i> -butyllithium	Ar = argon
N_2 = nitrogen (gas)	NaOH = sodium hydroxide

4.5 CHEMICAL METHODS

By varying the alkyl groups (-R) on the thiophene, phthalonitriles with carbon sidechains of different lengths were synthesized. From these the corresponding metal free and ruthenium complexed phthalocyanines were prepared.

Preparation of 2, 5-dialkylthiophenes compounds [4.3a-4.3e].



[4.3a-4.3e]

a, R = C₆H₁₃ c, R = C₁₂H₂₅ e = C₈H₁₅

b, R = C₈H₁₇ d, R = C₅H₁₁

Compounds [4.3a-4.3e] were synthesized according to procedures published by Cook *et al.*^{6,7} and Swarts *et al.*⁸

General Procedure A.

In a typical experiment, thiophene (3.47) (9 g, 0.107 mol) in dry THF (50 cm³) was treated with *n*-butyllithium in hexane (2.5M, 107 cm³, 0.267 mol, 2.5 eq.) at -78 °C in an argon atmosphere. The solution was allowed to warm to room temperature and stirred for 24 hours. The reaction was cooled again to -78 °C and alkylhalide (2.5 eq.) was added drop wise over 30 minutes. The mixture was then poured into iced water (500 cm³) and extracted into diethyl ether (3x 150 cm³). The combined organic layers were washed with brine (100 cm³) dried over magnesium sulfate, filtered and concentrated under reduced pressure to give the 2,5-dialkylthiophene as a pale yellow oil which was used without further purification.

2,5-Dihexylthiophene, [4.3a].^{6,7}

Using general procedure A: thiophene (**3.47**) (9 g, 0.107 mol), dry THF (50 cm³), *n*-butyllithium in hexane (2.5 M, 107 cm³, 0.267 mol, 2.5 eq), 1-bromohexane (40.3 g, 0.267 mol, 2.5 eq.) gave 2,5-dihexylthiophene [**4.3a**] (19 g, 70%) as a pale yellow oil: δ_{H} (300 MHz; C₆D₆, *Spectrum 1*) 6.66 (2H, s, H-3,4), 2.77 (4H, t, *J* 7.6 Hz, H-1',H-1''), 1.73 – 1.65 (4H, m, H-2',H-2''), 1.41-1.32 (12H, m, H-3',4',5', H-3'',4'',5''), 0.96 (6H, t, *J* 6.7 Hz, H-6', H-6''); δ_{C} (150.9 MHz; CDCl₃, *Spectrum 2*) 143.25, 123.33, 31.80, 31.74, 30.29, 28.96, 22.71, 14.15; IR $\nu_{\text{max}}/\text{cm}^{-1}$ (neat) (**plate 1**) 2956, 2925, 2854 (CH), 1458, 1378, 1232, 1027, 794, 724, 690 (CH₃).

2,5-Dioctylthiophene [4.3b].^{6,7}

Using general procedure A: thiophene [**3.47**] (9 g, 0.107 mol), dry THF (50 cm³), *n*-butyllithium in hexane (2.5 M, 107 cm³, 0.267 mol, 2.5 eq), 1-bromooctane (51.6 g, 0.267 mol, 2.5 eq.) gave 2,5-dioctylthiophene [**4.3b**] (20 g, 60%) as a pale yellow oil: δ_{H} (600 MHz, CDCl₃, *Spectrum 3*) 6.59 (2H, s, H-3, H-4), 2.77 (4H, t, *J* 7.7 Hz, H-1', H-1''), 1.69 – 1.67 (4H, m, H-2', H-2''), 1.40-1.31 (20H, m, H-(3'-H7'), H-(3''-H7'')), 0.92 (6H, t, *J* 6.9 Hz, H-8', H-8''); δ_{C} (150.9 MHz, CDCl₃, *Spectrum 4*) 143.27, 123.28, 31.94, 31.78, 30.23, 29.42, 29.30, 29.23, 22.73, 14.13; IR $\nu_{\text{max}}/\text{cm}^{-1}$ (neat) (**plate 2**) 2955, 2923, 2853 (CH), 1462, 1377, 793, 722, 690 (CH₃).

2,5-Didodecylthiophene, [4.3c].^{8,9}

Using general procedure A: thiophene [**3.47**] (9 g, 0.107 mol), dry THF (50 cm³), *n*-butyllithium in hexane (2.5 M, 107 cm³, 0.267 mol, 2.5 eq), 1-bromododecane (66.54 g, 0.267 mol, 2.5 eq.) gave 2,5-didodecylthiophene [**4.3c**] (34 g, 76%) as a pale yellow oil: δ_{H} (300 MHz, C₆D₆, *Spectrum 5*) 6.62 (2H, s, H-3, H-4), 2.77 (4H, t, *J* 7.5 Hz, H-1', H-1''), 1.71-1.69 (4H, m, H-2', H-2''), 1.37 (36H, s, H-(3'-H11'), H-(3''-H11'')), 1.02 (6H, t, *J* 6.79 Hz, H-12', H-12''); δ_{C} (150.9 MHz, CDCl₃, *Spectrum 6*) 143.21, 123.30, 32.10, 31.87, 30.31, 30.25, 29.86, 29.83, 29.75, 29.57, 29.54, 29.33, 22.85, 14.22; IR $\nu_{\text{max}}/\text{cm}^{-1}$ (neat) (**plate 3**) 2922, 2852 (CH), 1466, 1377, 794, 721 (CH₃).

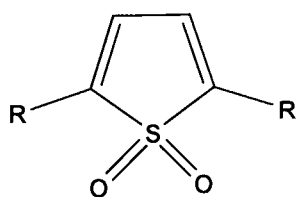
2,5-Diisopentylthiophene, [4.3d].

Using general procedure A: thiophene [3.47] (9 g, 0.107 mol), dry THF (50 cm³), n-butyllithium in hexane (2.5 M, 107 cm³, 0.267 mol, 2.5 eq), isopentylbromide (36.6 g, 0.267 mol, 2.5 eq.) gave 2,5-diiisopentylthiophene [4.3d] (20 g, 84 %) as a pale yellow oil: δ_{H} (300 MHz, C₆D₆, *Spectrum 7*) 5.59 (2H, s, H-3, 4), 2.42 (4H, t, *J* 7.41 Hz, H-1', H-1''), 1.51 – 1.40 (6H, m, H-2', 2'', H-3', 3''), 0.85 (12H, d, *J* 6.2 Hz, H-4', 5', H-4'', 5''); δ_{C} (150.9 MHz, CDCl₃, *Spectrum 8*) 144.13, 121.55, 35.36, 27.66, 22.24, 22.16; IR $\nu_{\text{max}}/\text{cm}^{-1}$ (neat) (**plate 4**) 2955, 2929, 2869, 2851 (CH), 1467, 1384, 1366, 1169, 1027, 794, 761, 597 (CH₃).

2,5-Di(2-cyclohexylethyl)thiophene, (3e).

Using general procedure A: thiophene [3.47] (9 g, 0.107 mol), dry THF (50 cm³), n-butyllithium in hexane (2.5 M, 107 cm³, 0.267 mol, 2.5 eq), 2-cyclohexylethylbromide (51 g, 0.267 mol, 2.5 eq.) gave 2,5-di(2-cyclohexylethyl)thiophene [4.3e] (22.5 g, 69%) as a pale yellow oil: δ_{H} (600 MHz, C₆D₆, *Spectrum 9*) 6.69 (2H, s, H-3,4), 2.81 (4H, t, *J* 7.94 Hz, H-1', H-1''), 1.74-1.69 (10H, m, H-3',4',8', H-3'',4'',8'') 1.67-1.63 (4H, m, H-2', H-2''), 1.27-1.19 (8H, m, H-5',7', H-5'',7'') 0.95-0.88 (4H, m, H-6', H-6''); δ_{C} (150.9 MHz, CDCl₃, *Spectrum 10*) 143.44, 123.30, 39.68, 37.38, 33.46-33.44, 27.78, 26.95, 26.93, 26.58; IR $\nu_{\text{max}}/\text{cm}^{-1}$ (neat) (**plate 5**) 2910, 2850 (CH), 1447, 1346, 1261, 1078, 1025, 962, 889, 843, 797, 689(CH₃); *m/z* (EI) 304 (M⁺, 65%), 126 (C₉H₁₈, 100%); HR MS: C₂₀H₃₂S(M + H⁺) requires 305.2303, found 305.2307.

Preparation of 2,5-dialkylthiophene 1,1-dioxides, [4.4a-4.4e]



[4.4a-4.4e]

a, R = C₆H₁₃ c, R = C₁₂H₂₅ e = C₈H₁₅
b, R = C₈H₁₇ d, R = C₅H₁₁

Method 1: Sodium perborate

General Procedure B.

To a stirred mixture of 2,5-dialkylthiophene (0.07 mol) in glacial acetic (350 cm³) was added solid NaBO₃·4H₂O (48.90 g, 0.49 mol, 7 eq.) over *ca.* 5 min with care being taken to maintain the internal temperature between 48 and 52⁰C. The reaction mixture was then stirred at 50⁰C for another 5 h. before it was left at room temperature for 16 h. The acetic acid was removed under reduced pressure and the solid residue stirred in H₂O (100 cm³) and filtered. The remaining solid was extracted with diethyl ether (100 cm³) and the organic solution washed with H₂O (100 cm³) and brine (100 cm³) before it was dried (MgSO₄). Removal of the solvent and recrystallisation of the waxy residue with absolute ethanol gave the 2,5-dialkylthiophene 1,1-dioxide.

Method 2: *m*-Chloroperoxybenzoic acid

General Procedure C.

A solution of 2,5-dialkylthiophene (3c) (0.015 mol) in dichloromethane (190 cm³) was stirred with *m*-chlorobenzoic acid (50-60% tech. grade, 9.38 g, 0.022 mol, 1.5 eq.) at 0°C in the presence of an excess of NaHCO₃ (37.5 g, 0.058 mol). The heterogeneous mixture was allowed to stand for 16 h at 5°C before the precipitate was filtered off and washed with dichloromethane (2 x 100 cm³). The combined organic phases were subsequently washed with 20% aqueous NaOH (2 x 100 cm³), water (2 x 100 cm³) and dried over MgSO₄ to give, after solvent removal and recrystallisation of the waxy residue from warm ethanol, the 2,5-dialkylthiophene 1,1-dioxide.

Method 3: Dimethyldioxirane

General Procedure D.

A mixture of H₂O (330 cm³), acetone (240 cm³) and NaHCO₃ (180 g, 2.14 mol) was added to a solution of 2,5-dialkylthiophene (0.015 mol) in dichloromethane (270 cm³) in a 3 litre 2-necked flask equipped with an efficient stirrer and a large CO₂ / acetone condenser. The resulting heterogeneous mixture was cooled in an ice bath before solid oxone (300 g, 1.97 mol, 131.4 eq.) was carefully added over 30 minutes with efficient stirring. Stirring continued for a further 16 hours at room temperature before water (1,500 cm³) was added to dissolve most inorganics. The decanted aqueous layer, and all remaining solids were extracted with dichloromethane (750 cm³), the combined organic phases washed with water (1,500 cm³) and dried with magnesium sulfate before solvent removal and recrystallisation of the residue from ethanol gave the 2,5-dialkylthiophene-1,1-dioxide.

2,5-Dihexylthiophene 1,1-dioxide, [4.4a]

Using general procedure D: 2,5-dihexylthiophene [4.3a] (3.8 g, 0.015 mol), DCM (270 cm³), H₂O (330 cm³), acetone (240 cm³), NaHCO₃ (180 g, 2.14 mol), oxone (300 g, 1.97 mol, 131.4 eq.) gave 2,5-dihexylthiophene 1,1-dioxide [4.4a] (2.4 g, 56.3%) as off white needles: m.p. 45.4 °C (Lit.⁶ mp 43-44 °C); δ_H (600 MHz, C₆D₆, *Spectrum 11*) 5.57 (2H, s, H-3,4), 2.39 (4H, t, *J* 7.7 Hz, H-1',1''), 1.54-1.52 (4H, m, H-2',2''), 1.30- 1.29 (4H, m, H-3',3''), 1.21-1.19 (8H, m, H-4',4'', H-5',5''), 0.95 (6H, t, *J* 7.3 Hz, H-6',6''); δ_C (150.9 MHz, CDCl₃, *Spectrum 12*) 143.95, 121.68, 31.37, 28.76, 26.54, 24.28, 22.48, 14.00; IR ν_{max}/cm⁻¹ (neat) (**plate 6**) 2954, 2925, 2872, 2857, 1469, 1431, 1278 (-SO₂), 1141 (-SO₂), 1114, 1027, 890, 842, 770, 723, 629, 579, 554.

2,5-Dioctylthiophene 1,1-dioxide, [4.4b]

Using general procedure B: 2,5-dioctylthiophene [4.3b] (21.56 g, 0.07 mol), glacial acetic (350 cm³), NaBO₃·4H₂O (48.90 g, 0.49 mol, 7 eq.) gave 2,5-dioctylthiophene 1,1-dioxide [4.4b] (3 g, 12.6%) as off white needles : m.p. 56 °C. (Lit.⁶ mp 52-53 °C); δ_H (300 MHz, C₆D₆, *Spectrum 13*) 5.62 (2H, s, H-3,4), 2.41 (4H, t, *J* 7.6 Hz, H-1',1''), 1.58-1.54 (4H, m, H-2',2''), 1.30-1.24 (20H, m, H-(3'-7'), H-(3''-7'')), 1.01 (6H, t, *J* 6.9 Hz, H-8',8''); δ_C (150.9MHz, CDCl₃, *Spectrum 14*) 143.98, 121.65, 31.79, 29.16, 29.12, 26.59, 24.28, 22.62, 14.07; IR ν_{max}/cm⁻¹ (neat) (**plate 7**) 2953, 2918, 2853, 1470, 1281 (-SO₂), 1142 (-SO₂), 1119, 1095, 869, 837, 770, 720, 629, 579, 569.

2,5-Didodecylthiophene 1,1-dioxide, [4.4c].^{8,9}

Using general procedure C: 2,5-didodecylthiophene [4.3c] (6.31 g, 0.015 mol) DCM (190 cm³), *m*-chloroperoxybenzoic acid (50-60% tech. grade, 9.38 g, 0.022 mol, 1.5 eq.), NaHCO₃ (37.5 g, 0.058 mol) gave 2,5-didodecylthiophene 1,1-dioxide [4.4c] (2.5 g, 36.8%) as off white needles: m.p. 72 °C (Lit.⁸ mp 73 °C); δ_H (600 MHz, C₆D₆, *Spectrum 15*) 5.59 (2H, s, H-3,4), 2.42 (4H, t, *J* 7.6 Hz, H-1',1''), 1.59-1.56 (4H, m, H-2',2''), 1.41 - 1.26 (36H, m, H-(3'-11'), H-(3''-11'')), 1.03 (6H, t, *J* 6.7 Hz, H-12',12''); δ_C (150.9 MHz, CDCl₃, *Spectrum 16*) 143.97, 121.65, 31.91, 29.62, 29.59, 29.54, 29.48,

29.34, 29.21, 29.12, 26.59, 24.28, 22.68, 14.10; IR $\nu_{\max}/\text{cm}^{-1}$ (neat) (**plate 8**) 2954, 2916, 2850, 1470, 1432, 1284 (-SO₂), 1137 (-SO₂), 1094, 851, 828, 770, 729, 619, 571.

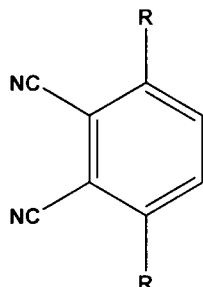
2,5-Diisopentylthiophene 1,1-dioxide, [4.4d].

Using general procedure D: 2,5-diisopentylthiophene [4.3d] (3.4 g, 0.015 mol), DCM (270 cm³), H₂O (330 cm³), acetone (240 cm³), NaHCO₃ (180 g, 2.14 mol), oxone (300 g, 1.97 mol, 131.4 eq.) gave 2,5-diisopentylthiophene 1,1-dioxide [4.4d] (1.87 g, 48.75%) as off white needles m.p. 56.5^oC; δ_{H} (300 MHz, C₆D₆, **Spectrum 17**) 5.59 (2H, s, H-3,4), 2.42 (4H, t, *J* 7.41 Hz, H-1',1''), 1.53-1.40 (6H, m, H-2',3', H-2'',3''), 0.85 (12H, d, *J* 6.2 Hz, H-4',5', H-4'',5''); δ_{C} (150.9 MHz, CDCl₃, **Spectrum 18**) 144.13, 121.55, 35.36, 27.66, 22.24-22.16 22.16; IR $\nu_{\max}/\text{cm}^{-1}$ (neat) (**plate 9**) 2957, 2928, 2869, 1470, 1434, 1385, 1367, 1277 (-SO₂), 1213, 1141 (-SO₂), 1119, 1030, 830, 754, 628, 576, 558.

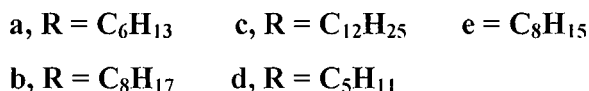
2,5-Di(2-cyclohexylethyl)thiophene 1,1-dioxide, [4.4e].

Using general procedure D: 2,5-di(2-cyclohexylethyl)thiophene [4.3e] (4.57 g, 0.015 mol), DCM (270 cm³), H₂O (330 cm³), acetone (240 cm³), NaHCO₃ (180 g, 2.14 mol), oxone (300 g, 1.97 mol, 131.4 eq.) gave 2,5-di(2-cyclohexylethyl)thiophene 1,1-dioxide [4.4e] (3.5 g, 69.5%) as off white needles: m.p. 111^oC; δ_{H} (600 MHz, C₆D₆, **Spectrum 19**) 5.58 (2H, s, H-3,4), 2.44 (4H, t, *J* 7.95 Hz, H-1',1''), 1.72-1.62 (10H, m, H-3',4',8', H-3'',4'',8''), 1.24-1.11 (8H, m, H-5',7', H-5'',7''), 0.85-0.79 (4H, m, H-6',6''); δ_{C} (150.9 MHz, CDCl₃, **Spectrum 20**) 144.32, 121.47, 37.20, 33.95, 33.00, 26.51, 26.19, 21.69; IR $\nu_{\max}/\text{cm}^{-1}$ (neat) (**plate 10**) 2957, 2918, 2850, 1469, 1445, 1385, 1367, 1277(-SO₂), 1139 (-SO₂), 1118, 1097, 841, 627, 610, 558; *m/z* (EI) 336.30 (M⁺, 33.42%), 185.15 (100%); C₂₀H₃₂O₂S(M + Na⁺) requires 359.2021, found 359.2196.

Preparation of 3, 6-dialkylphthalonitriles, [4.5a-4.5e].



[4.5a-4.5e]



General Procedure E.

In a typical experiment, 2,5-dialkylthiophene 1,1-dioxide (0.015 mol) and fumaronitrile (1.14 g, 0.015 mol, 1 eq.) in chloroform (1 cm³) were heated in a sealed tube at 150 °C for 18 hr. The contents of the tube were dissolved in chloroform and the solvent removed under reduced pressure at 90°C until the residue stopped liberating bubbles. The dark residue was then purified by column chromatography over silica gel with toluene as eluent to give the 3,6-dialkylphthalonitrile.

3,6-Dihexylphthalonitrile, [4.5a].⁶

Using general procedure E: 2,5-dihexylthiophene 1,1-dioxide [4.4a] (4.3 g, 0.015 mol), fumaronitrile (1.14 g, 0.015 mol, 1 eq.), chloroform (1 cm³) gave 3,6-dihexylphthalonitrile [4.5a] (1.4 g, 30.7%) as off white needles: m.p. 40 °C. (Lit.⁶ mp 38 °C); R_f(toluene) = 0.82; δ_H (600 MHz, CDCl₃, *Spectrum 21*) 7.48 (2H, s, H-4,5), 2.86 (4H, t, *J* 7.86 Hz, H-1',1''), 1.68-1.64 (4H, m, H-2',2''), 1.33-1.28 (12H, m, H-(3'-5'), H-(3''-5'')), 0.89 (6H, t, *J* 7.07 Hz, H-6',6''); δ_C (150.9 MHz, CDCl₃, *Spectrum 22*) 146.22 133.47, 115.59, 115.16, 34.40, 31.44, 30.66, 28.81, 22.48, 13.99; IR ν_{max}/cm⁻¹

(neat) (**plate 11**) 2954, 2924, 2854, 2228 (C≡N), 1464, 1375, 1284, 1231, 1170, 1115, 850, 722, 648.

3,6-Dioctylphthalonitrile, [4.5b].⁶

Using general procedure E: 2,5-dioctylthiophene 1,1-dioxide [4.4b] (5.0 g, 0.015 mol), fumaronitrile (1.14 g, 0.015 mol, 1 eq.), chloroform (1 cm³) gave 3,6-dioctylphthalonitrile [4.5b] (2.5 g, 40%) as off white needles m.p. 60.4 °C (Lit.⁶ mp. 59 °C); R_f(toluene) = 0.8; δ_H (600 MHz, CDCl₃, *Spectrum 23*) 7.47 (2H, s, H-4,5), 2.86 (4H, t, *J* 7.83 Hz, H-1',1''), 1.69-1.64 (4H, m, H-2',2''), 1.32-1.28 (20H, m, H-(3'-7'), H-(3''-7'')), 0.89 (6H, t, *J* 7.0 Hz, H-8',8''); δ_C (150.9 MHz, CDCl₃, *Spectrum 24*) 146.22, 133.47, 115.59, 115.16, 34.41, 31.78, 30.70, 29.24, 29.15, 29.12, 22.62, 14.06; IR ν_{max}/cm⁻¹ (neat) (**plate 12**) 2920, 2853, 2227(C≡N), 1463, 882, 851, 721.

3,6-Didodecylphthalonitrile, [4.5c].⁸

Using general procedure E: 2,5-Didodecylthiophene 1,1-dioxide [4.4c] (6.8 g, 0.015 mol), fumaronitrile (1.14 g, 0.015 mol, 1 eq.), chloroform (1 cm³) gave 3,6-Didodecylphthalonitrile [4.5c] (3.3 g, 48%) as off white needles : m.p. 78-80 °C. (Lit.⁸ mp 82 °C); R_f(toluene) = 0.82; δ_H (300 MHz, C₆D₆, *Spectrum 25*) 6.77 (2H, s, H-4,5), 2.60 (4H, t, *J* 7.74 Hz, H-1',1''), 1.51-1.33 (40H, m, H-(2'-11'), H-(2''-11'')), 1.04 (6H, t, *J* 6.0 Hz, H-12',12''); δ_C (150.9 MHz, CDCl₃, *Spectrum 26*) 146.20, 133.42, 115.63, 115.14, 34.41, 31.91, 30.71, 29.64, 29.62, 29.59, 29.48, 29.34, 29.30, 29.17, 22.68, 14.10; IR ν_{max}/cm⁻¹ (neat) (**plate 13**) 2954, 2915, 2850, 2228 (C≡N), 1470, 1284, 1125, 851, 770, 717, 630.

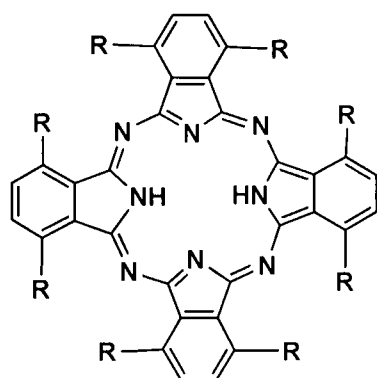
3,6-Diisopentylphthalonitrile, [4.5d].

Using general procedure E: 2,5-diisopentylthiophene 1,1-dioxide [4.4d] (3.43 g, 0.015 mol), fumaronitrile (1.14 g, 0.015 mol, 1 eq.), chloroform (1 cm³) gave 3,6-diisopentylphthalonitrile [4.5d] (2 g, 52%) as off white needles: m.p. 90.9 °C; R_f (toluene) = 0.75; δ_H (300 MHz, C₆D₆, **Spectrum 27**) 7.48 (2H, s, H-4,5), 2.87-2.84 (4H, m, H-1',1''), 1.67-1.63 (2H, m, H-3',3''), 1.59-1.52 (4H, m, H-2',2''), 0.99 (6H, d, J 6.6 Hz, H-4',5', H-4'',5''); δ_C (150.9MHz, CDCl₃, **Spectrum 28**) 146.43, 133.37, 115.64, 115.08, 39.90, 32.38, 27.87, 22.32; IR ν_{max}/cm^{-1} (neat) (**plate 14**) 2955, 2935, 2871, 2225(C≡N), 1562, 1469, 1384, 1368, 1323, 1245, 1169, 857, 758, 642.

3,6-Di(2-cyclohexylethyl)phthalonitrile, [4.5e].

Using general procedure E: 2,5-di(2-cyclohexylethyl)thiophene 1,1-dioxide [4.4e] (5.0 g, 0.015 mol), fumaronitrile (1.14 g, 0.015 mol, 1 eq.), chloroform (1 cm³) gave 3,6-di(2-cyclohexylethyl)phthalonitrile [4.5e] (2 g, 40%) as *off white needles*: m.p. 147.5 °C; δ_H (300 MHz, C₆D₆, **Spectrum 29**) 6.75 (2H, s, H-4,5), 2.60 (4H, t, J 8.27 Hz, H-1',1''), 1.75 (10H, m, H-(3',4',8'), H-(3'',4'',8''), 1.41-1.34 (2H, m, H-2',2''), 1.26 – 1.15 (8H, m, H-5',7', H-5'',7''), 0.99-0.88 (4H, m, H-6',6''); δ_C (150.9 MHz, CDCl₃, **Spectrum 30**) 146.56, 133.37, 115.59, 115.09, 38.51, 37.40, 33.06, 31.92, 26.49, 26.18. IR ν_{max}/cm^{-1} (neat) (**plate 15**) 2919, 2855, 2845, 2226 (C≡N), 2147, 1556, 1486, 1236, 1187, 882, 841, 660, 595, 557; m/z (EI) 348.30 (M⁺, 100%); C₂₄H₃₂N₂(M + Na)⁺ requires 371.2463, found 371.2455.

Preparation of 1,4,8,11,15,18,22,25-octaalkylphthalocyanines [4.6a-4.6e]



[4.6a-4.6e]

- a, R = C₆H₁₃ c, R = C₁₂H₂₅ e = C₈H₁₅
b, R = C₈H₁₇ d, R = C₅H₁₁

General Procedure F.

3,6-Dialkylphthalonitrile (0.001 mol) was dissolved in warm (80 °C) pentanol (10 cm³). An excess of clean lithium metal (0.35 g, 0.05 mol, 30-40 eq.) was added in small portions at 110°C and the mixture refluxed for 16 hours. The cooled (r.t) deep green coloured suspension was stirred with acetone (50 cm³), the solution filtered and the solids washed with acetone (50 cm³) before the combined acetone solutions were concentrated *in vacuo* to *ca.* 25 cm³. Acetic acid (50 cm³) was added, the heterogeneous mixture stirred for 30 minutes and the precipitate collected to afford after recrystallisation from THF-methanol the 1,4,8,11,15,18,22,25-octaalkylphthalocyanine.

1,4,8,11,15,18,22,25-octahexylphthalocyanine, [4.6a].^{6,7}

Using general procedure F: 3,6-dihexylphthalonitrile [4.5a] (0.3 g, 0.001 mol), warm pentanol (10 cm³), clean lithium metal (0.35 g, 0.05 mol) gave 1,4,8,11,15,18,22,25-octahexylphthalocyanine [4.6a] (0.14 g, 12%) as a green solid. δ_{H} (600 MHz, C₆D₆, *Spectrum 31*) 7.89 (8H, s, H-4,5 (x4)), 4.70 (16H, t, *J* 7.5 Hz, H-1'(x16)), 2.36-2.34 (16H, m, H-2'(x16)), 1.83-1.81 (16H, m, H-3'(x16)), 1.50-1.41 (16H, m, H-4'(x16)), 1.40-1.35 (16H, m, H-5'(x16)), 0.96 (24H, t, *J* 7.3 Hz, H-6'(x24)), -0.32 (2H, s, H-1(x2)); δ_{C} (150.9 MHz, CDCl₃, *Spectrum 32*) 138.60, 130.39, 32.68, 32.18, 30.41, 29.12, 22.68, 14.08; UV-vis (petroleum ether) λ_{max} /nm (log ϵ) 730 (01.06), 690 (0.88), 674 (0.34), 639 (0.14), 364 (0.34); IR ν_{max} /cm⁻¹ (neat) (plate 16) 3300 (N-H), 2953, 2924, 2854, 1891, 1578, 1465, 1304, 1141, 1019, 877, 763; MALDI-MS: *m/z* 1186.91 (M-H).

1,4,8,11,15,18,22,25-octaoctylphthalocyanine, [4.6b].^{1,2}

Using general procedure F: 3,6-dioctylphthalonitrile [4.5b] (0.5 g, 0.001 mol), warm pentanol (10 cm³), clean lithium metal (0.35 g, 0.05 mol) gave 1,4,8,11,15,18,22,25-octaoctylphthalocyanine [4.6b] (0.20 g, 10%) as a green solid: δ_{H} (600 MHz, C₆D₆, *Spectrum 33*) 7.91 (8H, s, H-4,5), 4.72 (16H, t, *J* 7.4 Hz, H-1' (x16)), 2.39-2.36 (16H, m, H-2' (x16)), 1.86-1.83 (16H, m, H-3' (x16)), (16H, m, H-4'(x16)), 1.41-1.39 (16H, m, H-5'(x16)), 1.33-1.31 (32H, m, H-6',7'(x16)), 0.95 (24H, t, *J* 7.0 Hz, H-8' (x24)), -0.29 (2H, s, H-1(x4)); δ_{C} (150.9 MHz, CDCl₃, *Spectrum 34*) 138.68, 130.50, 32.70, 31.90, 30.52, 29.92, 29.46, 29.34, 22.62, 14.05; UV-vis (petroleum ether) λ_{max} /nm (log ϵ) 730 (0.41), 695 (0.33), 674 (0.14), 639 (0.07), 364 (0.16); MALDI-MS: *m/z* 1411.16 (M-H); IR ν_{max} /cm⁻¹ (neat) (plate 17) 3298 (N-H), 2953, 2920, 2851, 1461, 1024, 873, 804, 750.

1,4,8,11,15,18,22,25-octadodecylphthalocyanine, [4.6c].⁹

Using general procedure F: 3,6-dioctylphthalonitrile [4.5c] (0.46 g, 0.001 mol), warm pentanol (10 cm³), clean lithium metal (0.35 g, 0.05 mol) gave 1,4,8,11,15,18,22,25-octadodecylphthalocyanine (6c) (0.22 g, 12%) as a green solid: δ_{H} (600 MHz, CDCl₃, *Spectrum 35*) 7.77 (8H, s, H-4,5 (x 4)), 4.34 (16H, t, *J* 7.1 Hz, H-1' (x16)), 2.07-2.02 (16H, m, H-2' (x16)), 1.56-1.53 (16H, m, H-3' (x16)), 1.28 - 1.21 (128H, m, H-(4'-11'))

(x16)), 0.90 – 0.83 (24H, m, H-12' (x 24)), -0.31 (2H, s, H-1 (x 2)); δ_C (150.9 MHz, $CDCl_3$, **Spectrum 36**) 138.56, 130.34, 32.65, 31.90, 30.43, 30.00, 29.71, 29.68, 29.64, 29.46, 29.34, 22.67, 14.08; UV-vis (petroleum ether) $\lambda_{max/nm}$ (log ϵ) 725 (0.6), 695 (0.52), 674 (0.20), 639 (0.10), 364 (0.22); MALDI-MS: m/z 1860.67(M-H); IR ν_{max}/cm^{-1} (neat) (**plate 18**) 3300 (N-H), 3297, 2918, 2850, 1483, 1304, 1139, 1017, 878, 790, 737, 720.

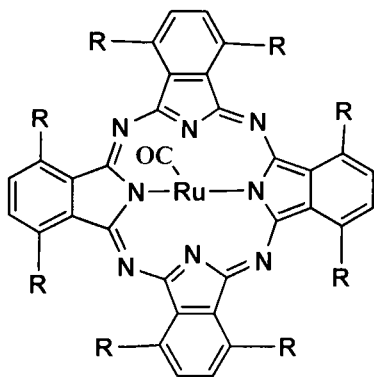
1,4,8,11,15,18,22,25-octa-isopentylphthalocyanine, [4.6d].¹²

Using general procedure F: 3,6-dioctylphthalonitrile [4.5d] (0.27 g, 0.001 mol), warm pentanol (10 cm³), clean lithium metal (0.35 g, 0.05 mol) gave 1,4,8,11,15,18,22,25-octaisopentylphthalocyanine [4.6d] (0.11 g, 10%) as a green solid: δ_H (600 MHz, $CDCl_3$, **Spectrum 37**) 7.88 (8H, s, 8H, H-4,5 (x 4)), 4.49 (16H, t, J 7.7 Hz, H-1' (x 16)), 1.94 (16H, dd, J 14.9, 7.1 Hz, H-2' (x 16)), 1.83-1.81 (8H, m, H-3' (x 8)), 1.01 (48H, d, J 6.6 Hz, H-4',5' (x 24)); δ_C (150.9 MHz, $CDCl_3$, **Spectrum 38**) 139.07, 130.77, 39.98, 30.50, 27.53, 22.97; MALDI-MS: m/z 1074.791(M); IR ν_{max}/cm^{-1} (neat) (**plate 19**) 3300 (N-H), 2921, 2854, 2226, 1455, 1021, 805, 718, 589; UV-vis (petroleum ether) $\lambda_{max/nm}$ (log ϵ) 285.0 (0.612), 360 (0.44), 705 (2.67), 725 (3.26).

1,4,8,11,15,18,22,25-octa(2-cyclohexylethyl)phthalocyanine, [4.6e]

Using general procedure F: 3,6-dioctylphthalonitrile [4.5e] (0.35 g, 0.001 mol), warm pentanol (10 cm³), clean lithium metal (0.35 g, 0.05 mol) gave 1,4,8,11,15,18,22,25-octa(2-cyclohexylethyl)phthalocyanine [4.6e] (0.19 g, 14%) as a green solid: δ_H (600 MHz, $CDCl_3$, **Spectrum 39**) 7.88 (8H, s, H-4,5 (x 4)), 4.48 (16H, t, J 7.7 Hz, H-1' (x 16)), 1.95-1.90 (32H, m, H-4',8' (x 16)), 1.69-1.64 (24H, m, H-2' (x 16), H-3' (x 8)), 1.27-1.18 (32H, m, H-5',7' (x 16)), 1.04-0.98 (16H, m, H-6' (x 16)); δ_C (150.9 MHz, $CDCl_3$, **Spectrum 40**) 139.14, 130.57, 77.21, 77.00, 76.79, 38.28, 37.26, 33.71, 29.89, 29.69, 26.73, 26.42; UV-vis (petroleum ether) $\lambda_{max/nm}$ (log ϵ) 734 (0.91), 695 (0.79), 674 (0.26), 639 (0.10), 364 (0.30); IR ν_{max}/cm^{-1} (neat) (**plate 20**) 3300 (N-H), 3302, 2910, 2848, 1596, 1508, 1425, 1313, 1032, 882, 816, 762, 716; MALDI-MS (m/z): 1396.04 (M).

Synthesis of 1,4,8,11,15,18,22,25-octaalkyl phthalocyaninoruthenium(II)
complexes



[4.8a-4.8e]

a, R = C₆H₁₃ c, R = C₁₂H₂₅ e, R = C₈H₁₅
b, R = C₈H₁₇ d, R = C₅H₁₁

General Procedure G.

To a flame dried flask under an argon atmosphere was added 1,4,8,11,15,18,22,25-octaalkylphthalocyanine (0.23 mmol) and triruthenium dodecacarbonyl (0.3 g, 0.47 mmol, 2 eq). Benzonitrile (10 cm³) was added and the reaction mixture was heated at reflux for 100 min. The cooled reaction mixture was poured onto cold methanol (400 cm³) causing the formation of some crystals. After cooling at 5 °C for a further 72 h, the excess solvent was decanted. The crude product was purified by flash column chromatography (eluting with methanol to remove benzonitrile and then with petroleum ether 40-60 °C). Reprecipitation (petroleum ether – methanol) gave the 1,4,8,11,15,18,22,25-octaalkylphthalocyaninoruthenium.

Carbonyl(1,4,8,11,15,18,22,25-octaethylphthalocyaninato)ruthenium(II), [4.8a].

Using general procedure G: 1,4,8,11,15,18,22,25-octaethylphthalocyanine [4.6a] (0.28 g, 0.23 mmol), triruthenium dodecacarbonyl (0.3 g, 0.47 mmol, 2 eq.), benzonitrile (10 cm³), gave carbonyl(1,4,8,11,15,18,22,25-octaethylphthalocyaninato)ruthenium(II) [4.8a] (0.25 g, 78%) as a dark blue amorphous solid: δ_{H} (600 MHz, CDCl₃, *Spectrum 41*) 7.87 (8H, s, H-4,5), 4.65-4.62 (8H, m, H-1' α (x8)), 4.59-4.55 (8H, m, H-1' β (x8)), 2.30-2.22 (16H, m, H-2'(x 16)), 1.75-1.68 (16H, m, H-3'(x 16)), 1.46-1.39 (16H, m, H-4'(x 16)), 1.38-1.34 (16H, m, H-5'(x 16)), 0.89 (24H, t, J 7.2 Hz, H-6' (x 24)); δ_{C} (150.9 MHz, CDCl₃, *Spectrum 42*) 183.34, 145.17, 137.95, 136.57, 129.79, 32.68, 32.31, 30.88, 29.10, 22.76, 14.15; UV-vis (petroleum ether) $\lambda_{\text{max/nm}}$ (log ϵ) 659 (0.51); IR $\nu_{\text{max/cm}^{-1}}$ (neat) (**plate 21**) 2953, 2925, 2855, 1958 (Ru-C=O), 1600, 1573, 1468, 1433, 1329, 1261, 1167, 1108, 1017, 911, 801, 726.1936; MALDI-MS(m/z) (**plate 28**): 1313.688(M), 1295(M-CO), C₈₁H₁₁₂N₈ORu (**plate 35**). requires 1314.8061800, found 1314.7997112. Anal. Calcd for C₈₁H₁₁₂N₈ORu.3CH₃OH: C, 71.49; H, 8.86; N, 7.94; Found C, 71.84; H, 8.72; N, 8.16.

Carbonyl(1,4,8,11,15,18,22,25-octaoctylphthalocyaninato)ruthenium(II), [4.8b].¹⁰

Using general procedure G: 1,4,8,11,15,18,22,25-octaoctylphthalocyanine [4.6b] (0.33 g, 0.23 mmol), triruthenium dodecacarbonyl (0.3 g, 0.47 mmol, 2 eq.), benzonitrile (10 cm³) gave carbonyl(1,4,8,11,15,18,22,25-octaoctylphthalocyaninato)ruthenium(II) [4.8b] (0.3 g, 86%) as a dark blue amorphous solid: δ_{H} (600 MHz, CDCl₃, *Spectrum 43*) 7.86 (8H, s, H-4,5(x 4)), 4.65-4.60 (8H, m, H-1' α (x 8)), 4.57-4.52 (8H, m, H-1' β (x 8)), 2.27-2.22 (16H, m, H-2' (x 16)), 1.72 - 1.67 (16H, m, H-3' (x 16)), 1.46-1.39 (16H, m, H-4' (x 16)), 1.35-1.29 (16H, m, H-5' (x 16)), 1.27-1.23 (32H, m, H-6',7' (x 16)), 0.84 (24H, t, J 6.9 Hz, H-8' (x 24)); δ_{C} (150.9 MHz, CDCl₃, *Spectrum 44*) 180.25 145.16, 137.93, 136.57, 129.72, 32.62, 31.91, 30.89, 30.01, 29.40, 29.36, 22.62, 14.02; UV-vis (petroleum ether) $\lambda_{\text{max/nm}}$ (log ϵ) 675 (0.18); IR $\nu_{\text{max/cm}^{-1}}$ (neat) (**plate 22**) 2954, 2922, 2852, 1963 (Ru-C=O), 1502, 1466, 1328, 1167, 1112, 913, 721; MALDI-MS (m/z) (**plate 29**): 1539.777(M), 1511.85(M-CO); C₉₇H₁₄₄N₈ORu (**plate 36**) requires 1539.0473960, found 1539.0501122.

Carbonyl(1,4,8,11,15,18,22,25-octadodecylphthalocyaninato)ruthenium(II), [4.8c]

Using general procedure G: 1,4,8,11,15,18,22,25-octadodecylphthalocyanine [4.6c] (0.43 g, 0.23 mmol), triruthenium dodecacarbonyl (0.3 g, 0.47 mmol, 2 eq.), benzonitrile (10 cm³) gave carbonyl(1,4,8,11,15,18,22,25-octadodecylphthalocyaninato)ruthenium(II) [4.8c] (0.32 g, 70%) as a *dark blue amorphous solid*: δ_{H} (600 MHz, C₆D₆ + drop pyridine, **Spectrum 45**) 7.95 (8H, d, *J* 22.9 Hz, H-4,5 (x4)), 4.96-4.70 (16H, m, H-1' (x16)), 2.49-2.41 (16H, m, H-2' (x16)), 1.89-1.84 (17H, m, H-3' (x16)), 1.57-1.37 (128H, m, H-(4'-11')), 0.95 (24H, t, *J* 6.7 Hz, H-12' (x24)); δ_{C} (150.9 MHz, C₆D₆ + pyridine, **Spectrum 46**) 181.24, 145.37, 138.13, 137.40, 130.08, 32.84, 32.36, 32.02, 31.14, 30.29, 29.91, 29.84, 29.59, 29.51, 29.15, 22.81, 14.07. ; IR $\nu_{\text{max}}/\text{cm}^{-1}$ (neat) 2920, 2851, 1965 (C=O), 1601, 1466, 1328, 1172, 1112, 913, 805, 721 ; UV-vis (petroleum ether) $\lambda_{\text{max/nm}}$ (log ϵ) 664.9 (0.38); IR $\nu_{\text{max}}/\text{cm}^{-1}$ (neat) (**plate 23**) 2921, 2852, 1967 (Ru-C=O), 1456, 1328, 1172, 1111, 1021, 803, 720; MALDI-MS (*m/z*) (**plate 30**): 1988.324(M), 1960.862(M - CO); C₁₃₀H₂₁₂N₈O₂Ru (**plate 37**) requires 2020.5810, found 2020.5658.

Carbonyl(1,4,8,11,15,18,22,25-octaisopentylphthalocyaninato)ruthenium(II), [4.8d].

Using general procedure G: 1,4,8,11,15,18,22,25-octaisopentylphthalocyanine [4.6d] (0.25 g, 0.23 mmol), triruthenium dodecacarbonyl (0.3 g, 0.47 mmol, 2 eq.), benzonitrile (10 cm³) gave carbonyl(1,4,8,11,15,18,22,25-octaisopentylphthalocyaninato)ruthenium(II) [4.8d] (0.18 g, 61%) as a *dark blue amorphous solid*: δ_{H} (600 MHz, CDCl₃, **Spectrum 47**) 7.86 – 7.81 (8H, d, *J* 13 Hz, H-4,5 (x4)), 4.67-4.61 (8H, m, H-1' α (x 8)), 4.60-4.55 (8H, m, H-1' β (x 8)), 2.12-2.08 (16H, m, H-2' (x 16)), 1.97 – 1.93 (8H, m, H-3' (x 8)), 1.09 (48H, d, *J* 6.5 Hz, H-4',5' (x 24)); δ_{C} (150.9 MHz, CDCl₃, **Spectrum 48**) 174.77, 145.03, 138.05, 136.62, 129.62, 40.29, 30.23, 27.13, 23.12; UV-vis (petroleum ether) $\lambda_{\text{max/nm}}$ (log ϵ) 665 (10); IR $\nu_{\text{max}}/\text{cm}^{-1}$ (neat) (**plate 24**) 2952, 2929, 2866, 1958 (Ru-C=O), 1601, 1502, 1449, 1329, 1180, 1104, 1025, 917, 794, 759; MALDI-MS (*m/z*) (**plate 31**): 1174.681(M-CO); C₇₃H₉₆N₈ORu (**plate 38**) requires 1202.6755670, found 1202.6745107. Anal. Calcd for C₇₃H₉₆N₈ORu. 3CH₃OH: C, 70.27; H, 8.39; N, 8.63; Found: C, 70.35; H, 7.97; N, 8.56.

Carbonyl[1,4,8,11,15,18,22,25-octa(2-cyclohexylethylphthalocyaninato)ruthenium(II), [4.8e].

Using general procedure G: 1,4,8,11,15,18,22,25-octa(2-cyclohexylethyl)phthalocyanine [4.6e] (0.33 g, 0.23 mmol), triruthenium dodecacarbonyl (0.3 g, 0.47 mmol, 2 eq.), benzonitrile (10 cm³) gave carbonyl[1,4,8,11,15,18,22,25-octa(2-cyclohexylethyl)phthalocyaninato)ruthenium(II) [4.8e] (0.25 g, 67%) as a *dark blue amorphous solid*: δ_{H} (600 MHz, CDCl₃, **Spectrum 49**) 7.84 (8H, s, H-4,5 (x 4)), 4.65-4.61 (8H, m, H-1' α (x 8)), 4.60-4.56 (8H, m, H-1' β (x 8)), 2.10 (16H, dd, J 14.4, 7.4 Hz, H-5' (x 16)), 2.02 (16H, s, br, H-7' (x 16)), 1.76 (16H, d, J 12.3 Hz, H-4' (x 16)), 1.73-1.65 (16H, m, H-8' (x 16)), 1.34-1.21 (24H, m, H-2' (x 16), H-3' (x 8)), 1.09 (16 H, dd, J 24.0, 12.0 Hz, H-6' (x 16)); δ_{C} (150.9 MHz, CDCl₃, **Spectrum 50**) 183.32, 145.13, 138.20, 136.56, 129.58, 38.70, 36.85, 33.88, 29.59, 26.82, 26.50; UV-vis (petroleum ether) $\lambda_{\text{max/nm}}$ (log ϵ) 664 (0.5); IR $\nu_{\text{max/cm}^{-1}}$ (neat) (**plate 25**) 2920, 2854, 2227, 1972 (Ru-C=O), 1456, 1326, 1077, 1035, 881, 796; MALDI-MS (m/z) (**plate 32**): 1494.863 (M-CO); Anal. Calcd for C₉₇H₁₂₈N₈ORu.3CH₃OH: C, 74.16; H, 8.72; N, 6.92; Found: C, 74.07; H, 8.26; N, 7.10.

Carbonyl(phthalocyaninato)ruthenium(II), [4.8f].¹⁷

UV-vis (toluene) $\lambda_{\text{max/nm}}$ (log ϵ) 634.98 (0.26); IR $\nu_{\text{max/cm}^{-1}}$ (neat) (**plate 26**) 2167.60, 2079.93, 2027.42, 1966.12 (Ru-C=O), 1648.60, 1570.68, 1543.91, 1499.90, 1437.20, 1001.45, 718.22; MALDI-MS (m/z) (**plate 33**): 614.338 (M-CO).

(1,4,8,11,15,18,22,25-Octaoctylphthalocyaninato)cobalt(II), [4.7b].

A stirred mixture of metal free 1,4,8,11,15,18,22,25-octaoctylphthalocyanine (0.08 g, 0.0057 mmol) [4.6b], cobalt(II) chloride (0.0029 g, 0.023 mmol) and pentanol (3 ml) was heated at 130 °C for 5 hr. Methanol (6 ml) was added, the precipitate filtered and washed with excess methanol, followed by recrystallisation from THF/Methanol to afford (1,4,8,11,15,18,22,25-octaoctylphthalocyaninato)cobalt(II) (0.06 g, 72 %) as a *blue amorphous solid*: δ_{H} (300 MHz, CDCl₃, **Spectrum 51**) 7.85 (8H, s, H-4,5 (x4)), 4.55-4.58 (16H, m, H-1' (x16)), 2.36-2.16 (16H, m, H-2' (x16)), 1.7-1.1 (80H, m, H-3'-4' (x32)), 0.96 (24H, t, J 7.3 Hz, H-8' (x24)); δ_{C} (151.9 MHz, CDCl₃, **Spectrum 52**) 132.63, 130.35,

128.71, 114.27, 40.93, 32.03, 31.28, 31.11, 30.68, 29.70, 22.79, 14.60; MALDI-MS (m/z) (plate 34): 1468.084 (M), IR $\nu_{\max}/\text{cm}^{-1}$ (neat) (plate 27) 2955.70, 2922.31, 2852.79, 1703.71, 1602.81, 1504.78, 1462.94, 1332.96, 1260.73, 1177.13, 1096.13, 924.82, 801.87, 743.45; UV-Vis (chloroform) λ_{\max}/nm ($\log \epsilon$) 705 (0.32).

4.6 References

1. (a) Higuchi, T.; Ohtake, H.; Herobe, M. *Tetrahedron Lett.* **1989**, *30*, 6545. (b) Higuchi, T.; Ohtake, H.; Herobe, M. *Tetrahedron Lett.* **1991**, *32*, 7435. (c) Higuchi, T.; Ohtake, H.; Herobe, M. *Tetrahedron Lett.* **1992**, *33*, 2521. (d) Higuchi, T.; Ohtake, H.; Herobe, M. *Tetrahedron Lett.* **1989**, *30*, 6545.
2. Berkessel, A.; Kaiser, P.; Lex, J. *Chem. Eur. J.* **2003**, 4746-4756.
3. Che, C-M.; Huang, J-S. *Chem. Commun.*, **2009**, 3996-4015.
4. Gross, Z.; Ini, S. *J. Org. Chem.* **1997**, *62*, 5514-5521.
5. Larsen, E.; Jorgensen, K. A. *Acta Chem. Scand.* **1989**, *43*, 259-263.
6. McKeown, N. B.; Chambrier, I.; Cook, M. J.; *J. Chem. Soc. Perkin Trans. 1*, **1990**, 1169.
7. Chambrier, I.; Cook, M.J.; Cracknell, S. T. and McMurdo, J. *J. Mater. Chem.*, **1993**, *3*(8), 841-849.
8. Swarts, J. C.; Langner, N. K-H. and Cook, M. J. *J. Mater. Chem.*, **2000**, *10*, 8.
9. Davis, W. L.; *Ph.D Thesis*, University of the Free State, Bloemfontein, South Africa, 2003.
10. Cammidge, A. N.; Berber, G.; Chambrier, I.; Hough, P. W and Cook, M. J. *Tetrahedron* **2005**, *61*, 4067-4074.
11. Berber, G.; Cammidge, A. N.; Chambrier, I.; Cook, M. J.; Hough, P. W. *Tetrahedron Lett.* **2003**, *44*, 5527.
12. Chambrier, I.; Cook, M. J. and Powell, A. K. *J. Chem. Soc. Chem. Commun.*, **1992**, 1169.
13. Liu, J.-Y.; Jiang, X.-J.; Fong, W.-P. and Ng, K. P. *Metal-Based Drugs*, **2008**, 284691.
14. (a) Gorbunova, Y.G.; Enakieva, Y.Y.; Sakharov, S.G. and Tsivadze, A.Y. *Russ. Chem. Bull.* **2004**, *53*, 74. (b) Dudnik, A.S.; Ivanov, A.V.; Tomilova, L.G. and Zafirov, N.S. *Russian Journal of Coordination Chemistry*, **2004**, *30*, 110-114.
15. Poon, K.; Yan, Y.; Li, X. and Ng, D.P. *Organometallics*, **1999**, *18*, 3528.
16. Zhang, R., Yu, W.-Y.; Wong, K.-Y. and Che, C.-M. *J. Org. Chem.* **2001**, *66*, 8145-8153.

17. Capobianchi, A.; Paoletti, A. M.; Pennesi, G.; Caminiti, R. and Ercolani, C. *Inorg. Chem.*, **1994**, *33*, 4635-4640.
18. Buitendach, B. E. *M.Sc Thesis*, University of The Free State, Bloemfontein, South Africa, 2008.
19. Gottlieb, H. E.; Kotlyar, V.; Nudelman, A. *J. Org. Chem.* **1997**, *62*, 7512-7515.

Chapter 5

Epoxidation with ruthenium phthalocyanine catalysts

5.1 Introduction

Although some research has been carried out on Fe, Mn, and Co phthalocyanines as epoxidation catalysts,¹ most of the studies on phthalocyanines had the objective of comparing the activity and stability of these complexes with that of the porphyrin equivalents. Development of the oxidation chemistry of phthalocyanines has also been hampered by the poor solubility of these compounds in common organic solvents due to aggregation, but since examples with alkyl substituents at the 1,4,8,11,15,18,22,25 (nonperipheral) sites have shown much improved solubility, these compounds were considered to be very attractive in the epoxidation of alkenes. With the series of nonperipherally alkyl substituted ruthenium phthalocyanines [4.8a-4.8f]¹ in hand, attention was subsequently turned towards testing these complexes as epoxidation catalysts on a series of alkenes. Since substituted pyridine-*N*-oxides, especially 2,6-dichloropyridine-*N*-oxide (2,6-DCPNO) [5.2], gave good results as stoichiometric oxidants in the epoxidation of alkenes with ruthenium porphyrins,⁹ the study was kicked off by using this oxidant and extended to the evaluation of other substituted pyridine-*N*-oxides.

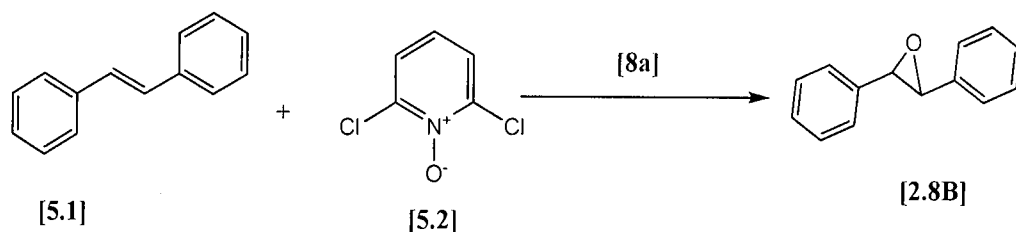
¹ For the purpose of simplification, the following abbreviations will be used for the catalysts: carbonyl(1,4,8,11,15,18,22,25-octahexylphthalocyaninato)ruthenium(II) [8a] - RuPc-C6, carbonyl(1,4,8,11,15,18,22,25-octa-octylphthalocyaninato)ruthenium(II) [8b] - RuPc-C8, carbonyl(1,4,8,11,15,18,22,25-octadodecylphthalocyaninato)ruthenium(II) [8c] - RuPc-C12, carbonyl(1,4,8,11,15,18,22,25-octaisopentylphthalocyaninato)ruthenium(II) [8d] - RuPc-Isopentyl and carbonyl[1,4,8,11,15,18,22,25-octa(2-cyclohexylethyl)phthalocyaninato]ruthenium(II) [8e] - RuPc-Cyclohex and carbonyl(phthalocyaninato)ruthenium(II) [8f] - RuPc-Unsub.

5.2 Results and discussion

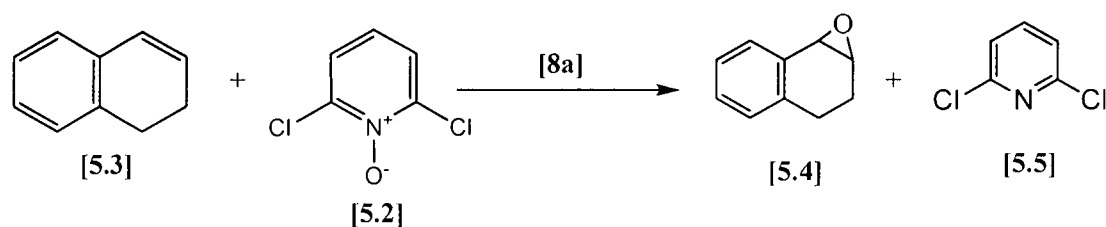
5.2.1 Epoxidation of 1,2-dihydronaphthalene [5.3] and *trans*-stilbene [5.1] catalyzed by RuPc-C6 [8a] and RuPc-Isopentyl [8d].

A. Effect of solvent & temperature

In order to determine whether ruthenium Pcs would catalyse the epoxidation of alkenes at all and to find the optimum conditions of solvent and temperature for the epoxidation of alkenes with these catalysts, it was decided to start the investigation by subjecting *trans*-stilbene (TSB) [5.1] (Scheme 5.1) and 1,2-dihydronaphthalene (DHN) [5.3] (Scheme 5.2) to two ruthenium phthalocyanine complexes, *i.e.* [8a] and [8d] (refer to Scheme 4.4, Chapter 4). Since no report on the utilization of ruthenium phthalocyanines in the epoxidation of alkenes could be located in literature, it was decided to initiate the investigation with the conditions reported for epoxidations based on the ruthenium porphyrin systems.^{3,8,9}



Scheme 5.1: Ruthenium phthalocyanine catalyzed epoxidation of *trans*-stilbene [5.1].



Scheme 5.2: Ruthenium phthalocyanine catalyzed epoxidation of 1,2-dihydronaphthalene [5.3].

Thus 1,2-dihydronaphthalene [5.3] and *trans*-stilbene [5.1] were reacted with 2,6-dichloropyridine-*N*-oxide (2,6-DCPNO) [5.2] in the presence of [8a] and [8d] (0.5-0.1 mol%) in a range of solvents and temperatures varying between 30 - 125 °C (Table 5.1 and 5.2). In order to be able to quantify the reaction products by GC, dodecane was added to the reaction mixture as internal standard. While product epoxide [2.8B] was identified by comparing the GC retention times with that of authentic samples obtained commercially, product [5.4] was identified by GC-MS.

The investigation was started at 30 °C in DCM, but poor epoxide yields (<6%) and conversions were obtained, even after two days of reaction, so the reaction temperature was increased to 45 °C and the solvent evaluation process continued at that temperature. At the higher temperature, yields for both [5.3] and [5.1] were still low (both 13 %) so the solvent was changed to toluene, which led to a marginal increase in both the epoxide yield (16 %) and conversion (22 %) for [5.3] (Table 5.1, entries 1 and 2), while the yield and conversion for [5.1] showed a slight decrease (Table 5.1, entries 3 and 4). In ethylacetate (Table 5.1, entry 5) the yield and conversion was 12 % and 17 % respectively. When the solvent was changed to THF and acetonitrile, no reaction was observed for [5.3], so [5.1] was not subjected to these conditions. The absence of reaction in THF and acetonitrile is probably explicable in terms of coordination of these strongly coordinating solvents to the ruthenium catalyst.

Table 5.1: Epoxidation of DHN [5.3] and *trans*-stilbene [5.1] with 2,6-dichloropyridine *N*-oxide [5.2] catalyzed by 0.1 mol % [8a] and [8d] in solvents as indicated.^[a]

Entry	Cat.	Olefin	Solvent	Conversion[%] ^b	Epoxide Yield [%]
1	[8a]	[5.3]	Toluene	22	16
2	[8a]	[5.3]	Dichloromethane	17	13
3	[8d]	[5.1]	Toluene	22	12
4	[8d]	[5.1]	Dichloromethane	26	13
5	[8a]	[5.3]	Ethylacetate	17	12
6	[8a]	[5.3]	THF	No reaction	No reaction
7	[8a]	[5.3]	CH ₃ CN	No reaction	No reaction

^[a] Reaction conditions: solvent, 45 °C, 48 h, catalyst/substrate/oxidant molar ratio = 1:1000:1500; ^[b] conversions were determined by GC using dodecane as internal standard.

Based on these results and the fact that reaction temperatures would be limited by the boiling point of DCM, toluene was selected as solvent for all future reactions. Furthermore, Berkessel and co-workers¹⁰ noted that higher reaction temperatures (125 °C) promote conversion rates, yields, and turnover frequencies (TOF; product/catalyst molar ratio per hour) in the ruthenium porphyrin/*N*-oxide system. The optimum temperature for these reactions with regard to epoxide yield, conversion, and turnover frequency, which was determined over the first 30 – 120 min of the reaction, was subsequently determined by subjecting [5.3] and [5.1] to epoxidation with 2,6-dichloropyridine-*N*-oxide [5.2] and 0.1 mol% of RuPcs [8a] and [8d] as catalysts.

For 1,2-dihydronaphthalene [5.3], at 115 °C and 90 °C, almost complete substrate conversion was observed after 3 h and 6 h respectively, whereas at 60 °C acceptable conversion (84 %) could only be achieved after 48 h (Table 5.2, entry 1-5). A similar

pattern was observed with *trans*-stilbene [5.1], though longer reaction time was required because of its lower reactivity compared to DHN [5.3] (Table 5. 2, entry 6-9).

Table 5.2: Temperature effect on the epoxidation of DHN [5.3] and *trans*-stilbene [5.1] with 2,6-dichloropyridine *N*-oxide [5.2] catalyzed by ruthenium Pc [8a] and [8d] at 0.1 mole % in toluene.^[a]

Entry	Cat.	Olefin	Temp [°C]	Time [h]	Conv. [%]	Epoxide yield (selectivity)[%]	TOF [h ⁻¹]
1	[8a]	[5.3]	60	48	84	68 (81)	46
2	[8a]	[5.3]	90	6	100	80 (80)	600
3	[8a]	[5.3]	115	3	>98	74 (76)	1,120
4	[8d]	[5.3]	60	48	84	57 (68)	138
5	[8d]	[5.3]	90	6	100	77 (77)	770
6	[8a]	[5.1]	60	48	23	21 (91)	30
7	[8a]	[5.1]	90	48	>99	82 (82)	120
8	[8d]	[5.1]	90	48	72.5	56 (77)	104
9	[8d]	[5.1]	115	8	83	61 (74)	174

^[a] Reaction conditions: Toluene (2ml), catalyst/substrate/oxidant molar ratio = 1:1000:1500

The rate at which epoxide is formed also increases with temperature. This is evident from the drastic rise in turnover frequency. With [8a] as catalyst, the TOF rose from 46 to 1,120 (Table 5.2, entry 1 and 3) for the DHN [5.3] reaction as the temperature was raised from 60°C to 115°C, and from 30 to 120 (Table 5.2, entry 6 and 7) for TSB [5.1] with an increase in temperature from 60 to 90°C. However, although the epoxide formed faster at higher temperatures, the catalyst also decomposed faster as was evident from the rapid color change of the reaction mixture from blue to brown. The selectivity is however not significantly affected by temperature. For example, for the DHN [5.3] reaction catalyzed by [8a], the selectivity was 81%, 80% and 76% when the reaction was

performed at 60, 90 and 115 °C, respectively (Table 5.2, entry 1-3). The selectivity tended to drop when the reaction was left for longer than 48 h or soon after complete substrate conversion was attained.

B. Reaction kinetics

As expected, the reactivity of ruthenium complexes depends on the nature of the substrate (Figure 5.1). Similarly to oxidation and epoxidation with ruthenium porphyrin complexes,^{11,12} these reactions also showed an induction period of *ca.* 30 min at the lower temperatures (Figure 5.1, graphs d & f). This induction period could be arising from the formation of the active oxidative species, *i.e.* binding of the oxidant to the catalyst. At higher temperatures (90°C and 115°C) the induction period is very short, so it could be concluded that there is an inverse relationship between reaction temperature and induction time.

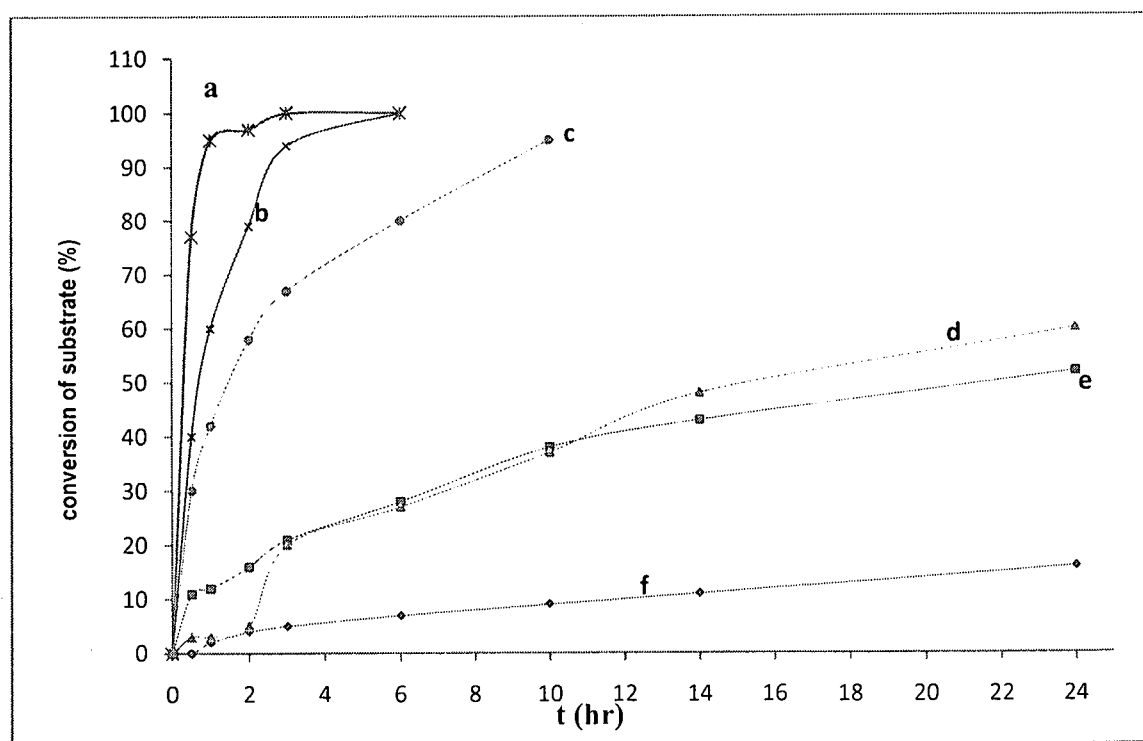


Figure 5.1. Kinetics for the epoxidation of DHN [5.3] and TSB [5.1] with 2,6-DCPNO [5.2] catalyzed by [8a] and [8d] at 0.1 mol% and at the temperatures indicated (catalyst/substrate/oxidant molar ratio = 1:1000:1500). a = [8d], [5.3], 115°C. b = [8a], [5.3], 90°C. c = [8d], [5.1], 115°C. d = [8a], [5.3], 60°C. e = [8d], [5.1], 90°C. f = [8a], [5.1], 60°C.

C. Influence of catalyst concentration

The effect of catalyst concentration on the epoxidation rate was investigated with *trans*-stilbene [5.1] as substrate and concentrations of [8a] ranging between 0.1 and 0.45 mol% over a 24 hour period at 90 °C. While it is apparent from Figure 5.2 that the epoxidation rate is higher at higher catalyst concentration, the overall epoxide yield and conversion for the 0.23 mol% and 0.45 mol% reactions appear to be very close (Table 5.3, entry 1 and 2 and Figure 5. 2). This indicates that once a certain threshold catalyst concentration is attained, the epoxidation rate is unaffected by a further increase in catalyst concentration. A possible explanation for this observation could be that catalyst aggregation, which reduces the availability of active catalyst, is more profound once a certain threshold concentration is reached. The fact that selectivity at 0.23 and 0.45 mol % catalyst concentrations were marginally higher than at 0.1 mol% (97%, 95% and 84%, respectively) is inexplicable at this stage and might be due to experimental error or some hitherto unknown effect.

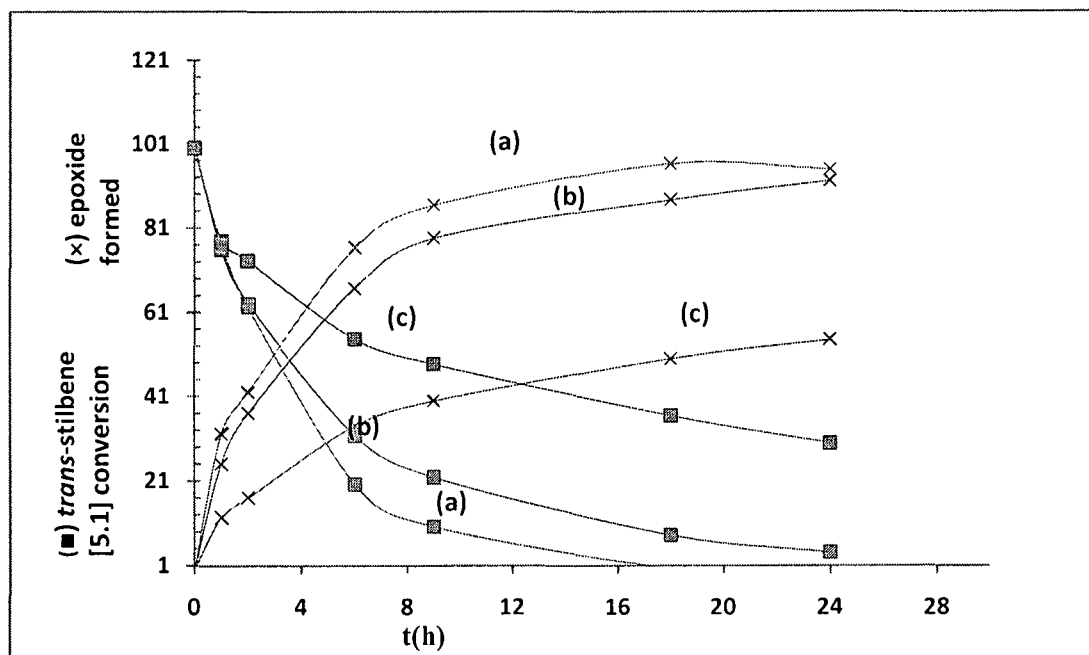


Figure 5.2. Kinetics of epoxidation of *trans*-stilbene [5.1] with different catalyst [8a] concentrations $[\text{cat}]_0 = 0.4 \text{ mol \%}$ (a), 0.2 mol \% (b), 0.1 mol \% (c), at 90°C for 24 h. (x) epoxide formed, (■) *trans*-stilbene [5.1] conversion.

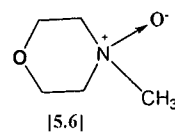
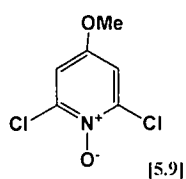
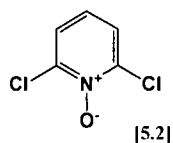
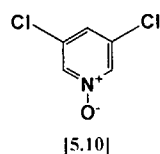
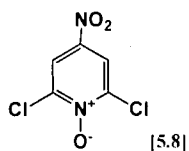
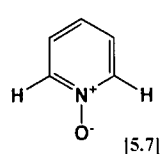
Table 5.3: Influence of catalyst concentration on *trans*-stilbene [5.1] epoxidation with 2,6-dichloropyridine-*N*-oxide [5.2] catalyzed by [8a]^a.

Entry	Cat. mol%	Conversion (%)	Yield (%)	Selectivity (%)
1	0.1	68	57	84
2	0.2	>95	92	97
3	0.4	100	95	95

^aData at 24 h.

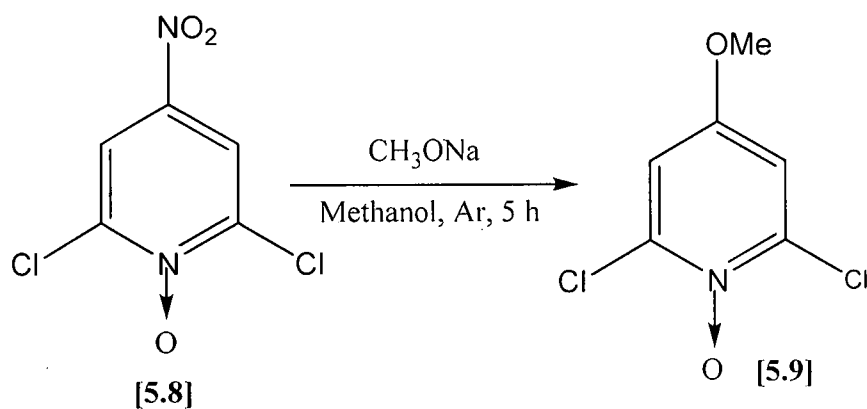
D. Effect of oxidant

Since it was reported that 2,6-disubstitution on pyridine-*N*-oxides is a prerequisite for this type of oxidant to be effective in the epoxidation of alkenes with ruthenium porphyrin catalysts¹⁴ and that 2,6-dichloropyridine-*N*-oxide [5.2] is the oxidant of choice in these reactions,¹¹ it was decided to test the applicability of these results to the ruthenium Pc catalytic system and to also evaluate different *N*-oxides as well as other common oxidants with regard to their epoxidation capabilities in the ruthenium Pc system. A series of potentially interesting oxidants, commercially available hydrogen peroxide, *tert*-butyl hydroperoxide (TBHP), iodobenzene diacetate, *N*-methylmorpholine-*N*-oxide [5.6], and pyridine-*N*-oxides [5.7], [5.8], [5.10] and [5.2] were therefore selected to be tested in the epoxidation of *trans*-stilbene [5.1] with the ruthenium phthalocyanine catalysts [8a] and [8d]. 2,6-Dichloro-4-methoxypyridine-*N*-oxide [5.9] was prepared in the laboratory and included in the evaluation.



Pyridine-*N*-oxides [5.8] and [5.9] were selected to study the effect of deactivating and activating groups, respectively, on the epoxidation in terms of yields, selectivity and epoxidation rates, while [5.2], [5.7] and [5.10] were selected to examine the necessity of substitution on the 2 and 6 positions of the pyridine-*N*-oxide.

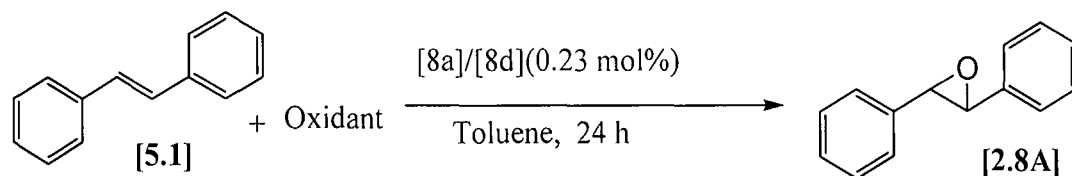
N-oxide [5.9] was prepared from [5.8] according to a literature procedure (Scheme 5.3).²⁰ The spectroscopic data for this compound [¹H NMR (spectrum 53) and ¹³C NMR (spectrum 54)] are identical to those reported.²⁰ Another confirmation for the structure of [5.9] was obtained by GC-MS, which revealed the presence of the peak expected for the molecular ion at *m/z* 192.97 (100%).



Scheme 5.3

The selected oxidants were thus tested in the epoxidation of *trans*-stilbene [5.1] with 0.23 mol% of [8a] or [8d] in toluene at 90 °C (H₂O₂ and TBHP reactions were done at room temperature) (Table 5.4). As for the porphyrin system, 2,6-dichloropyridine-*N*-oxide [5.2] proved to be superior to all other reagents with regard to both catalysts, giving conversions of 100 and 51 % respectively with the two catalysts (Table 5.4 entry 1 and entry 2, respectively). Interestingly, oxidant [5.10], with no substitution in the 2 and 6 positions, but still deactivated by chloro substituents, still reacted albeit at much lower conversion and selectivity than the 2,6-dichloro equivalent [5.2] (Table 5.4 entry 3 and 4 *versus* 1 and 2).

Table 5.4: Epoxidation of *trans*-stilbene [5.1] catalyzed by [8a] and [8d] at 0.23 mol % with different oxidants.^[a]



Entry	Catalyst	Oxidant	Conv %	Yield (%)
1	8a	[5.2]	100	95
2	8d	[5.2]	51	30
3	8a	[5.10]	52	42
4	8d	[5.10]	35	32
5	8a	[5.8]	36	32
6	8d	[5.8]	18	14
7	8a	[5.9]	45	37
8	8d	[5.9]	32	27
9	8a	[5.7]	No reaction	No reaction
10	8d	[5.7]	No reaction	No reaction
11	8a	[5.6]	No reaction	No reaction
12	8d	[5.6]	No reaction	No reaction
13	8a	iodobenzene diacetate	No reaction	No reaction
14	8d	iodobenzene diacetate	No reaction	No reaction
15	8a	TBHP	No reaction	No reaction
16	8d	TBHP	No reaction	No reaction
17	8a	H ₂ O ₂	No reaction	No reaction
18	8d	H ₂ O ₂	No reaction	No reaction

^a Reaction conditions: Toluene, 80 °C, catalyst/substrate/oxidant molar ratio = 1:500: 750 for 24 h.

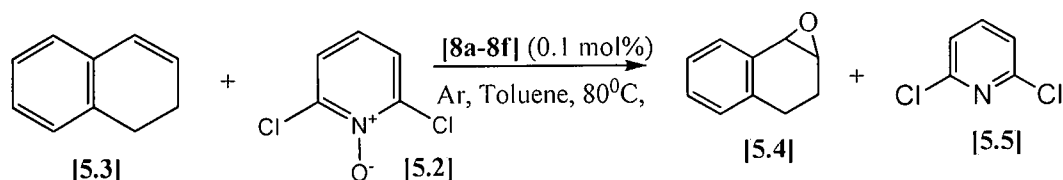
Substitution at the 2 and 6 positions are therefore not necessary to prevent strong coordination of the deoxygenated heteroaromatic product to the ruthenium, which would deactivate the catalyst and hinder further oxygen transfer, as was claimed for the porphyrin system.^{9a} From the results obtained it however seems necessary to have a deactivated pyridine ring since unsubstituted pyridine-N-oxide [5.7] gave no reaction at all (Table 5.4, entries 9 and 10). Excessive deactivation of the pyridine N-oxide as in the case of [5.8] with an electron withdrawing 4-nitro group in addition to the 2,6-dichloro substitution resulted in a decrease in conversion and yield, though, compared to [5.2] (Table 5.4, entries 5 and 6 *versus* 1 and 2). Activation of the 2,6-dichloropyridine-N-oxide base skeleton by an additional 4-methoxy group as in [5.9] also deactivated the oxidant compared to [5.2] (Table 5.4, entries 7 and 8 *versus* 1 and 2), but activated it compared to [5.8] (Table 5.4, entries 7 and 8 *versus* 5 and 6). The idea that deactivated or less basic nitrogen is a prerequisite for successful epoxidation with these catalysts was substantiated by the failure of *N*-methylmorpholine-*N*-oxide [5.6], to give any reaction, while other common oxidants like iodobenzene diacetate, *tert*-butylhydroperoxide (TBHP), and hydrogen peroxide (H₂O₂), also failed in this application. Similar results were obtained by Berkessel using chiral ruthenium porphyrin catalysts.¹⁰

5.2.2 Control Reactions

In order to ensure that the ruthenium catalyst was in fact catalyzing the reaction, epoxidation reactions in the absence of ruthenium Pc were performed under the same conditions for each of the substrates (DHN [5.3] and TSB [5.1]) and oxidants. In most cases no epoxide or just trace amounts ($\leq 0.59\%$) of epoxide could be detected after two days' reaction time. Reactions with the metal free Pc also gave only traces of the epoxide.

5.2.3 Epoxidation of 1,2-dihydronaphthalene [5.3] with RuPc catalysts

Since 1,2-dihydronaphthalene [5.3] has found wide application as substrate in the evaluation of epoxidation catalysts and Berkessel and Frauenkron¹⁰ and Che *et al.*²² reported TONs of 880 (48 h) and 890 (3 h) with homogeneous chiral ruthenium porphyrins and 870 (24 h) for soluble polymer-supported ruthenium porphyrin catalysts with 1,2-dihydronaphthalene [5.3] as substrate, this compound was selected for full evaluation of the catalytic capabilities of the prepared RuPc catalysts. Thus 1,2-dihydronaphthalene [5.3] was reacted with 2,6-dichloropyridine-*N*-oxide [5.2] in the presence of 0.1 mol % (catalyst : substrate ratio 1:1000) of the prepared RuPcs [8a-8e] (refer to Scheme 4.4, Chapter 4) (Scheme 5.4).



Scheme 5.4

While complete substrate conversion to the epoxide [5.4] was observed in 4 hours at 80 °C and high yields (77-83 %) and selectivities (77-85 %) were obtained with all the substituted ruthenium Pcs [8a-8e], the fact that only 42 % conversion could be reached (even at a catalyst concentration of 0.45 mole %) with the unsubstituted RuPc [8f], clearly indicated that substituted RuPcs were superior in catalytic activity to the unsubstituted equivalent [8f] (Table 5.5). Turnover numbers of up to 830 (in 4 h) were also comparable to those reported by Che *et al.*²² RuPc-Isopentyl [8d] proved to be the most active catalyst attaining a maximum epoxide yield within 1 h (Figure 5.3).

Table 5.5: 1,2-Dihydronaphthalene [5.3] epoxidation with RuPcs at 0.1 mole % catalyst concentration.^[a]

Entry	Cat.	Conv. (%)	Yields ^[b] (%)	Selectivity (%)	TON in 6h
1	8f (0.45 mol %)	42	35	76	77
2	8a	100	82	82	820
3	8b	100	80	80	800
4	8c	100	80	80	800
5	8d	100	77	77	770
6	8e	100	83	85	830

^[a] Reaction conditions: Toluene, 80°C, catalyst/substrate/oxidant molar ratio = 1:1000:1500 for 6 h. ^[b] [5.4] identified by GC-MS.

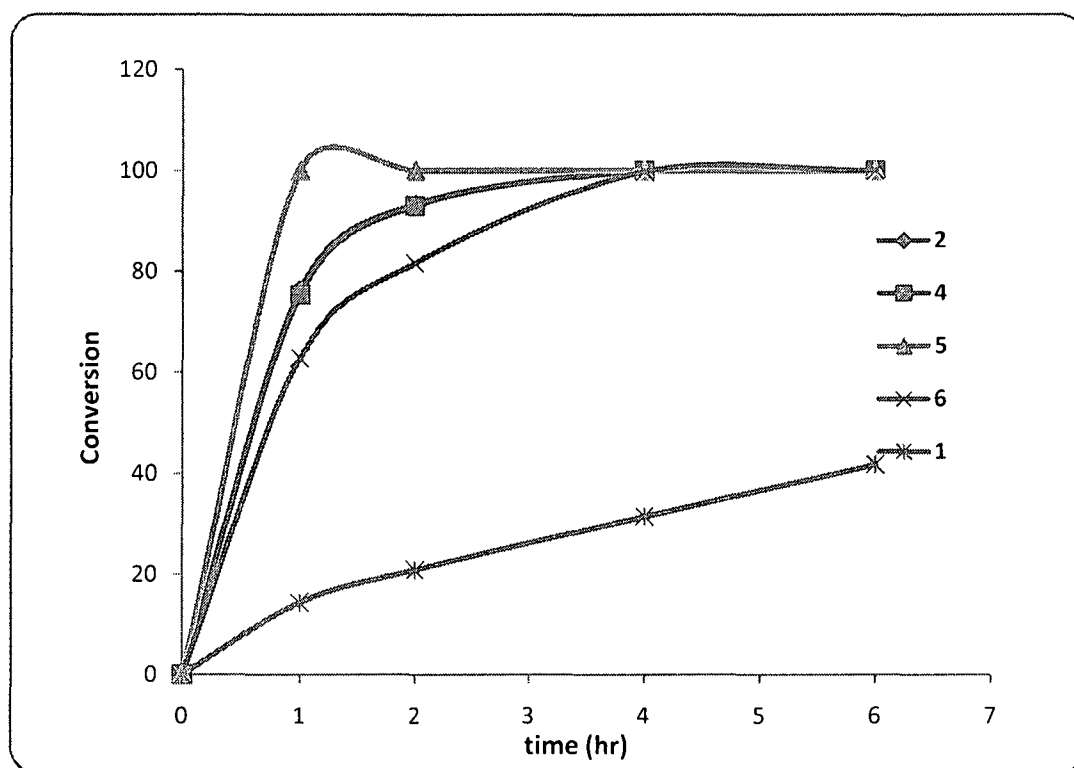


Figure 5.3: Time course plot for epoxidation of DHN [5.3] with RuPcs (0.1 mole % catalyst concentration) at 80°C (catalyst/substrate/oxidant molar ratio = 1:1000:1500). **1** = **8f**, **2** = **8a**, **4** = **8c**, **5** = **8d**, **6** = **8e**. The graphs for catalysts **8a** (**2**) and **8c** (**4**) overlap.

Since complete substrate consumption was achieved by the alkylsubstituted ruthenium Pc when the catalyst/substrate/oxidant molar ratio = 1:1000:1500 (0.1 mole % catalyst concentration) was employed, further evaluation of the activity and stability of the ruthenium complexes in the epoxidation of 1,2-dihydronaphthalene [5.3] was performed at a catalyst : substrate ratio of 1:5000 (Table 5.6). High turnovers (TON; product/catalyst molar ratio) of 2300 - 2800 in 12 h were achieved (Table 5.6, entry 1-5) at a turnover frequency of 260 – 457 hr⁻¹ (Table 5.6) prior to catalyst degradation (evident from the change in color of the reaction mixture from blue to brown).

Table 5.6: 1,2-Dihydronaphthalene [5.3] epoxidation catalyzed by ruthenium Pcs at 0.02 mol % catalyst concentration.^[a]

Entry	Catalyst	Conversion (%) ^[b]	TOF (h ⁻¹)	TON in 12 h
1	8a	53	286	2700
2	8b	49	295	2500
3	8c	57	300	2800
4	8d	51	457	2500
5	8e	46	260	2300

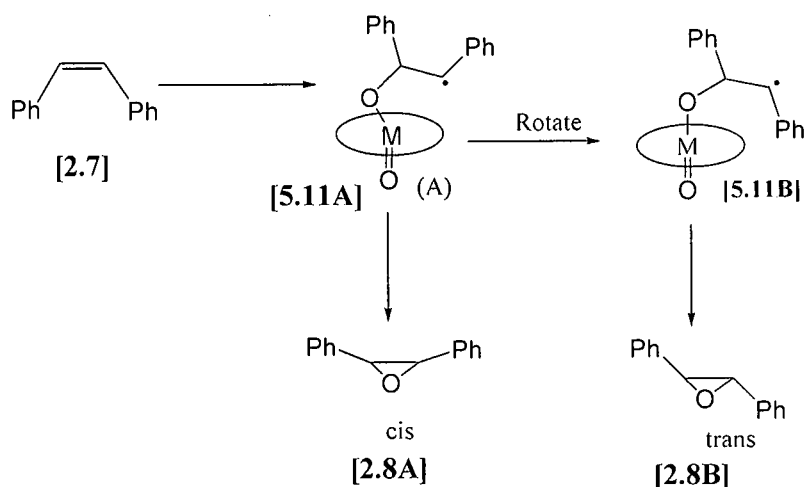
^[a] Reaction conditions: Toluene, 80 °C, catalyst/substrate/oxidant molar ratio = 1:5000: 5000 for 12 h.

5.2.4 Catalytic epoxidation of *cis*-stilbene [2.7] with phthalocyanine ruthenium complexes using 2, 6-dichloropyridine-N-oxide [5.2] as oxidant; catalyst activity and stability.

In the porphyrin catalyzed epoxidation of unfunctionalized alkenes and metal catalyzed oxidation in general, *cis*-stilbene [2.7] oxidation is of particularly high interest. This is mainly because the products obtained during the epoxidation of this substrate directly indicate the type of mechanism involved. Furthermore, since *cis*-stilbene [2.7] does not have an allylic H, the possibility of competing oxidation reactions on the allylic position

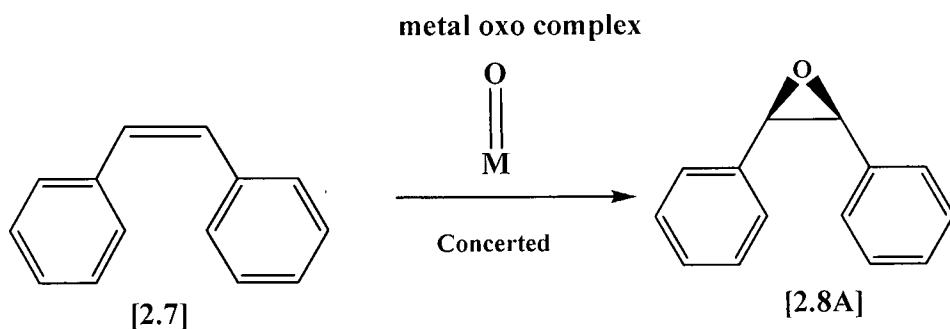
is eliminated. Consequently, *cis*-stilbene [2.7] has been used to probe stereoselectivity especially for the metalloporphyrin and salen-manganese catalyzed oxidation systems.^{15,16} A mechanism involving a “side-on approach” to the oxo-metal complex ($M=O$) offers a widely accepted explanation for the relatively high reactivity of the *cis*-alkenes over the *trans*-alkenes in these systems.²⁶

One of the most far reaching mechanisms in metal catalyzed epoxidation was put forward by Castellino and Bruice¹⁵ to explain (i) the formation of mixtures of *trans*- [2.8B] and *cis*-stilbene oxides [2.8A] and (ii) the formation of the *cis*-epoxide [2.8A] only, in the epoxidation of *cis*-stilbene [2.7] with iron or manganese porphyrin systems. For (i) these authors suggested a stepwise process involving a radical intermediate ([5.11A], Scheme 5.5) which allows for rotation about the carbon-carbon single bond to give the more stable *trans*- product [2.8B]. The ratio of *cis/trans* epoxide ([2.8A] / [2.8B]) formed depended on the type of catalyst and reaction conditions and in most cases the *trans*-oxide [2.8B] dominated.



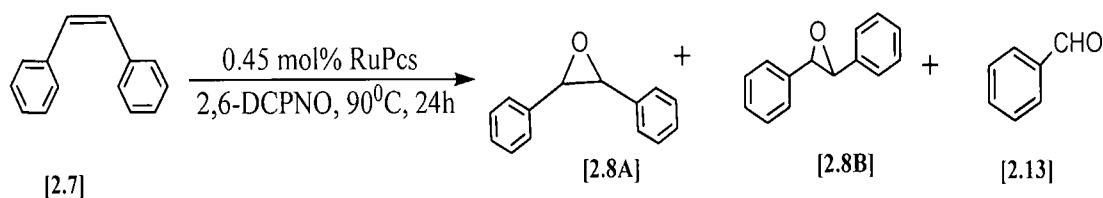
Scheme 5.5: Radical pathway for *cis*-stilbene [2.7] epoxidation.

Leung *et al.*¹⁷ also acknowledged this mechanism for *cis*-stilbene [2.7] epoxidation with nonsterically bulky ruthenium porphyrin complexes where mixtures of *cis*-[2.8A] and *trans*-epoxides [2.8B] were observed, the *trans*-epoxide [2.8B] dominating. In (ii) above, the *cis*-epoxide [2.8A] is thought to be formed through a concerted mechanism (Scheme 5.6).



Scheme 5.6: Concerted oxene transfer.

Using *cis*-stilbene [2.7] as substrate, the mechanistic properties of the Pc ligands were evaluated in reactions with 0.45 mol% of all six RuPc complexes at 90 °C (Scheme 5.7). For the straight chain alkyl substituted complexes RuPc-C6 [8a], RuPc-C8 [8b], and RuPc-C12 [8c], increasing the substituent chain length did not significantly affect overall yields, as all three catalysts gave high yields (83 – 86 %) and conversions of almost 100 %. The ratio of the *cis* : *trans* epoxide product was high (Table 5.7, entry 2-6) and did not change with the catalyst. The superior epoxide yields with the alkyl substituted RuPcs [8a-8c] could be attributed to the increased solubility associated with the alkyl side chains and a concomitant decrease in aggregation as chain length increases. The poor activity of the RuPc-Cyclohex [8e] could probably be due to the influence of the steric bulk of the ligands on the oxygen transfer process.



Scheme 5.7

The small amounts of *trans*-epoxide [2.8B] (*ca.* 4 - 6 %) observed in all of the reactions might be attributed to some *trans*-stilbene [5.1] being present as impurity in the commercially available samples of *cis*-stilbene [2.7], which was sold as having a purity of only 96 %. The almost exclusive formation of *cis*-stilbene oxide [2.8A] with all the RuPcs suggests that the RuPcs [8a-8e] react with the stilbene [2.7] in a concerted manner as shown in Scheme 5.6.

Table 5.7: *Cis*-stilbene [2.7] epoxidation catalyzed by ruthenium Pcs at 0.45 mol% concentration^[a]

Entry	Catalyst	Conv. (%)	Yields (%)		
			[2.8A]	[2.8B]	[2.13]
1	8f	20	11	1	1
2	8a	100	84	4	2
3	8b	100	86	4	1
4	8c	100	85	5	1
5	8d	94	83	4	2
6	8e	76	60	4	1

^[a] Reaction conditions: Toluene, 90°C, catalyst/substrate/oxidant = 1:220:330 for 24 h.

The cleavage product, benzaldehyde [2.13], was only observed after 15 hours of reaction time and amounted to only 2 % after 24 hours. The relative amounts of the [2.8B] and [2.13] formed did also not vary with the different ligands attached to the metal complex. Since the epoxide yields dropped over prolonged reaction times (>15 h) and the benzaldehyde [2.13] was only observed after *ca.* 15 h, it could be concluded that this product possibly originated from decomposition (over oxidation) of the stilbene oxide [2.7]. This was confirmed by a control experiment where *cis*-stilbene oxide [2.7] was subjected to the reaction conditions present during the reaction resulting in extensive transformation into benzaldehyde [2.13] (within 15 h) as was observed by Brassan and Morvillo.^{18a,b}

The activity and stability of all six catalysts in the epoxidation of *cis*-stilbene [2.7] was further evaluated through the determination of turnover number (TON) and frequency (TOF) (Table 5.8). In this case, the catalyst (0.1 mol %) was reacted with 1000 eq. of substrate and 1500 eq. oxidant at 90°C for 48 hours. Since catalyst concentrations were lower, reaction rates also dropped with the consequence of increased decomposition of the epoxide [2.8A] to benzaldehyde [2.13] and thus lower epoxide yields. High TONs of up to 570 after 48h for RuPc-C12 [8c] at TOFs of 25 to 45 h⁻¹ were however obtained.

Table 5.8: *Cis*-stilbene [2.7] epoxidation by ruthenium Pcs in 0.1 mol% concentration^[a].

Entry	Cat.	Conv. [%]	Yields			Selectivity [%] ^[b]	TOF(h ⁻¹)[TON] ^[c]
			[2.8A]	[2.8B]	[2.13]		
1	8a	64	40	3	9	77	41 [520]
2	8b	66	44	3	10	77	40 [560]
3	8c	72	46	2	9	81	45 [570]
4	8d	55	34	3	13	68	32 [490]
5	8e	46	26	3	5	76	25 [340]

^[a] Reaction conditions: Toluene (2ml), 90°C, catalyst/substrate/oxidant molar ratio = 1:1000:1500 for 48 h [b] 2.8A/(2.8A+2.8B+2.13). [c] TONs after 48 h.

Compared to the alkyl substituted RuPcs [8a-8e], the unsubstituted ruthenium Pc, Pc-Unsub [8f], were much less reactive even at the early stages of the reaction (< 2 h) when the concentration of catalyst and substrate were still high (Figure 5.4, 0.45 mol % RuPc). Yields of less than 10% were recorded with RuPc-Unsub [8f] after the first 2 hrs of the reaction compared to the 30-60 % for the alkyl substituted equivalents.

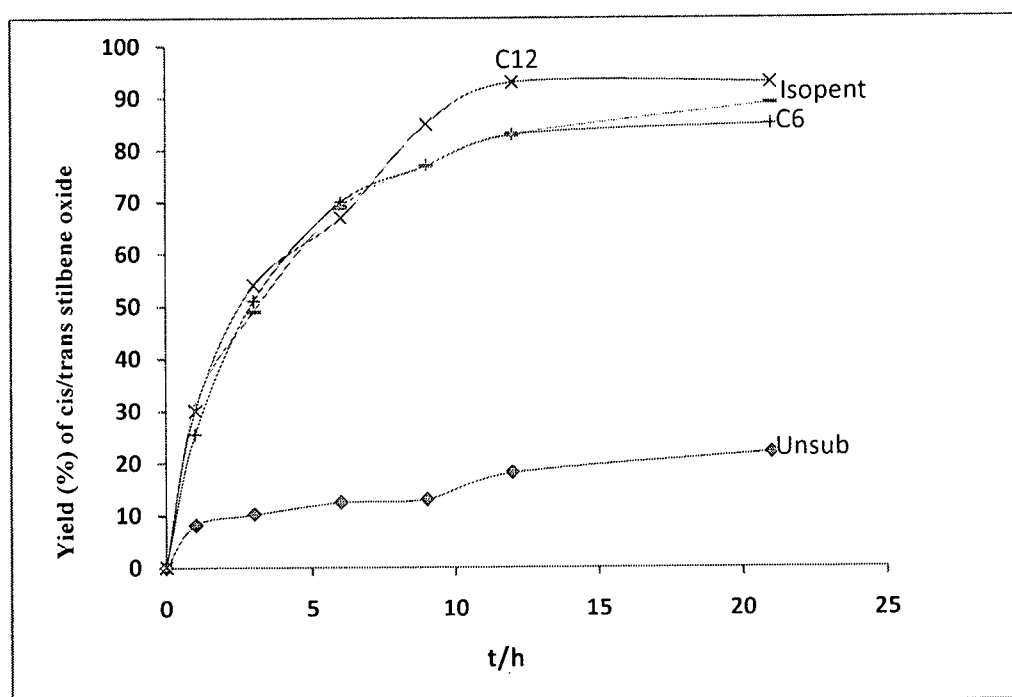
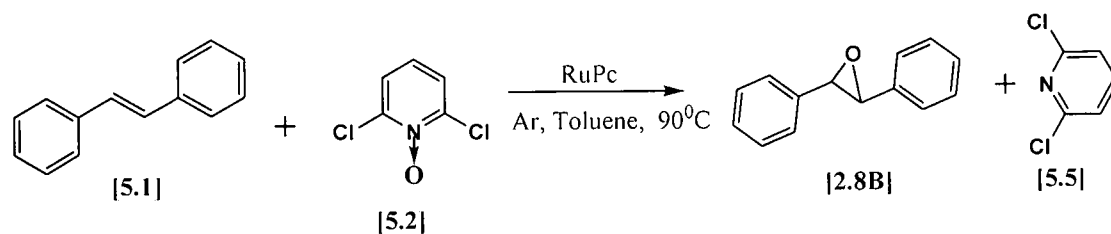


Figure 5.4. Reaction progress for *cis*-stilbene [2.7] epoxidation with 0.45 mol% catalysts in toluene (2 ml) at 90°C. RuPc-Unsub [8f], RuPc-C6 [8a], RuPc-C12 [8c], and RuPc-Isopentyl [8d].

5.2.5 Epoxidation of *trans*-stilbene [5.1] with ruthenium phthalocynine complexes using 2,6-dichloropyridine-N-oxide [5.2] as oxidant.

In order to compare the activity of the ruthenium Pc complexes towards *cis*- and *trans*-stilbene [5.1] epoxidation with 2,6-DCPNO, *trans*-stilbene [5.1] was thus subjected to reactions with the RuPc catalysts. The investigation was conducted with three catalyst: substrate ratios, i.e. 1:220 (0.45 cat mole %), 1:1000 (0.1 cat mole %) and finally 1:5000

(0.02 cat mole %) in an attempt to obtain higher TONs. In each case *trans*-stilbene oxide [2.8B] was the sole product of epoxidation (Scheme 5.8).



Scheme 5.8

In an attempt to obtain higher TONs epoxidation at a catalyst: substrate ratio of 1:220 (0.45 mol %) resulted in complete conversion, with excellent selectivities (>75 %), for all catalysts within 15 hours, the only exception being the unsubstituted RuPc complex [8f] (Table 5.8, entry 1), for which little epoxidation was observed (Table 5.9, entry 1). From the reaction progress graph (Figure 5.5), it is clear that the optimum yields were reached after *ca.* 10 and 12 hours, respectively, for the reactions with RuPc-C6 [8a] and RuPc-Cyclohexyl [8e] and that the epoxide again showed some decomposition with an incidental drop in yield towards the end of the reaction period.

Table 5.9: *Trans*-stilbene [5.1] epoxidation by ruthenium Pcs at 0.45 mole % catalyst concentration.^[a]

Entry	Catalyst	Conv. [%] ^b	Yield (%)	Selectivity (%)
1	8f	27	18	67
2	8a	100	99	99
3	8b	100	99	99
4	8c	100	100	100
5	8d	100	75	75
6	8e	95	84	76

^[a] Reaction conditions: Toluene, 90°C, catalyst/substrate/oxidant molar ratio = 1: 220: 330 for 24 h. ^[b] Conversions were determined by GC using dodecane as internal standard.

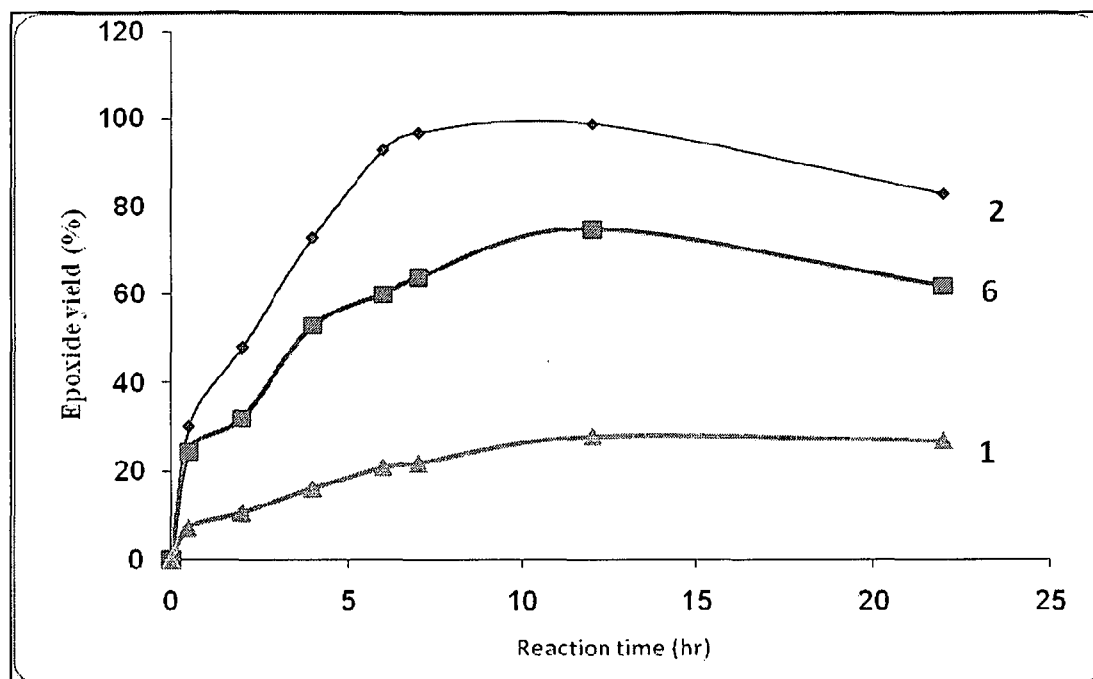


Figure 5.5: Reaction progress for *trans*-stilbene [5.1] epoxidation with 0.45 mol% in toluene (2 ml) at 90°C with complexes 1= RuPc-Unsub [8f], 2= RuPc-C6 [8a] and 6= RuPc-Cyclohexyl [8e].

In order to determine optimum catalyst activity and to investigate possible differences between the catalysts, the catalyst concentration was lowered to 0.1 mol % (catalyst/alkene/2,6-DCPNO = 1:1000:1500) and the reactions repeated. The selectivity and conversions for the alkyl substituted RuPc [8a-8e] were still relatively high (77-87 % and 68-100 % respectively) (Table 5.10, entry 1-5), while turnovers of up to 840 were obtained (Table 5.10, entry 3) after 48 hours.

These results undoubtedly showed that the attachment of alkyl substituents to the non-peripheral positions of phthalocyanines does improve the catalytic activity of these complexes. While it seemed that the activity, yield, and selectivity for the linear alkyl substituted complexes RuPc-C6 [8a], RuPc-C8 [8b] and RuPc-C12 [8c] (Table 5.10, entries 1-3) were the same within experimental error, it was clear that these catalysts showed better activities than the more bulky complexes, RuPc-Isopentyl [8d] and RuPc-Cyclohexyl [8e] (Table 5.10, entries 4 and 5). This observation is in agreement with that

of Groves who also found that oxygen transfer is sensitive to the steric bulk in the vicinity of the active metal centre.²⁶

Table 5.10: *Trans*-stilbene [5.1] epoxidation catalyzed by ruthenium Pcs at 0.1 mole % catalyst concentration.^a

Entry	Catalyst	Conversion (%) ^b	Yield (%)	Selectivity (%)	TON after 48 h
1	8a	100	82	82	820
2	8b	100	78	78	780
3	8c	100	84	84	840
4	8d	73	56	77	560
5	8e	68	59	87	590

^[a] Reaction conditions: Toluene (2ml), 90°C, catalyst/substrate/oxidant molar ratio = 1:1000:1500 for 48 h. ^[b] Conversions were determined by GC using dodecane as internal standard.

These results greatly contrast those obtained in the homogeneous and heterogeneous epoxidation of *trans*-stilbene [5.1] by the ruthenium porphyrin/*N*-oxide system as reported by Hirobe,¹⁹ Gross,²⁰ Berkesel,¹⁰ and Zhang.²¹ These workers reported poor or no epoxidation of this substrate even with highly electron deficient ruthenium porphyrin complexes. The best conversion and turnover with homogeneous chiral ruthenium porphyrins was reported to be *ca.* 21 % and 270 (after 16 h)^{14a} respectively, while heterogeneous polymer-supported ruthenium porphyrin catalysts gave 88% conversion and 870 TON (after 24 h).²² The poor reactivity of *trans*-stilbene [5.1] in homogeneous epoxidation with these systems was attributed to steric hindrance during the 'side on' approach of the bulky *trans*-stilbene [5.1] to the active site of the metal complex. It is thought that the incoming substrate, due to its angle of approach to the reactive centre, is blocked by the plane of the metal complex and the substituents on the metal complex such that it does not get to the **Ru=O** site (*cf.* Scheme 2.10). More bulky substituents on the porphyrin periphery decreased the reactivity even more.²³

On the basis of these widely accepted views, the facile epoxidation of *trans*-stilbene [5.1] by the alkylsubstituted ruthenium phthalocyanines suggest a difference in either the orientation of the substituents around the metal oxo ($\text{Ru}=\text{O}$) moiety or an approach to the reactive site different from the 'side-on' view (Fig. 5.7). As mentioned earlier, non-peripherally substituted Pcs are non-planar,²⁴ adopting a saddled shape structure. For example, the metal free isopentyl phthalocyanine is inclined at an angle of 32° from the core of the complex. Such inclination, if the same in the ruthenium phthalocyanine complexes prepared in this study, will expose the reactive metal oxo ($\text{Ru}=\text{O}$) part of the complex and therefore facilitate its interaction with the substrate. On the other hand, a mechanism involving a 'top on' approach (Fig. 5.7) of the olefin to the $\text{Ru}=\text{O}$ as suggested by Liu *et al.*²³ will sufficiently account for such high activity despite the bulkiness of the ligands.

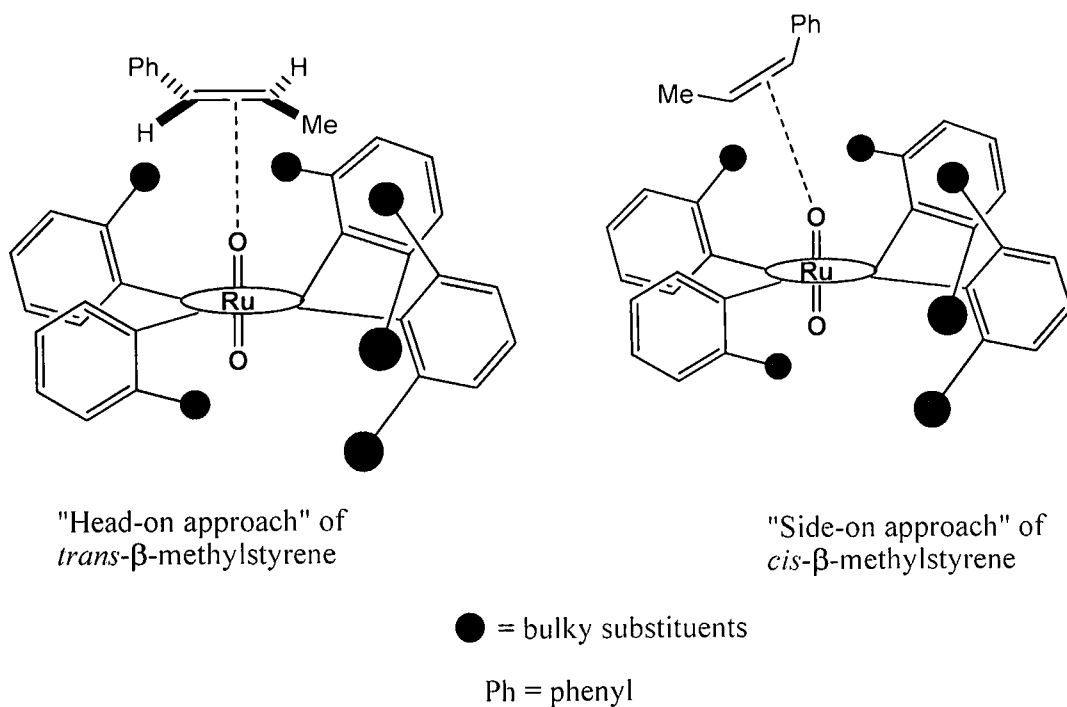


Figure 5.7²³

In order to determine if some of the catalyst might have been deactivated by aggregation and to see if differences in catalyst activity could be accentuated, the catalyst concentration was reduced even further to 0.02 mol % (catalyst:alkene:2,6-DCPNO = 1:5000:5000) and the reaction repeated with all the prepared catalysts [8a-8e]. As indicated in Table 5.11, all of the catalysts, except RuPc-Cyclohex [8e], proved to be quite active with turnover frequencies (TOF) of *ca.* 170 h⁻¹. Although yields and conversions dropped quite dramatically when compared to the reactions at 0.45 mole % (Table 5.9), the increase in turnover numbers indicated that the catalyst were still active up to the end of the reactions in the previous runs (at the higher concentrations). Again the high activity of RuPc-C12 [8c] relative to the other catalysts is reflected in its higher turnover frequency (TOF). Since the best results reported in literature for the homogeneous epoxidation of *trans*-stilbene [5.1] by Gross²⁰ and Che¹¹ contained TONs of 243 (after 48 h) and 270 (after 16 h) respectively, it could be concluded that RuPc-C12 [8c] (Table 5.11, entry 4) with a turnover number of 1,200 (after 48 h) is the best catalyst for the epoxidation of *trans*-stilbene [5.1] described to date.

Table 5.11: *Trans*-stilbene [5.1] epoxidation catalyzed by ruthenium phthalocyanines at 0.02 mole % catalyst concentration.^a

Entry	Catalyst	Conversion (%) ^b	Yield (%)	TOF (h ⁻¹)	TON ^c
1	8a	22	22	151	1,085
2	8b	23	23	169	1,150
3	8c	24	24	147	1,200
4	8d	18	17	139	850
5	8e	20	20	93	1,002

^[a] Reaction conditions: Toluene (2ml), 90°C, catalyst/substrate/oxidant molar ratio = 1:5000:5000 for 48 h. ^[b] Conversions were determined by GC using dodecane as internal standard. ^[c] Turnover number after 48 h.

5.2.6 Competitive epoxidation of *cis*- [2.7] and *trans*-stilbene [5.1] with ruthenium phthalocyanine complexes.

Since it is claimed in literature that the homogeneous⁹ and heterogeneous²⁵ ruthenium porphyrin-*N*-oxide systems show preference towards the epoxidation of *cis*-stilbene [2.7] over the *trans*-isomer [5.1] (94% *cis*-epoxide [2.8A] vs 5% *trans*-epoxide [2.8B] and 93% *cis*-epoxide [2.8A] vs 31% *trans*-epoxide [2.8B] respectively), this aspect of the current RuPc catalysts was subsequently evaluated. Thus competitive epoxidation of a 1:1 mixture of *cis*- [2.7] and *trans*-stilbene [5.1] were carried out with a catalyst concentration of 0.23 mol% over a 24 h reaction period.

The ratios of *trans*-epoxide [2.8B]: *cis*-epoxide [2.8A] (Table 5.12) and the kinetic profiles (Figure 5.6, RuPc-C6 [8a]) both indicate the *trans*-epoxide [2.8B] to form 1.14-1.35 times faster than the *cis*-epoxide [2.8A]. This represents the opposite of what was found for the porphyrin system (*vide supra*) and resembles the *m*-chloroperoxybenzoic acid epoxidation of *cis*- [2.7] and *trans*-stilbene [5.1] in methylene chloride.²⁶

Table 5.12: *Cis/trans*-stilbene [2.7/5.1] epoxidation catalyzed by RuPcs at 0.23 mole % catalyst concentration.^[a]

Entry	Catalyst	<i>Trans</i> -epoxide [2.8B]	<i>Cis</i> -epoxide [2.8A]	Ratio (2.8B/2.8A)
1	8f	16	12	1.35
2	8a	91	70	1.3
3	8b	89	74	1.2
4	8c	98	73	1.34
5	8d	84	74	1.14
6	8e	37	31	1.19

^[a] Reaction conditions: 0.23 mol% catalyst, 1:1 mixture of *cis*- [2.7] and *trans*-stilbene [5.1] for 24 h

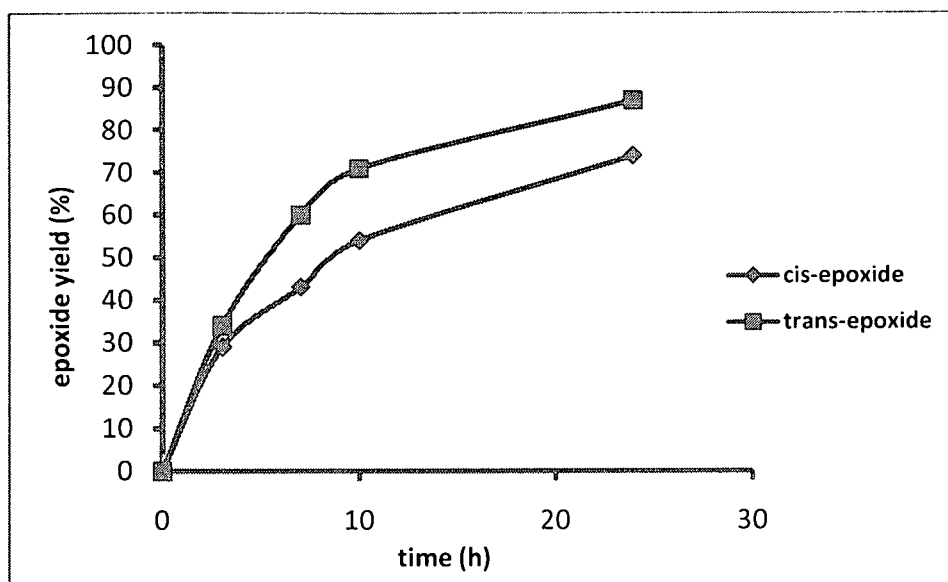


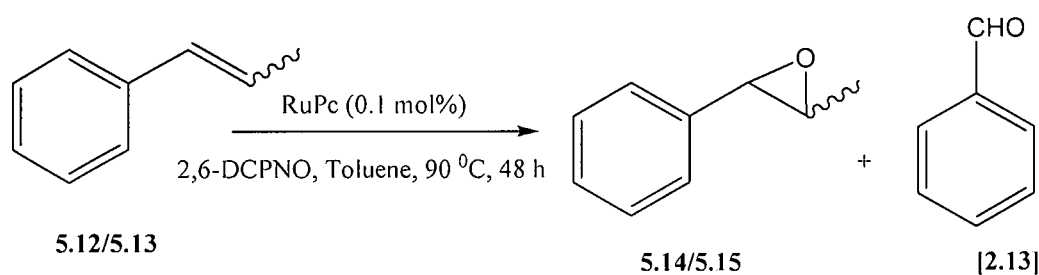
Figure 5.6: Time course plot for RuPc-C6 [8a] (0.23 mol%) catalyzed epoxidation of a 1:1 mixture of *cis*- [2.7] and *trans*-stilbene [5.1] at 90 °C for 24 h.

Since the *cis*- [2.8A] and *trans*-epoxides [2.8B] were formed at almost equal rates, it seems reasonable to conclude that both substrates have equal reactivity towards the oxidizing Ru=O complex and that there is an equal chance of oxygen transfer to either substrate. Contrary to the porphyrin-iodosylbenzene and porphyrine-*N*-oxide systems, variation in the alkyl substituents did not have any marked influence on the selectivities. However, the overall epoxidation rate dropped for the most bulky complex RuPc-Cyclohex [8e] (Table 5.12, entry 6).

The fact that the selectivities did not change with bulkier substituents further indicate that transfer of oxygen from the generated Ru=O species to substrates encounter almost no interference from the alkyl substituents or from the phenyl groups on the stilbenes.

5.2.7 Epoxidation of *cis*- [5.12] and *trans*- β -methylstyrene [5.13] over ruthenium Pc complexes.

As the conjugated phenyl groups in stilbenes [5.1] and [2.7] are slightly electron withdrawing, one of these groups was subsequently replaced by a methyl group to investigate the activity of the ruthenium phthalocyanines in this scenario. Epoxidation of *cis*- [5.12] and *trans*- β -methylstyrene [5.13] was thus investigated with 0.1 mol% of the catalysts for 48 h at 90 °C.



cis-isomer = [5.12] and [5.14]

trans-isomer = [5.13] and [5.15]

Scheme 5.9

For both epoxides ([5.14] and [5.15]), high conversions (74 – 90 %) and yields (67 – 75 %), good selectivities (80 – 88 %), and moderate turnovers (670 - 750 in 48 h) were obtained for all RuPcs [8a-8d], except RuPc-cyclohex [8e] for which only moderate conversions (53 and 62 % respectively), yields (46 and 49 % respectively) and TONs (460 and 490, respectively, in 48 h) were found (Tables 5.13 and 5.14). In comparison, the unsubstituted RuPc (8f) gave extremely low conversions (10%), yields (4 – 7 %), and TONs (50 – 70 in 48 h), while both substrates also produced minor amounts (1-6%) of the C=C bond cleavage product, benzaldehyde [2.13]. Since the epoxide selectivity was similar for all of the alkyl substituted ruthenium Pcs, it could be concluded that the substituents do not really interfere with the transfer of oxygen to the substrate.

Table 5.13: *Trans*- β -methylstyrene [5.12] epoxidation catalyzed by ruthenium Pcs at 0.1 mole % catalyst concentration.^[a]

<i>Entry</i>	<i>Catalyst</i>	Conv. (%) ^[b]	Yield (%) ^[c]	Selectivity (%) ^[d]	<i>TON</i> in 48 h
5.15(2.13)					
1	8f	10	4 (1)	50	50
2	8a	84	70 (3)	83	700
3	8b	82	68 (4)	83	680
4	8c	85	75 (6)	88	750
5	8d	84	67 (3)	80	670
6	8e	62	49 (3)	79	490

^[a] Reaction conditions: Toluene, 90^oC, catalyst/substrate/oxidant molar ratio = 1:1000:1500 for 48 h. [b] Conversions were determined by GC using dodecane as internal standard. [c] [5.15] identified by GC-MS. 5.14 and 5.15 could not distinguished from each other as their retention times were identical (23.04 min). [d] Epoxide selectivity.

Since the Fe(II)Pc/PhIO system reported on by Jorgenson^{1a} gave only 63 % conversion with a turnover number of < 50 in the epoxidation of *trans*- β -methylstyrene [5.13], it is evident that the alkylsubstituted ruthenium Pcs tested during the current investigation are considerably more reactive than the Jorgenson system.^{1a} The homogeneous ruthenium porphyrin/*N*-oxide system with a substrate conversion of only 24 % at the same catalyst loading is also inferior to the current RuPc catalysts in the epoxidation of *trans*- β -methylstyrene,²¹ while the heterogeneous ruthenium porphyrin/*N*-oxide system, which gave a TON of up to 890 (24 h)²² in the epoxidation of [5.13], can be viewed equally active when compared to the RuPc complexes [8a-8e].

Table 5.14: *Cis*- β -methylstyrene [5.13] epoxidation catalyzed by ruthenium Pcs at 0.1 mol% catalyst concentration.^[a]

Entry	Catalyst	Conv. (%) ^[b]	Yields (%) 5.14(2.13) ^c	Selectivity (%) ^[d]	TON in 48h
1	8f	10	7(1)	70	70
2	8a	88	72 (4)	82	720
3	8b	87	70 (4)	81	700
4	8c	90	72 (3)	80	720
5	8d	74	67 (3)	87	670
6	8e	53	46 (3)	87	460

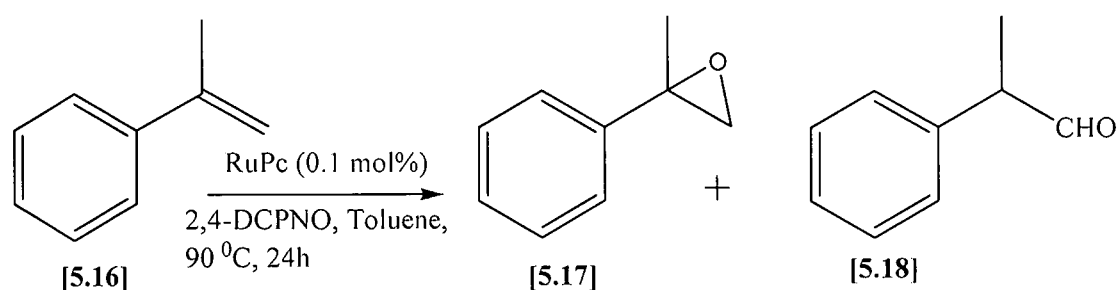
^[a] Reaction conditions: Toluene, 90°C, catalyst/substrate/oxidant molar ratio = 1:1000:1500 for 48 h. ^[b] Conversions were determined by GC using dodecane as internal standard. ^[c] Products identified by GC-MS. **5.14** and **5.15** could not be distinguished from each other as their retention times were identical (23.04 min). ^[d] Epoxide selectivity.

The high reactivity of *trans*- β -methylstyrene [5.13] with the bulky alkyl substituted ruthenium phthalocyanines [8e] again contradicted the 'side on approach' model, which, if operational, should have resulted in little or no activity in the current epoxidations as the eight bulky alkyl substituents should have crowded the Ru=O moiety enough to prevent the substrate from reaching it 'side on'.

5.2.8 Epoxidation of α -methylstyrene [5.16] over phthalocyanine ruthenium catalysts.

The isomeric α -methylstyrene [5.16] was subsequently evaluated to investigate the effect of 1,1-disubstitution of the substrate *versus* 1,2-substitution. Thus, treatment of α -methylstyrene [5.16] with all ruthenium Pcs [8a-8f] (0.1 mole %) and 2,6-dichloropyridine-*N*-oxide [5.2] for 48 h afforded 2-phenyl-1-epoxypropane [5.17] together with small quantities (up to 3%) of aldehyde [5.18]. Under the prevailing conditions, substrate conversions of 74 - 88 % as well as selectivities of > 66 % were

again obtained for the substituted RuPcs [8a-8e] while turnovers between 660 and 750 were found after 48 h. As for the β -methylstyrenes [5.12 and 5.13], the RuPc [8e] was the worst of the substituted ruthenium catalysts giving only 53 % conversion with a turnover number of 480 in 48 h (Table 5.15, entry 5).



Scheme 5.10

Table 5.15: α -Methylstyrene [5.16] epoxidation catalyzed by RuPcs at 0.1 mole % catalyst concentration.^[a]

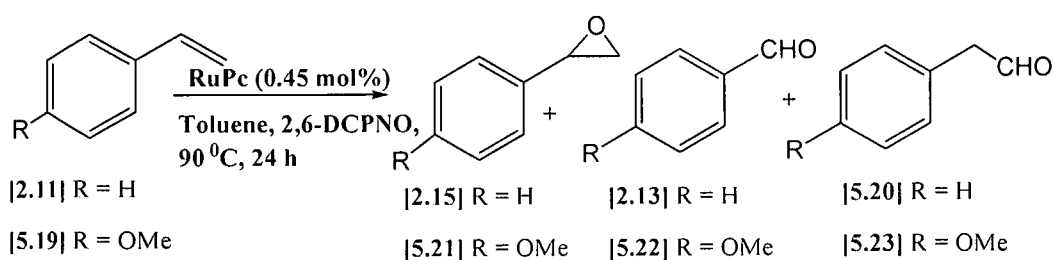
Entry	Catalyst	Conv. (%) ^b	Yields (%) ^c 5.17(5.18)	Selectivity (%) ^d	TON in 48 h
1	8f	18	12(<1)	66	120
2	8a	88	72(3)	82	750
3	8b	87	70 (2)	80	720
4	8c	79	52(12)	66	640
5	8d	74	64 (2)	86	660
6	8e	53	46 (2)	87	480

^[a] Reaction conditions: Toluene, 90 °C, catalyst/substrate/oxidant molar ratio = 1:1000:1500 for 48 h [b] Conversions were determined by GC using dodecane as internal standard. [c] Products identified by GC-MS. [d] Epoxide selectivity.

Conversions and yields were remarkably comparable to those obtained for the epoxidation of *cis*- β -methylstyrene [5.13] in the presence of all the catalysts except for RuPc-C12 [8c], which performed considerably poorer with this substrate (79 % conversion, 52 % yield, 66 % selectivity and 640 TON in 48 h *versus* 90 % conversion, 72 % yield, 80 % selectivity and 720 TON in 48h for *cis*- β -methylstyrene [5.13]; Tables 5.14 and 5.15). The reason for this outlier result is not understood, but the similarities points to the absence of steric interference between the methyl group in α -methylstyrene [5.16] and the catalyst geometry in the transition state.

5.2.9 Epoxidation of styrene [2.11] and 4-methoxystyrene [5.19] over ruthenium Pc catalysts.

Due to its high reactivity and tendency towards polymerization, it was decided to investigate the catalytic activity of the ruthenium Pcs towards the epoxidation of the difficult to handle substrate, styrene [2.11]. Treatment of styrene [2.11] with 0.45 mol% of the catalysts for 24 hr, gave the styrene epoxide [2.15] in low to moderate conversions and selectivities towards the expected product (Table 5.16). The sought after product [2.15] was accompanied by fairly large amounts of the cleavage products, benzaldehyde [2.13] and phenylacetaldehyde [5.20] (Scheme 5.11).



Scheme 5.11

While no clear trend or influence on selectivity could be identified originating from the alkylsubstituents attached to the Pcs, it was noticed that reaction time played a crucial role in the product distribution. With the RuPc-C12 [8c] reaction for example, a product

distribution of 57, 36 and 15 % yields for [2.15], [2.13] and [5.20] respectively, were obtained at 28 % conversion after 24 h. When the reaction with RuPc-C8 [8b] was left to run for 36 h, [2.13] became the main product with a product distribution of 38, 17, and 25 % for [2.13], [5.20], and [2.15] respectively (77 % substrate conversion). Similar variations in the product ratios were observed in the epoxidation of styrene with 0.1 mol% of [Ru^{II}(F₂₀-tpp(CO))] [2.20h], [Ru^{II}(2,6-Cl₂tpp(CO))] [2.20j], or [Ru^{II}(F₂₈-tpp(CO))] [2.20i] and 2,6-dichloropyridine-*N*-oxide [5.2], PhIO [2.9] or TBHP as oxidants.³² Deactivation of the ruthenium catalyst by the aldehyde³⁴ might explain why prolonged reaction times did not result in substantially better conversions and yields.

Table 5.16: Styrene [2.11] epoxidation catalyzed by ruthenium Pcs at 0.45 mole % catalyst concentration.^[a]

Entry	Catalyst	Conv. (%) ^[b]	Selectivity (%)		
			[2.15]	[2.13]	[5.20]
1	8f	7	35	20	19
2	8a	39	39	33	15
3	8b	44	42	29	18
4	8c	28	57	36	15
5	8d	35	51	31	17
6	8e	17	41	35	12

^[a] Reaction conditions: Toluene, 90^oC, catalyst/substrate/oxidant molar ratio = 1:220:330 for 24 h. ^[b] Conversions were determined by GC using dodecane as internal standard.

Since the conversion rates for styrene [2.11] with all of the RuPcs were rather low, it was decided to extend the investigation to the more electron rich 4-methoxystyrene [5.19]. (Ep)oxidation of [5.19] (Table 5.17) catalyzed by 0.45 mol% of the RuPc complexes [8a-8e] in toluene gave ([5.21], [5.22] and [5.23]) with high substrate conversions (67 - 92 % within 24 hours), but only moderate selectivities towards the desired epoxide product. The epoxide [5.21], however, remained the main product. It could therefore be concluded that while the electron donating properties of the 4-methoxy group had a

beneficial effect on the production of the desired epoxide, it also enhanced further/parallel oxidation of the product/styrene to the aldehydes [5.22] and [5.23].

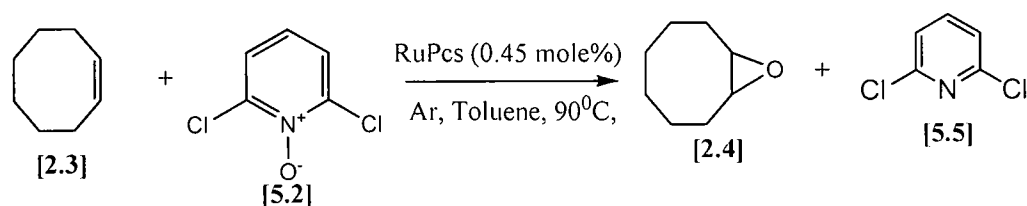
Table 5.17: 4-Methoxystyrene [5.19] epoxidation catalyzed by ruthenium Pcs at 0.45 mole % catalyst concentration.^[a]

Entry	Catalyst	Conv. (%) ^[b]	Selectivity(%)		
			[5.21]	[5.22]	[5.23]
1	8a	90	51	29	14
2	8b	92	44	25	14
3	8c	69	32	25	7
4	8d	67	64	21	13
5	8e	51	41	35	12

^[a] Reaction conditions: Toluene, 90°C, catalyst/substrate/oxidant molar ratio = 1:220:330 for 24 h. ^[b] Conversions were determined by GC using dodecane as internal standard.

5.2.10 Epoxidation of cyclooctene [2.3] over phthalocynine ruthenium complexes.

With the performance of the ruthenium phthalocyanines [8a-8f] being evaluated in the epoxidation of various substrates with the double bonds conjugated to phenyl rings, it was thus decided to extend the investigation to the epoxidation of an isolated double bond. As the epoxidation of cyclooctene [2.3] have been investigated with a variety of catalytic systems,^{1a, 30, 31} this substrate was selected for this purpose. With 0.45 mol% of the alkylsubstituted ruthenium phthalocyanine complexes [8a-8f], the catalytic epoxidation of cyclooctene [2.3] with 2,6-dichloropyridine *N*-oxide [5.2] proceeded efficiently to afford cyclooctene oxide [2.4] as the only product (Scheme 5.12) in high yields (68-86 %) and selectivity (80–87 %) (Table 5.18) within 15 h.



Scheme 5.12

The unsubstituted RuPc **[8f]** gave very low epoxide yields (Table 5.18, entry 1). Substrate conversion was low for the unsubstituted RuPc **[8f]** (15 %) but high for the alkylsubstituted RuPcs **[8a-8e]** (78-100 %) (Table 5.18, entry 1-6). Compared to the other complexes, the epoxide formed faster with Rupc-C6 **[8a]** (2, Figure 5.8).

Table 5.18: Cyclooctene **[2.3]** epoxidation with RuPcs at a catalyst concentration of 0.45 mole %.^[a]

Entry	Catalyst	Conversion (%) ^[b]	Yields (%)	Selectivity (%)
1	8f	15	10	67
2	8a	100	82	86
3	8b	100	84	84
4	8c	100	86	86
5	8d	93	74	80
6	8e	78	68	87

^[a] Reaction conditions: Toluene, 90°C, catalyst/substrate/oxidant molar ratio = 1:220:330 for 20 h. ^[b] Conversions were determined by GC using dodecane as internal standard.

Using 0.23 mol% catalysts, 48 h was required for high substrate conversion (93%, Table 5.19, entry 3) to be realized. 99 % Substrate conversion was realized in 24 h when the same reaction was catalyzed by 0.2 mole % immobilized ruthenium porphyrins at 25 °C.²⁵ Although epoxide yields were still good (> 62 %, except for RuPc-Cyclohex **[8e]**) with 0.23 mol% catalyst, a slight drop in selectivity was noticed (Table 5.19), probably due to the extended reaction time.

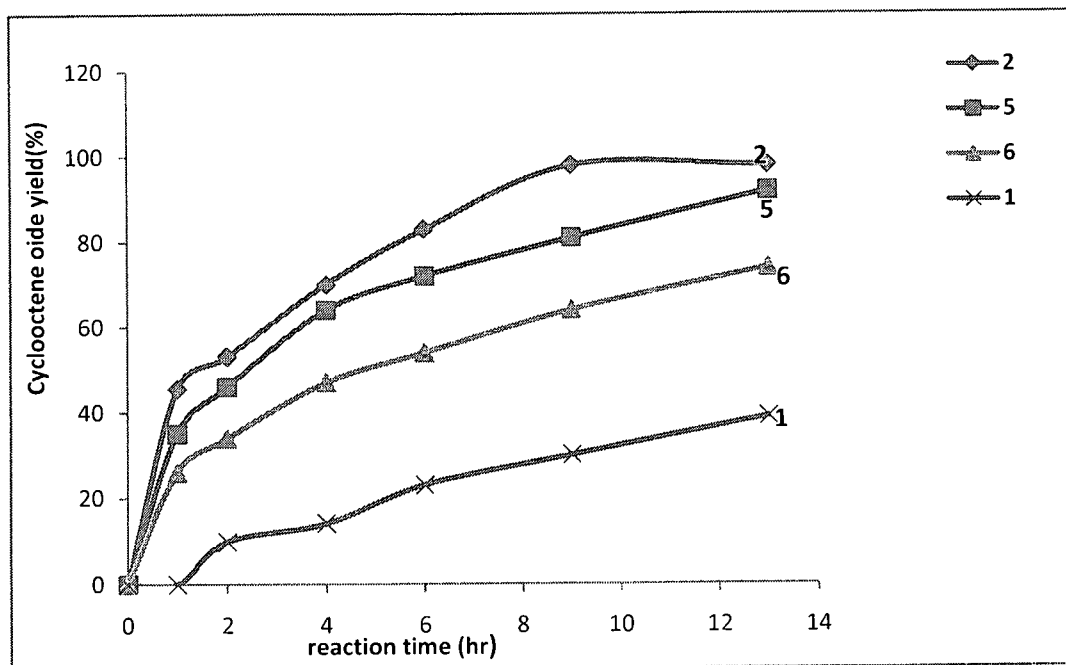


Figure 5.8: Time course plot for ruthenium phthalocyanine catalyzed epoxidation of cyclooctene [2.3] at 90°C and 0.45 % catalyst load (catalyst/substrate/oxidant molar ratio = 1:220:330). **1**= RuPc-Unsub [8f], **2**= RuPc-C6 [8a], **5** = RuPc-Isopentyl [8d], **6**= RuPc-Cyclohexyl [8e].

High turnovers (up to 365 TO in 48 h) were recorded for the epoxidation of cyclooctene [2.3] with these complexes at a maximum rate of 43 TO/h (Table 5.19, entry 2). The yields and TON are higher than those reported for the Fe(II)Pc catalyzed epoxidation of this substrate with PhIO.²⁷

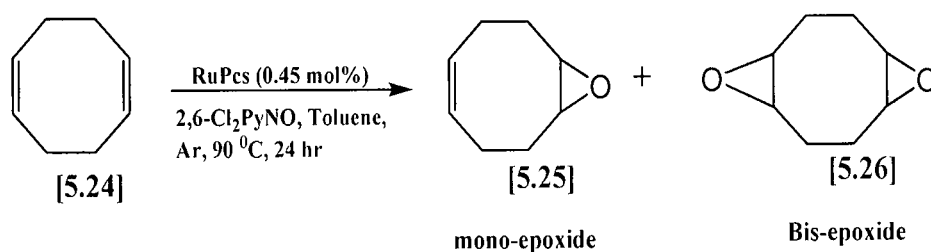
Table 5.19: Cyclooctene [2.3] epoxidation with RuPcs at catalyst concentration of 0.23 mole %.^[a]

Entry	Cat.	Conv. (%) ^[b]	Yields (%)	TON after 48h (TOF) ^[c]	Selectivity (%)
1	8a	79	61	305 (43)	77
2	8b	93	73	362 (41)	73
3	8c	87	73	365 (40)	84
4	8d	82	62	310 (42)	76
5	8e	66	44	220 (40)	67

^[a] Reaction conditions: Toluene, 90°C, catalyst/substrate/oxidant molar ratio = 1:500:750 for 48 h. ^[b] Conversions were determined by GC using dodecane as internal standard. ^[c] TOF after 2 hr of reaction.

5.2.11 Epoxidation of 1,5-cyclooctadiene [5.24] over phthalocyanine ruthenium catalysts.

After establishing that cyclooctene [2.3] could indeed be epoxidized in good yield and selectivity by ruthenium phthalocyanine catalysts, it was decided to study the selectivity of these catalysts towards the epoxidation of one of two equal double bonds. 1,5-Cyclooctadiene [5.24], which can be epoxidized to the *mono-epoxide* [5.25] or *bis-epoxide* [5.26] (Scheme 5.13), was thus selected as model compound.



Scheme 5.13

Employing 0.45 mole % catalysts, GC-MS analysis showed that 1,5-cyclooctadiene [5.24] epoxidized to the mono-epoxide [5.25] only. There was no indication of the formation of the bis-epoxide [5.26] even when the reaction time was extended. Bhattacharjee and Anderson²⁸ reported similar observations in the manganese-salen/O₂-aldehyde system and explained that [5.25], once formed, is more reluctant to undergo further oxidation to [5.26] compared to the oxidation of [5.24]. The alkyl substituted ruthenium Pcs [8a-8e] (Table 5.20, entry 2-6) were once again more active than the unsubstituted ruthenium Pc [8f] (Table 5.16, entry 1). The observed conversions (48-62%) and selectivity (46-65%) for the oxidation of 1,5-cyclooctadiene [5.24] by the various catalysts are lower in comparison to that of cyclooctene [2.3] (Tables 5.18 and 5.19). Previous work by Larsen and Jorgensen²⁷ showed that the epoxidation of this substrate with the iron(II) Pc/iodosylbenzene system afforded a mixture of both epoxides [mono-epoxide [5.25] (25%), di-epoxide [5.26] (5%)], whereas only the *bis-epoxide* [5.26] was selectively formed in 76 % yield by a polymer supported ruthenium porphyrin/*N*-oxide system.²⁹

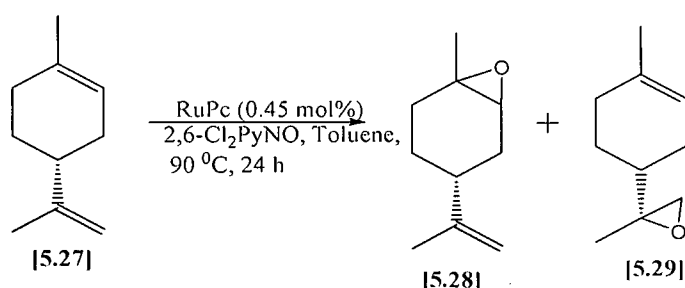
Table 5.20: 1,5-Cyclooctadiene [5.24] epoxidation with RuPcs at 0.45 mole % catalyst concentration.^[a]

Entry	Catalyst	Conv. (%) ^[b]	Yield (%) ^c	Selectivity to [5.25] (%)	TON after 24 h
1	8f	11	5	45	11
2	8a	52	24	46	53
3	8b	48	31	65	68
4	8c	62	34	55	75
5	8d	50	24	48	53
6	8e	53	28	53	62

^[a] Reaction conditions: Toluene, 90°C, catalyst/substrate/oxidant molar ratio = 1:220:330 for 24 h. ^[b] Conversions were determined by GC using dodecane as internal standard. ^[c] Product identified by GC-MS.

5.2.12 Epoxidation of limonene [5.27] over phthalocyanine ruthenium catalysts.

In order to investigate the selectivity of the catalysts under investigation towards the epoxidation of two non-equal double bonds, limonene [5.27] was selected as substrate. When (+)-limonene [5.27] was exposed to epoxidation conditions with 0.45 mol % of the ruthenium phthalocyanine complexes for 24 hrs, the electron-rich trisubstituted double bond was favoured to afford the epoxide [5.28] (Scheme 5.14).



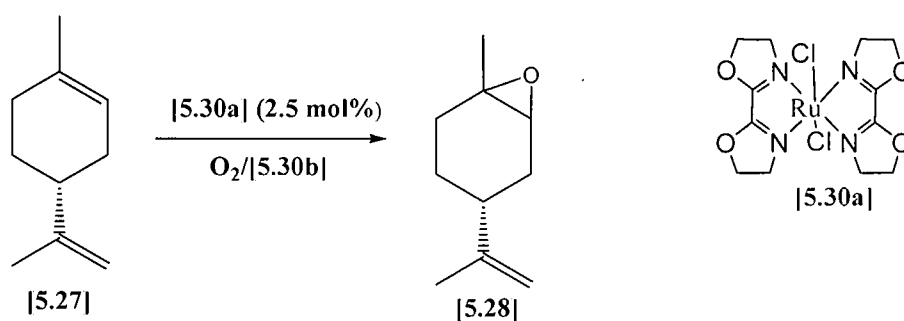
Scheme 5.14

Table 5.21: (+)-Limonene [5.27] catalyzed epoxidation by RuPcs at 0.45 mole % catalyst concentration ^[a]

Entry	Catalyst	Conv. (%) ^[b]	Yield (%)	Selectivity to [5.28] (%)	TON after 24 h
1	8f	13	trace	---	----
2	8a	100	40	40	88
3	8b	100	40	40	88
4	8c	100	42	42	92
5	8d	92	47	51	103
6	8e	96	46	48	101

^[a] Reaction conditions: Toluene, 90 °C, catalyst/substrate/oxidant molar ratio = 1:220:330 for 24 h. ^[b] Conversions were determined by GC using dodecane as internal standard..

Comparable results were obtained for all the alkyl substituted ruthenium phthalocyanine [8a-8e] catalyzed reactions with conversions above 92 % (Table 5.21, entry 2-6). Yields (40-47 %) and selectivity (40-51%) were however low. This result is similar to that reported for the ruthenium-bisoxazole [5.30a] catalyzed epoxidation of this substrate by molecular oxygen and isobutylaldehyde [5.30b] as co-reductant (Scheme 5.15).³⁰

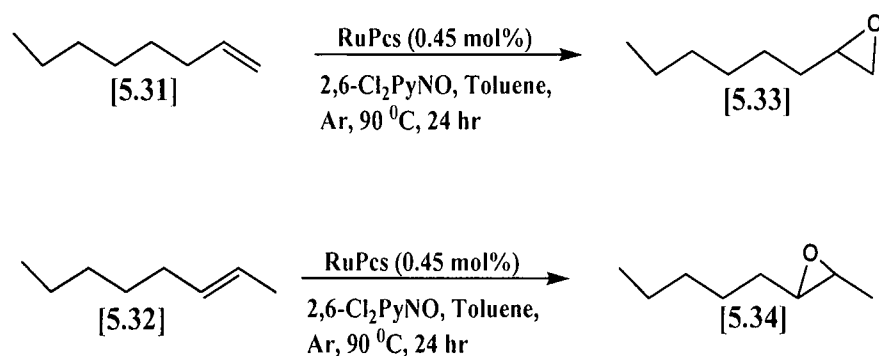


Scheme 5.15

Contrary to the current results, the epoxidation of limonene [5.27] with the homogeneous ruthenium porphyrin/*N*-oxide system previously reported, resulted in mixtures of both [5.28] and [5.29] in varying ratios being obtained.³¹ Yields and selectivities were considerably lower than that obtained for the epoxidation of cyclooctene [2.3] (Tables 5.18 and 5.19).

5.2.13 Epoxidation of aliphatic acyclic alkenes over phthalocyanine ruthenium catalysts.

The focus was finally shifted to the epoxidation of aliphatic acyclic substrates, and specifically those amongst the most difficult to oxidize substrates according to Table 5.22. 1-Octene [5.31] and *trans*-2-octene [5.32], with respective relative epoxidation TOFs of *ca.* 24 and 500, were thus selected as substrates.



Scheme 5.16

Only trace amounts ($\sim 2\%$) of the corresponding epoxides [5.33]/[5.34] could be detected after 24 h in the presence of 0.45 mol% catalyst, and excess 2,6-DCPNO [5.2] (3 eq.) (Scheme 5.16). Increasing the catalyst load to up to 3 mol% or raising the temperature to 100°C did not increase the yield of the epoxide [5.33]/[5.34] at all. The conversion (up to *ca.* 5 %) obtained for both 1-octene [5.31] and *trans*-2-octene [5.32], was comparable to that obtained with the chiral ruthenium porphyrin catalyzed epoxidation of 1-octene [5.31].¹⁰

Table 5.22: General relative catalytic epoxidation rates of alkenes.³³

Alkene	Relative TOFs
Ethylene ($\text{CH}_2=\text{CH}_2$)	1
$\text{RCH}=\text{CH}_2$	24
$\text{RCH}=\text{CHR}$	500
$\text{R}_2\text{C}=\text{CH}_2$	500
$\text{R}_2\text{C}=\text{CHR}$	6500
$\text{R}_2\text{C}=\text{CR}_2$	Very great

5.2.14 Epoxidation of *trans*-stilbene [5.1] over phthalocyanine cobalt Pc [7b].

In order to study the effect metal centres could have on the epoxidation of alkenes in the phthalocyanine/*N*-oxide system; CoPc-C8 [7b] was employed in the epoxidation of *trans*-stilbene [5.1] under the same conditions reported for its ruthenium counterpart with 0.45 mol% catalyst concentration for 24 h. No reaction was observed. This result wasn't totally unexpected as the application of other metalloporphyrins, such as Mn, Fe, Co, Mo and Rh porphyrin complexes in the porphyrin/*N*-oxide system gave no reaction as well.¹⁰

5.3 Conclusions

In this study it was demonstrated for the first time that ruthenium phthalocyanines can be used in the epoxidation of alkenes and that non-peripherally alkyl substituted ruthenium phthalocyanines in particular are highly active catalysts with true catalytic activities at very low concentrations (< 0.45 mole %). Complete conversion and high turnovers (> 800 in 48 h for 0.45 % catalyst load) comparable to or better than those published for other catalytic systems could be obtained for 1,2-dihydronaphthalene [5.3] and *trans*-stilbene [5.1]. At low catalyst load (0.02 mole %), TONs larger than 2000 in 12 h and TOFs above 260 h⁻¹ were obtained for 1,2-dihydronaphthalene [5.3]. The same catalyst load gave TONs above 1000 in 48 h and TOFs above 90 h⁻¹ for *trans*-stilbene [5.1]. Results for the other substrates commonly used to evaluate the activity of epoxidation catalysts, i.e. *cis*-stilbene [2.7], *cis*- [5.12] and *trans*- β -methylstyrene [5.13], α -methylstyrene [5.16], styrene [2.11], 4-methoxystyrene [5.19], cyclooctene [2.3], 1,5-cyclooctadiene [5.24], limonene [5.27] and 1-octene [5.31], were comparable to those reported for other catalytic systems.

All substituted ruthenium phthalocyanines performed markedly better as epoxidation catalysts than the unsubstituted equivalent for all substrates tested, most probably because of reduced levels of aggregation in solution due to the acquired "saddle shape" of substituted ruthenium phthalocyanines with non-peripheral substituents. Increasing the steric bulk of substituents attached to the phthalocyanine lowered the catalytic activity with a general order of reactivity RuPc-C6 [8a] = RuPc-C8 [8b] ~ RuPc-C12 [8c] >

RuPc-Isopentyl [8d] > RuPc-Cyclohex [8e]. RuPc-Cyclohex [8e] had the lowest activity towards all substrates evaluated, which might be ascribed to steric congestion.

These ruthenium phthalocyanines, all of them novel except for RuPc-C8 [8b], proved to be highly effective towards the epoxidation of conjugated and cyclic alkenes and, in the presence of non-equal double bonds, showed selectivity towards the more substituted double bond. The origin of aldehyde formation during epoxidation, and especially in the case of styrene, need to be investigated as deactivation of the ruthenium catalyst by the aldehyde¹⁹ might explain why prolonged reaction times did not result in substantially better conversions and yields. 1-Octene [5.31] and *trans*-2-octene [5.32] epoxidation failed with these catalysts, but is in accordance with the known low reactivity of these substrates.

The unexpected facile epoxidation of *trans*-stilbene [5.1] by these catalysts suggested the approach of the alkene to the metal oxo moiety to be different from the "side-on" approach proposed for alkene epoxidation by porphyrins, whereas a step-wise mechanism with intermediate radical formation (which allows for rotation around the C-C* bond) was furthermore ruled out by the stereospecific epoxidation of *cis*-stilbene [2.7]. A "top on" approach and concerted oxygen transfer mechanism seems to prevail with concomitant stereoretention.

5.4 Future work

This study focused on the effect of non-peripheral substituents on the activity of ruthenium phthalocyanines. Future work will thus include the effect of substitution on the peripheral positions. For both of these systems the effect of activating *versus* deactivating substituents will have to be investigated.

The mechanism of the reaction needs further investigation and the rate-determining step in the catalytic process will have to be determined by obtaining kinetic data for the reaction.

Catalyst activity will have to be improved for it to be able to epoxidize high carbon number alkenes like 1-octene, whereas substituted acyclic alkenes will have to be included in the evaluation of the catalysts.

5. 5 Experimental

5.5.1 Gas chromatography (GC) and tandem gas chromatography-mass spectrometry (GC-MS)

GC analyses were performed on a Shimadzu GC-2010 fitted with a PONA column (50.0 m x 0.20 mm x 0.50) and FID detector. The N₂/Air (carrier gas) linear velocity was 1.07 mL/min and the injector and detector temperatures 200 °C and 290 °C, respectively. Injections were made in the split mode. The initial column temperature of 60 °C was kept for 5 min. where after it was increased to 250 °C at 5 °C /min and kept at this temperature for the rest of the analysis. Retention times were compared to those of commercially available samples. Where indicated in the discussion, products were identified by GC-MS analyses on a Shimadzu GC-MS Qp-2010 fitted with a similar column and operated under the same conditions as the GC.

Quantitative analyses were performed using dodecane as internal standard. Response factors (R_f) of reactants and products were determined by injecting standard solutions containing dodecane as internal standard:

$$R_f = \frac{A_x \times M_s}{A_s \times M_x}$$

$$\text{Therefore, } M_x = \frac{A_x \times M_s}{R_f \times A_s}$$

R_f : Response factor

M_x : Moles of reactant to be calibrated; A_x : Integrated area of the calibrant peak

A_s : Moles of dodecane; M_s : integrated area of the dodecane peak

The amounts of reactants and products contained in the analyzed reaction solutions could be determined by integration of the detected peaks:

$$M_x = \frac{A_x \times M_s}{R_f \times A_s}$$

M_x : Moles of analyzed compound; A_x : integrated area of peak

5.5.2 Preparation of 2,6-dichloro-4-methoxypyridine-*N*-oxide [5.9].

A sodium methoxide methanol solution (2.6 ml, 13 mmol, 1.4 eq.) were added to a suspension of 2,6-dichloro-4-nitropyridine-*N*-oxide (2g, 9.6 mmol) in methanol (100 ml) under nitrogen at 0 °C. The solution was stirred for 4 h at room temperature, washed with water (40 ml), and extracted with dichloromethane (100 ml). After evaporation of the solvent, the product was isolated by flash chromatography on silica with methanol: ethyl acetate (1:9, v/v). By recrystallization from ethyl acetate, 2,6-dichloro-4-methoxypyridine-*N*-oxide [5.9] ($R_f = 0.5$, 800 mg, 40 %) was obtained as off white needles. δ_H (600 MHz, $CDCl_3$, *Spectrum 53*) 7.04 (2H, s, H-1 x 2), 3.88 (3H, s, H-1' x 3); δ_C (151.9 MHz, $CDCl_3$, *Spectrum 54*) 155.53, 143.70, 111.47, 56.57; m/z (EI) 192.97 (100%).

5.5.3 Epoxidation

A 15 ml Schlenk flask was charged with the catalyst (0.5 μ mol, 1eq. Table 5.23), the olefin,* dodecane* (internal standard) and dry toluene (2ml) under an argon atmosphere. 2,6-Dichloropyridine-*N*-oxide* was added and the solution stirred at 90 °C. The reactions were followed by gas chromatographic analysis.

Table 5.23. Catalyst load (0.5, μ mol, 1eq).

Catalyst	[8a]	[8b]	[8c]	[8d]	[8e]	[8f]	[7b]
Load (mg)	0.66	0.77	1	0.6	0.76	0.32	0.73

* Quantities as indicated in Table 5.24.

Table 5.24 Reagent proportions.

Catalyst (mole %)	Olefin	Dodecane	2,6-DNPNO (nr)
0.45	110 μmol , 220 eq.	25 μl , 110 μmol , 220 eq.	27 mg, 165 μmol , 330 eq.
0.23	250 μmol , 500 eq.	57 μl , 250 μmol , 500 eq.	61 mg, 375 μmol , 750 eq.
0.1	500 μmol , 1000 eq.	114 μl , 500 μmol , 1000 eq.	122 mg, 750 μmol , 1500 eq.
0.02	2500 μmol , 5000 eq.	570 μl , 2500 μmol , 5000 eq.	615 mg, 3750 μmol , 7500 eq.

5.5.3.1 Epoxidation of *cis*-stilbene [2.7]

Retention time in minutes:

	Rt (min.)
<i>cis</i> -stilbene [2.7]	35.13
<i>cis</i> -stilbene oxide [2.8A]	37.06
<i>trans</i> -stilbene oxide [2.8B]	55.96
benzaldehyde [2.13]	17.49
dodecane	26.32
2,6-DCPNO [5.2]	33.20
2,6-dichloropyridine (2,6-DCP) [5.5]	22.23

5.5.3.2 Epoxidation of *trans*-stilbene [5.1]

Retention time in minutes:

	Rt (min.)
<i>trans</i> -stilbene [5.1]	55.63
<i>trans</i> -stilbene oxide [2.8B]	55.96
dodecane	26.32
2,6-DCPNO [5.2]	33.20
2,6-dichloropyridine (2,6-DCP) [5.5]	22.23

5.5.3.3 Epoxidation of 1:1 *cis*- stilbene [2.7] and *trans*-stilbene [5.1]

Retention time in minutes:

	Rt (min.)
<i>trans</i> -stilbene [5.1]	55.63
<i>trans</i> -stilbene oxide [2.8B]	55.96
<i>cis</i> -stilbene [2.7]	35.13
<i>cis</i> -stilbene oxide [2.8A]	37.06
dodecane	26.32
2,6-DCPNO [5.2]	33.20
2,6-dichloropyridine (2,6-DCP) [5.5]	22.23

5.5.3.4 Epoxidation of 1,2-dihydronaphthalene [5.3]

Retention time in minutes:

	Rt (min.)
1,2-dihydronaphthalene [5.3]	25.04
1,2-dihydronaphthalene-oxide [5.4]	30.21, 30.34
Dodecane	26.32
2,6-DCPNO [5.2]	33.20
2,6-dichloropyridine (2,6-DCP) [5.5]	22.23

5.5.3.5 Epoxidation of cyclooctene [2.3]

Retention time in minutes:

	Rt (min.)
cyclooctene [2.3]	20.19
cyclooctene oxide [2.4]	23.04
dodecane	26.32
2,6-DCPNO [5.2]	33.20
2,6-dichloropyridine (2,6-DCP) [5.5]	22.23

5.5.3.6 Epoxidation of 1,5-cyclooctadiene [5.24]

Retention time in minutes:

	Rt (min.)
1,5-cyclooctadiene [5.24]	20.19
1,5-cyclooctadiene oxide [5.25]	23.04
dodecane	26.32
2,6-DCPNO [5.2]	33.20
2,6-dichloropyridine (2,6-DCP) [5.5]	22.23

5.5.3.7 Epoxidation of limonene [5.27]

Retention time in minutes:

	Rt (min.)
limonene [5.27]	20.66
limonene oxides [5.28]	24.03, 24.19
dodecane	26.32
2,6-DCPNO [5.2]	33.20
2,6-dichloropyridine (2,6-DCP) [5.5]	22.23

5.5.3.8 Epoxidation of *trans*- β -methylstyrene [5.13]

Retention time in minutes:

	Rt (min.)
<i>trans</i> - β -methylstyrene [5.13]	20.19
<i>trans</i> - β -methylstyrene oxide [5.15]	23.04
dodecane	26.32
2,6-DCPNO [5.2]	33.20
2,6-dichloropyridine (2,6-DCP) [5.5]	22.23

5.5.3.9 Epoxidation of *cis*- β -methylstyrene [5.12]

Retention time in minutes:

	Rt (min.)
<i>cis</i> - β -methylstyrene [5.12]	20.19
<i>cis</i> - β -methylstyrene oxide [5.14]	23.04
dodecane	26.32
2,6-DCPNO [5.2]	33.20
2,6-dichloropyridine (2,6-DCP) [5.5]	22.23

5.5.3.10 Epoxidation of styrene [2.11]

Retention time in minutes:

	Rt (min.)
styrene [2.11]	15.13
styrene oxide [2.15]	21.24
phenylacetaldehyde [5.20]	20.15
benzaldehyde [2.13]	17.25
dodecane	26.32
2,6-DCPNO [5.2]	33.20
2,6-dichloropyridine (2,6-DCP) [5.5]	22.23

5.5.3.11 Epoxidation of *p*-methoxystyrene [5.19]

Retention time in minutes:

	Rt (min.)
<i>p</i> -methoxystyrene [5.19]	28.24
<i>p</i> -methoxystyrene oxide [5.21]	28.35
4-methoxybenzaldehyde [5.22]	17.2
4-methoxyphenylacetaldehyde [5.23]	27.06
dodecane	26.32
2,6-DCPNO [5.2]	33.20
2,6-dichloropyridine (2,6-DCP) [5.5]	22.23

5.5.3.12 Epoxidation of α -methylstyrene [5.16]

Retention time in minutes:

	Rt (min.)
α -methylstyrene [5.16]	18.55
α -methylstyrene oxide [5.17]	21.07
2-phenylpropanal [5.18]	25.69
dodecane	26.32
2,6-DCPNO [5.2]	33.20
2,6-dichloropyridine (2,6-DCP) [5.5]	22.23

5.5.3.13 Epoxidation of 1-Octene [5.31]

Retention time in minutes:

	Rt (min.)
1-octene [5.31]	11.79
1-octene oxide [5.33]	19.56
dodecane	26.32
2,6-DCPNO [5.2]	33.20
2,6-dichloropyridine (2,6-DCP) [5.5]	22.23

5.6 References

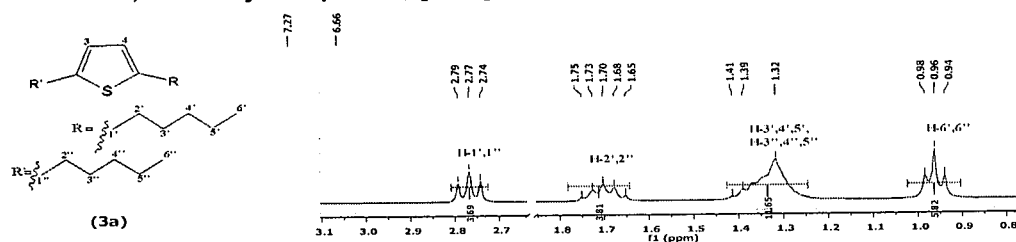
1. (a) Larsen, E.; Jorgensen, K. A. *Acta Chem. Scand.* **1989**, *43*, 259-263. (b) Safari, N.; Bahadoran, F. *J. Mol. Catal. A: Chem.* **2001**, *171*, 115-121. (c) Mahtab, P.; Safari, N.; Abbas Ali, S. *Iran. J. Chem. Eng.* **2006**, *25*, 4. (d) Ebadi, A.; Safari, N.; Peyrovi, M. N. *Applied Catalysis A: General* **2007**, *321*, 135-139. (e) Gonzalez, L. M.; Villa de P. A. L.; Montes de C., C. and Sorokin, A. *Tetrahedron Lett.* **2006**, *47*, 6465-6468.
2. Sorokin, A. B.; Mangematin, S.; Pergrale, C. *J. Mol. Catal. A: Chem.* **2002**, 182-183, 267-281.
3. Che, C.-M. and Huang, J.-S. *Chem. Commun.* **2009**, 3996-4015.
4. Takeda, T.; Irie, R.; Shinoda, Y.; Katsuki, T. *Synlett* **1999**, *7*, 1157.
5. (a) Zhang, J.-L. and Che, C.-M. *Chem. Eur. J.* **2005**, *11*, 3899-3914. (b) Leung, W.-H.; Che, C.-M. *Inorg. Chem.* **1987**, *26*, 2289.
6. Capobianchi, A.; Paoletti, A. M.; Pennesi, G.; Caminiti, R. and Ercolani, C. *Inorg. Chem.*, **1994**, *33*, 4635-4640.
7. Balkus, Jr.; K. J.; Eissa, M. and Levado, R. *J. Am. Chem. Soc.*, **1995**, *117*, 10753-10754.
8. Berkessel, A.; Kaiser, P.; Lex, J. *Chem. Eur. J.* **2003**, *9*, 4746-4756.
9. (a) Higuchi, T.; Hirobe, M. *J. Mol. Catal. A: Chem.* **1996**, *113*, 403-422, (b) Higuchi, T.; Ohtake, H.; Hirobe, M. *Tetrahedron Lett.* **1989**, *30*, 6545.
10. Berkessel, A. and Frauenkron, M. *J. Chem. Soc. Perkin Trans. 1*, **1997**, 2265
11. Zhang, R.; Yu, W.-Y.; Wong, K.-Y. and Che, C.-M. *J. Org. Chem.* **2001**, *66* (24), 8145-8153.
12. Groves, J.T.; Bonchio, M.; Carofiglio, T. and Shalyaev, K. *J. Am. Chem. Soc.* **1996**, *118*, 8961-8962.
13. Neumann, R. and Dahan, M. *J. Am. Chem. Soc.*, **1998**, *120*, 11969-11976.
14. (a) Gross, Z. and Ini, S. *Org. Lett.* **1999**, *1*, 13, 2077-2080. (b) Gross, Z.; Ini, S.; Kapon, M. and Cohen, S. *Tetrahedron Lett.* **1996**, *37*, 7325.

15. (a) Castellino, A. J. and Bruce, T. C. *J. Am. Chem. Soc.* **1988**, *110*, 158-162. (b) Dalton, C. T.; Ryan, K. M.; Wall, V. M.; Bousquet, C. and Gilheany, D. G. *Topics in catalysis* **1998**, *5*, 75-91
16. (a) Leung, W.-H.; and Che, C.-M. *Inorg. Chem.* **1989**, *28*, 26, 4619-4622. (b) Katsuki, T. *Coordination Chemistry Reviews* **1995**, *140*, 189-214.
17. Leung, W.-H.; Che, C.-M. *J. Am. Chem. Soc.* **1989**, *111*, 8812-8818
18. (a) Bressan, M. and Morvillo, A. *J. Chem. Soc., Chem. Commun.* **1988**, 650-651. (b) Morvillo, A.; Bressan, M. *J. Mol. Catal. A: Chem.* **1997**, *125*, 119-125. (c) Chatterjee, D. *Inorganica Chimica Acta* **2008**, *361*, 2177-2182.
19. Higuchi, T.; Hirobe, M. *J. Mol. Catal. A: Chem.* **1996**, *113*, 403-422,
20. Gross, Z. and Ini, S. *Org. Lett.* **1999**, *1*, 13, 2077-2080.
21. Zhang, R.; Yu, W.-Y.; Wong, K.-Y. and Che, C.-M. *J. Org. Chem.* **2001**, *66* (24), 8145-8153.
22. Zhang, J.-L. and Che, C.-M. *Org. Lett.* **2002**, *4* (11), 1911-1914.
23. Liu, C.-J.; Yu, W.-Y.; Che, C.-M. and Yeung, C.-H. *J. Org. Chem.* **1999**, *64* (20), 7365-7374.
24. Chambrier, I.; Cook, M. J. and Wood, P. T. *Chem. Commun.* **2000**, 2133-2134.
25. Nestler, O. and Severin, K. *Org. Lett.* **2001**, *3*(24), 3907-3909.
26. Groves, J. T.; Nemo, T.E. *J. Am. Chem. Soc.* **1983**, *105*, 5786-5791.
27. Larsen, E.; Jorgensen, K. A. *Acta Chem. Scan.* **1989**, *43*, 259.
28. Bhattacharjee, S.; Anderson, J. A. *J. Mol. Catal. A: Chem.* **2006**, *249*, 103-110.
29. Yu, X-Q.; Huang, J-S.; Yu, W-H. and Che, C-H. *J. Am. Chem. Soc.* **2000**, *122*, 5337-5342.
30. Kesavan, V. and Chandrasekaran, S. *J. Chem. Soc., Perkin Trans. 1*, **1997**, 3115-3116.
31. Liu, C.-J.; Yu, W.-Y.; Li, S.-G. and Che, C.-M. *J. Org. Chem.* **1998**, *63*, 7364-7369.
32. Zhang, J.-L. and Che, C.-M. *Chem. Eur. J.* **2005**, *11*, 3899-3914.
33. Kolar, J. US Patent, 3350422; **1967**.
34. Seyler, J. W.; Fanwick, P. E.; Leidner, C. R. *Inorg. Chem.* **1992**, *31*, 3699.

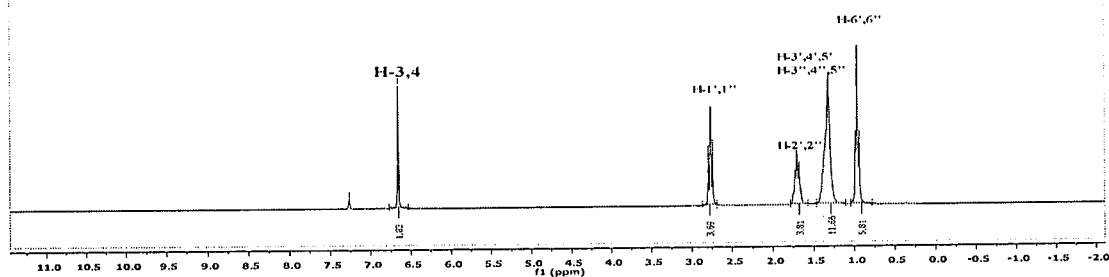
Appendix

^1H - NMR and ^{13}C - NMR

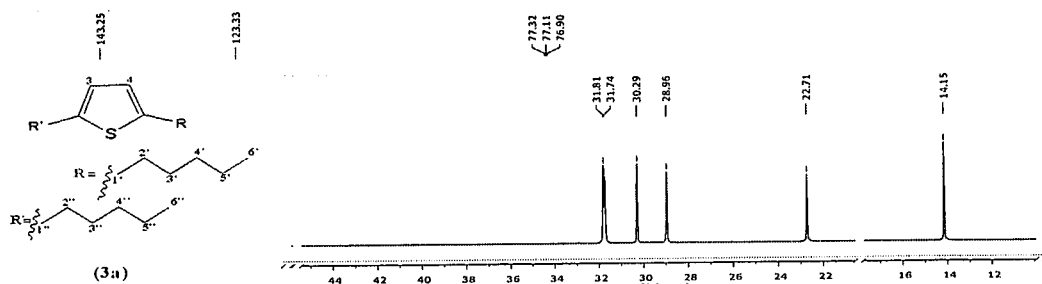
Spectrum 1: 2,5-Dihexylthiophene, [4.3a].



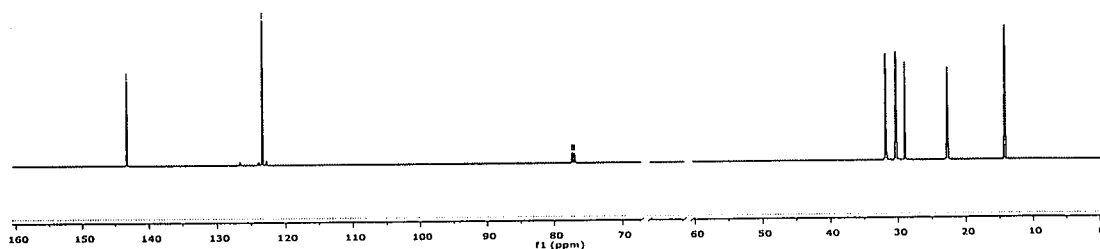
δ_{H} (300 MHz; C_6D_6 , Spectrum 1) 6.66 (2H, s, H-3,4), 2.77 (4H, t, J 7.6 Hz, H-1',H-1''), 1.73-1.65 (4H, m, H-2',H-2''), 1.41-1.32 (12H, m, H-3',4',5', H-3'',4'',5''), 0.96 (6H, t, J 6.7 Hz, H-6', H-6'')



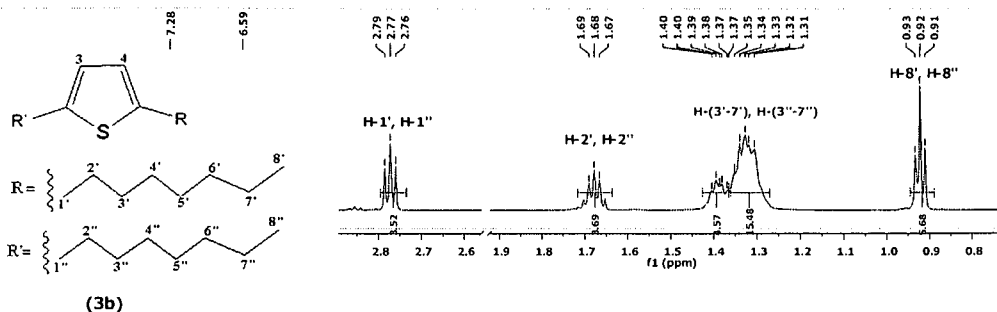
Spectrum 2: 2,5-Dihexylthiophene, [4.3a].



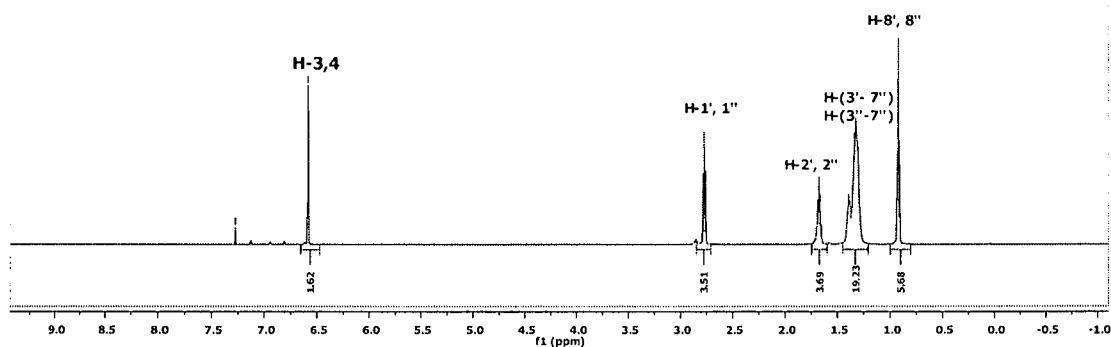
δ_{C} (150.9 MHz; CDCl_3 , Spectrum 2) 143.25, 123.33, 31.80, 31.74, 30.29, 28.96, 22.71, 14.15



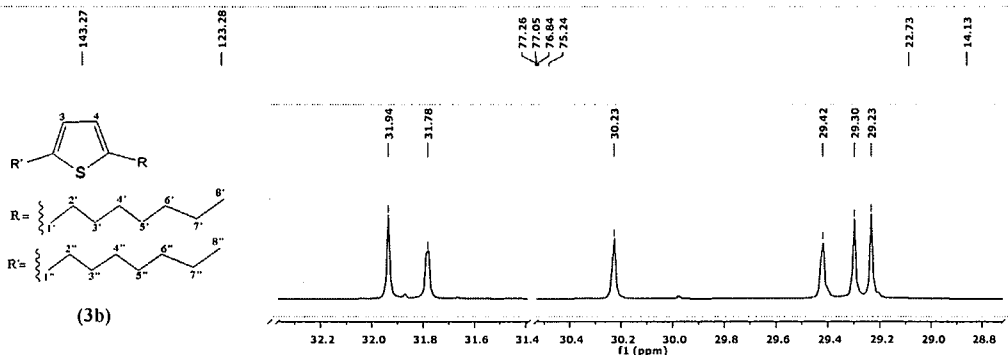
Spectrum 3: 2,5-Dioctylthiophene, [4.3b].



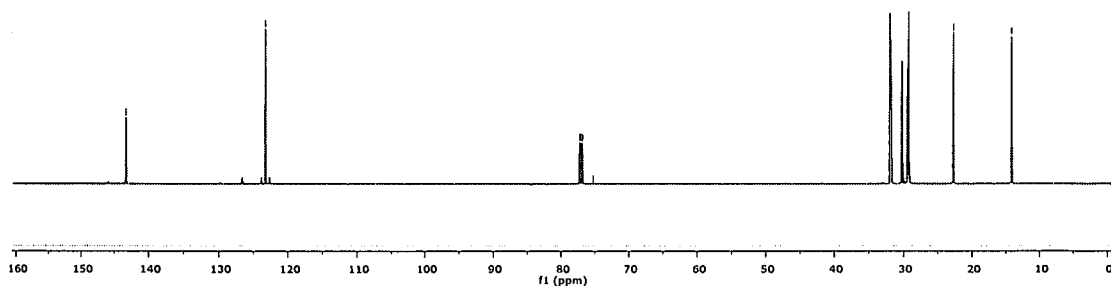
δ_H (600 MHz, $CDCl_3$, *Spectrum 3*) 6.59 (2H, s, H-3, H-4), 2.77 (4H, t, J 7.7 Hz, H-1', H-1''), 1.69-1.67 (4H, m, H-2', H-2''), 1.40-1.31 (20H, m, H3'-H7'), H3''-H7''), 0.92 (6H, t, J 6.9 Hz, H-8', H-8'')



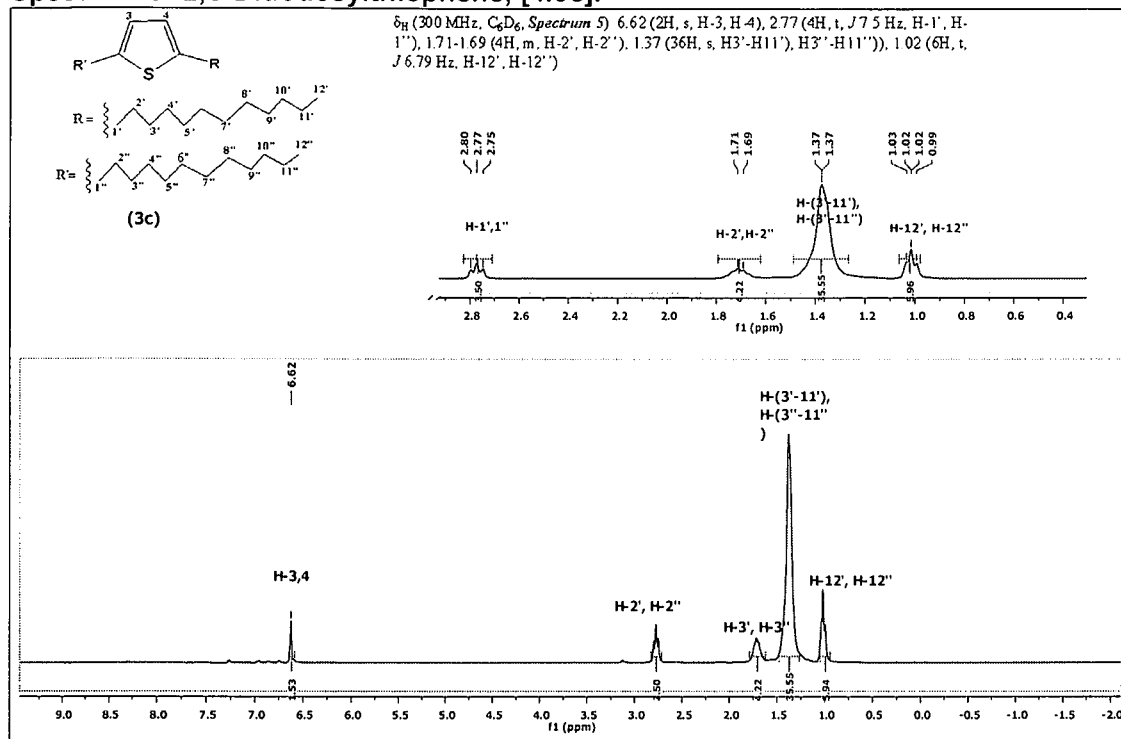
Spectrum 4: 2,5-Dioctylthiophene, [4.3b].



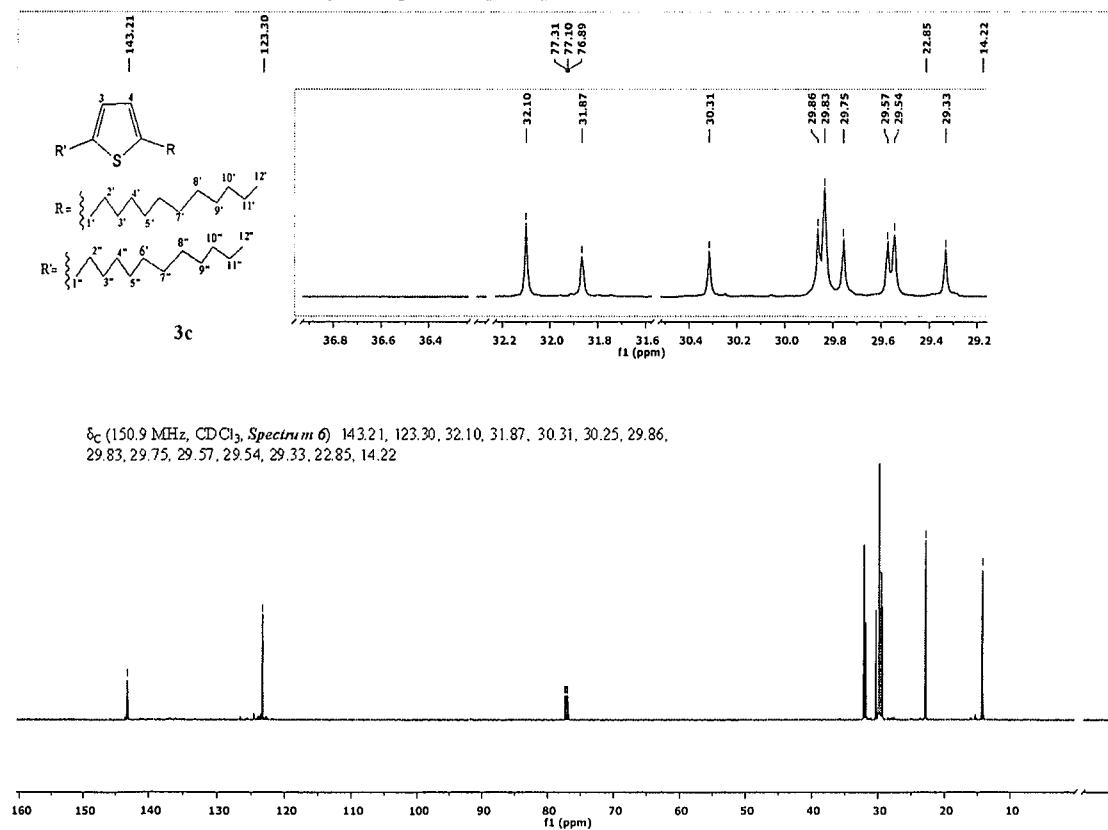
δ_C (150.9 MHz, $CDCl_3$, *Spectrum 4*) 143.27, 123.28, 31.94, 31.78, 30.23, 29.42, 29.30, 29.23, 22.73, 14.13



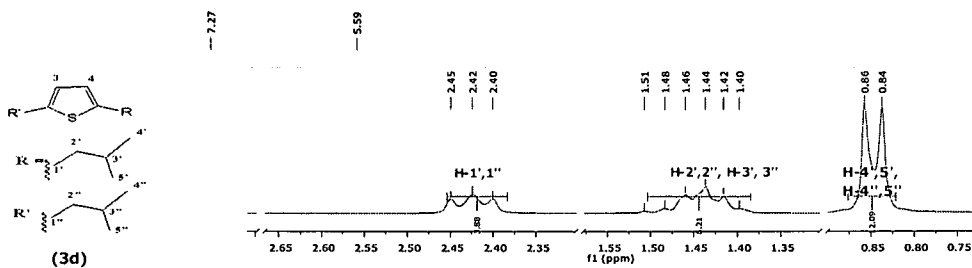
Spectrum 5: 2,5-Didodecylthiophene, [4.3c].



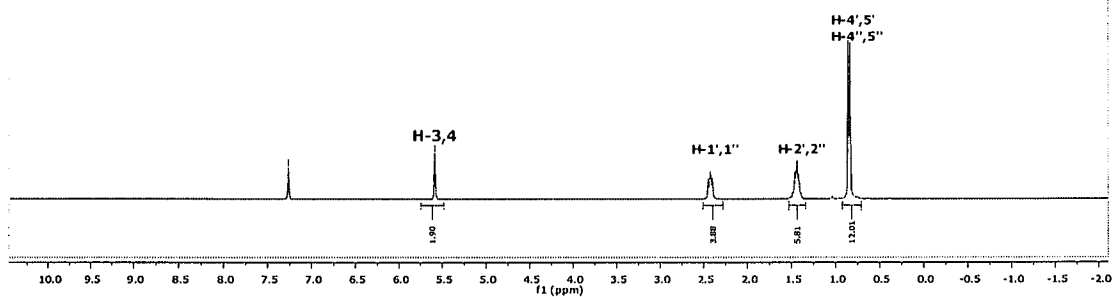
Spectrum 6: 2,5-Didodecylthiophene, [4.3c].



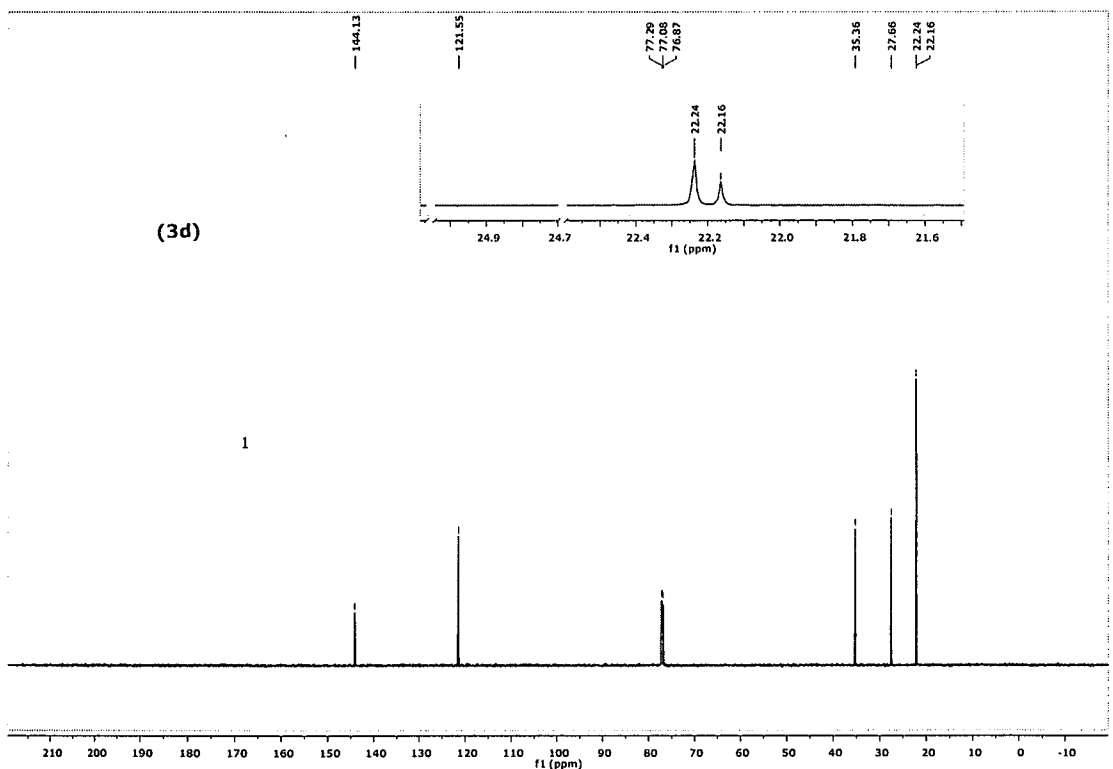
Spectrum 7: 2,5-Diisopentylthiophene, [4.3d].



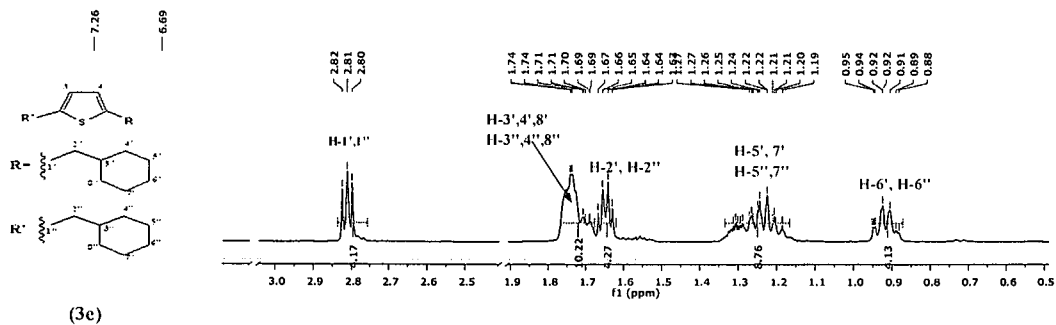
δ_{H} (300 MHz, CDCl_3 , Spectrum 7) 5.59 (2H, s, H-3, 4), 2.42 (4H, t, J 7.41 Hz, H-1', H-1''), 1.51–1.40 (6H, m, H-2', 2'', H-3', 3''), 0.85 (12H, d, J 6.2 Hz, H-4', 5', H-4'', 5'')



Spectrum 8: 2,5-Diisopentylthiophene, [4.3d].

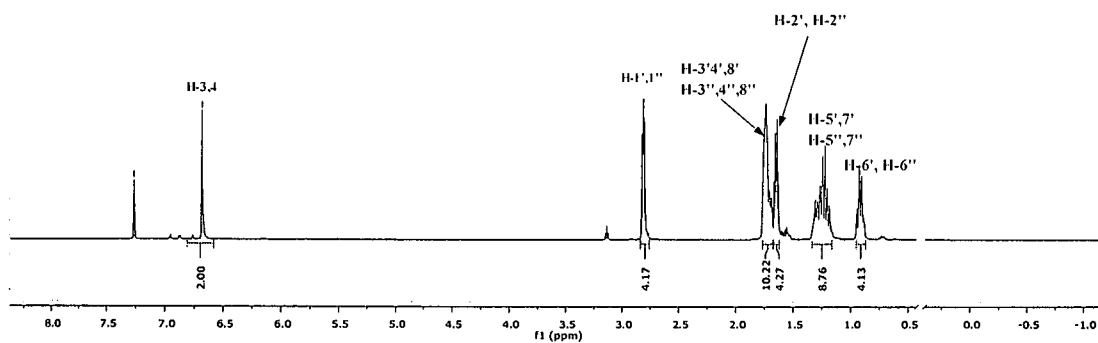


Spectrum 9: 2,5-Di(2-cyclohexylethyl)thiophene, [4.3e].

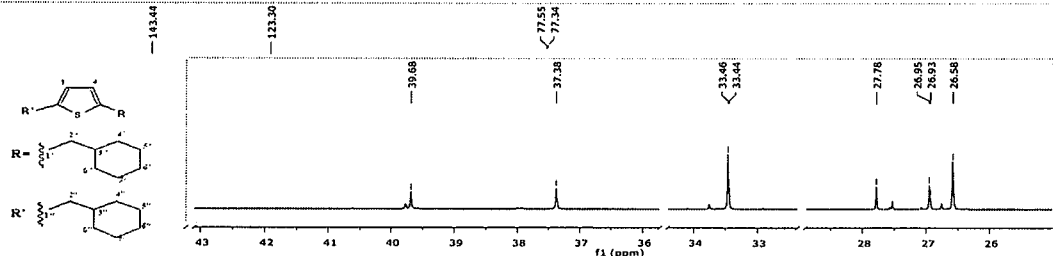


(3c)

δ_H (600 MHz, C_6D_6 , *Spectrum 9*) 6.69 (2H, s, H-3,4), 2.81 (4H, t, J 7.94 Hz, H-1', H-1''), 1.74-1.69 (10H, m, H-3',4',8', H-3'',4'',8''), 1.67-1.63 (4H, m, H-2', H-2''), 1.27-1.19 (8H, m, H-5',7', H-5'',7'') 0.95-0.88 (4H, m, H-6', H-6'')

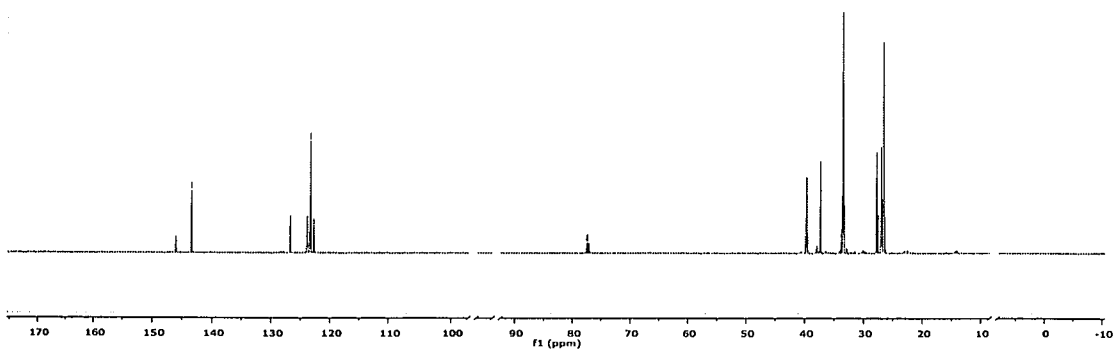


Spectrum 10: 2,5-Di(2-cyclohexylethyl)thiophene, [4.3e].

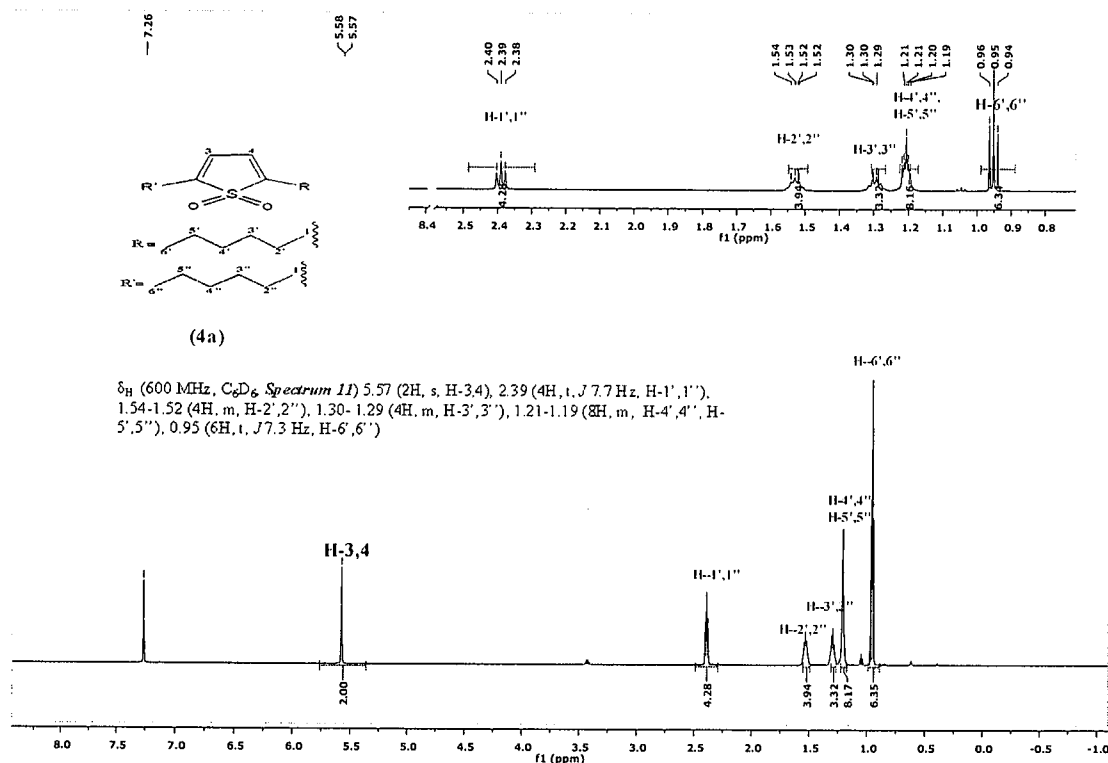


(3c)

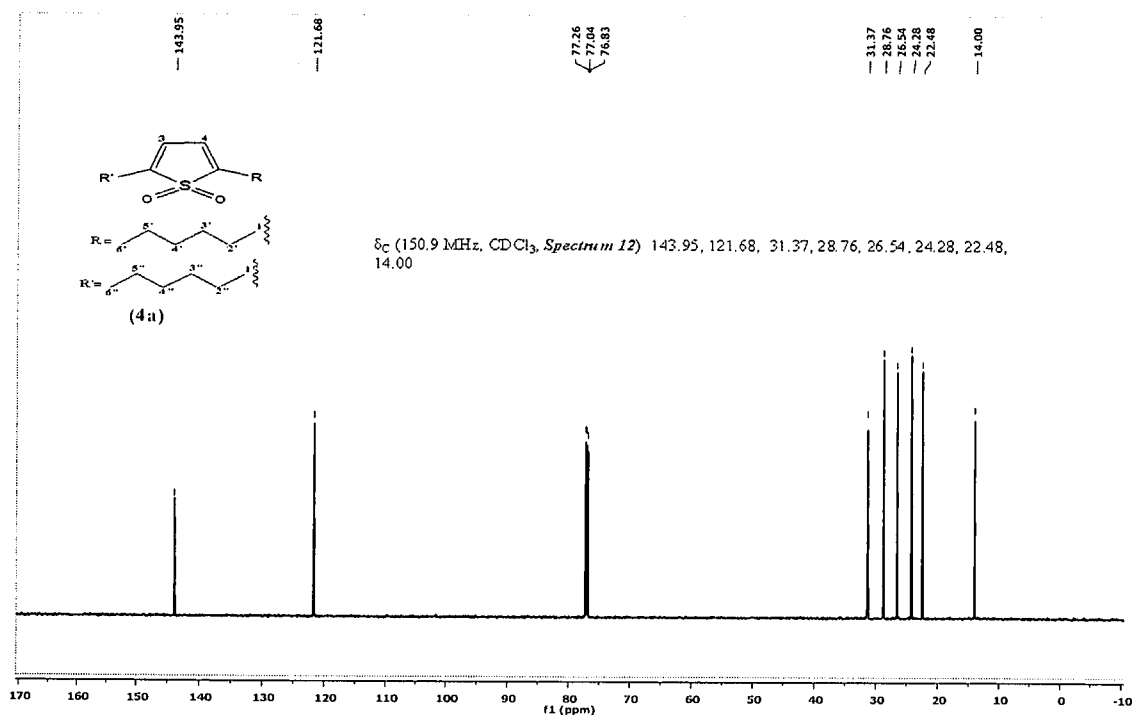
δ_C (150.9 MHz, $CDCl_3$, *Spectrum 10*) 143.44, 123.30, 39.68, 37.38, 33.46-33.44, 27.78, 26.95, 26.93, 26.58



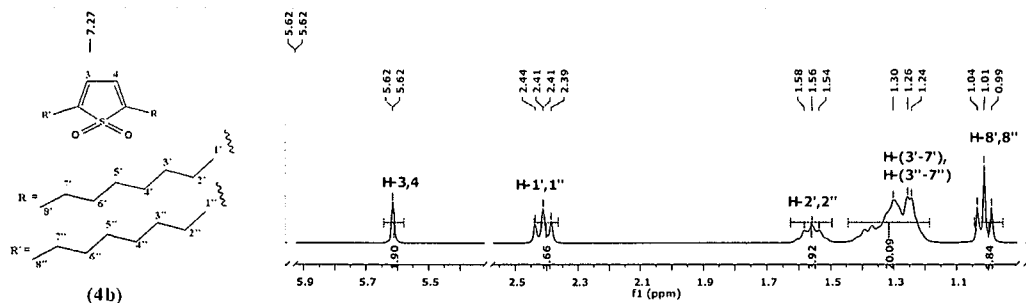
Spectrum 11: 2,5-Dihexylthiophene 1,1-dioxide, [4.4a].



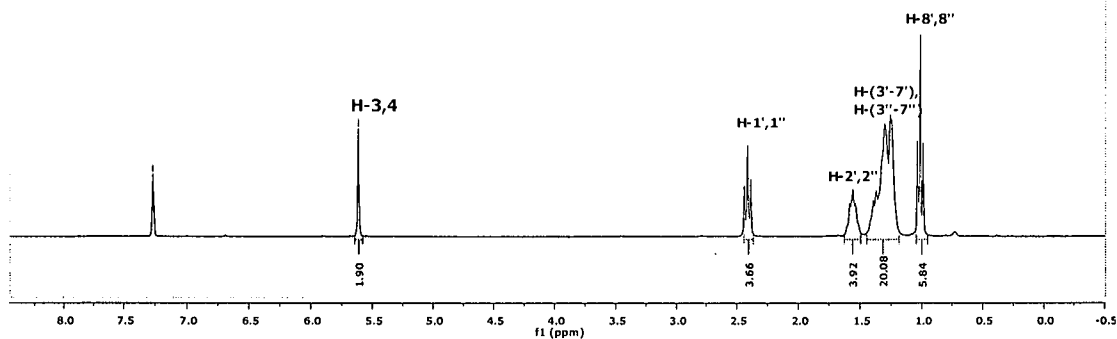
Spectrum 12: 2,5-Dihexylthiophene 1,1-dioxide, [4.4a].



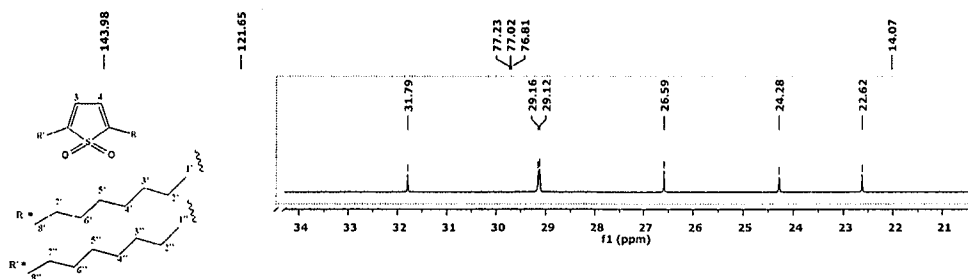
Spectrum 13: 2,5-Dioctylthiophene 1,1-dioxide, [4.4b].



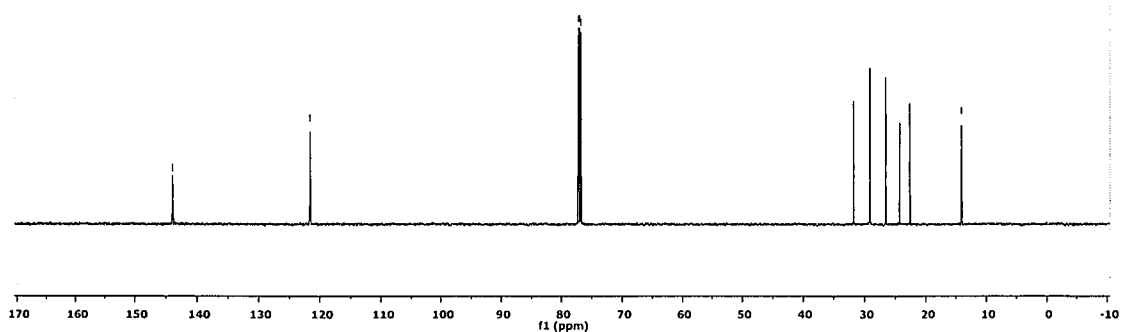
δ_H (300 MHz, C_6D_6 , *Spectrum 13*) 5.62 (2H, s, H-3,4), 2.41 (4H, t, J 7.6 Hz, H-1',1''), 1.58-1.54 (4H, m, H-2',2''), 1.30-1.24 (20H, m, H-(3'-7'), H-(3''-7'')), 1.01 (6H, t, J 6.9 Hz, H-8',8'')



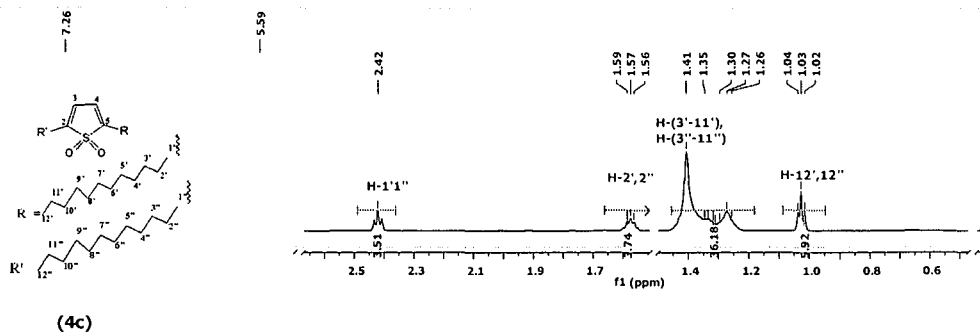
Spectrum 14: 2,5-Dioctylthiophene 1,1-dioxide, [4.4b].



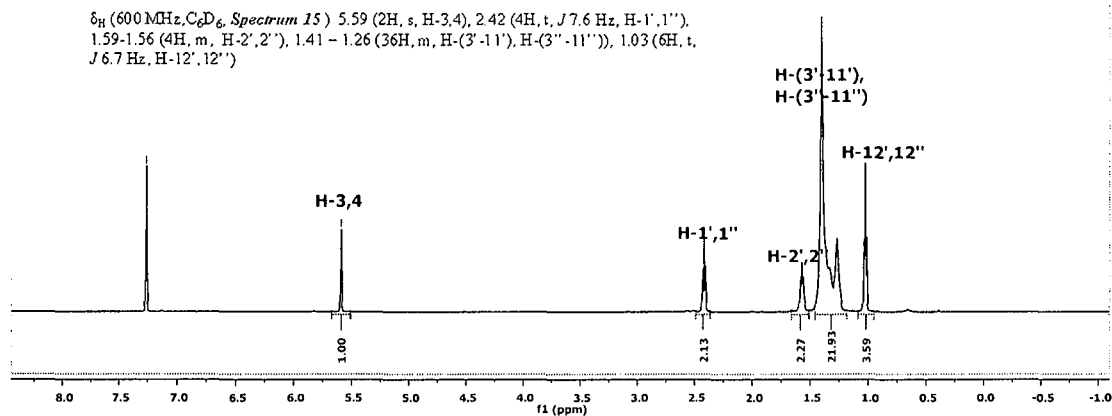
(4b) δ_C (150.9MHz, $CDCl_3$, *Spectrum 14*) 143.98, 121.65, 31.79, 29.16, 29.12, 26.59, 24.28, 22.62, 14.07



Spectrum 15: 2,5-Didodecylthiophene 1,1-dioxide, [4.4c].

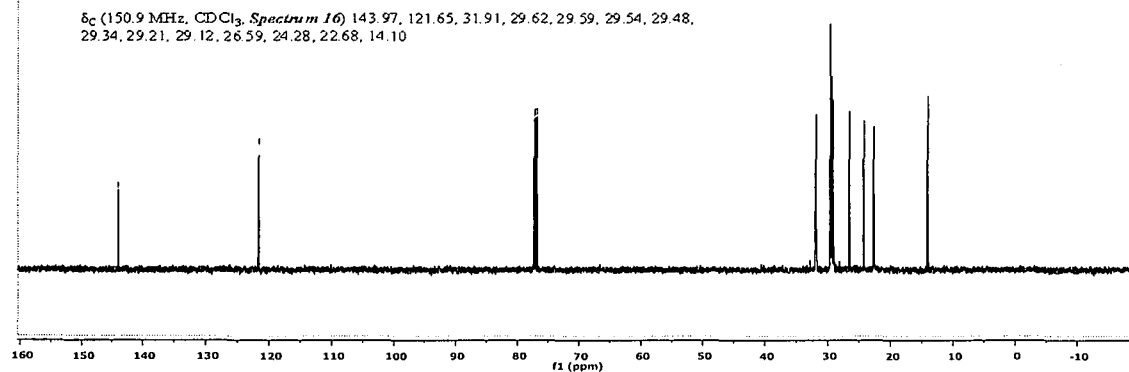
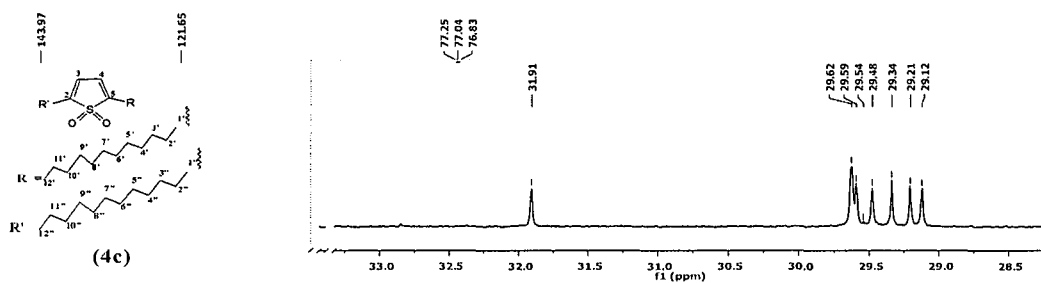


δ_H (600 MHz, C_6D_6 , Spectrum 15) 5.59 (2H, s, H-3,4), 2.42 (4H, t, J 7.6 Hz, H-1',1''), 1.59-1.56 (4H, m, H-2',2''), 1.41-1.26 (36H, m, H-(3'-11'), H-(3'-11'')), 1.03 (6H, t, J 6.7 Hz, H-12',12'')

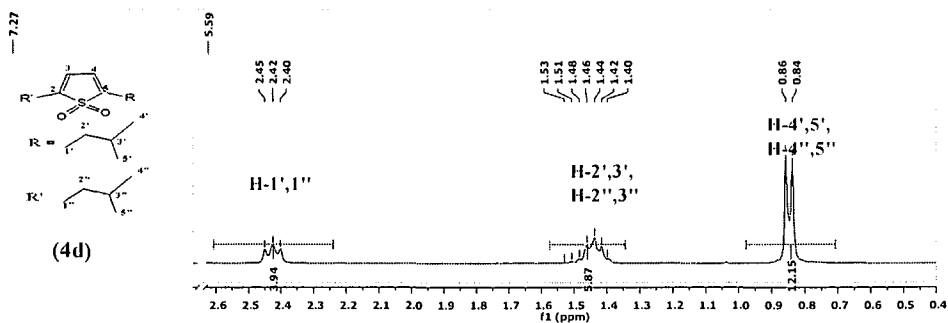


δ_C (150.9 MHz, $CDCl_3$, Spectrum 16) 143.97, 121.65, 31.91, 29.62, 29.59, 29.54, 29.48, 29.34, 29.21, 29.12, 28.59, 24.28, 22.68, 14.10

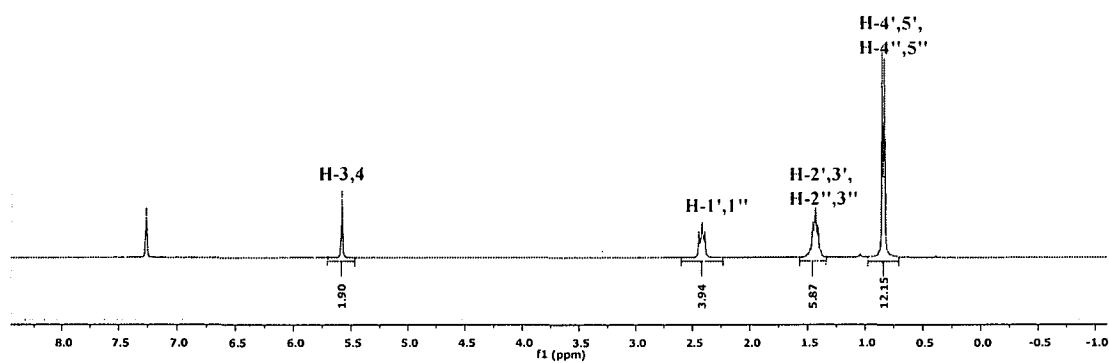
Spectrum 16: 2,5-Didodecylthiophene 1,1-dioxide, [4.4c].



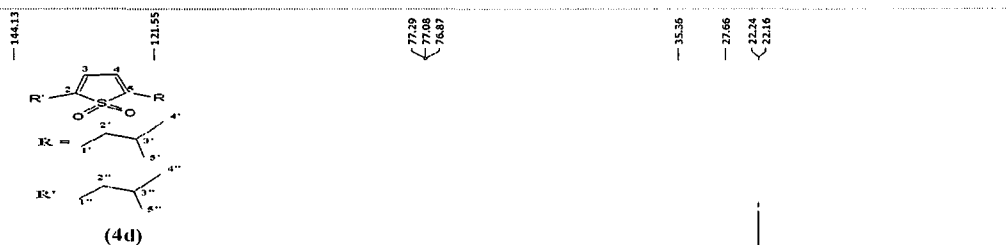
Spectrum 17: 2,5-Diisopentylthiophene 1,1-dioxide, [4.4d].



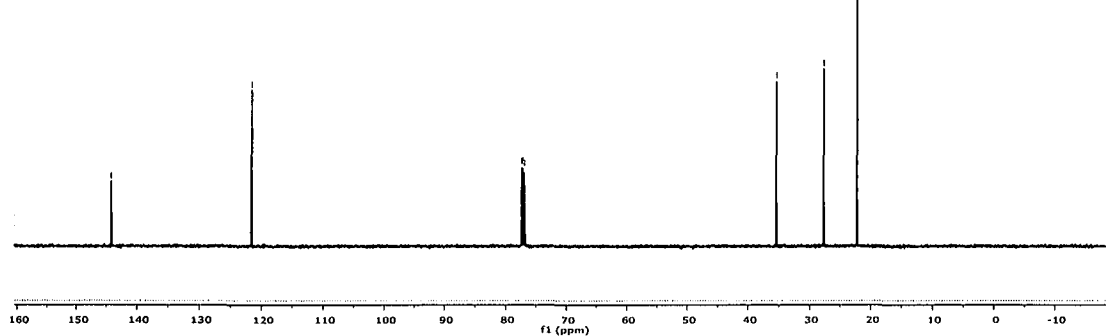
δ_H (300 MHz, C_6D_6 , *Spectrum 17*) 5.59 (2H, s, H-3,4), 2.42 (4H, t, J 7.41 Hz, H-1',1''), 1.53-1.40 (6H, m, H-2',3', H-2'',3''), 0.85 (12H, d, J 6.2 Hz, H-4',5', H-4'',5'')



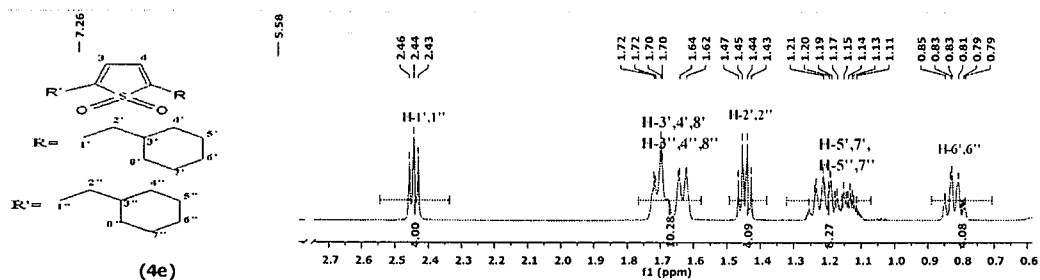
Spectrum 18: 2,5-Diisopentylthiophene 1,1-dioxide, [4.4d].



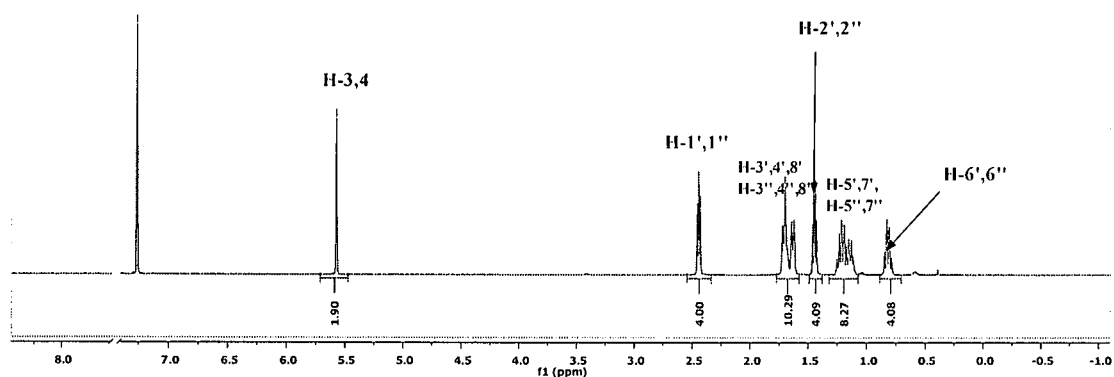
δ_C (150.9 MHz, $CDCl_3$, *Spectrum 18*) 144.13, 121.55, 35.36, 27.66, 22.24, 22.16, 22.16



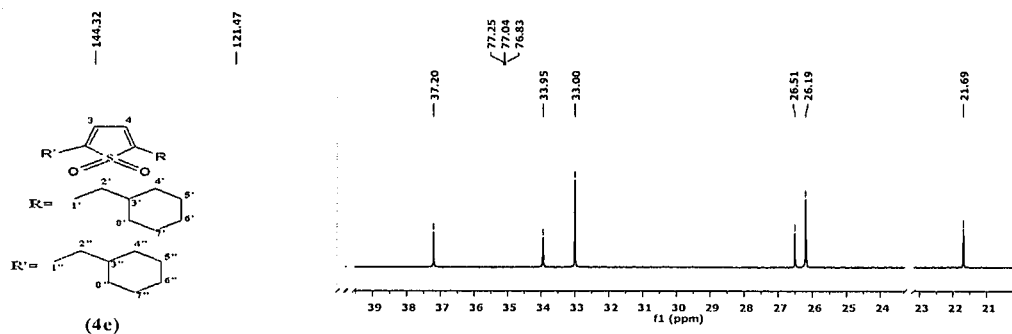
Spectrum 19: 2,5-Di(2-cyclohexylethyl)thiophene 1,1-dioxide, [4.4e].



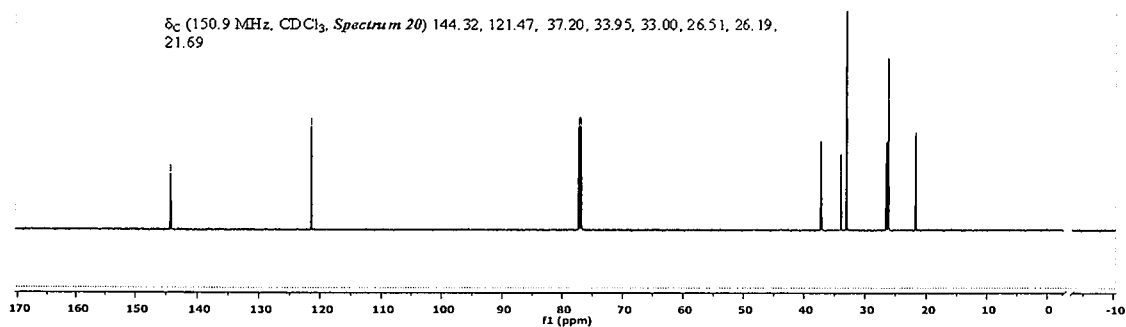
δ_H (600 MHz, C_6D_6 , *Spectrum 19*) 5.58 (2H, s, H-3,4), 2.44 (4H, t, J 7.95 Hz, H-1',1''), 1.72-1.62 (10H, m, H-3',4',8', H-3'',4'',8''), 1.45 (4H, dd, J 6.81, 15.71 Hz, H-2',2''), 1.24-1.11 (8H, m, H-5',7', H-5'',7''), 0.85-0.79 (4H, m, H-6',6'')



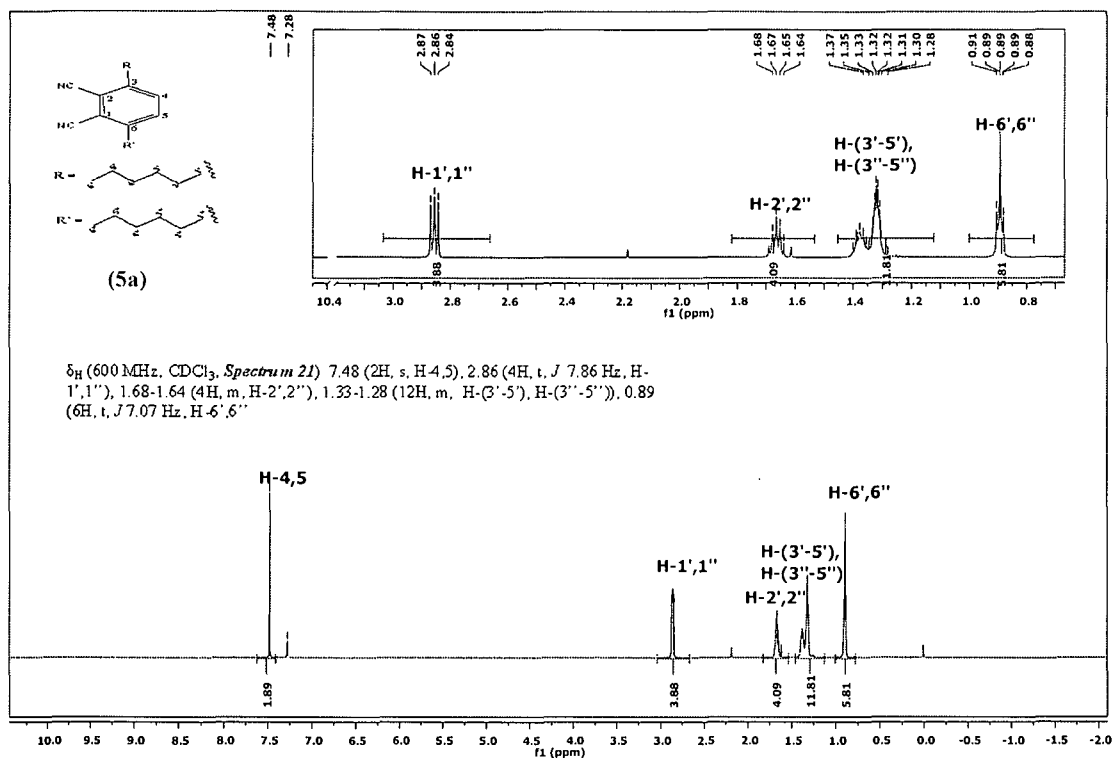
Spectrum 20: 2,5-Di(2-cyclohexylethyl)thiophene 1,1-dioxide, [4.4e].



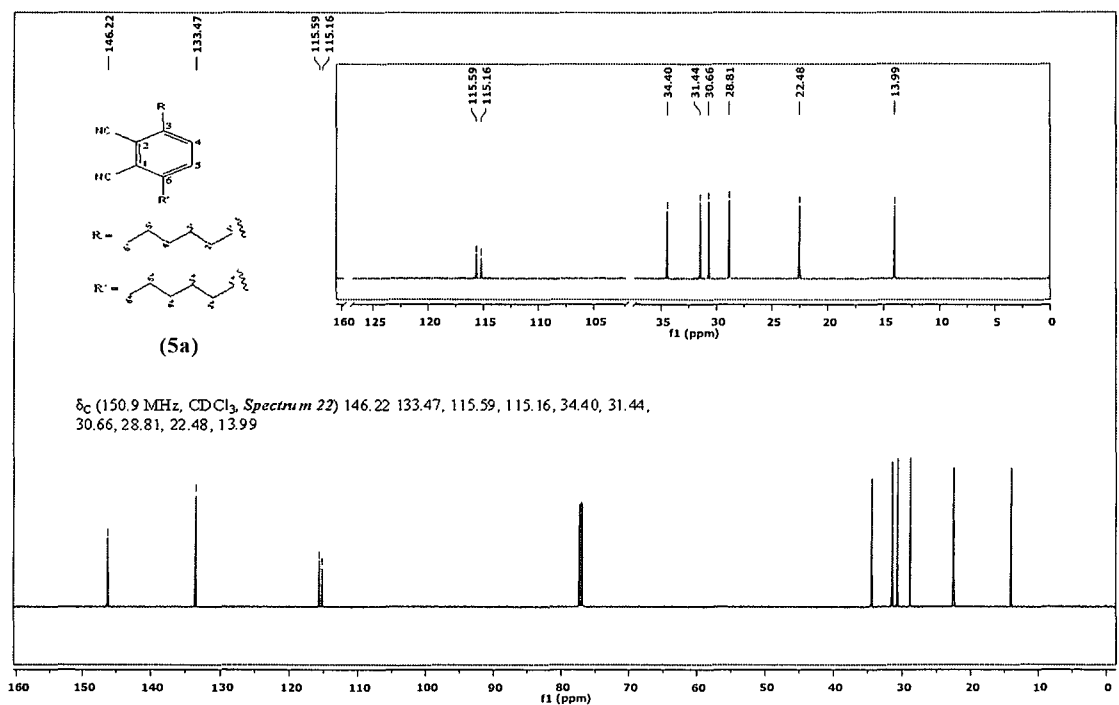
δ_C (150.9 MHz, $CDCl_3$, *Spectrum 20*) 144.32, 121.47, 37.20, 33.95, 33.00, 26.51, 26.19, 21.69



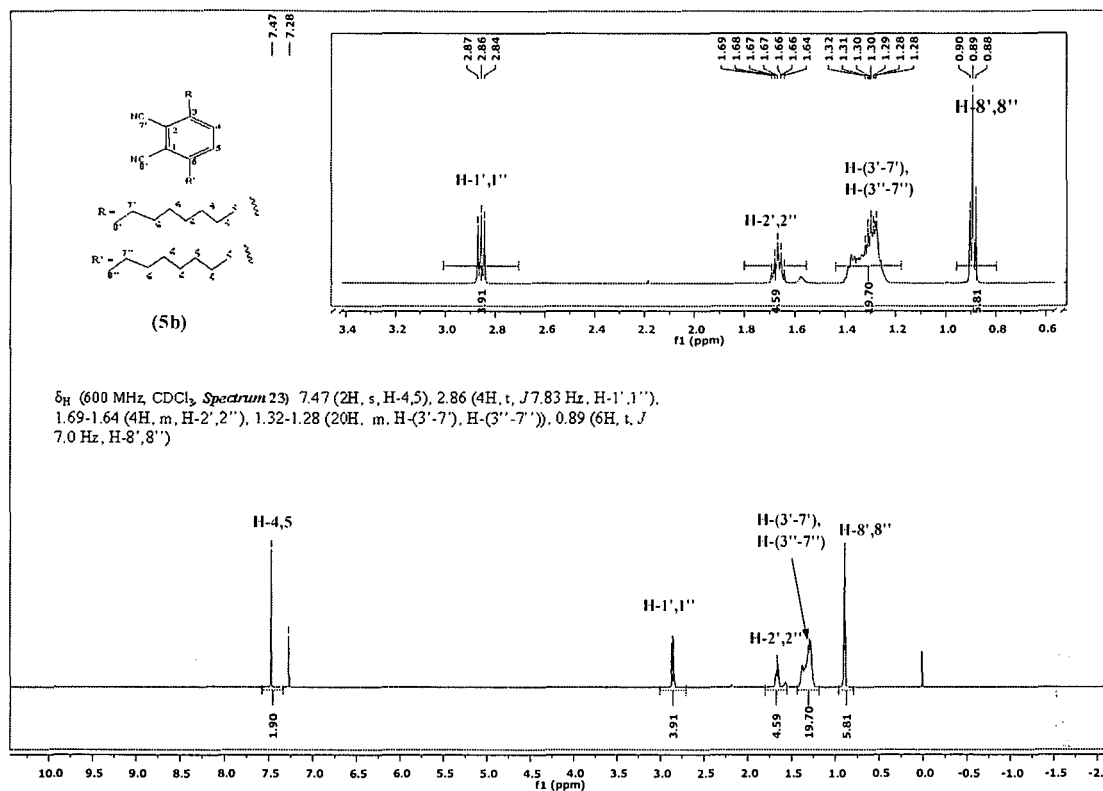
Spectrum 21: 3,6-Dihexylphthalonitrile, [4.5a].



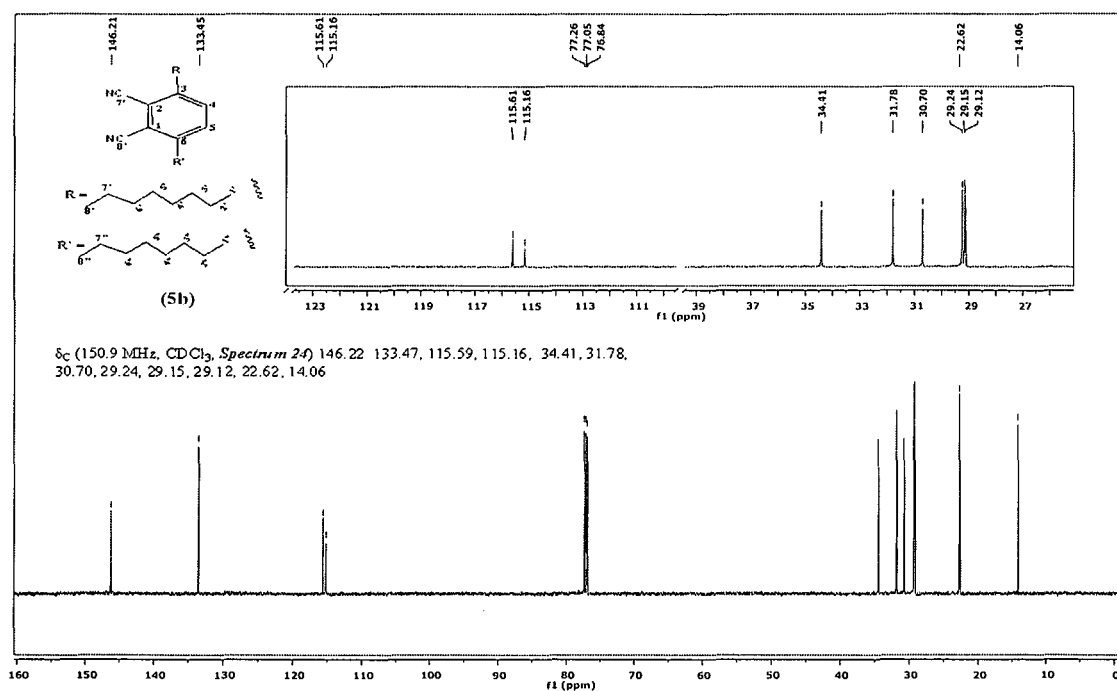
Spectrum 22: 3,6-Dihexylphthalonitrile, [4.5a].



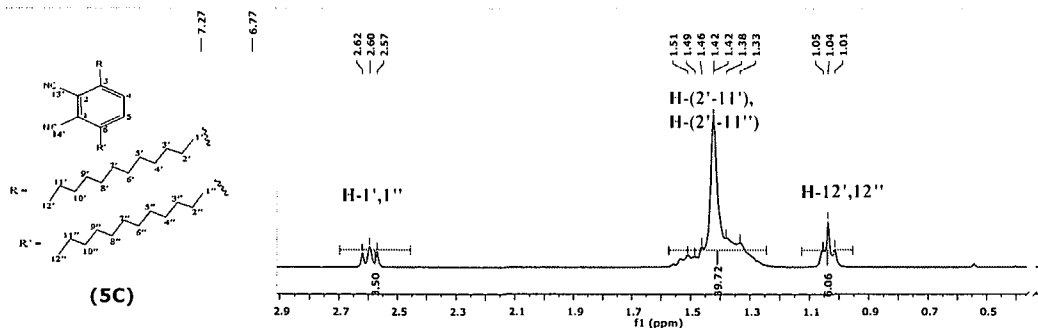
Spectrum 23: 3,6-Dioctylphthalonitrile, [4.5b].



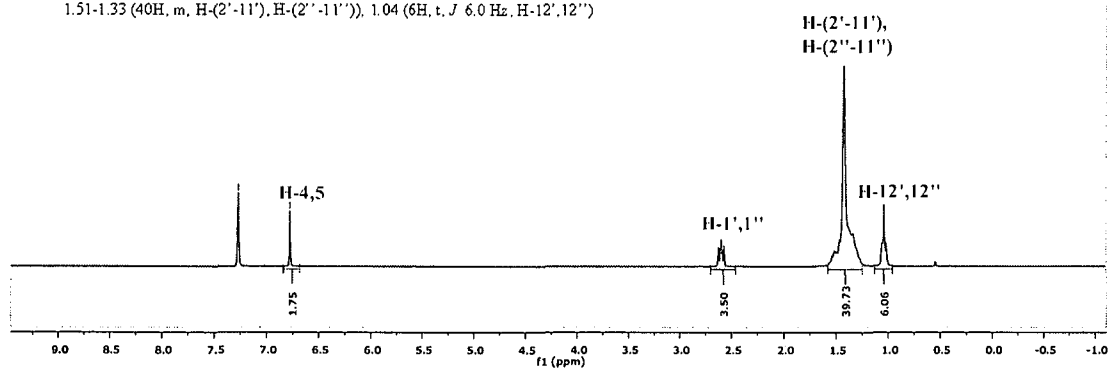
Spectrum 24: 3,6-Dioctylphthalonitrile, [4.5b].



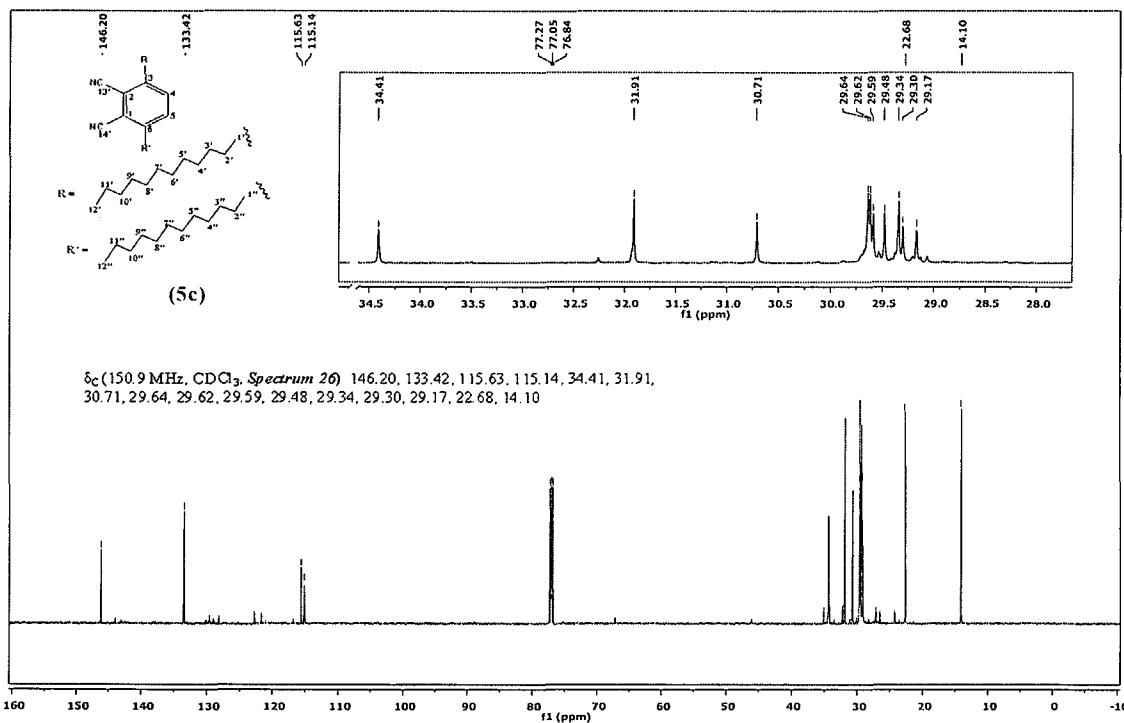
Spectrum 25: 3,6-Didodecylphthalonitrile, [4.5c].



δ_{H} (300 MHz, CDCl_3 , Spectrum 25) 6.77 (2H, s, H-4,5), 2.60 (4H, t, J 7.74 Hz, H-1',1''), 1.51-1.33 (40H, m, H-(2'-11'), H-(2''-11'')), 1.04 (6H, t, J 6.0 Hz, H-12',12'')

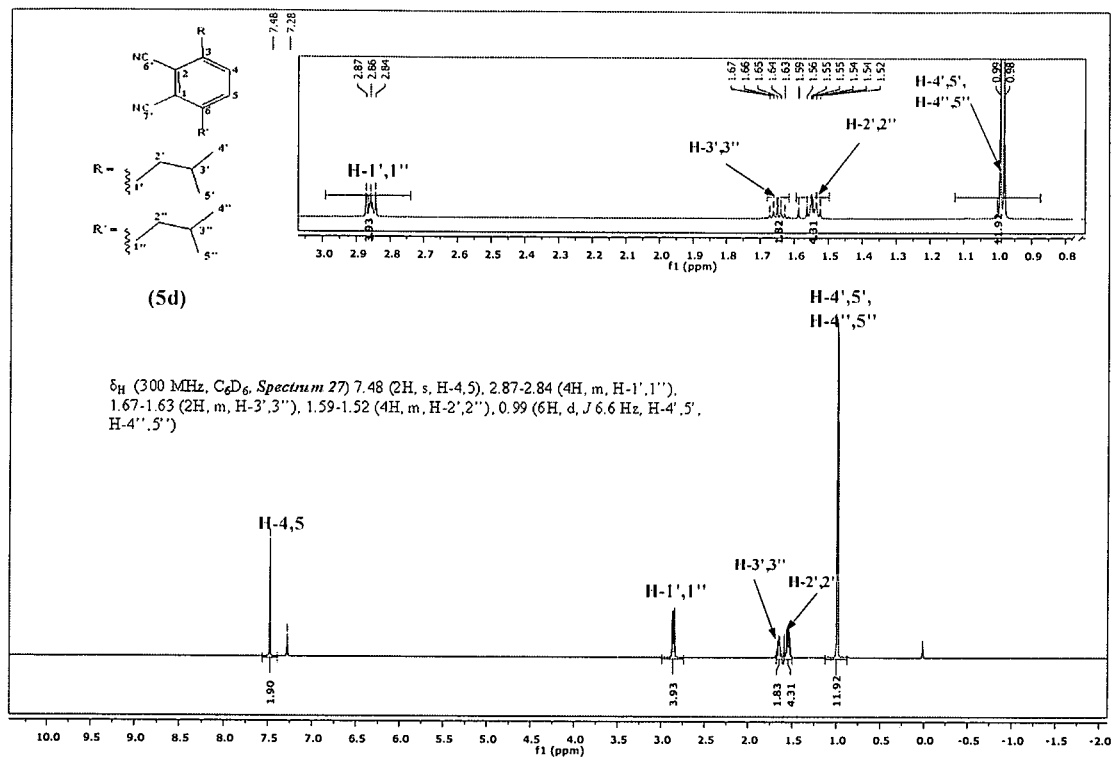


Spectrum 26: 3,6-Didodecylphthalonitrile, [4.5c].

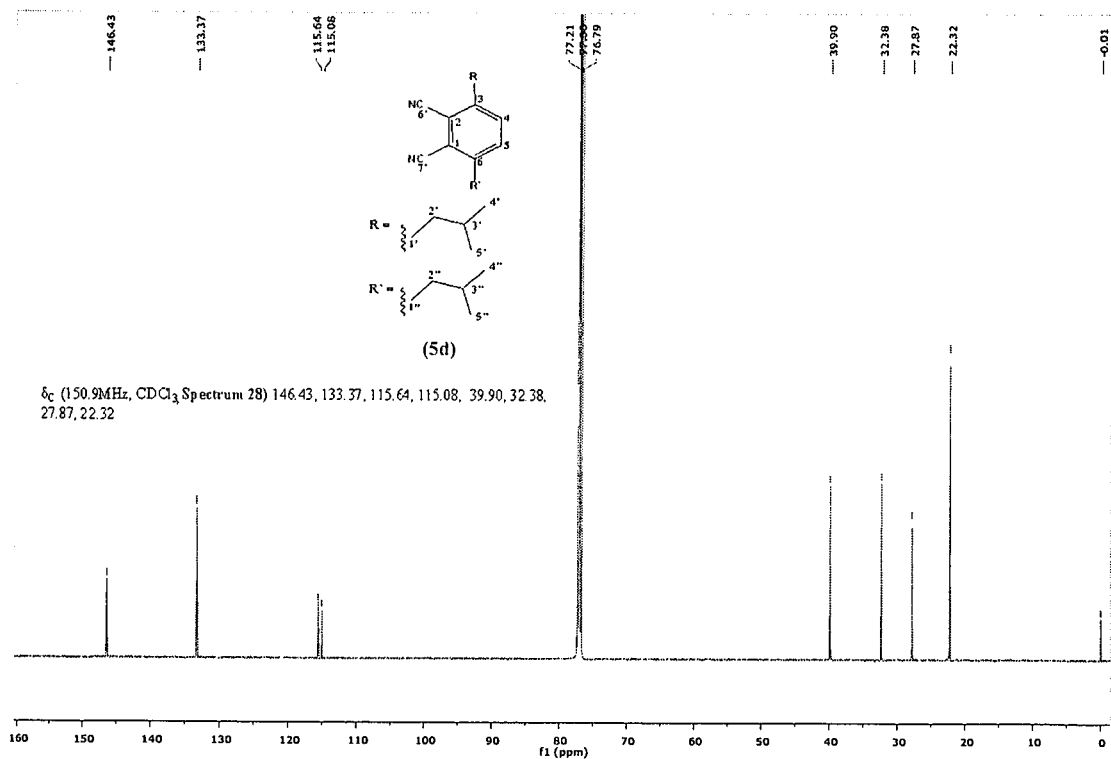


δ_{C} (150.9 MHz, CDCl_3 , Spectrum 26) 146.20, 133.42, 115.63, 115.14, 34.41, 31.91, 30.71, 29.64, 29.62, 29.59, 29.48, 29.34, 29.30, 29.17, 22.68, 14.10

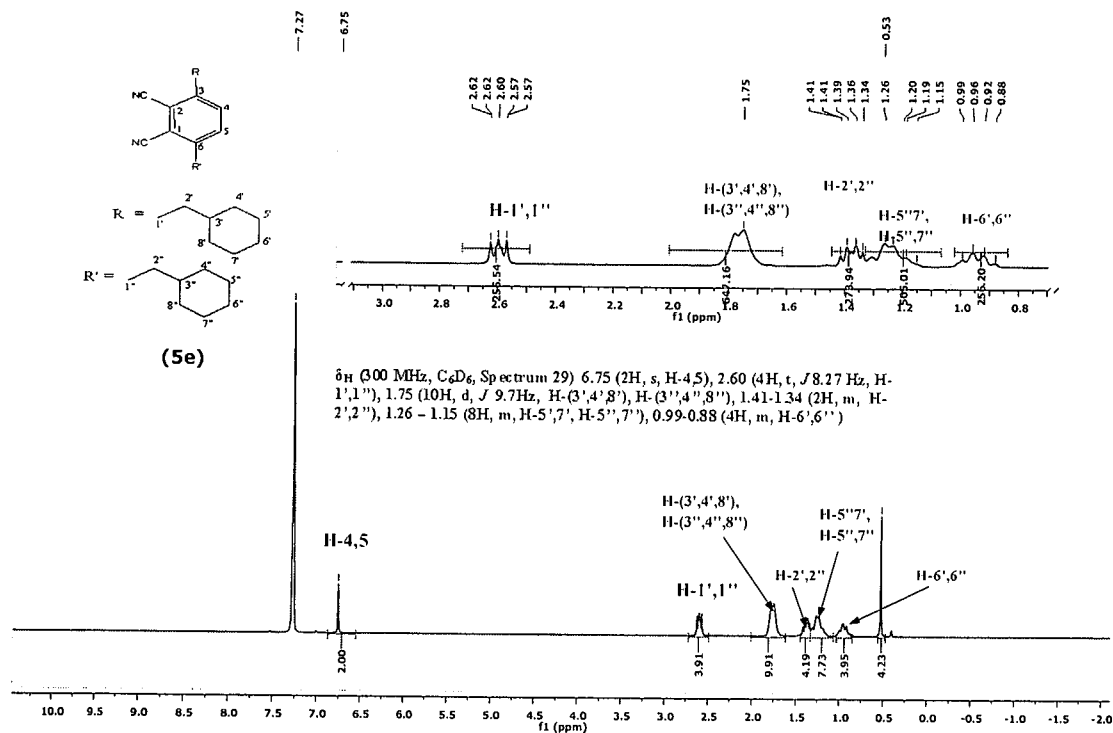
Spectrum 27: 3,6-Diisopentylphthalonitrile, [4.5d].



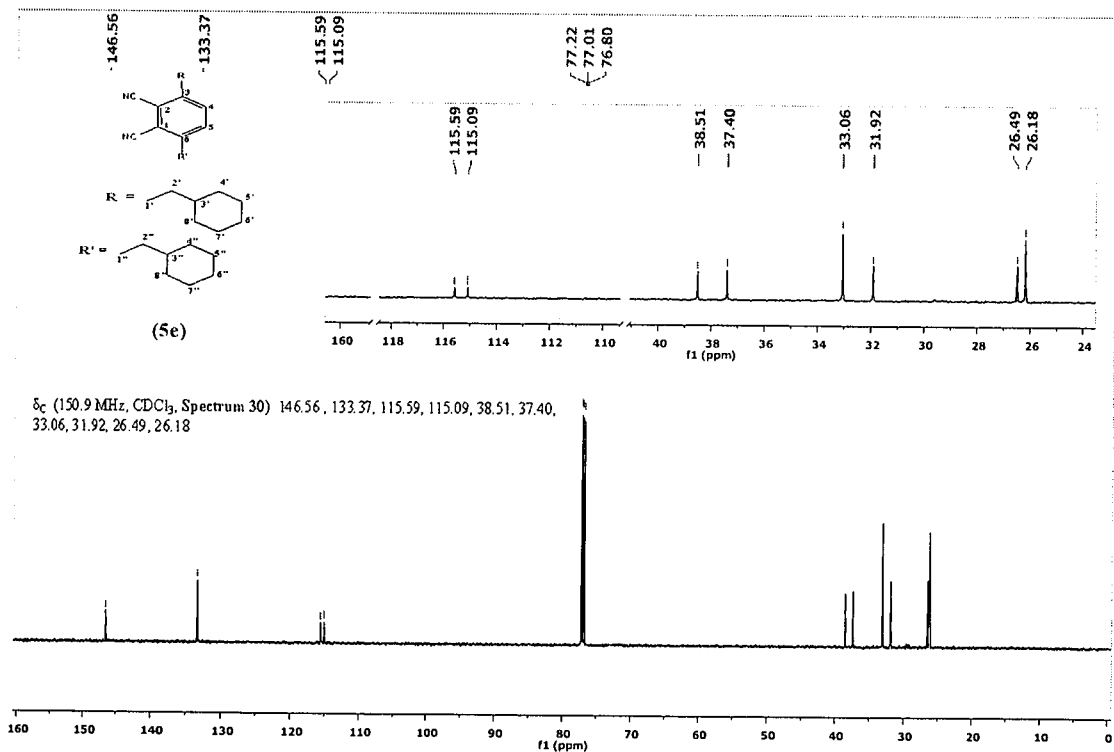
Spectrum 28: 3,6-Diisopentylphthalonitrile, [4.5d].



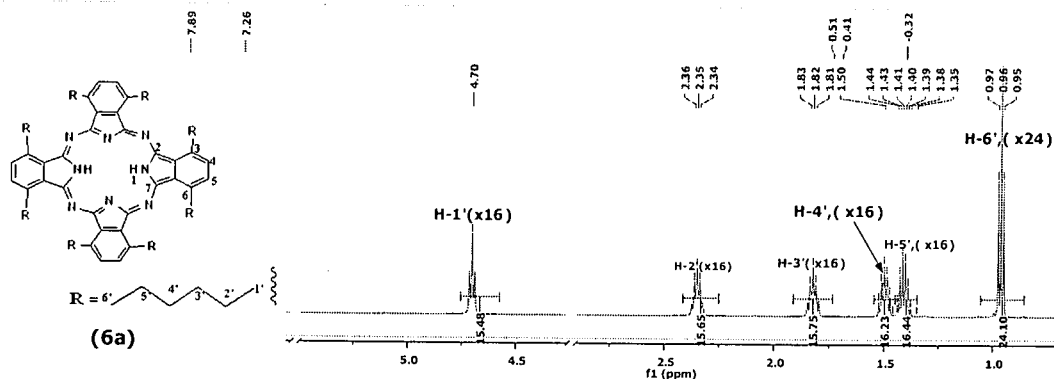
Spectrum 29: 3,6-Di(2-cyclohexylethyl)phthalonitrile, [4.5e].



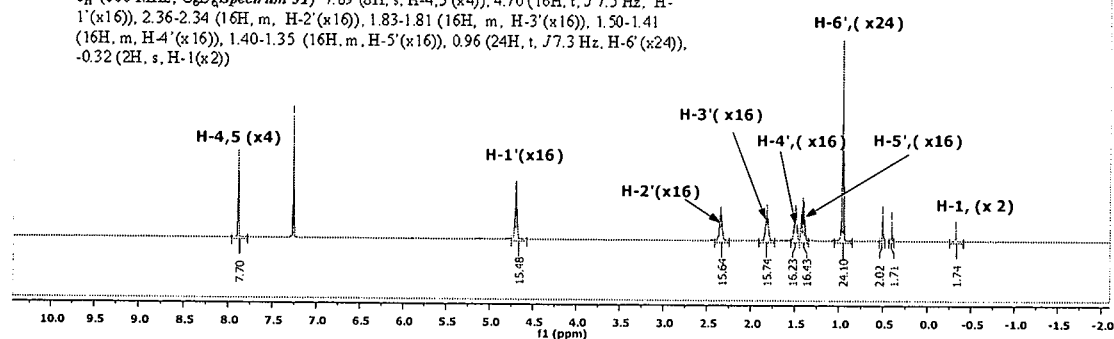
Spectrum 30: 3,6-Di(2-cyclohexylethyl)phthalonitrile, [4.5e].



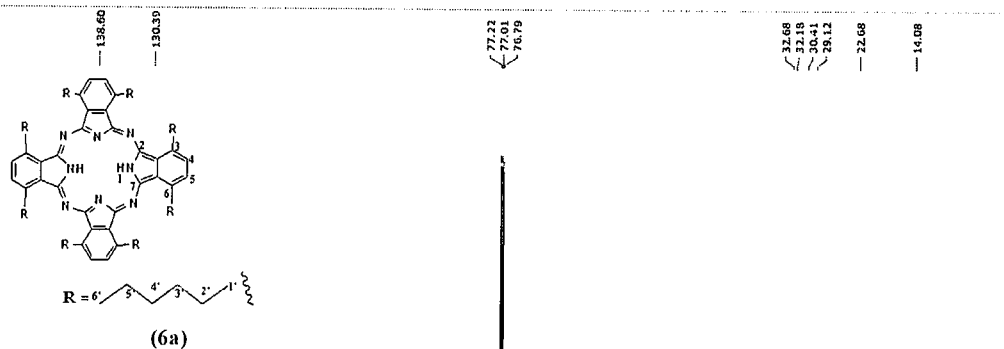
Spectrum 31: 1,4,8,11,15,18,22,25-octahexylphthalocyanine, [4.6a].



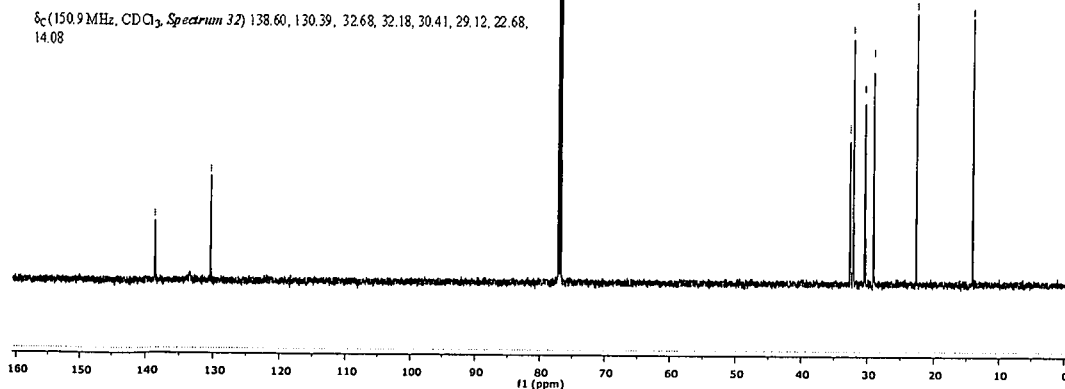
δ_H (600 MHz, C_6D_6 , Spectrum 31) 7.89 (8H, s, H-4,5 (x4)), 4.70 (16H, t, J 7.5 Hz, H-1' (x16)), 2.36-2.34 (16H, m, H-2' (x16)), 1.83-1.81 (16H, m, H-3' (x16)), 1.50-1.41 (16H, m, H-4' (x16)), 1.40-1.35 (16H, m, H-5' (x16)), 0.96 (24H, t, J 7.3 Hz, H-6' (x24)), -0.32 (2H, s, H-1 (x2)).



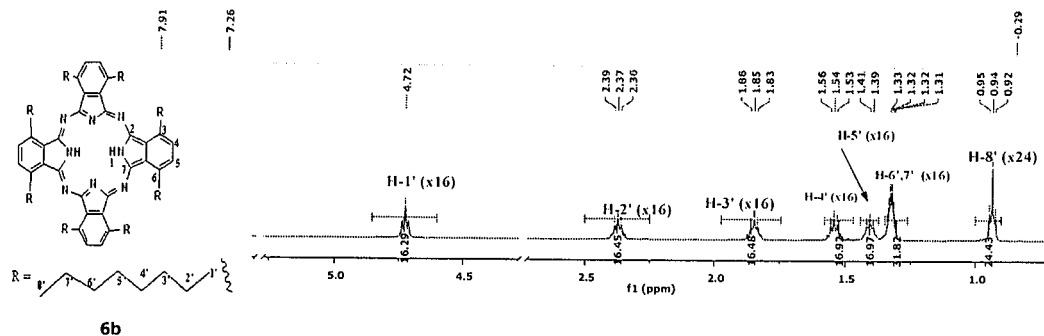
Spectrum 32: 1,4,8,11,15,18,22,25-octahexylphthalocyanine, [4.6a].



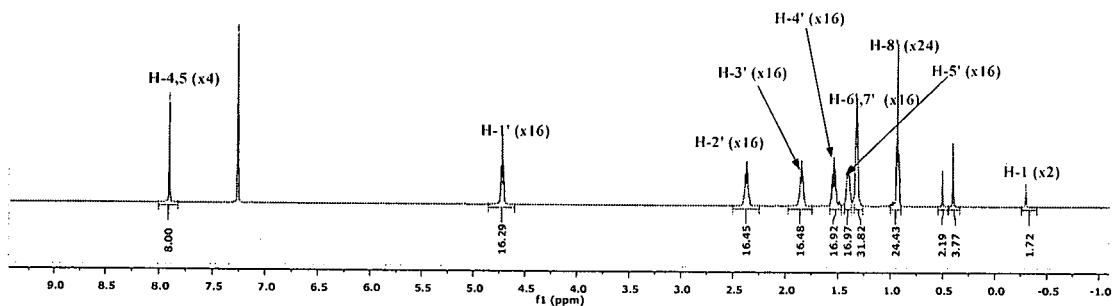
δ_C (150.9 MHz, $CDCl_3$, Spectrum 32) 138.60, 130.39, 32.68, 32.18, 30.41, 29.12, 22.68, 14.08.



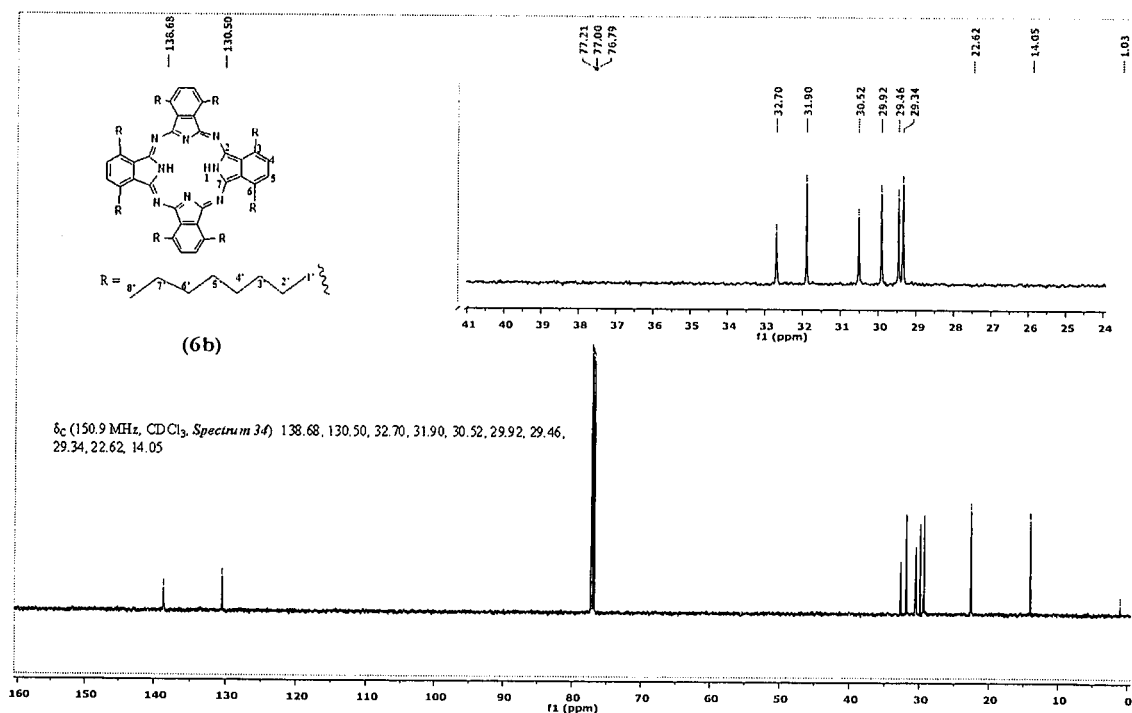
Spectrum 33: 1,4,8,11,15,18,22,25-octaethylphthalocyanine, [4.6b].



δ_H (600 MHz, C_6D_6 , Spectrum 33) 7.91 (8H, s, H-4,5), 4.72 (16H, t, J 7.4 Hz, H-1' (x16)), 2.39-2.36 (16H, m, H-2' (x16)), 1.86-1.83 (16H, m, H-3' (x16)), 1.53 (16H, m, H-4' (x16)), 1.41-1.39 (16H, m, H-5' (x16)), 1.33-1.31 (32H, m, H-6',7' (x16)), 0.95 (24H, t, J 7.0 Hz, H-8' (x24)), -0.29 (2H, s, H-1(x4))

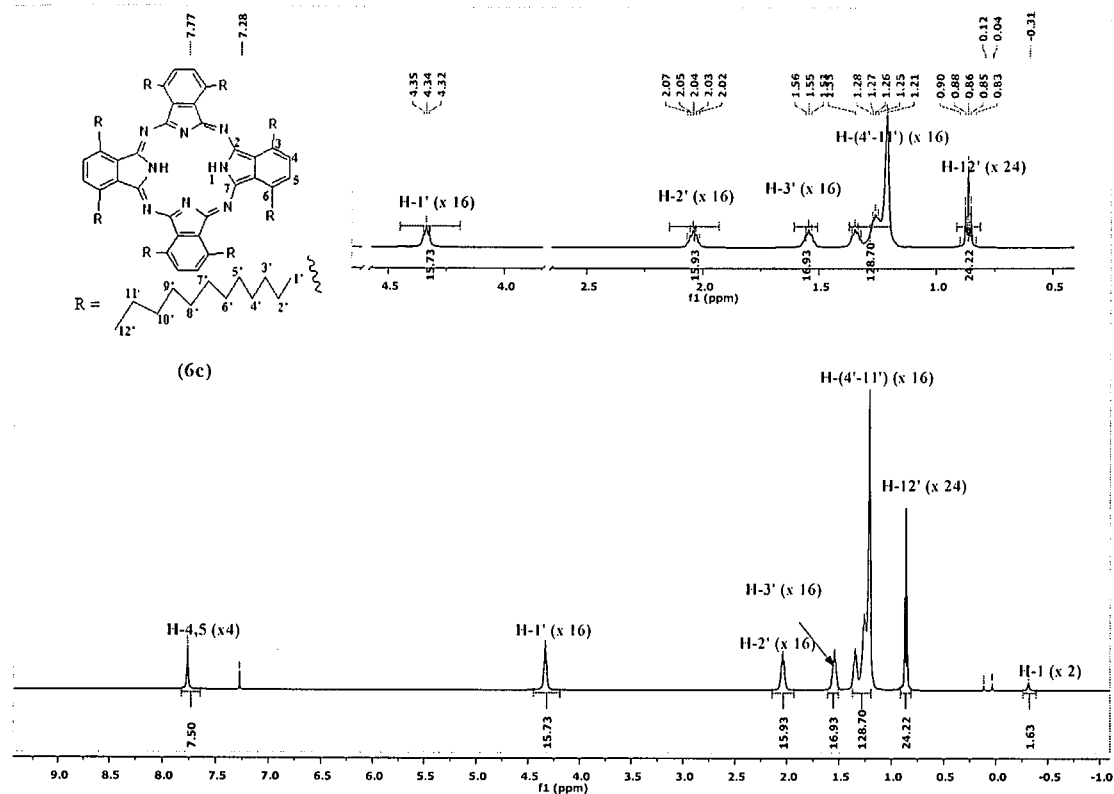


Spectrum 34: 1,4,8,11,15,18,22,25-octaethylphthalocyanine, [4.6b].

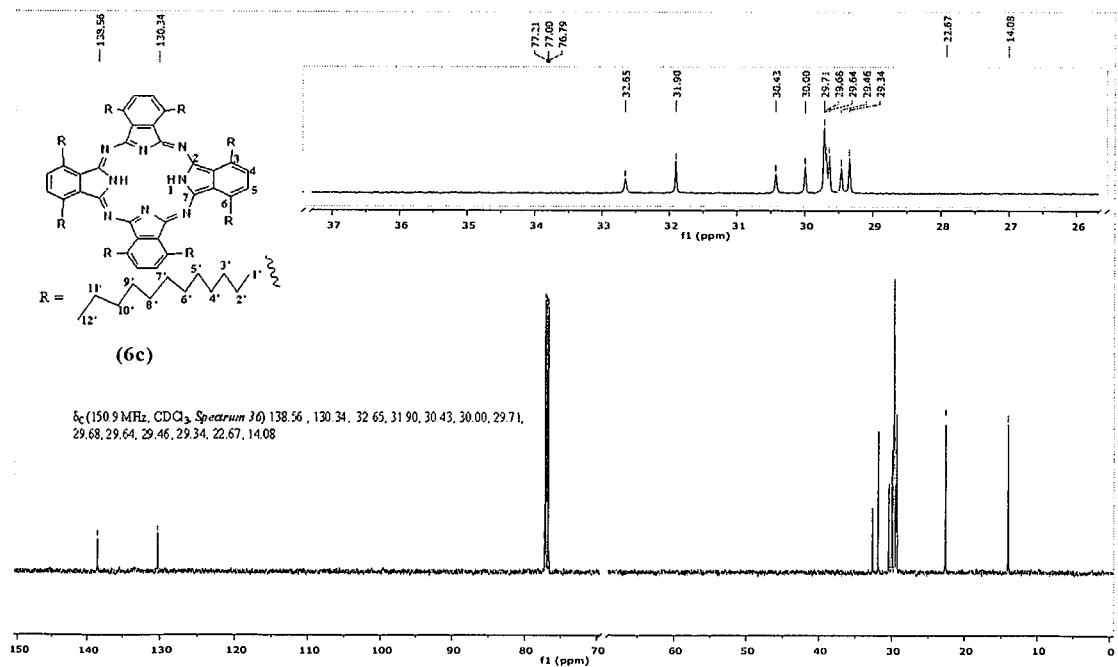


δ_C (150.9 MHz, $CDCl_3$, Spectrum 34) 138.68, 130.50, 32.70, 31.90, 30.52, 29.92, 29.46, 29.34, 22.62, 14.05

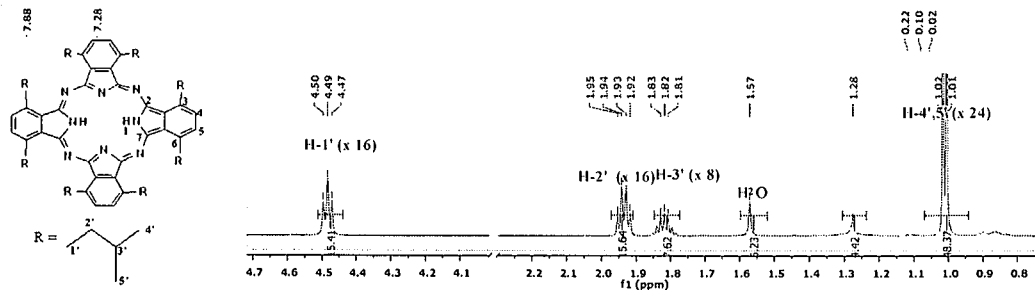
Spectrum 35: 1,4,8,11,15,18,22,25-octadodecylphthalocyanine, [4.6c].



Spectrum 36: 1,4,8,11,15,18,22,25-octadodecylphthalocyanine, [4.6c].

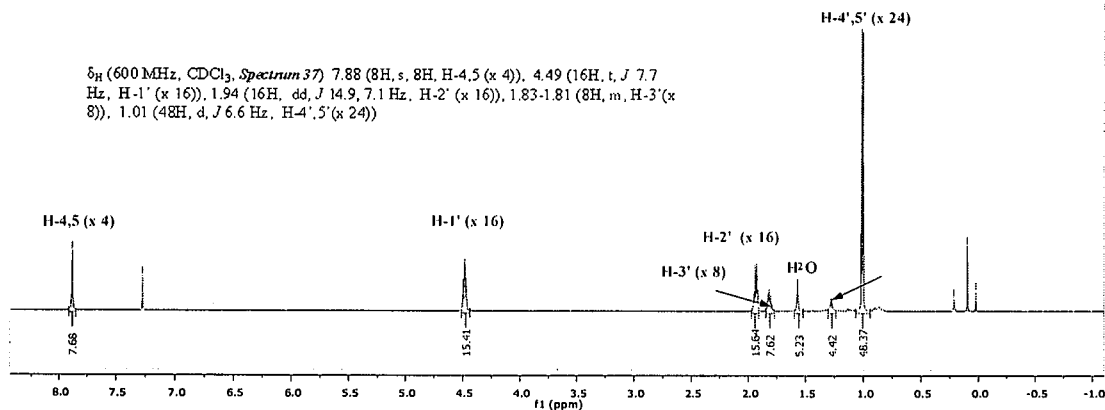


Spectrum 37: 1,4,8,11,15,18,22,25-octa-isopentylphthalocyanine, [4.6d].

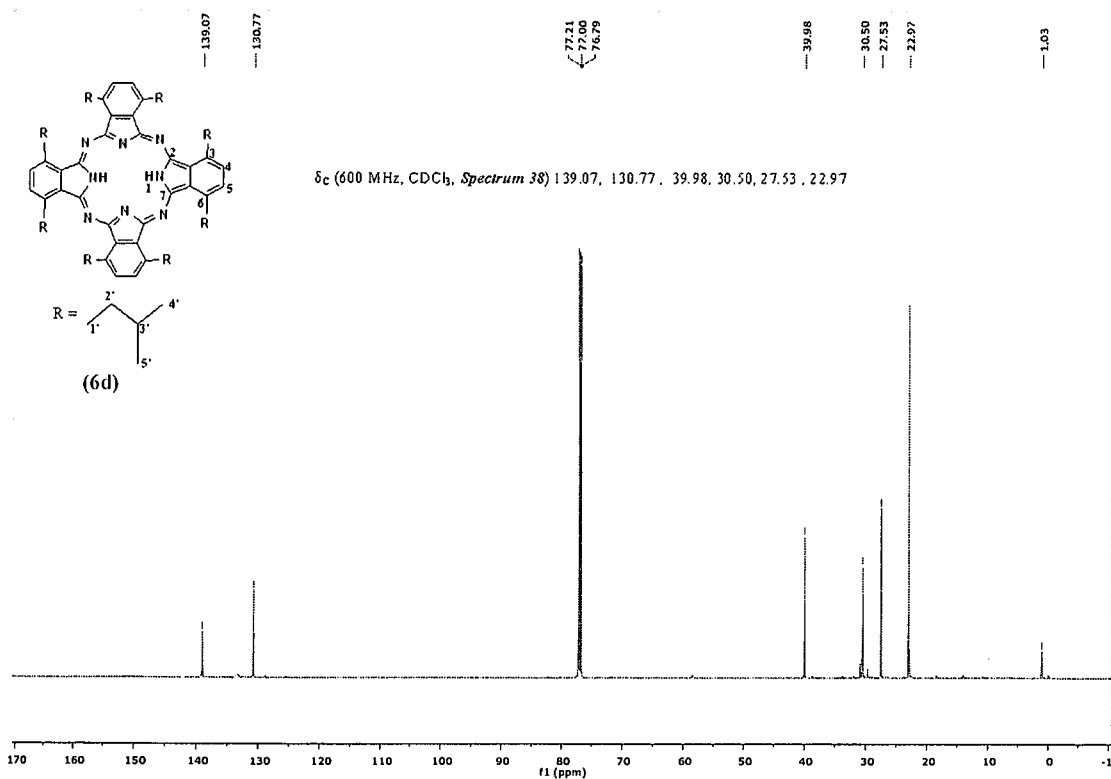


(6d)

δ_H (600 MHz, $CDCl_3$, Spectrum 37) 7.88 (8H, s, 8H, H-4,5 (x 4)), 4.49 (16H, t, J 7.7 Hz, H-1' (x 16)), 1.94 (16H, dd, J 14.9, 7.1 Hz, H-2' (x 16)), 1.83-1.81 (8H, m, H-3' (x 8)), 1.01 (48H, d, J 6.6 Hz, H-4',5' (x 24))



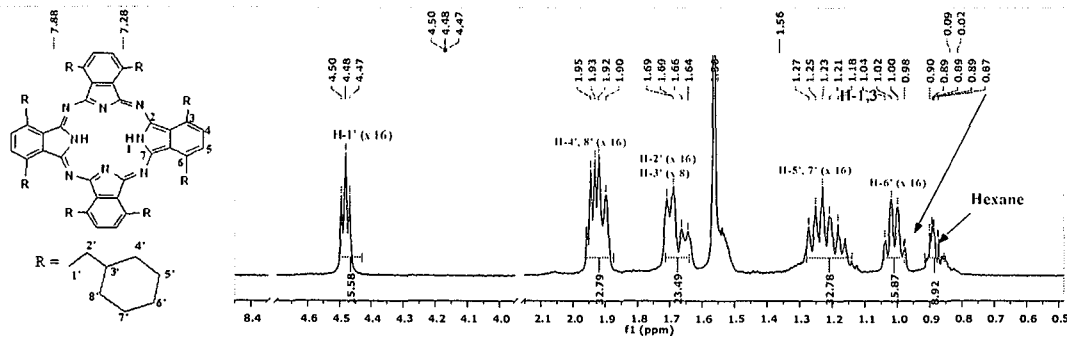
Spectrum 38: 1,4,8,11,15,18,22,25-octa-isopentylphthalocyanine, [4.6d].



δ_C (600 MHz, $CDCl_3$, Spectrum 38) 139.07, 130.77, 39.98, 30.50, 27.53, 22.97

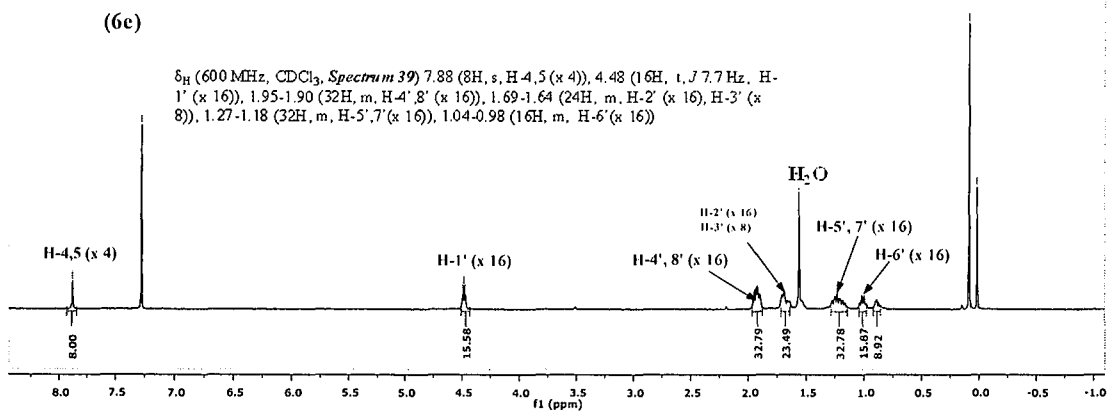
(6d)

Spectrum 39: 1,4,8,11,15,18,22,25-octa(2-cyclohexylethyl)phthalocyanine, [4.6e]

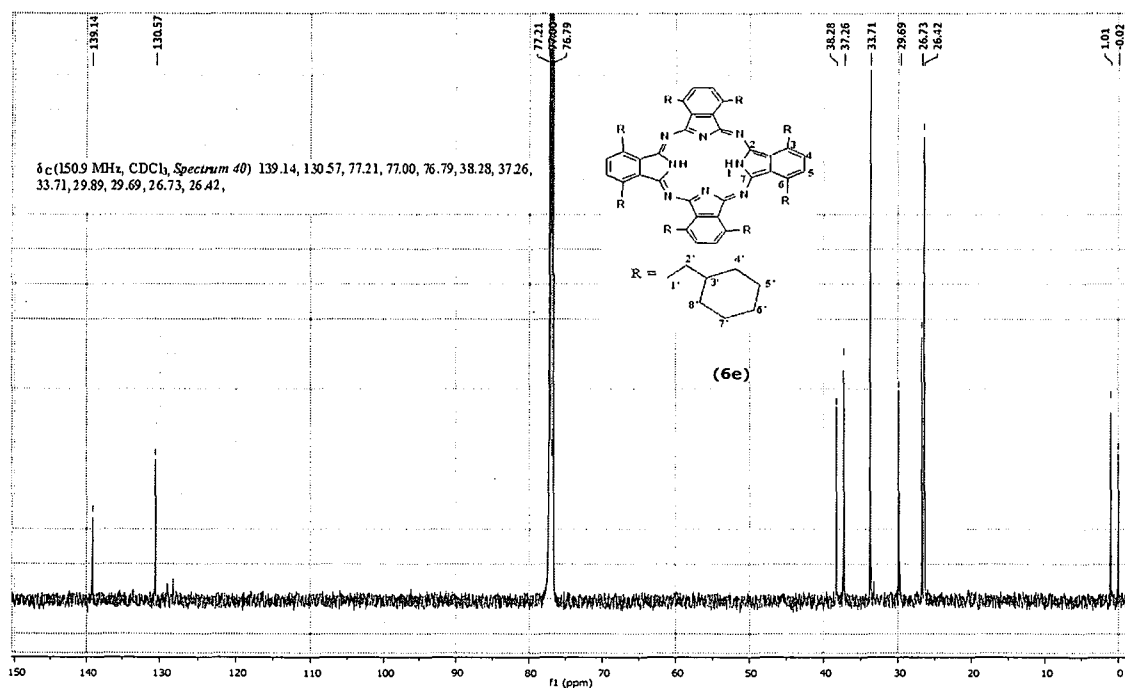


(6e)

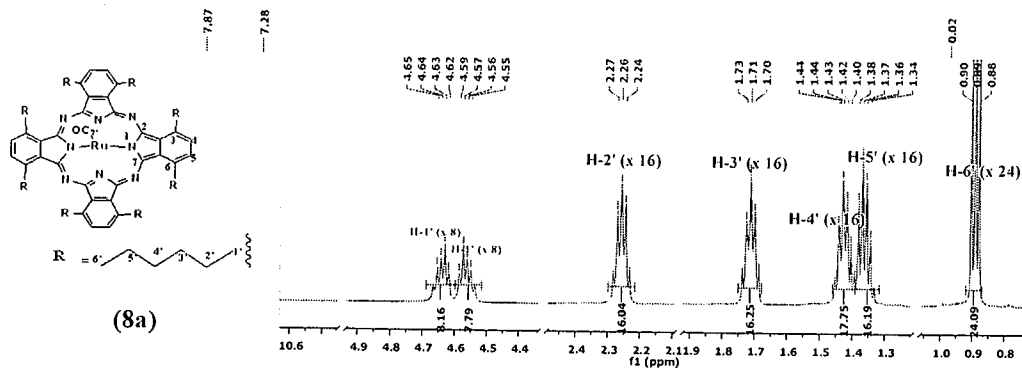
δ_H (600 MHz, $CDCl_3$, *Spectrum 39*) 7.88 (8H, s, H-4,5 (x 4)), 4.48 (16H, t, J 7.7 Hz, H-1' (x 16)), 1.95-1.90 (32H, m, H-4', 8' (x 16)), 1.69-1.64 (24H, m, H-2' (x 16), H-3' (x 8)), 1.27-1.18 (32H, m, H-5', 7' (x 16)), 1.04-0.98 (16H, m, H-6' (x 16))



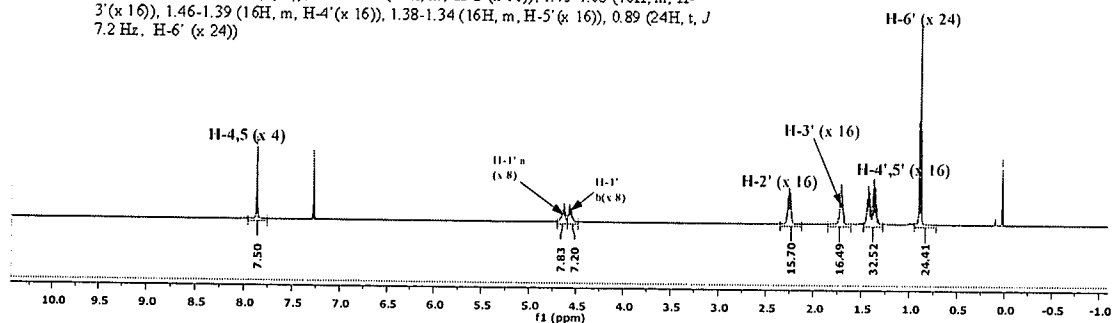
Spectrum 40: 1,4,8,11,15,18,22,25-octa(2-cyclohexylethyl)phthalocyanine, [4.6e].



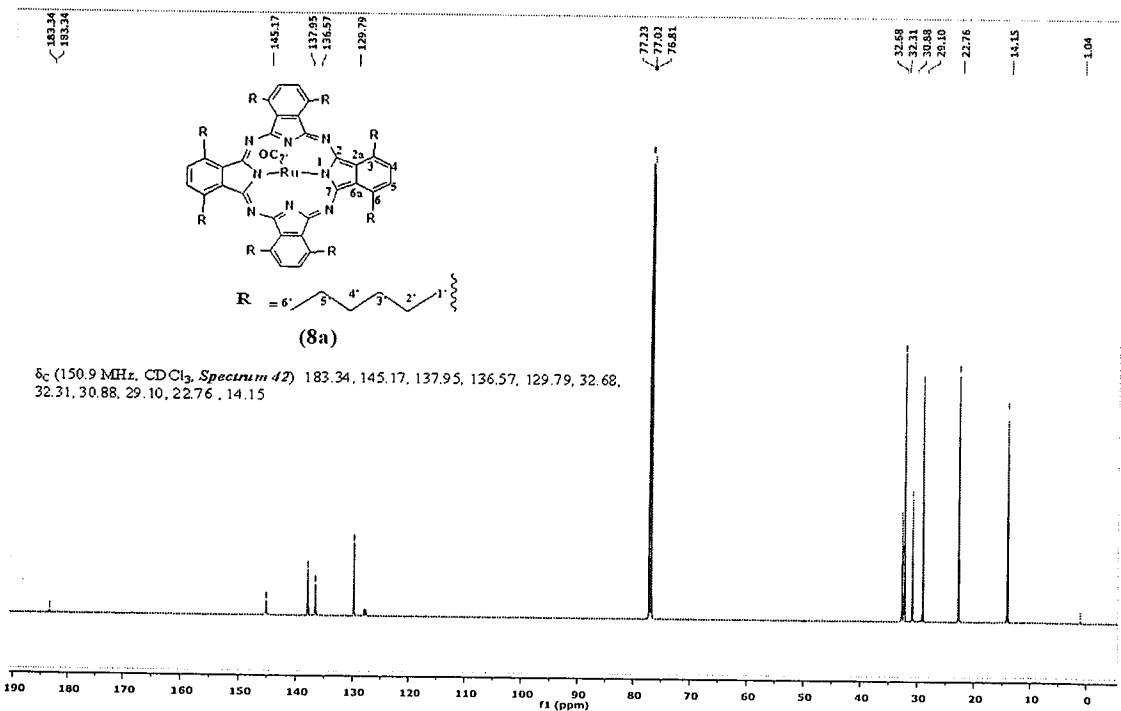
Spectrum 41: Carbonyl(1,4,8,11,15,18,22,25-octahexylphthalocyaninato)ruthenium(II), [4.8a].



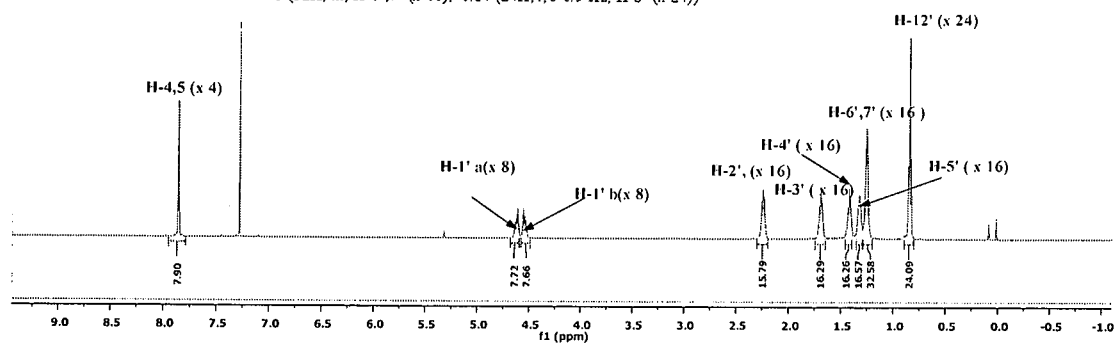
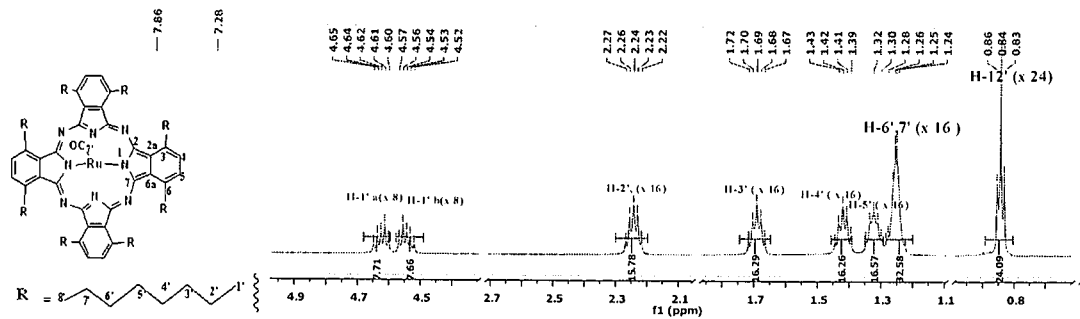
δ_H (600 MHz, $CDCl_3$, *Spectrum 41*) 7.87 (8H, s, H-4,5), 4.65-4.62 (8H, m, H-1' α (x8)), 4.59-4.55 (8H, m, H-1' β (x8)), 2.30-2.22 (16H, m, H-2'(x 16)), 1.75-1.68 (16H, m, H-3'(x 16)), 1.46-1.39 (16H, m, H-4'(x 16)), 1.38-1.34 (16H, m, H-5'(x 16)), 0.89 (24H, t, J 7.2 Hz, H-6'(x 24))



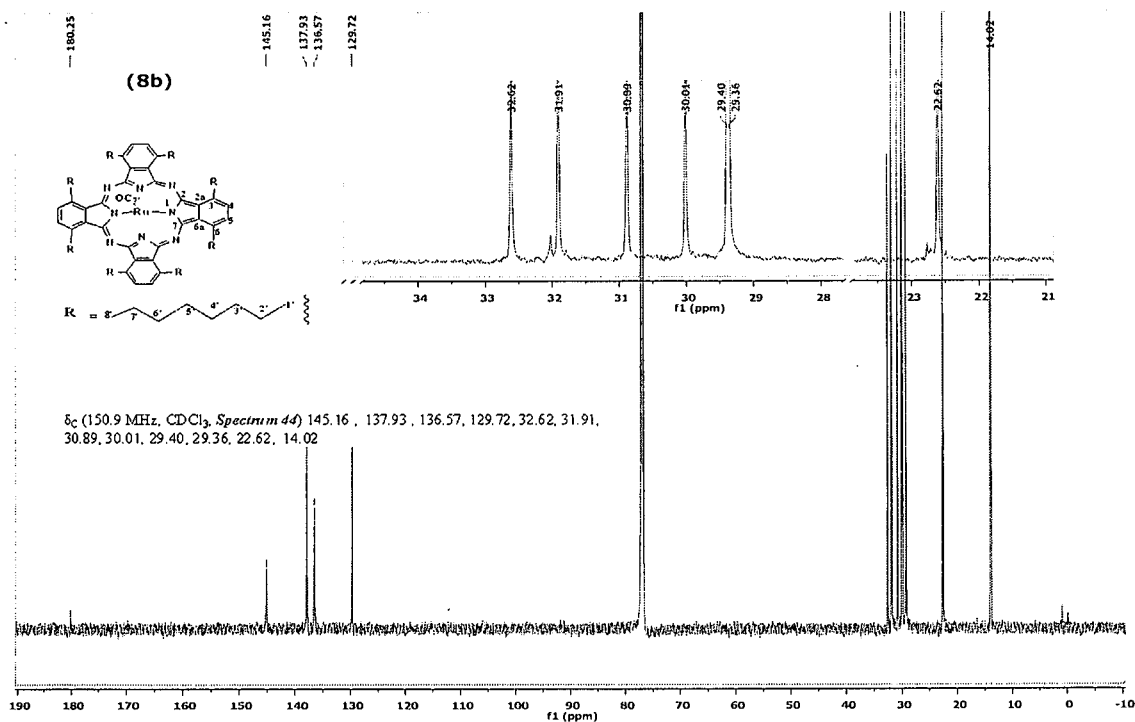
Spectrum 42: Carbonyl(1,4,8,11,15,18,22,25-octahexylphthalocyaninato)ruthenium(II), [4.8a].



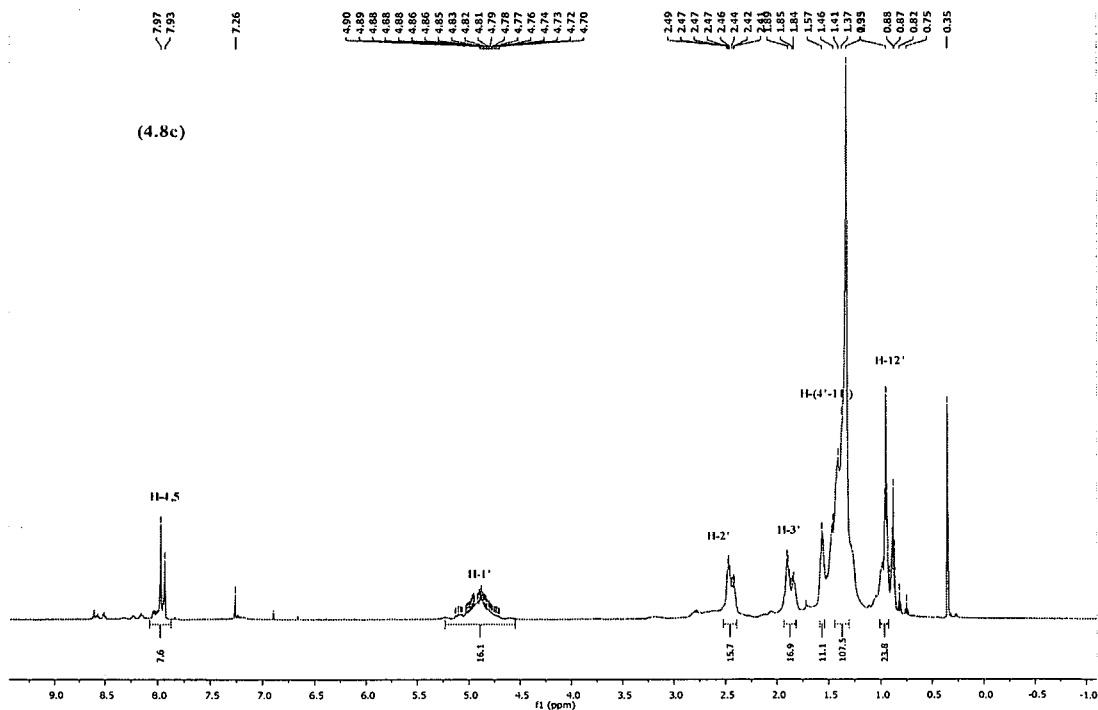
Spectrum 43: Carbonyl(1,4,8,11,15,18,22,25-octaoctylphthalocyaninato)ruthenium(II), [4.8b].



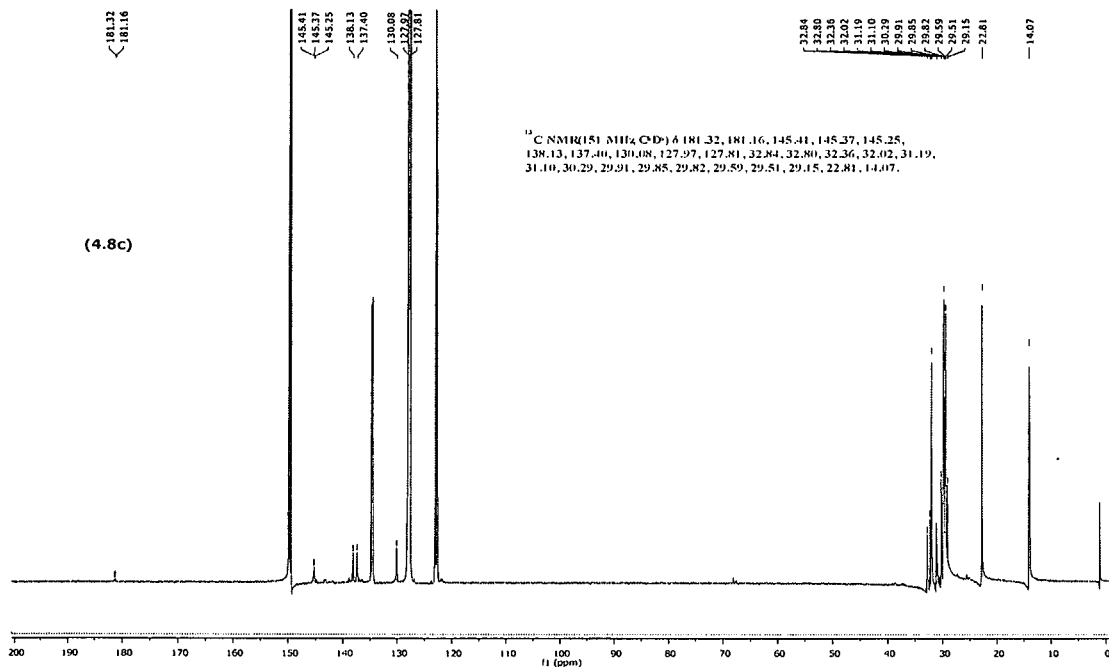
Spectrum 44: Carbonyl(1,4,8,11,15,18,22,25-octaocetylphthalocyaninato)ruthenium(II), [4.8b].



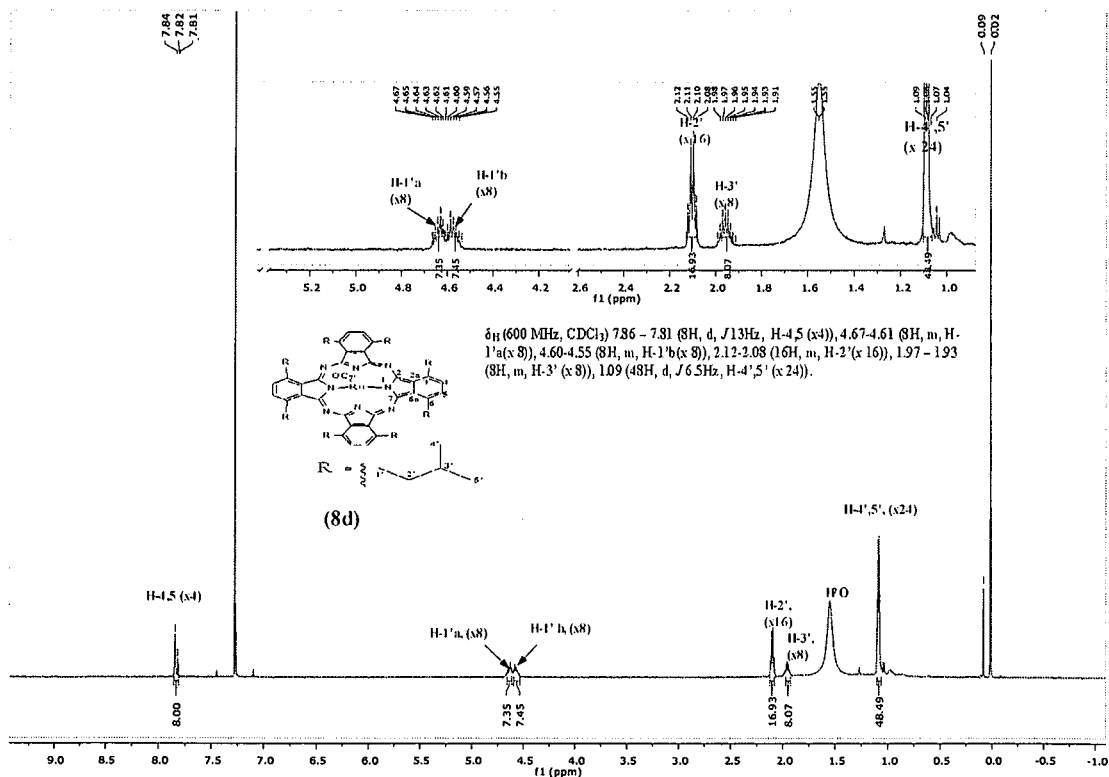
Spectrum 45: Carbonyl(1,4,8,11,15,18,22,25-octadodecylphthalocyaninato)ruthenium(II), [4.8c]



Spectrum 46: Carbonyl(1,4,8,11,15,18,22,25-octadecylphthalocyaninato)ruthenium(II), [4.8c].



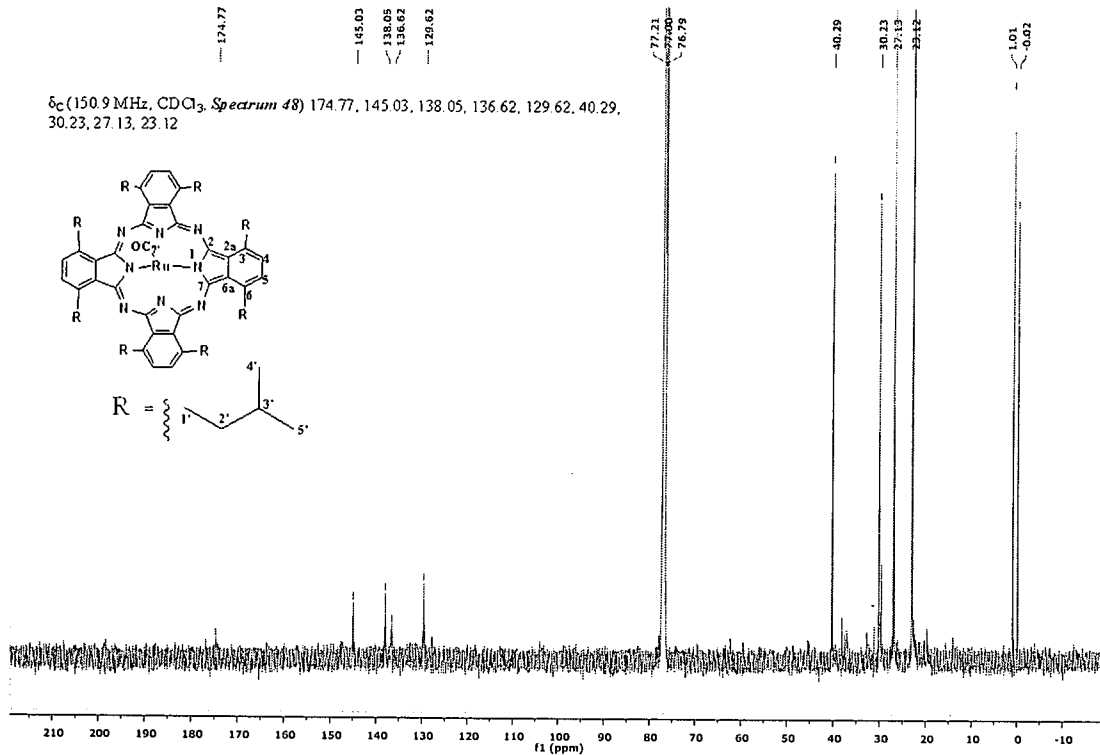
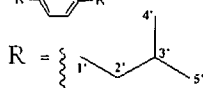
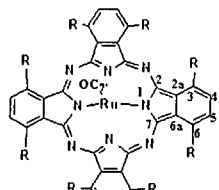
Spectrum 47: Carbonyl(1,4,8,11,15,18,22,25-octaisopentylphthalocyaninato)ruthenium(II), [4.8d].



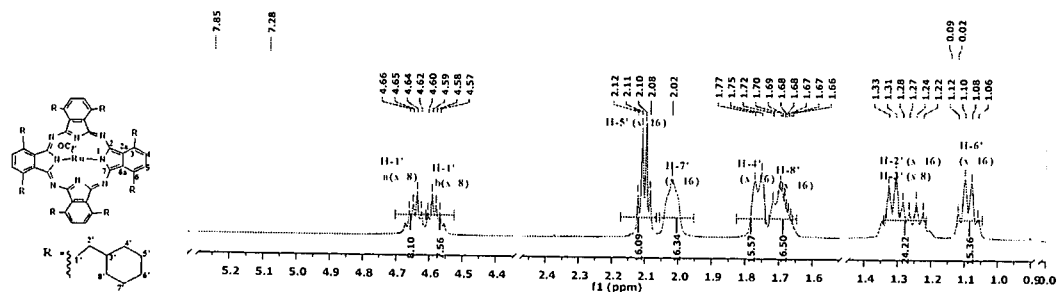
Spectrum 48: Carbonyl(1,4,8,11,15,18,22,25-octaisopentylphthalocyaninato)ruthenium(II), [4.8d].

Spectrum 48: Carbonyl(1,4,8,11,15,18,22,25-octaisopentylphthalocyaninato)ruthenium(II), [4.8d].

δ_C (150.9 MHz, $CDCl_3$, Spectrum 48) 174.77, 145.03, 138.05, 136.62, 128.62, 129.62, 40.29, 30.23, 27.13, 23.12

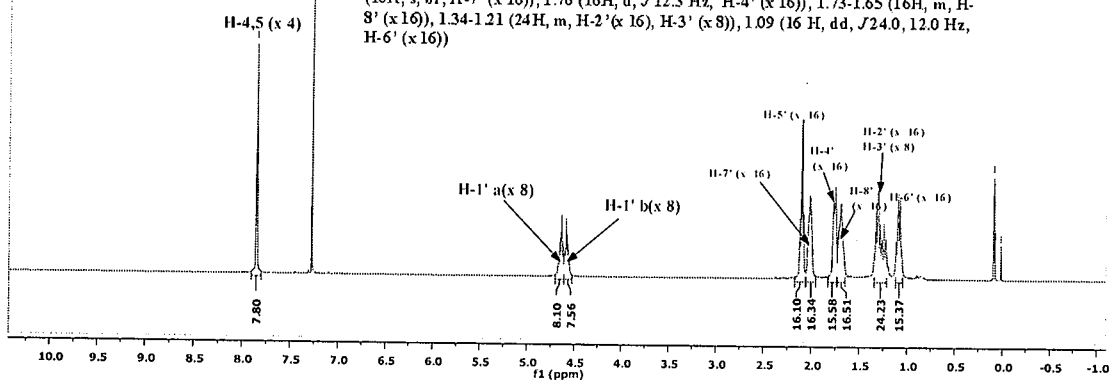


Spectrum 49: Carbonyl(1,4,8,11,15,18,22,25-octa(2- cyclohexylethylphthalocyaninato)ruthenium(II), [4.8e].



(8c)

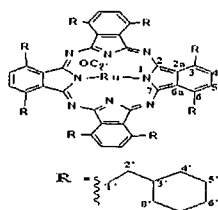
δ_H (600 MHz, $CDCl_3$, *Spectrum 49*) 7.84 (8H, s, H-4,5 (x 4)), 4.65-4.61 (8H, m, H-1' α (x 8)), 4.60-4.56 (8H, m, H-1' β (x 8)), 2.10 (16H, dd, J 14.4, 7.4 Hz, H-5' (x 16)), 2.02 (16H, s, br, H-7' (x 16)), 1.76 (16H, d, J 12.3 Hz, H-4' (x 16)), 1.73-1.65 (16H, m, H-8' (x 16)), 1.34-1.21 (24H, m, H-2' (x 16), H-3' (x 8)), 1.09 (16 H, dd, J 24.0, 12.0 Hz, H-6' (x 16))



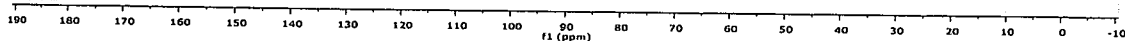
Spectrum 50: Carbonyl(1,4,8,11,15,18,22,25-octa(2- cyclohexylethylphthalocyaninato)ruthenium(II), [4.8e].



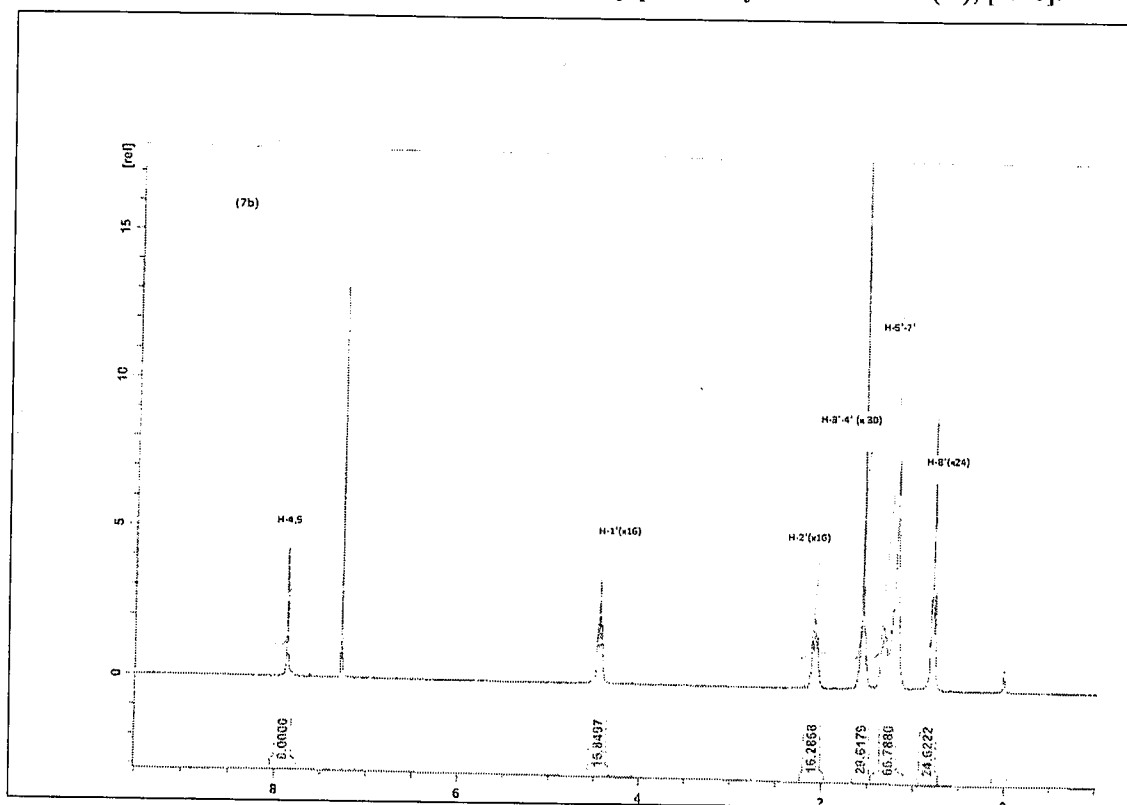
δ_C (150.9 MHz, $CDCl_3$, *Spectrum 50*) 183.32, 183.30, 145.13, 138.20, 136.56, 129.58, 38.70, 36.85, 33.88, 29.59, 26.82, 26.50



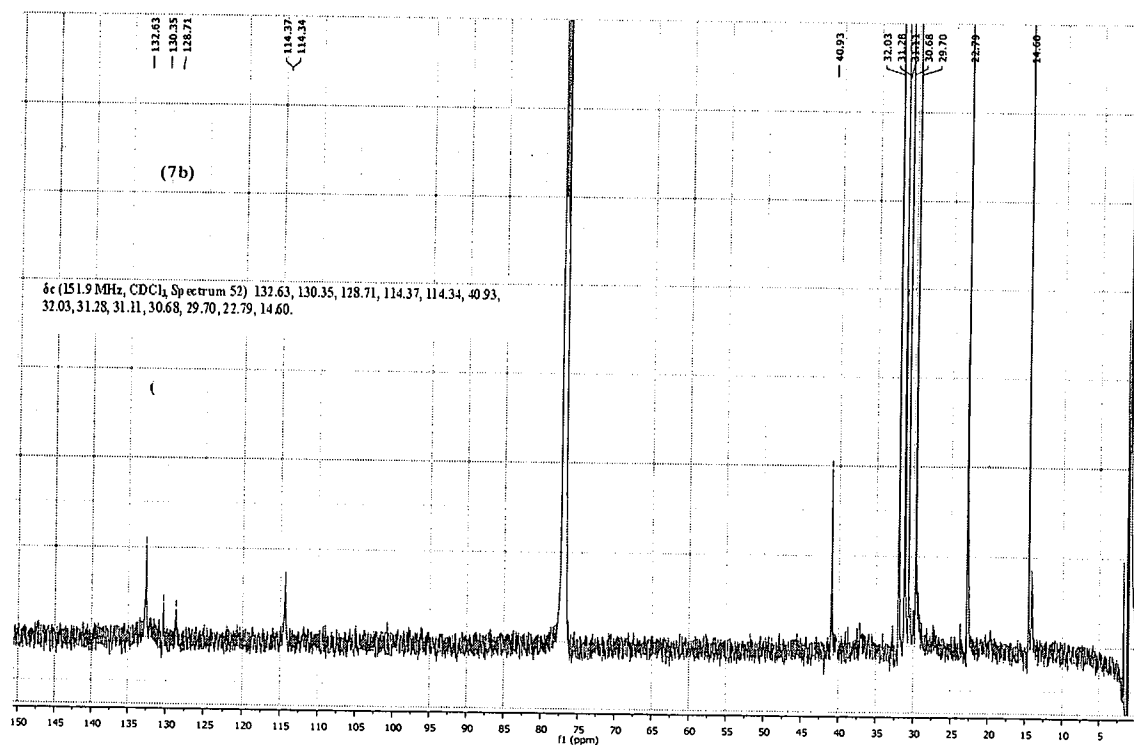
(8c)



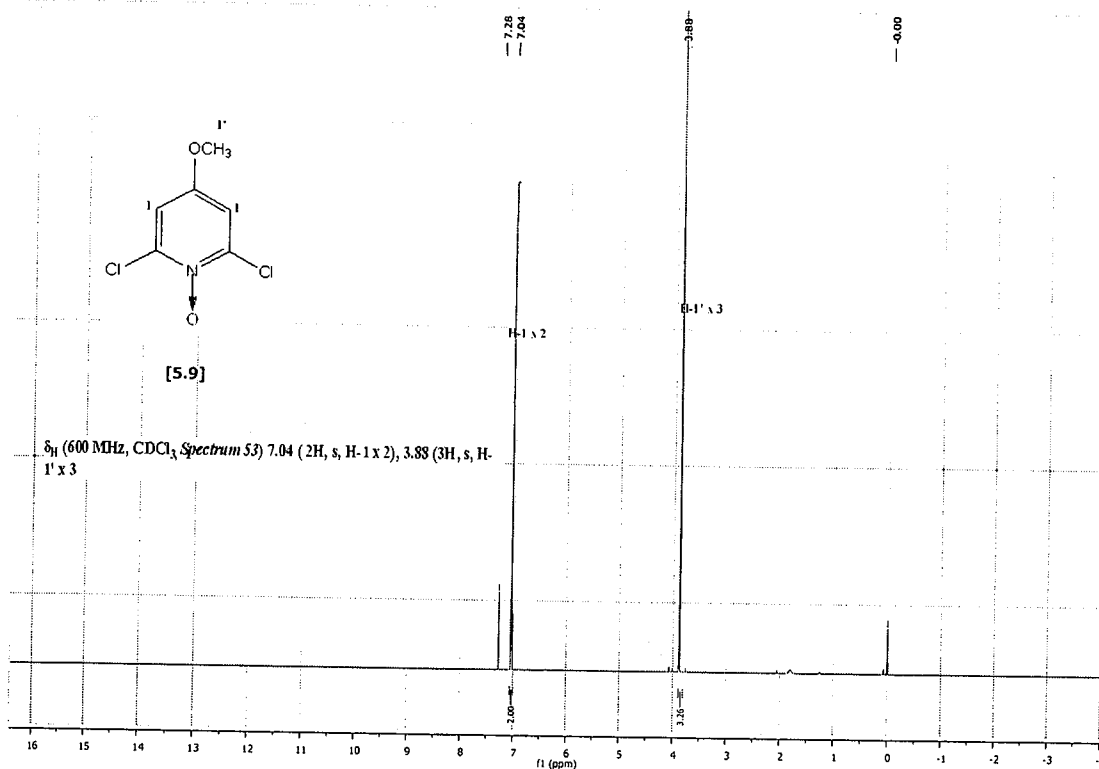
Spectrum 51: 1,4,8,11,15,18,22,25-Octaoctylphthalocyaninato cobalt(II), [4.7b].



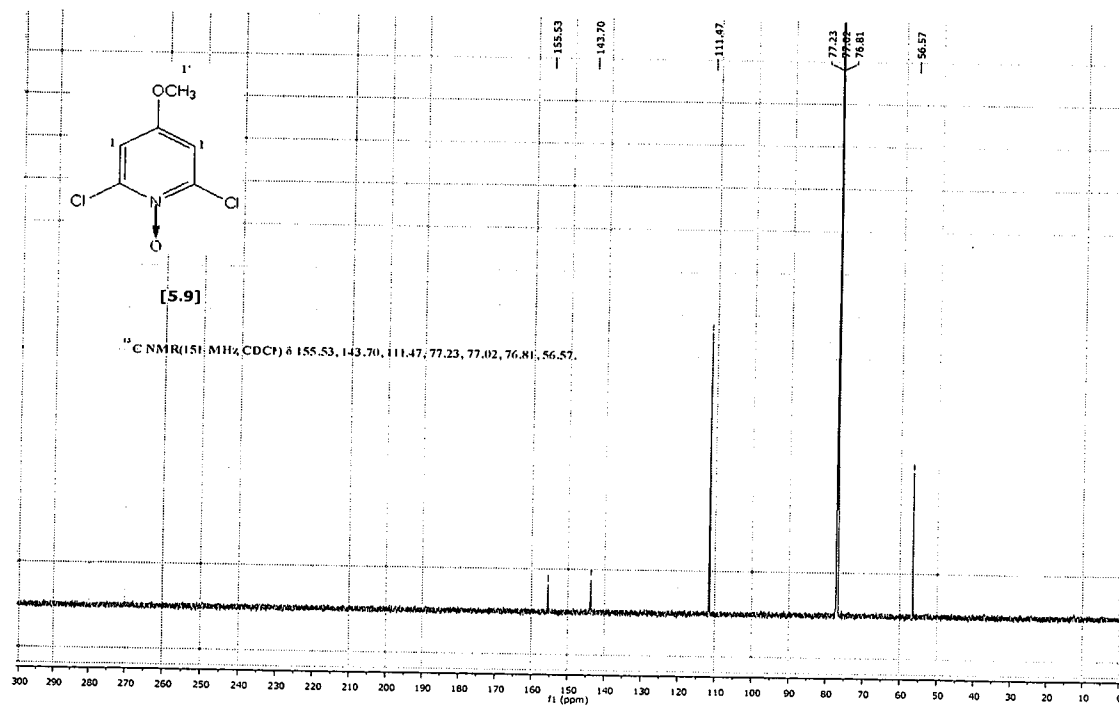
Spectrum 52: 1,4,8,11,15,18,22,25-Octaoctylphthalocyaninato cobalt(II), [4.7b].



Spectrum 53: 2,6-dichloro-4-methoxypyridine N-oxide [5.9]



Spectrum 54: 2,6-dichloro-4-methoxypyridine N-oxide [5.9]



FT-IR SPECTRA

Plate 1: 2,5-Dihexylthiophene, [4.3a]

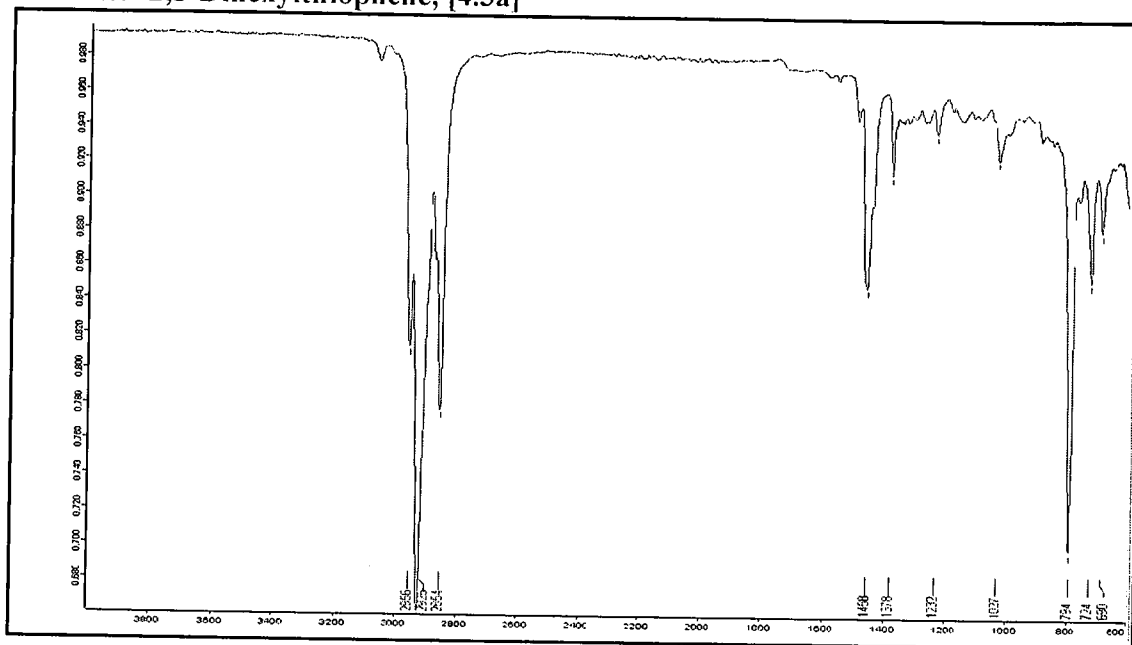


Plate 2: 2,5-Dioctylthiophene, [4.3b]

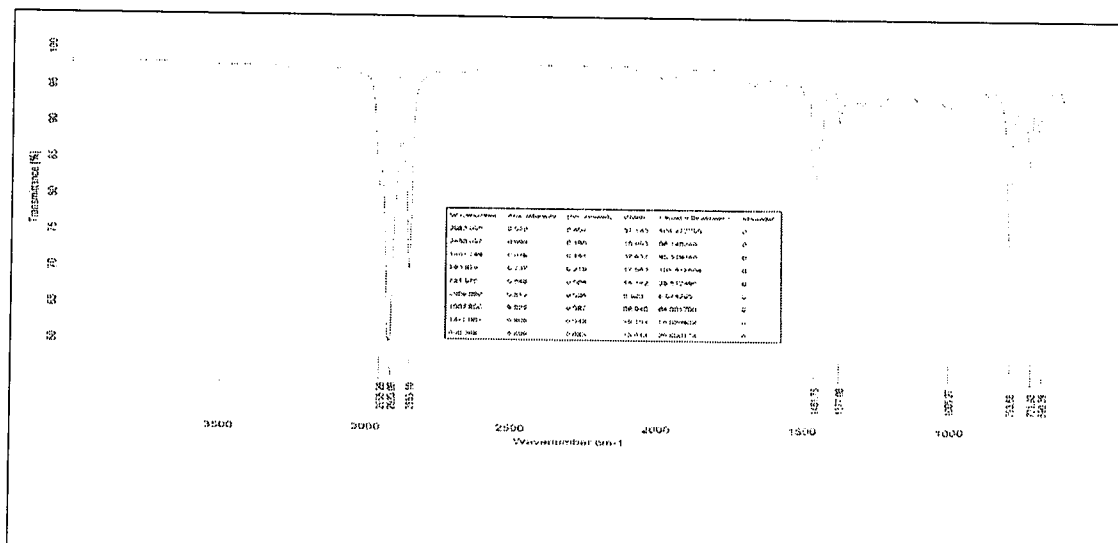


Plate 3: 2,5-Didodecylthiophene, [4.3c]

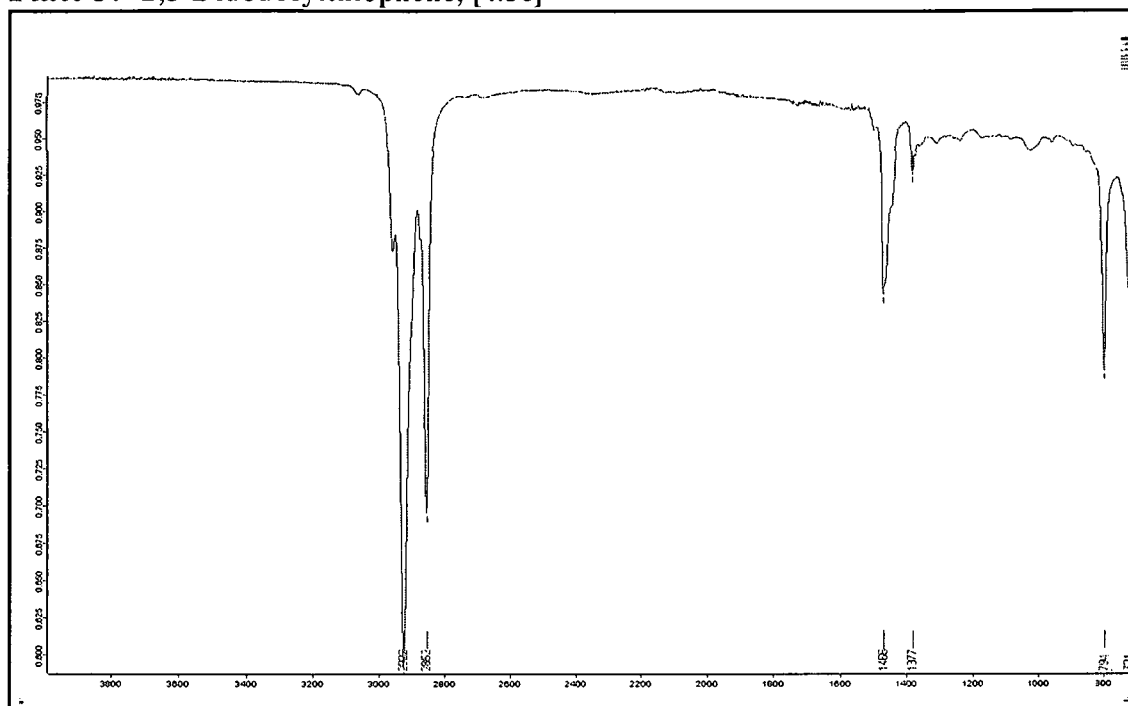


Plate 4: 2,5-Diisopentylthiophene, [4.3d]

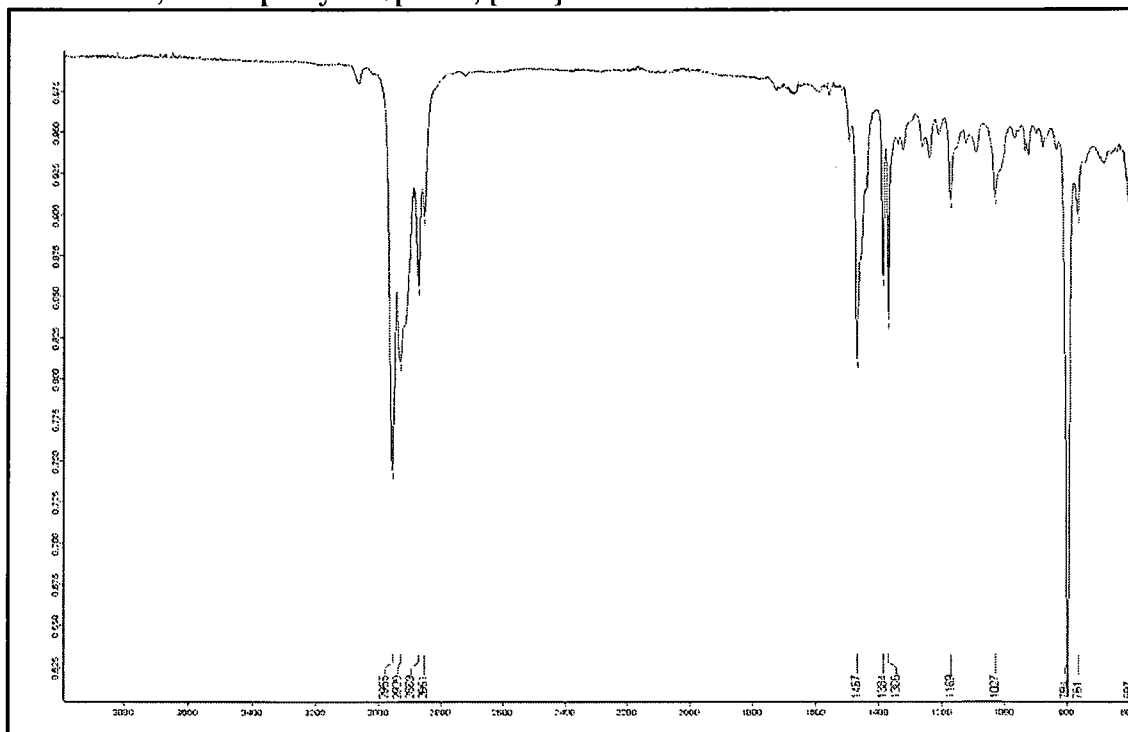


Plate 5: 2,5-Di(2-cyclohexylethyl)thiophene, [4.3e]

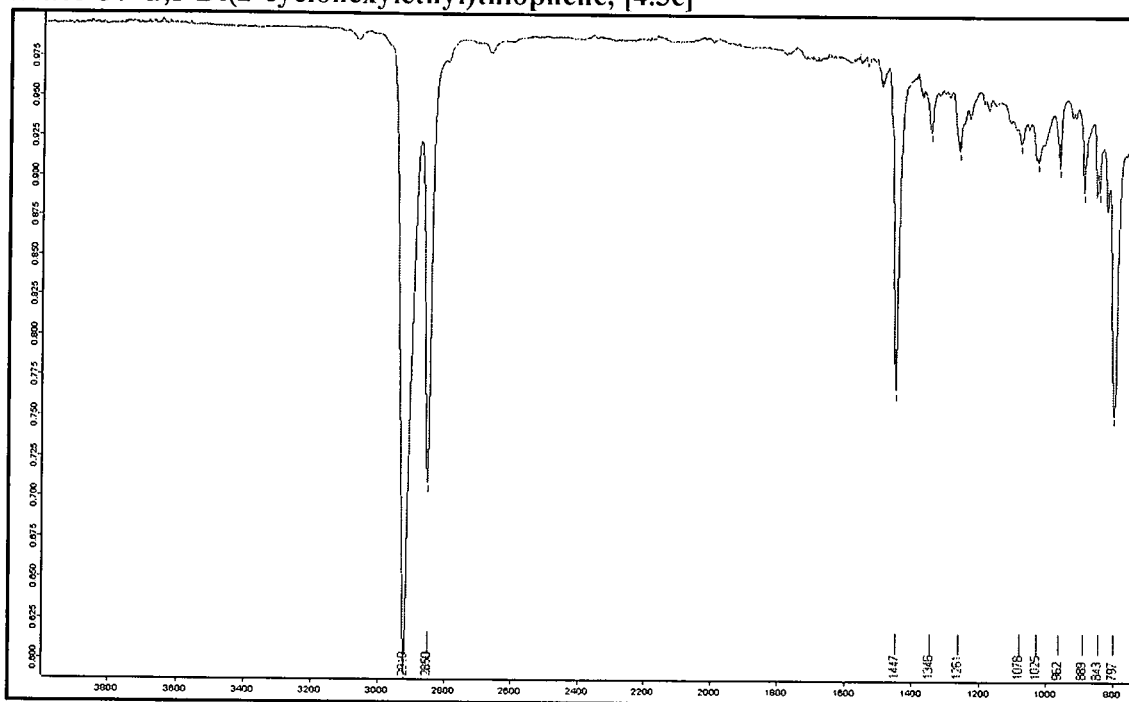


Plate 6: 2,5-Dihexylthiophene 1,1-dioxide, [4.4a]

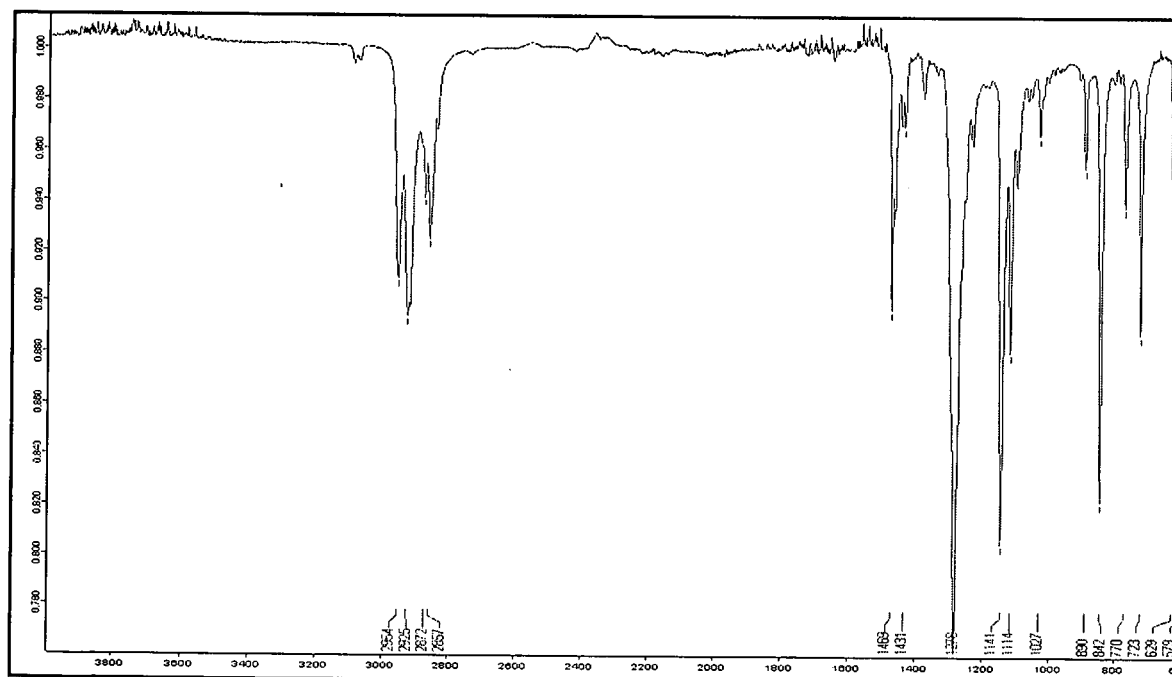


Plate 7: 2,5-Dioctylthiophene 1,1-dioxide, [4.4b]

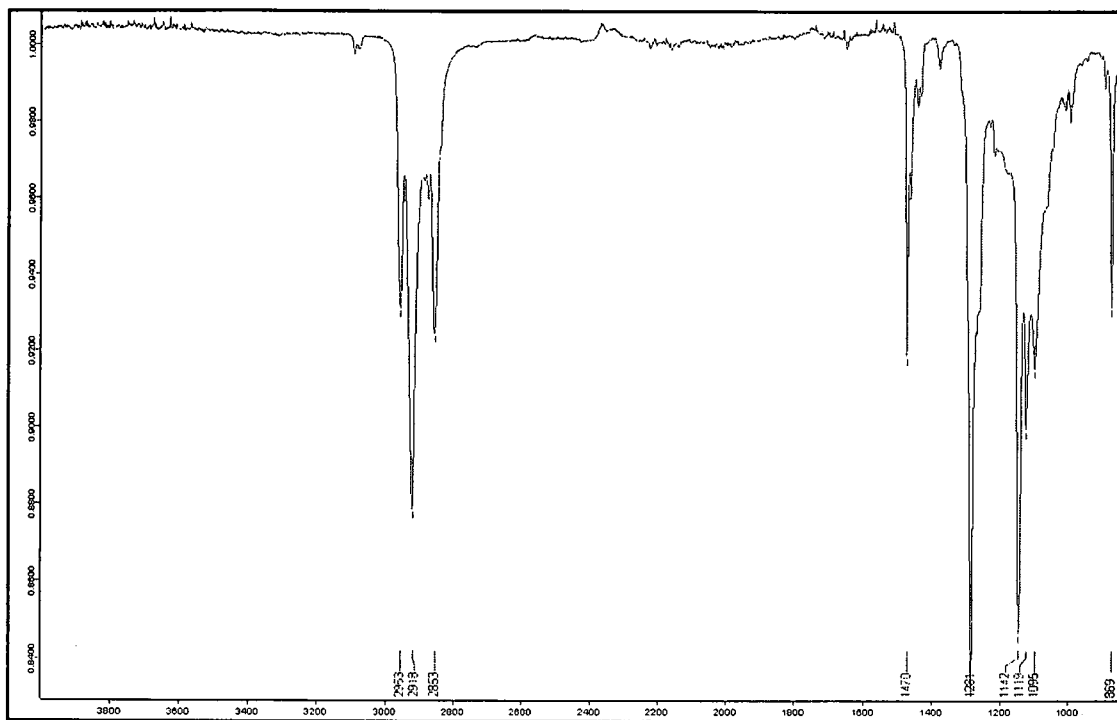


Plate 8: 2,5-Didodecylthiophene 1,1-dioxide, [4.4c]

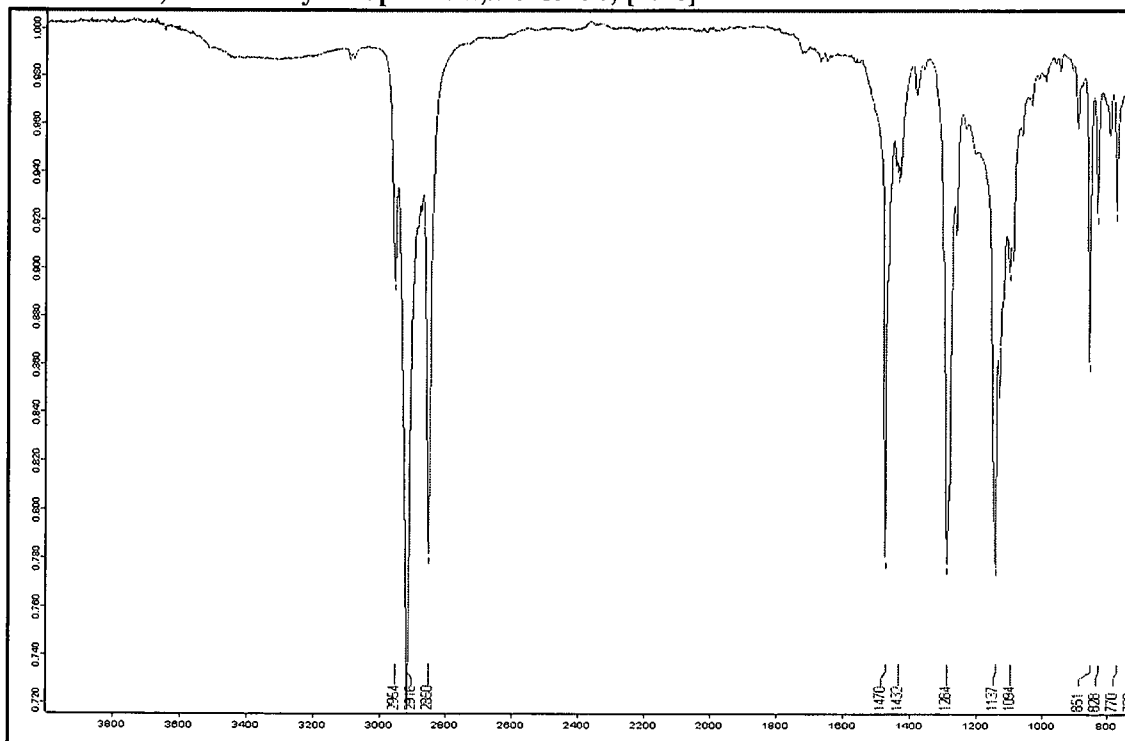


Plate 9: 2,5-Diisopentylthiophene 1,1-dioxide, [4.4d]

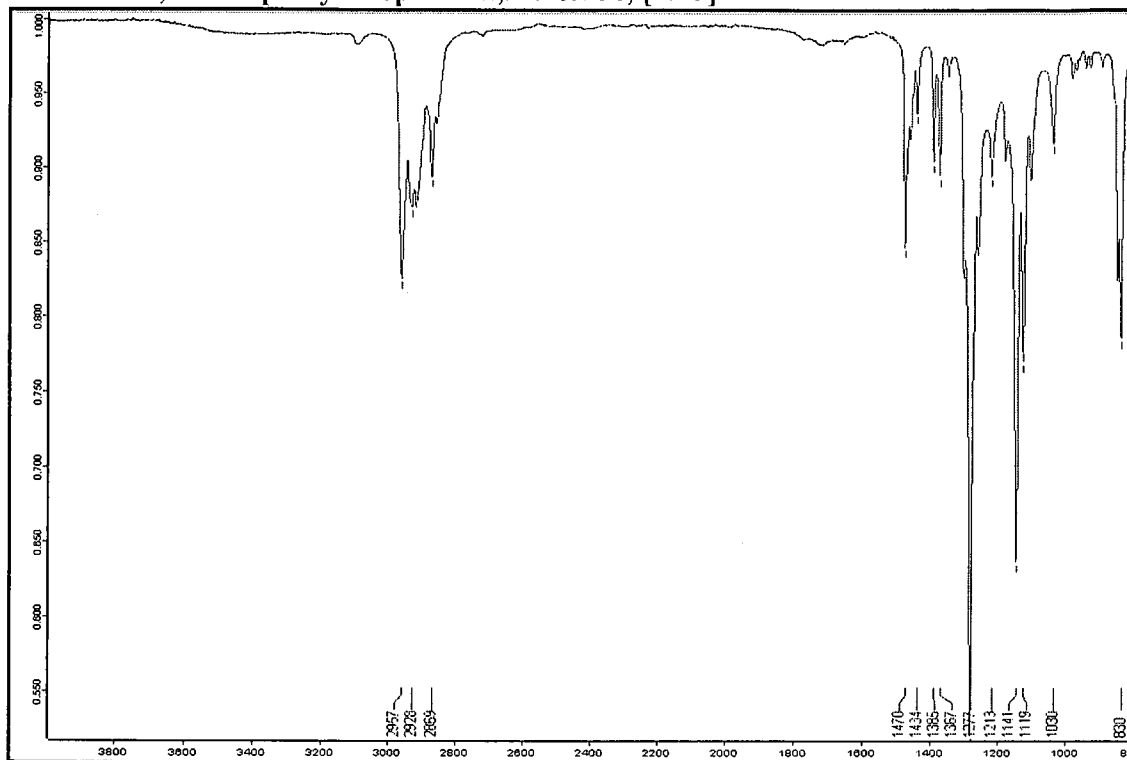


Plate 10: 2,5-Di(2-cyclohexylethyl)thiophene 1,1-dioxide, [4.4e]

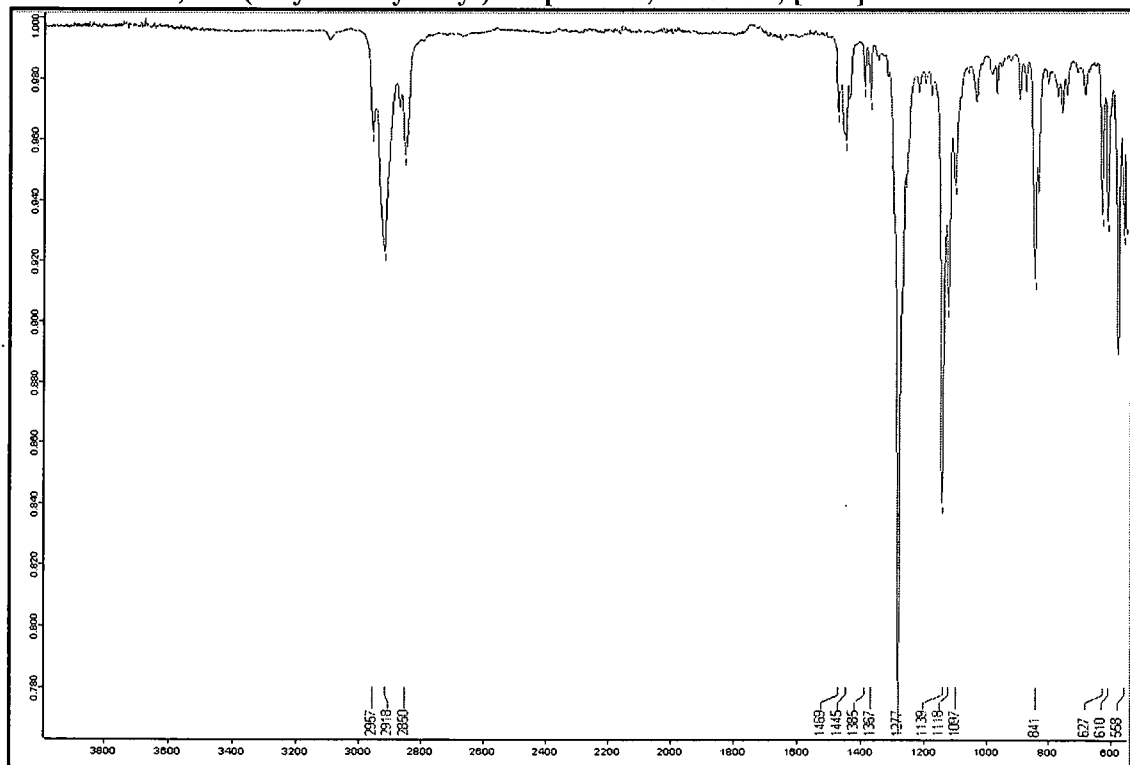


Plate 11: 3,6-Dihexylphthalonitrile, [4.5a].

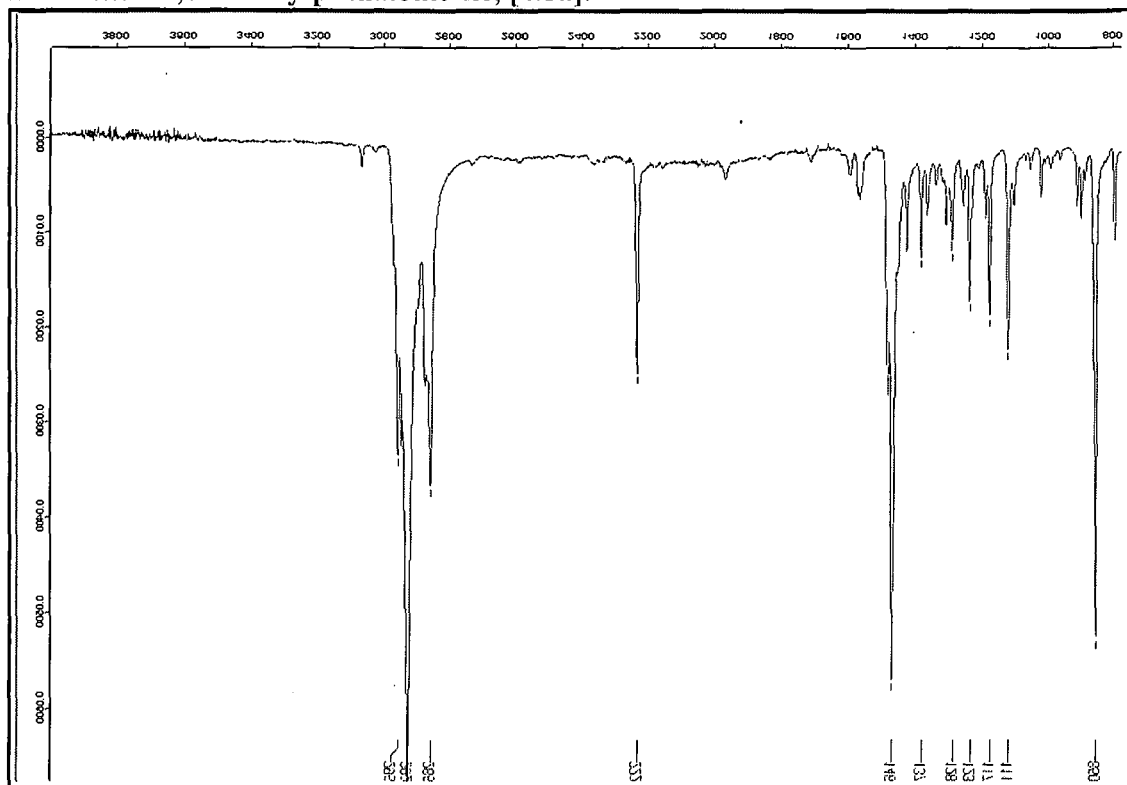


Plate 12: 3,6-Dioctylphthalonitrile, [4.5b]

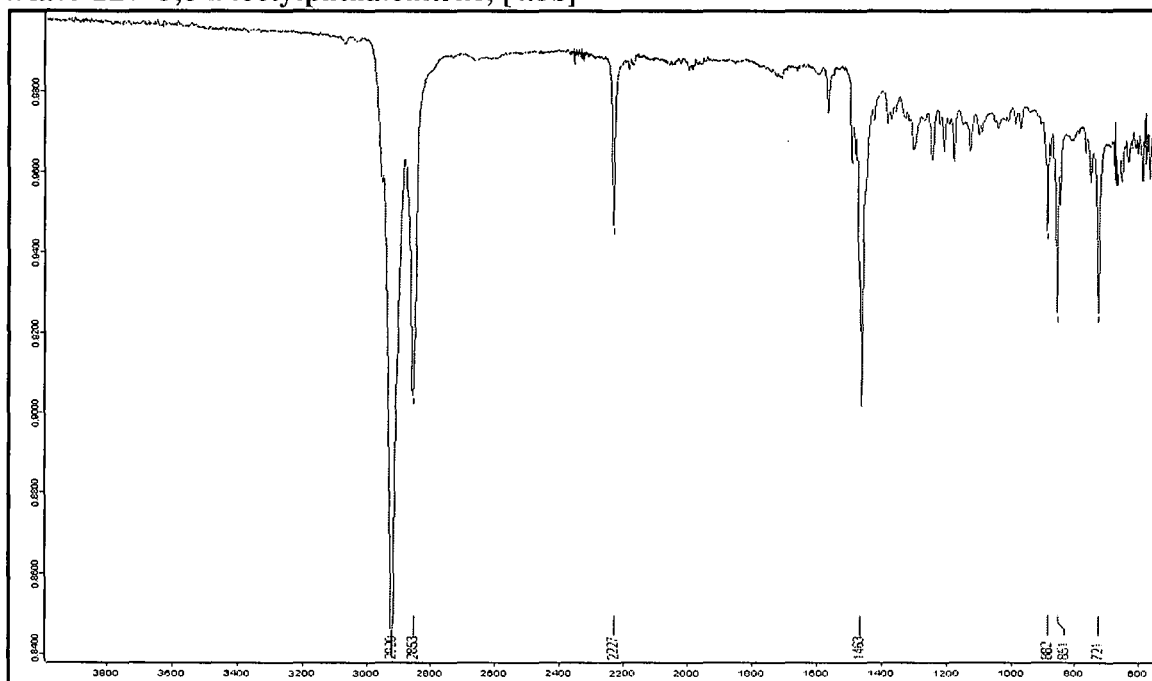


Plate 13: 3,6-Didodecylphthalonitrile, [4.5c]

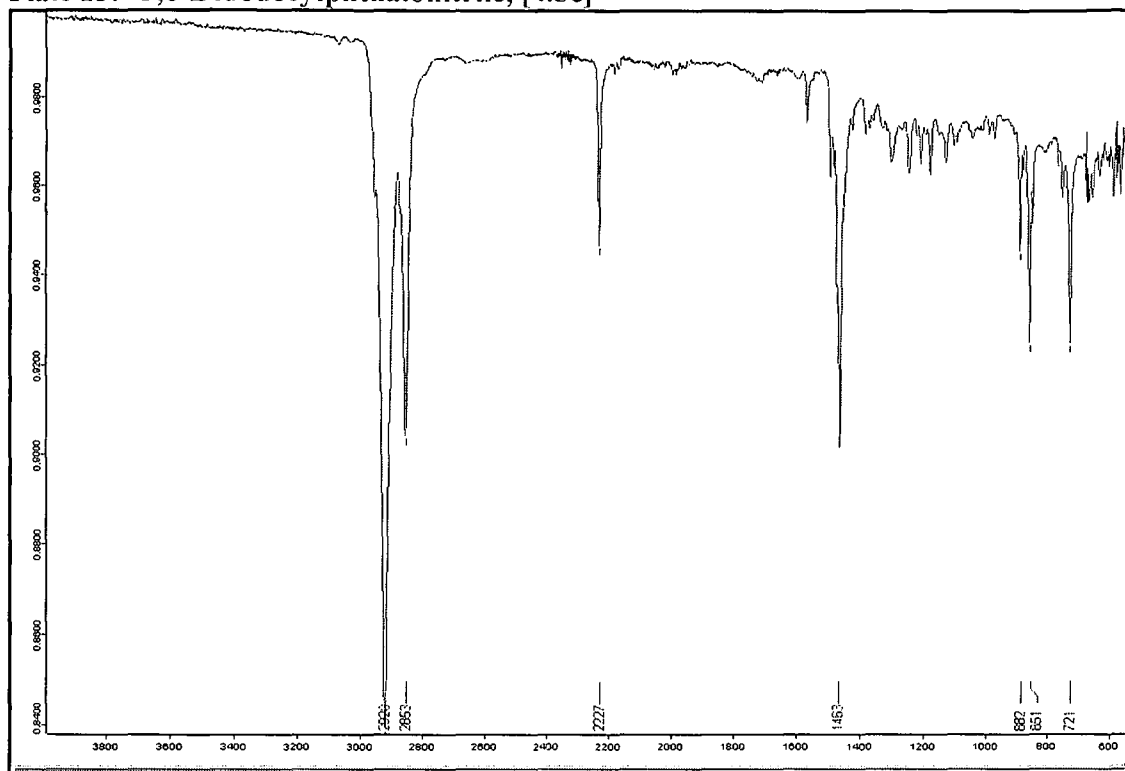


Plate 14: 3,6-Diisopentylphthalonitrile, [4.5d]

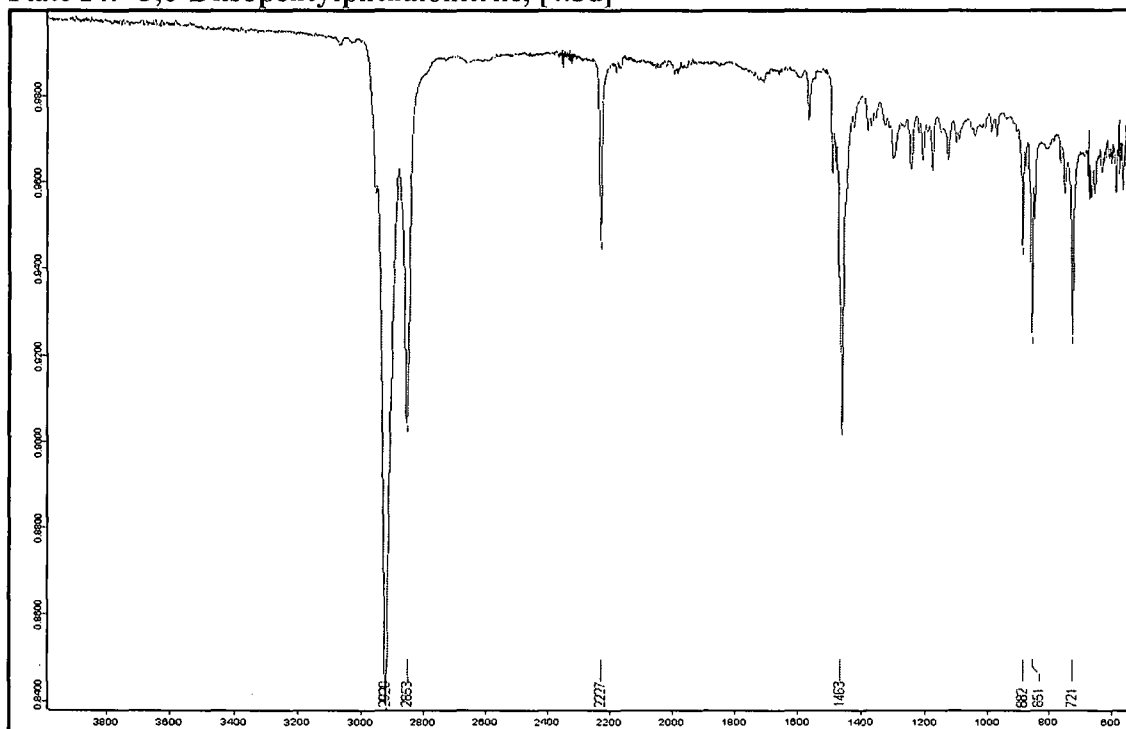


Plate 15: 3,6-Di(2-cyclohexylethyl)phthalonitrile, [4.5e].

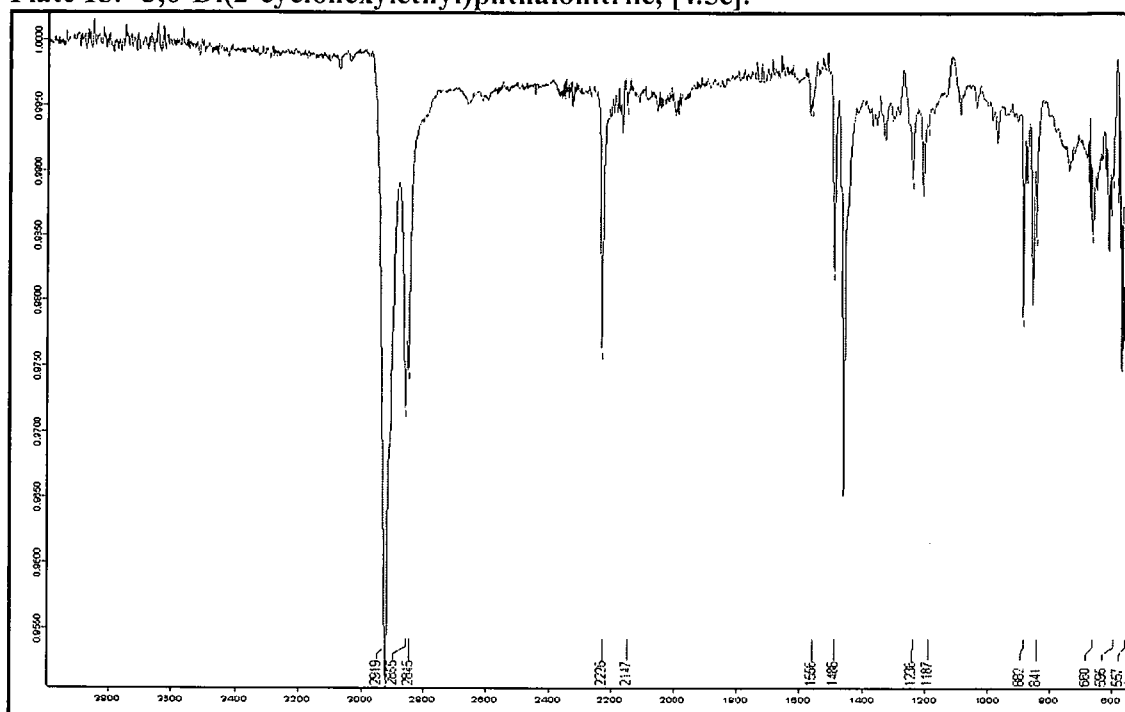


Plate 16: 1,4,8,11,15,18,22,25-octahexylphthalocyanine, [6.6a].

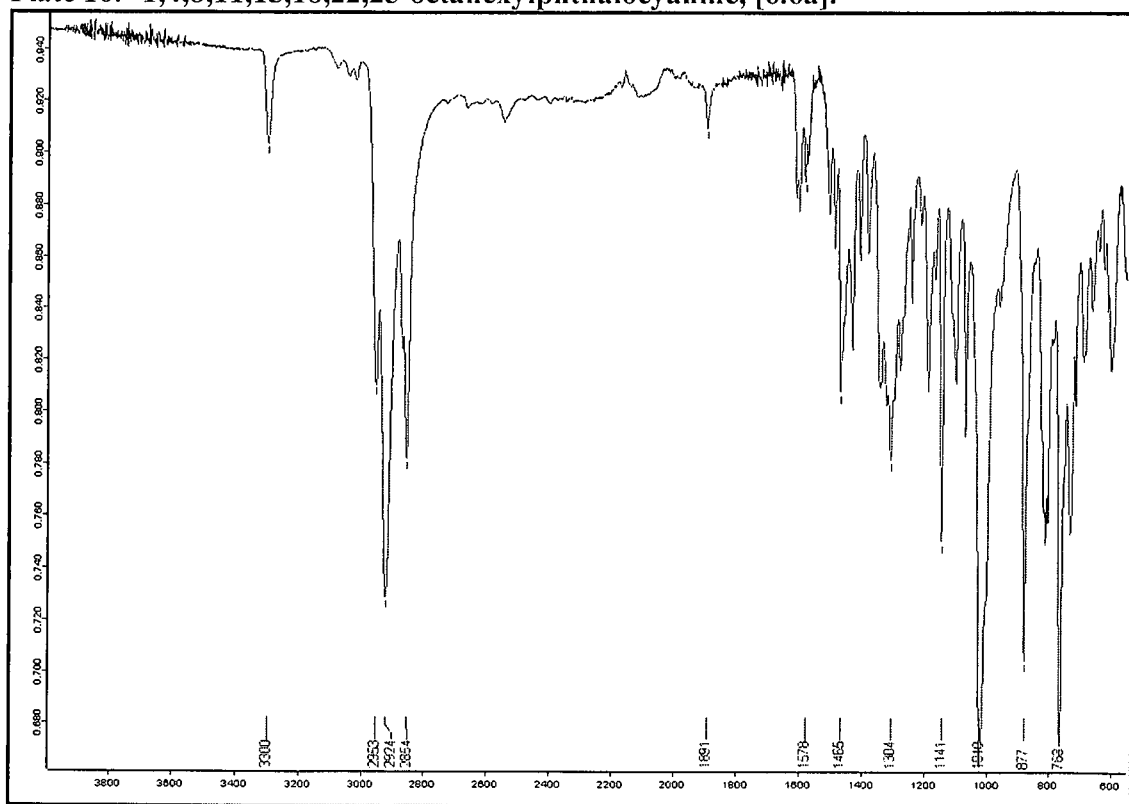


Plate 17: 1,4,8,11,15,18,22,25-octaoylphthalocyanine, [6.6b]

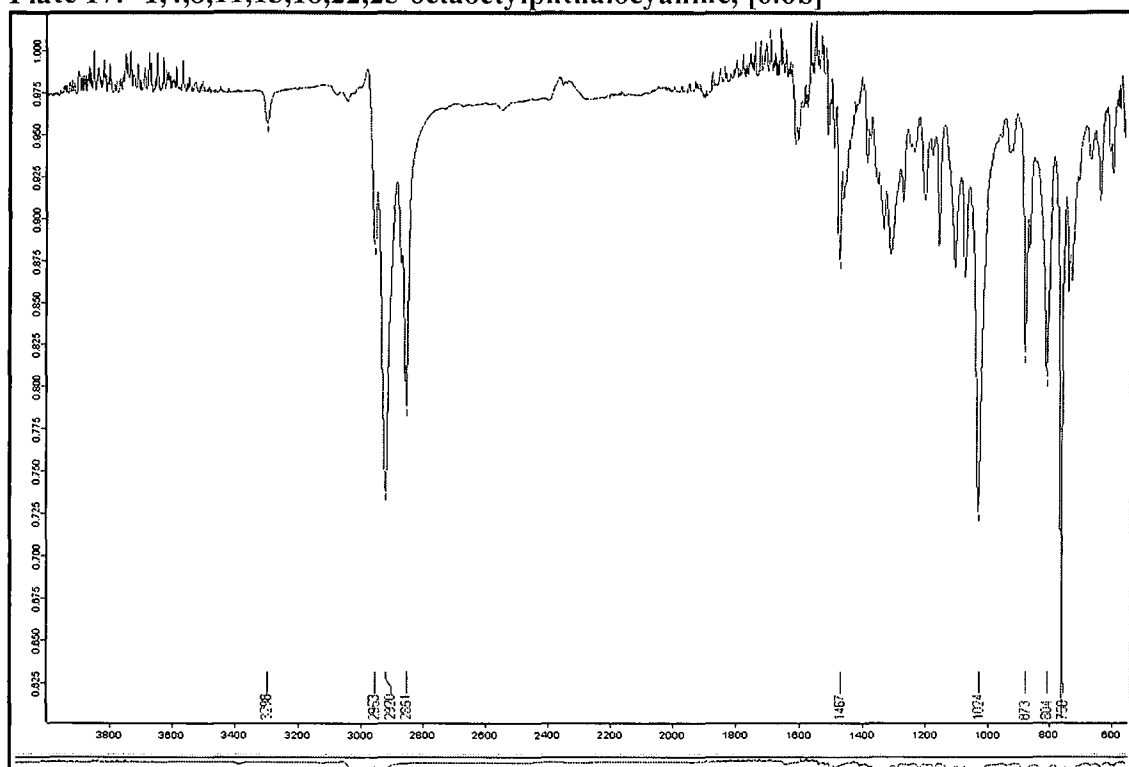


Plate 18: 1,4,8,11,15,18,22,25-octadodecylphthalocyanine, [6.6c]

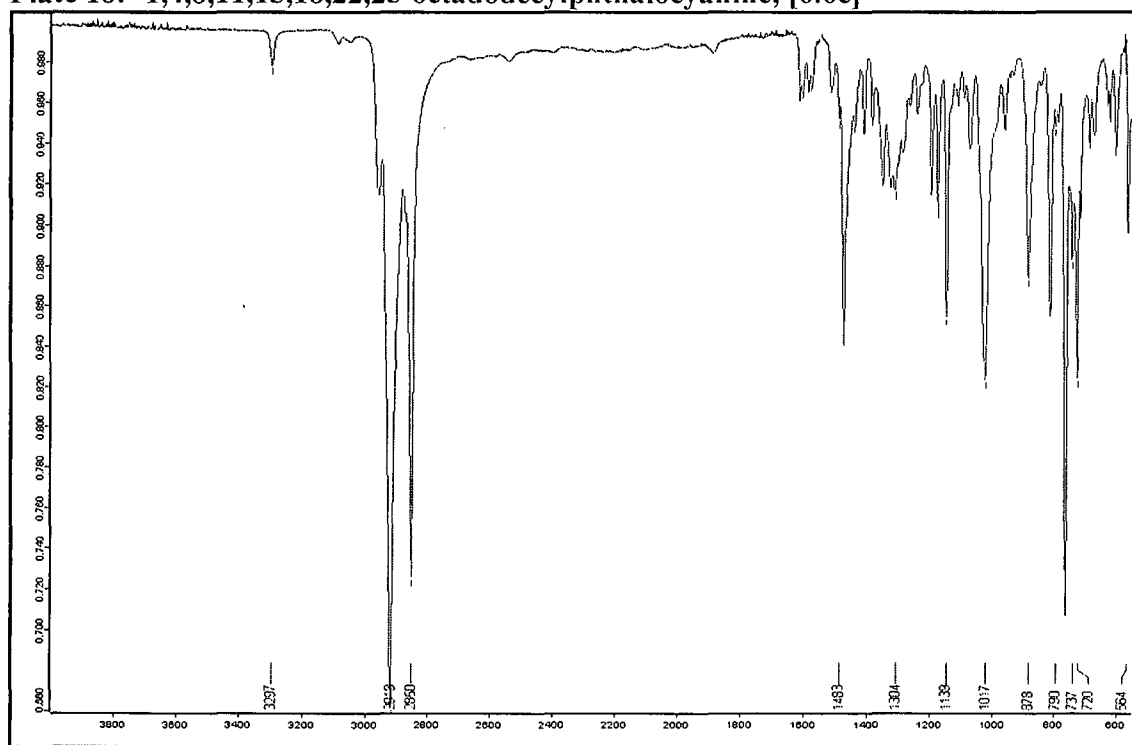


Plate 19: 1,4,8,11,15,18,22,25-octaisopentylphthalocyanine, [6.6d]

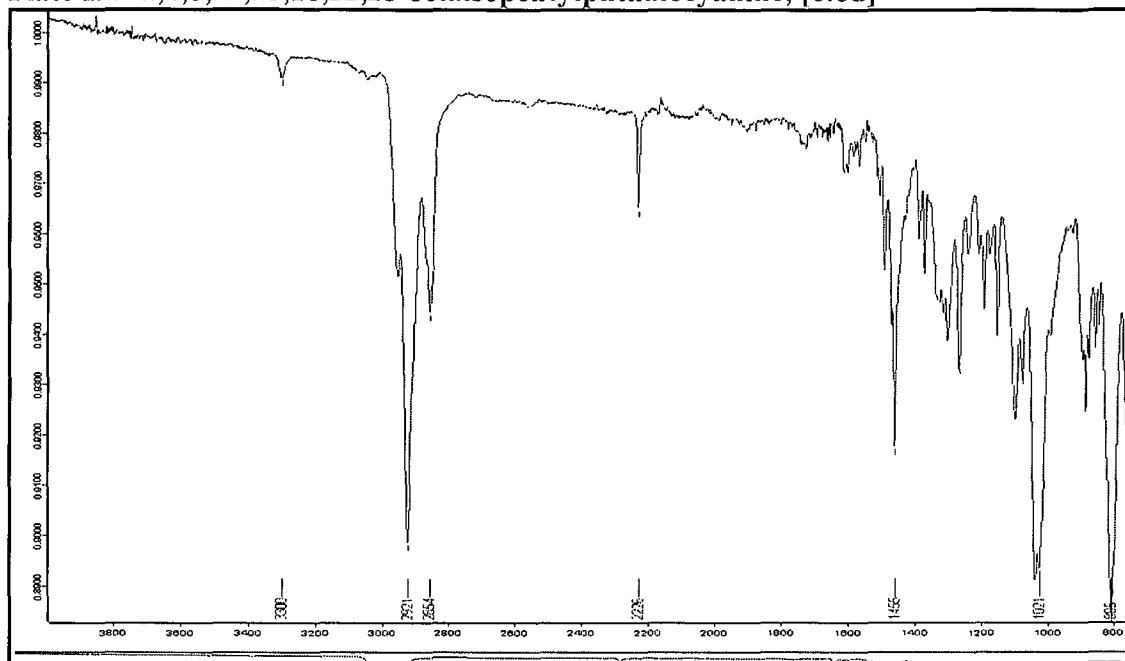


Plate 20: 1,4,8,11,15,18,22,25-octa(2-cyclohexylethyl)phthalocyanine, [6.6e]

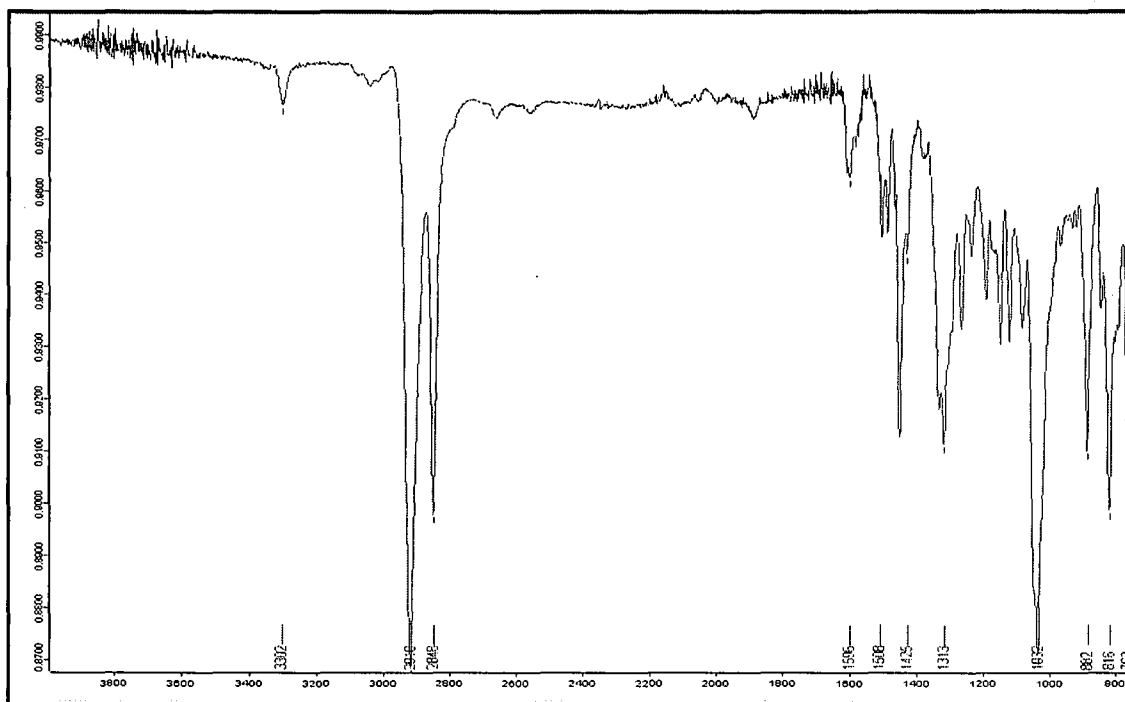


Plate 21: Carbonyl(1,4,8,11,15,18,22,25-octahexylphthalocyaninato)ruthenium(II), [4.8a]

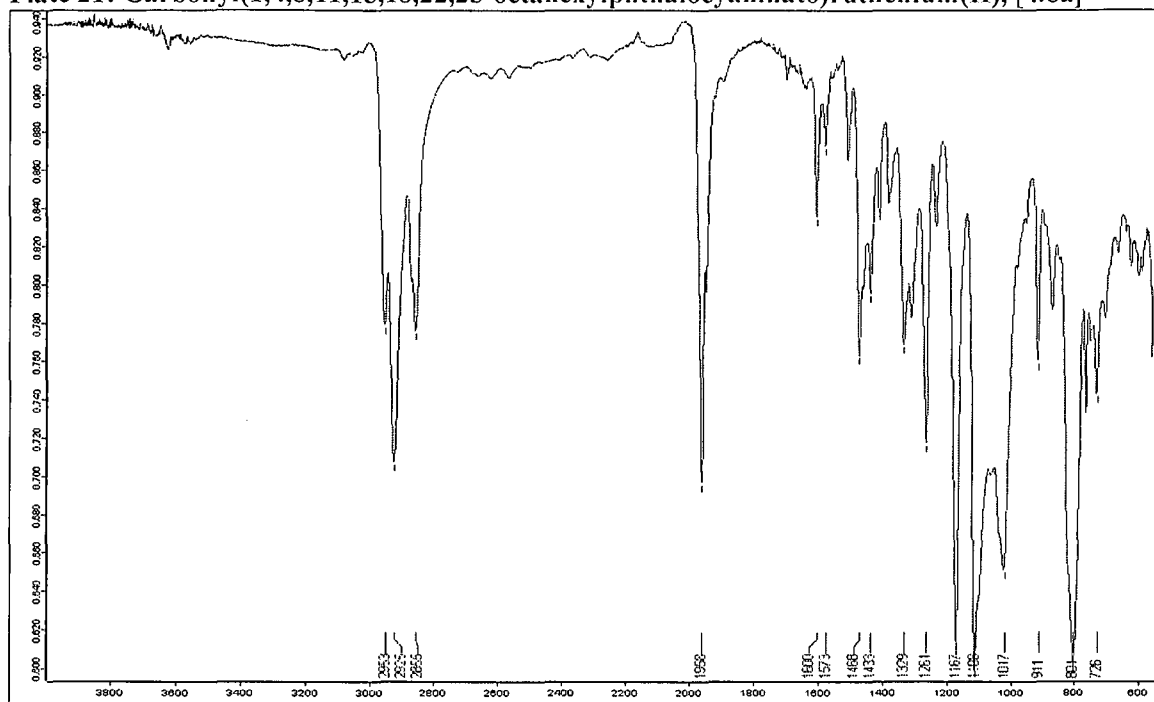


Plate 22: Carbonyl(1,4,8,11,15,18,22,25-octaoctylphthalocyaninato)ruthenium(II), [4.8b].

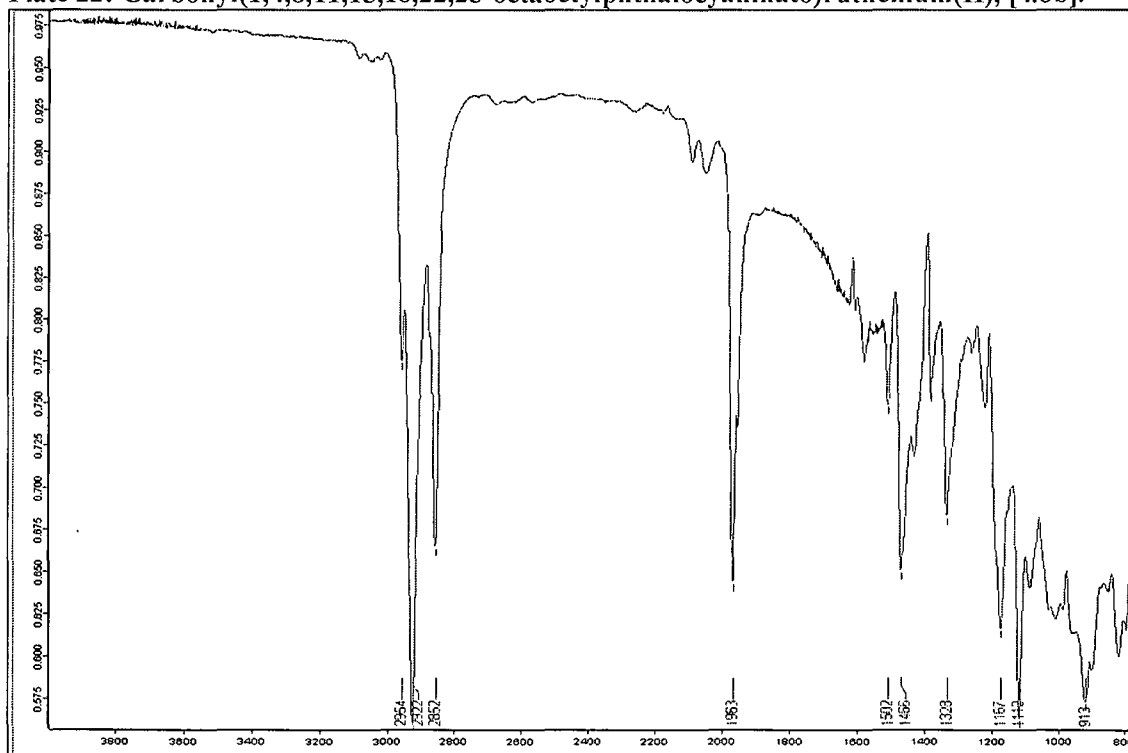


Plate 23: Carbonyl(1,4,8,11,15,18,22,25-octadecylphthalocyaninato)ruthenium(II), [4.8c]

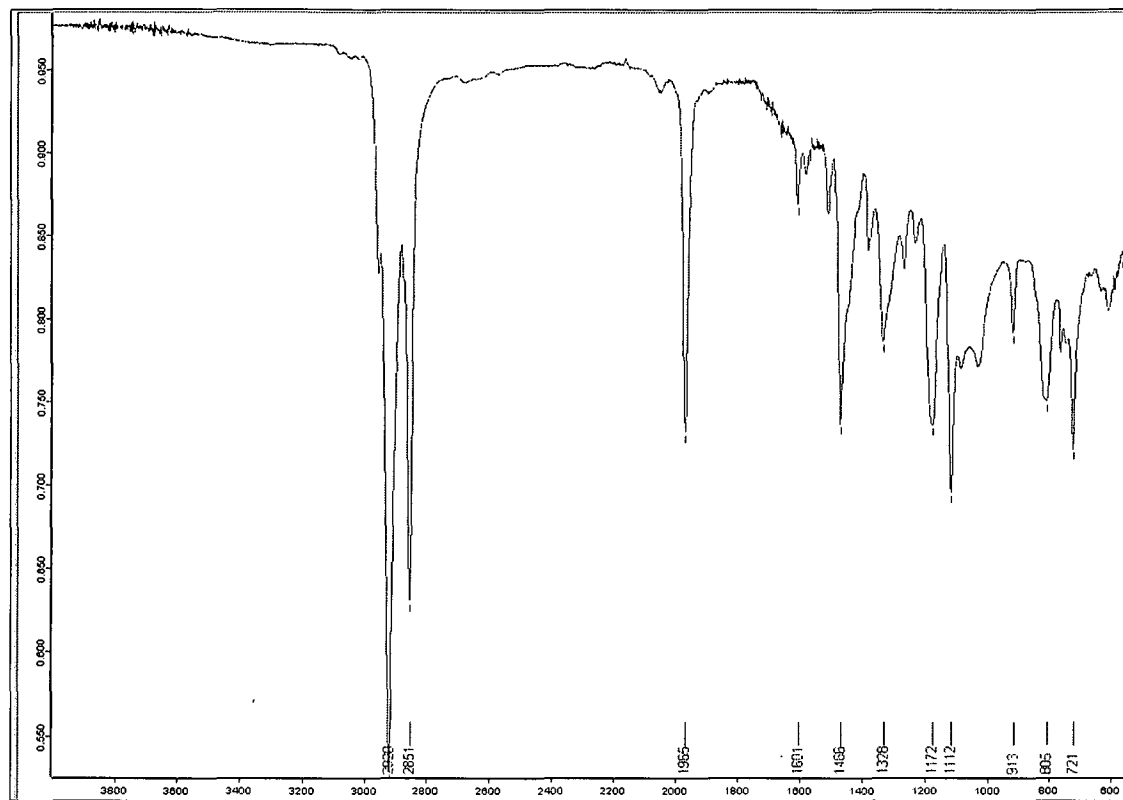


Plate 24: Carbonyl(1,4,8,11,15,18,22,25-octaisopentylphthalocyaninato)ruthenium(II), [4.8d]

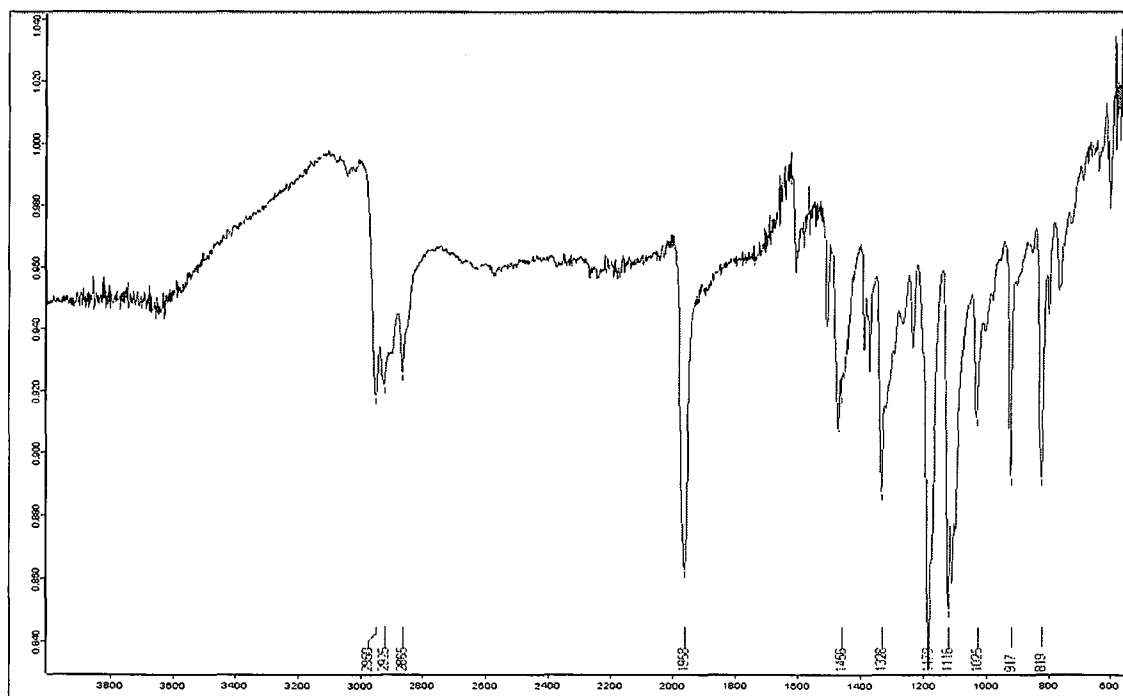


Plate 25: Carbonyl(1,4,8,11,15,18,22,25-octa(2-cyclohexylethylphthalocyaninato)ruthenium(II), [4.8e].

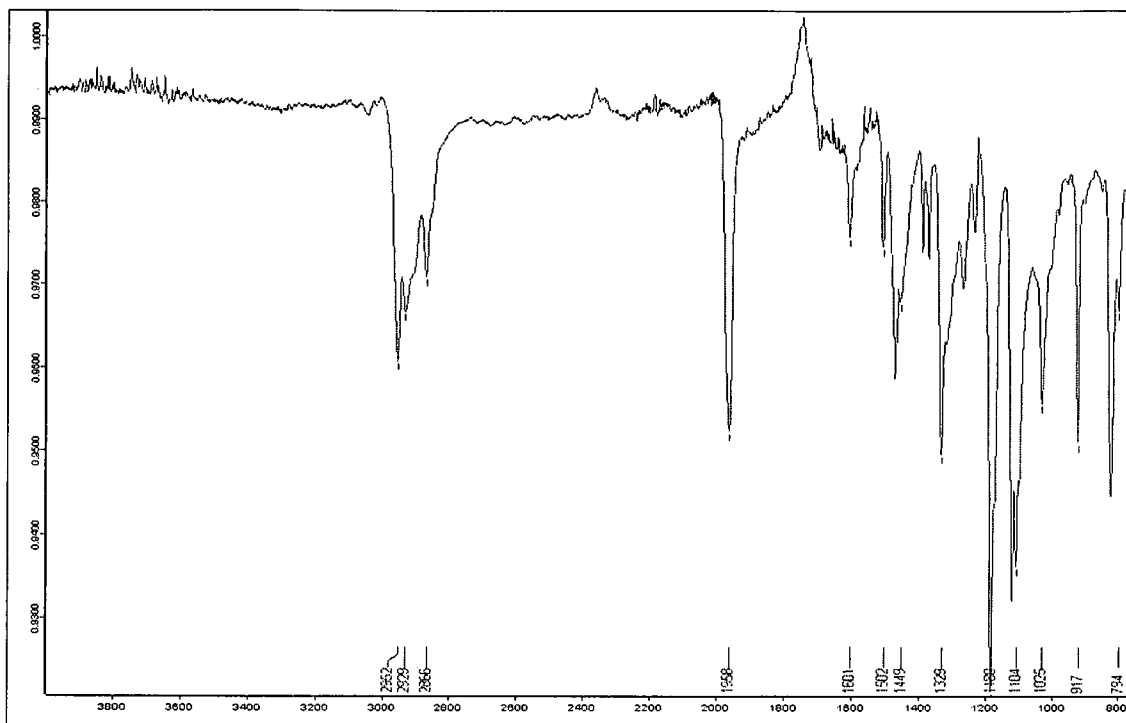


Plate 26: Carbonyl(phthalocyaninato)ruthenium(II), [4.8f].

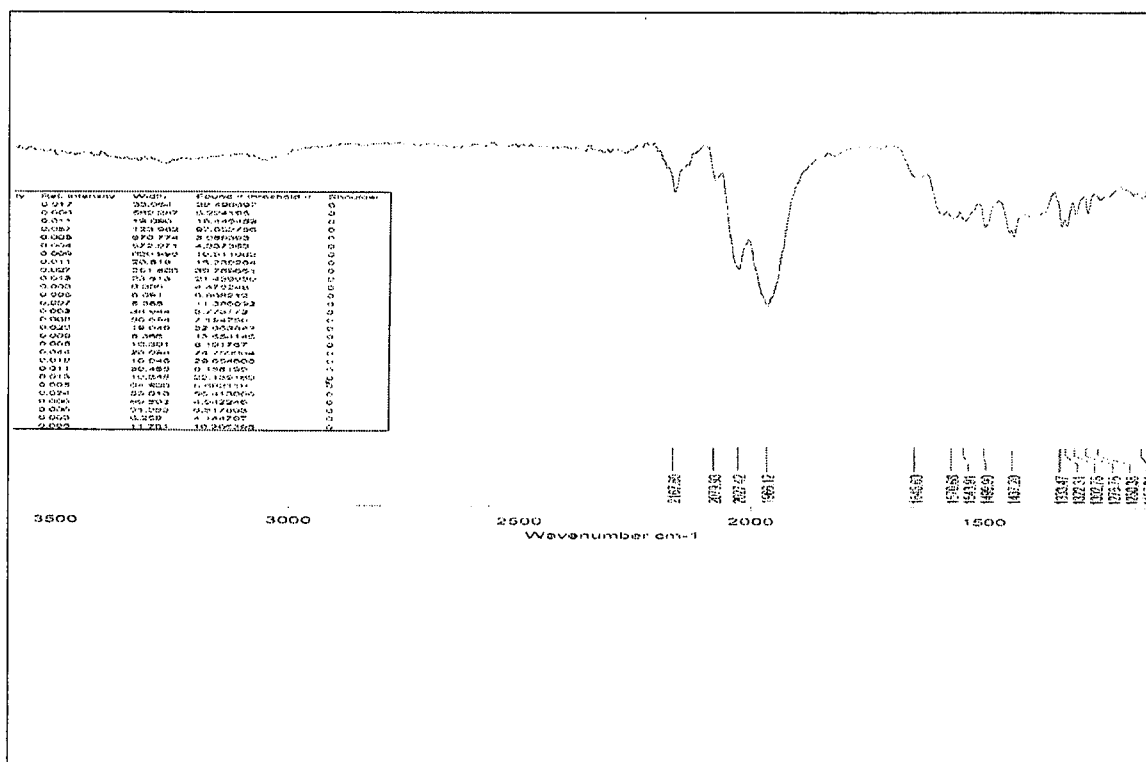
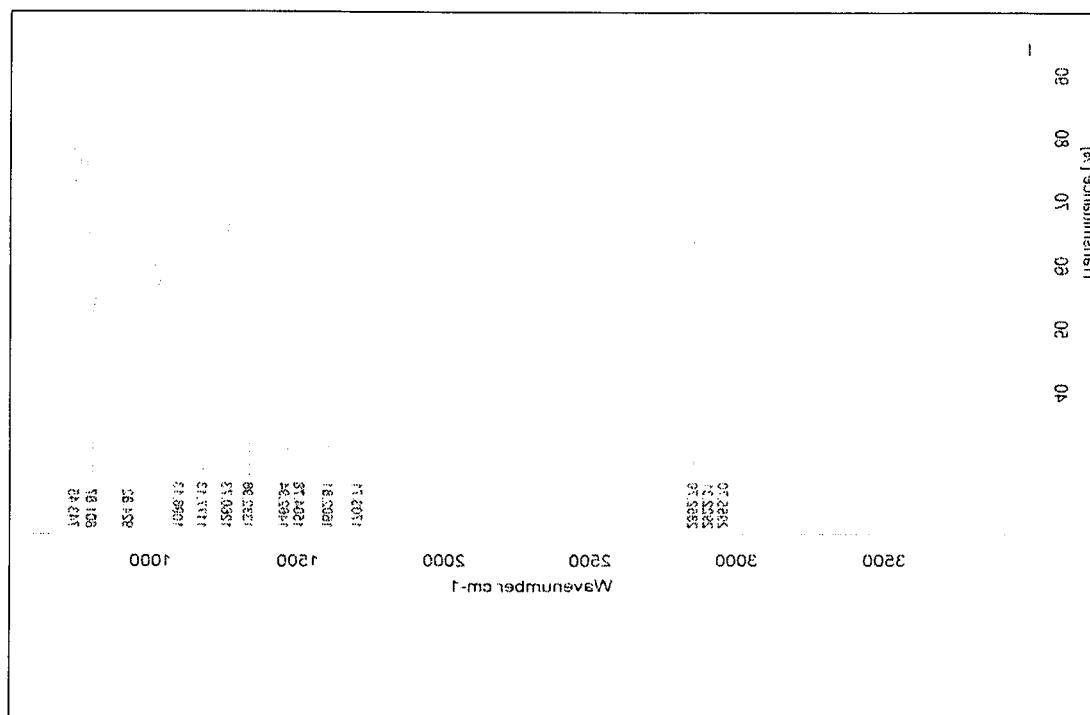


Plate 27: (1,4,8,11,15,18,22,25-Octaocetylphthalocyaninato)cobalt(II), [4.7b].



MALDI-TOF MS

Plate 28: Carbonyl(1,4,8,11,15,18,22,25-octahexylphthalocyaninato)ruthenium(II), [4.8a]

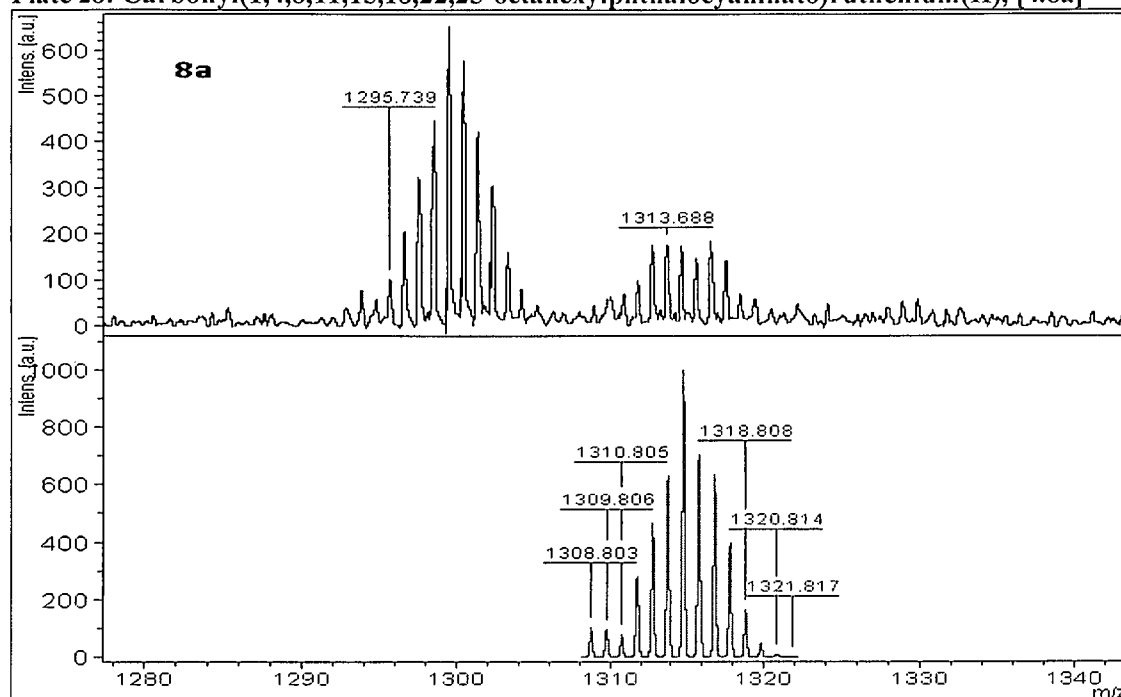


Plate 29: Carbonyl(1,4,8,11,15,18,22,25-octaoctylphthalocyaninato)ruthenium(II), [4.8b]

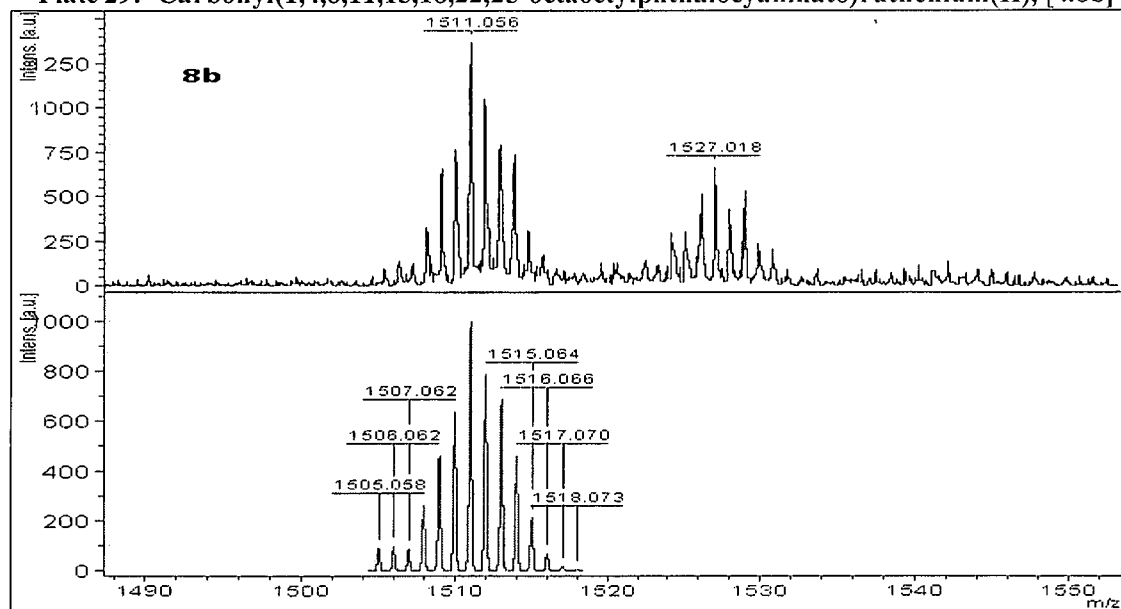


Plate 30: Carbonyl(1,4,8,11,15,18,22,25-octadecylphthalocyaninato)ruthenium(II), [4.8c]

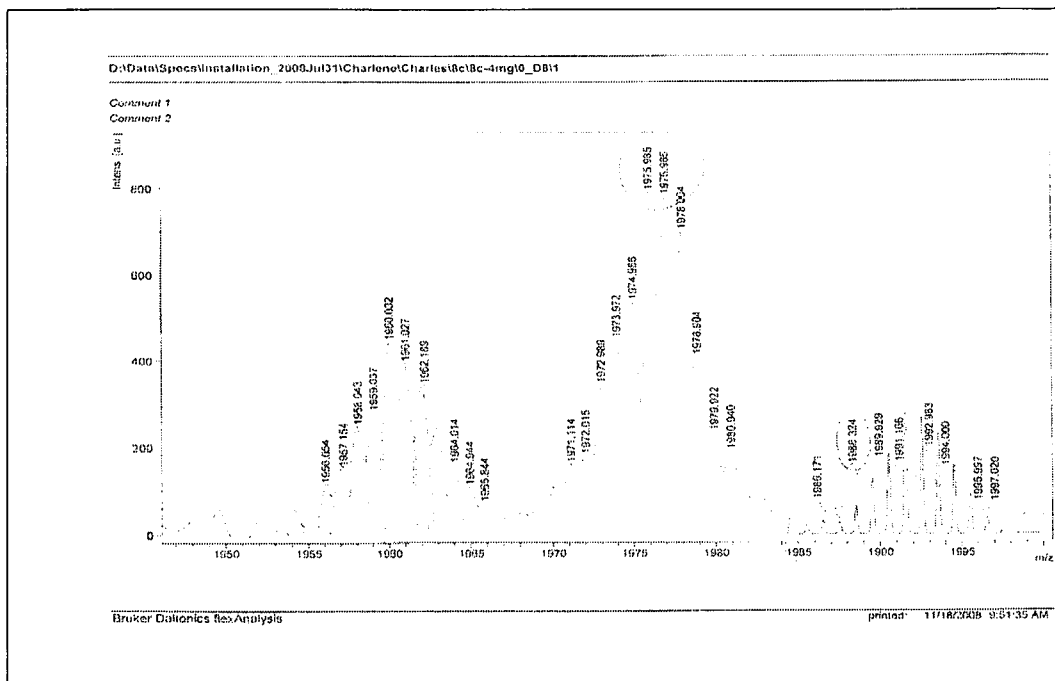


Plate 31: Carbonyl(1,4,8,11,15,18,22,25-octaisopentylphthalocyaninato)ruthenium(II), [4.8d].

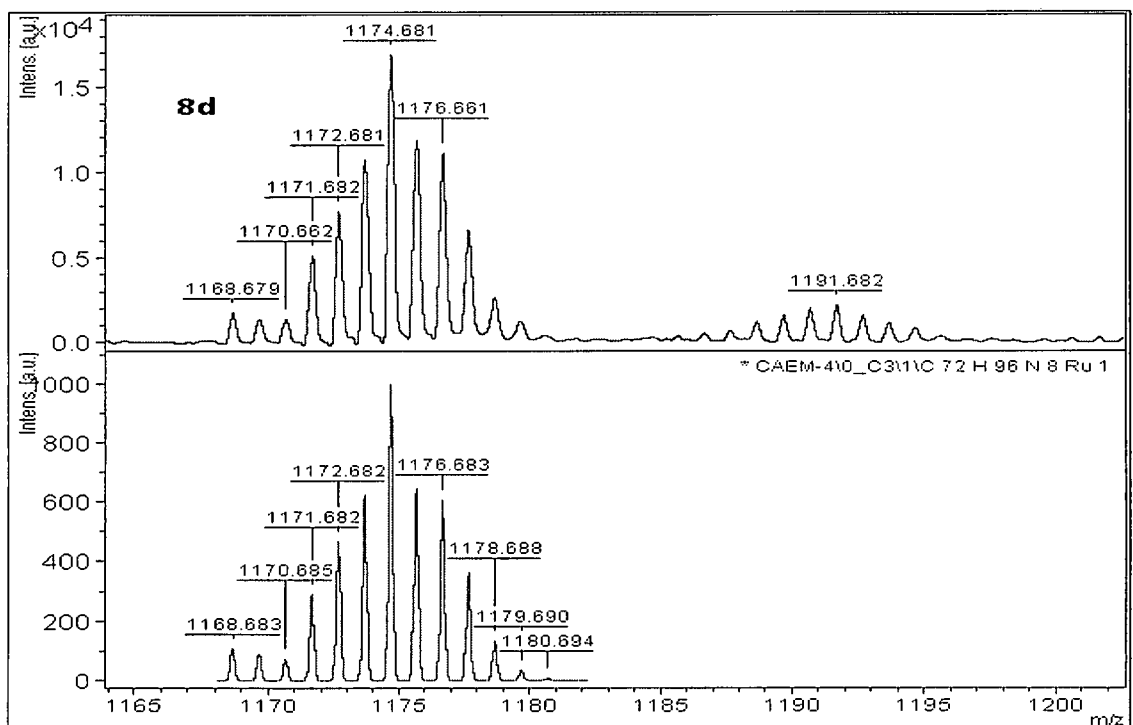


Plate 32: Carbonyl(1,4,8,11,15,18,22,25-octa(2- cyclohexylethylphthalocyaninato)ruthenium(II), [4.8e].

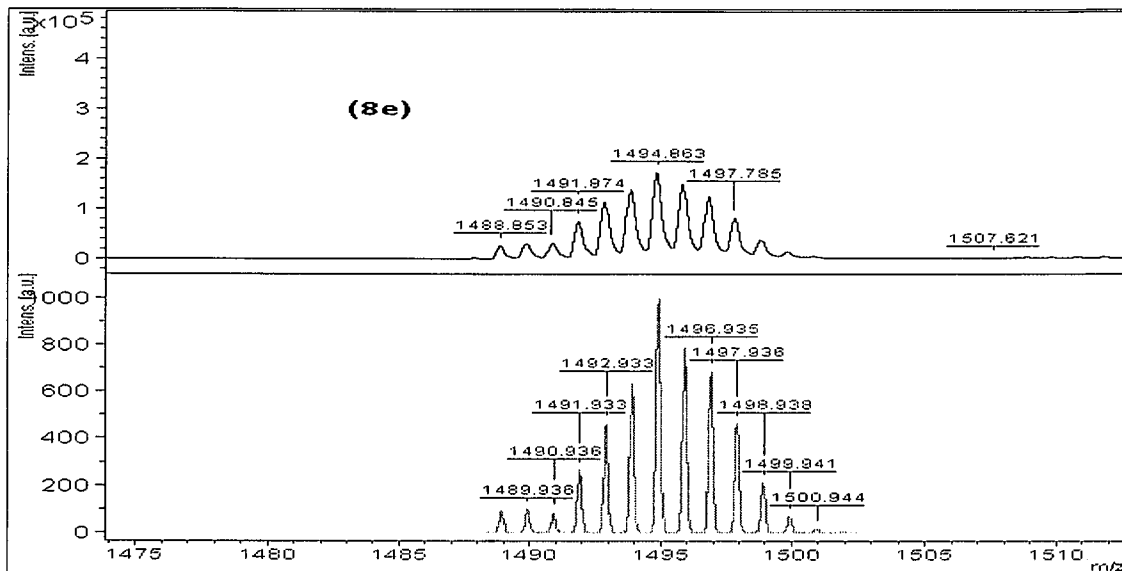


Plate 33: Carbonyl(phthalocyaninato)ruthenium(II), [4.8f].

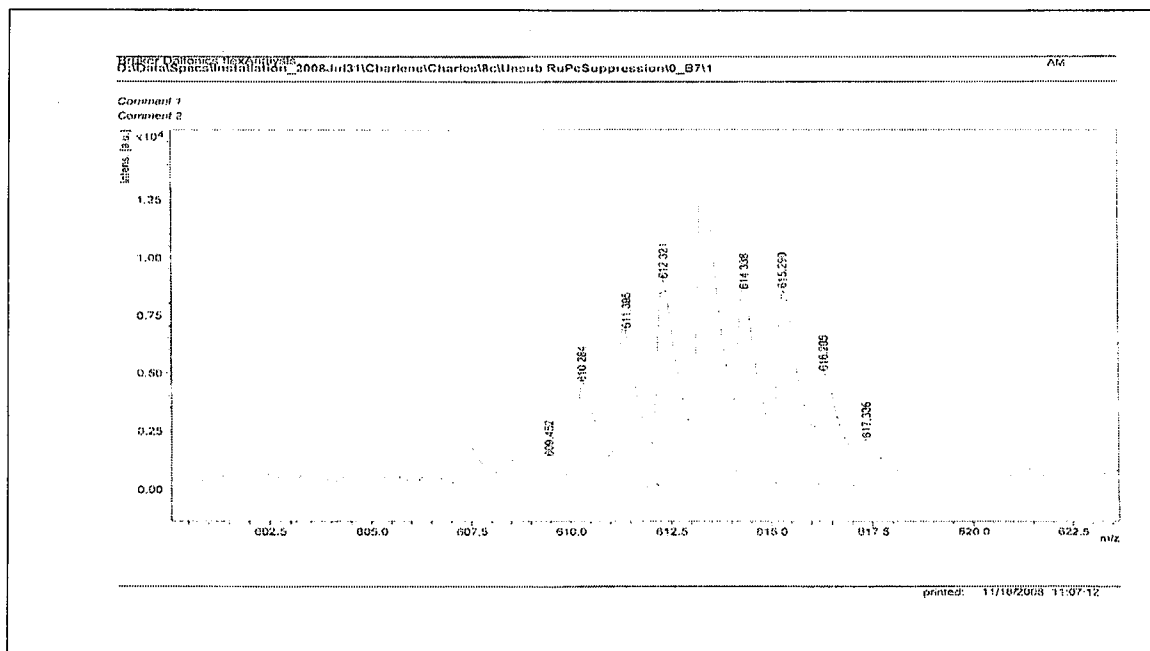
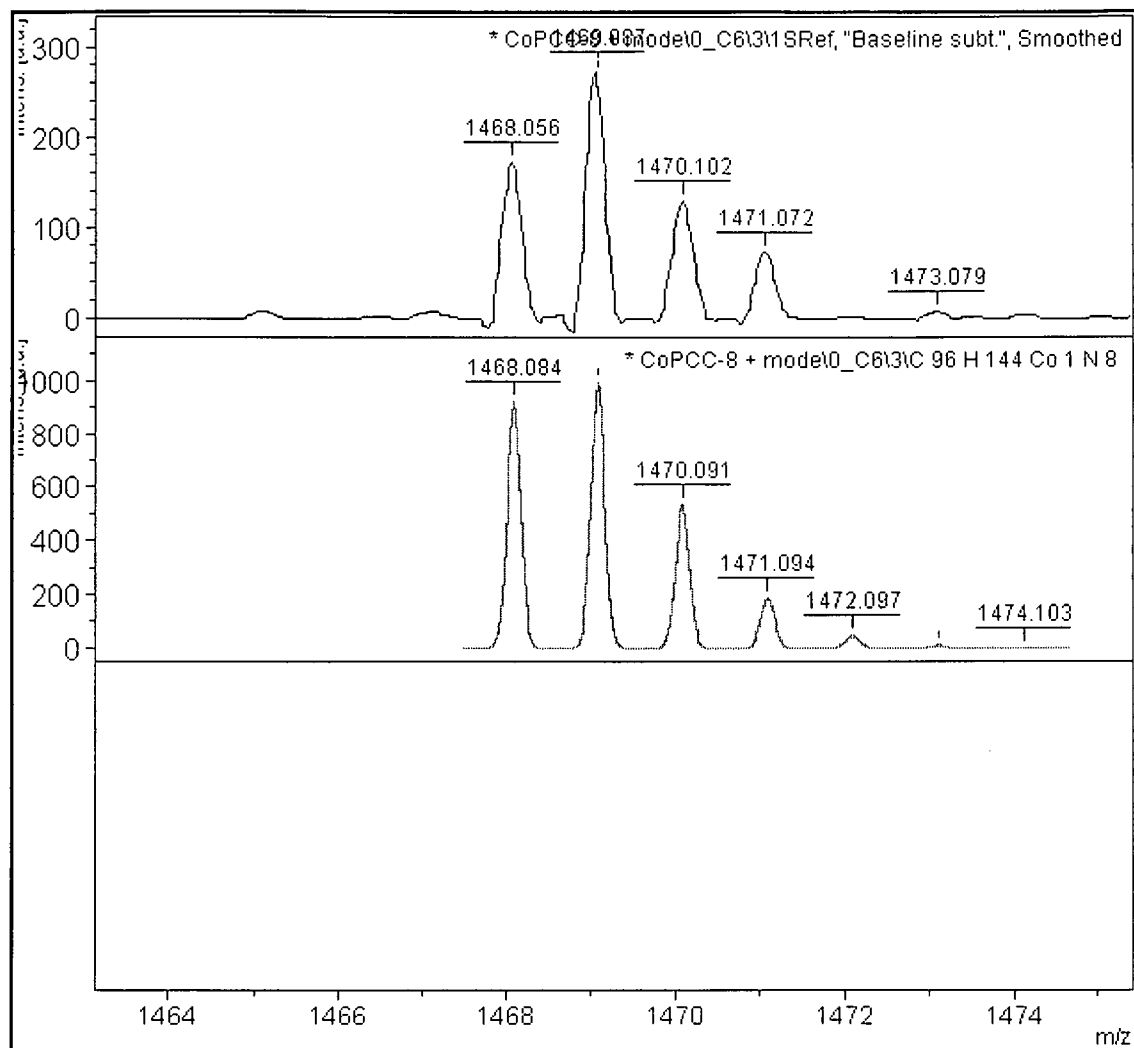


Plate 34: (1,4,8,11,15,18,22,25-Octaoctylphthalocyaninato)cobalt(II), [4.7b].



HRMS

Plate 35: Carbonyl(1,4,8,11,15,18,22,25-octaethylphthalocyaninato)ruthenium(II), [4.8a]

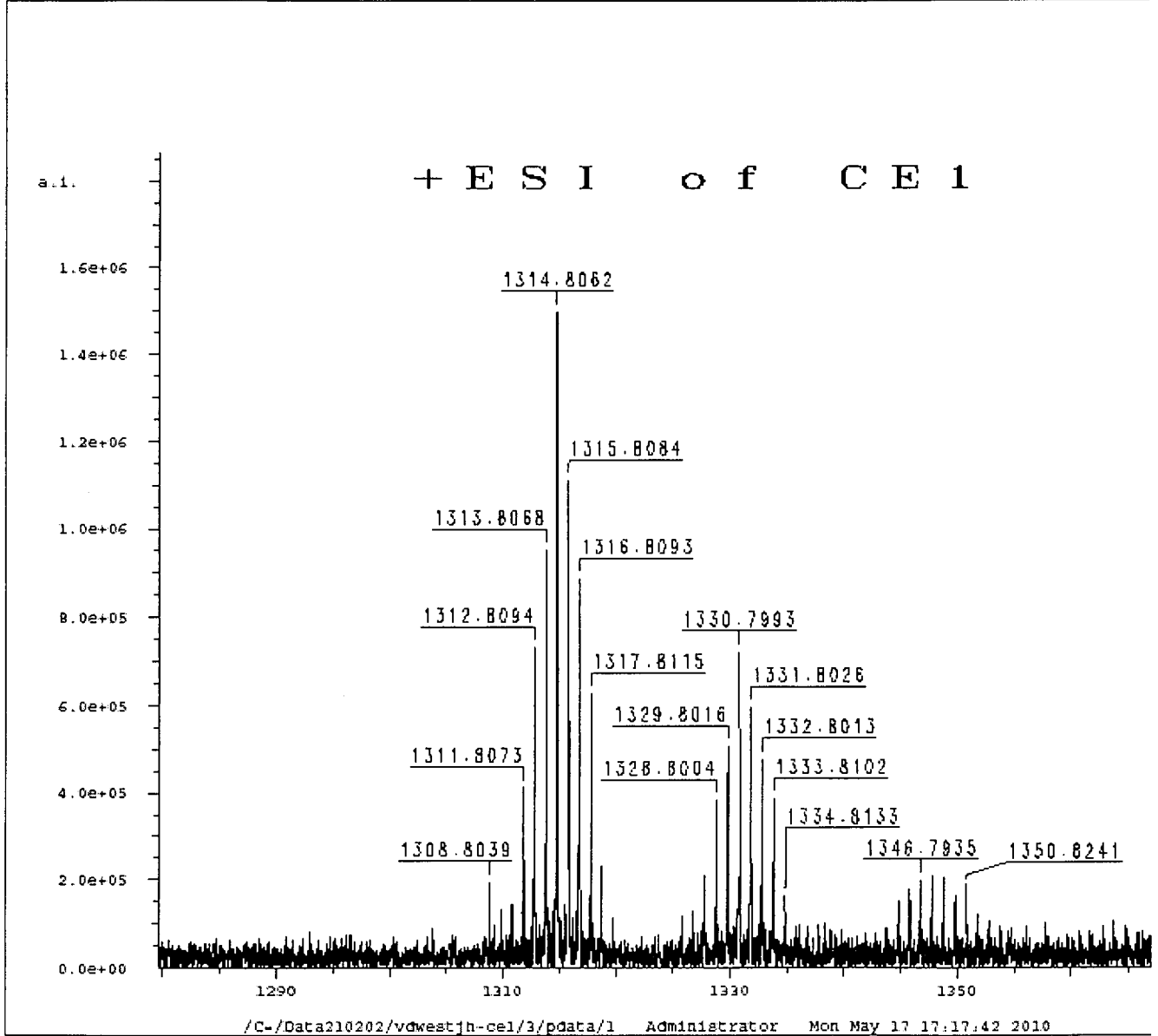


Plate 36: Carbonyl(1,4,8,11,15,18,22,25-octaoctylphthalocyaninato)ruthenium(II), [4.8b]

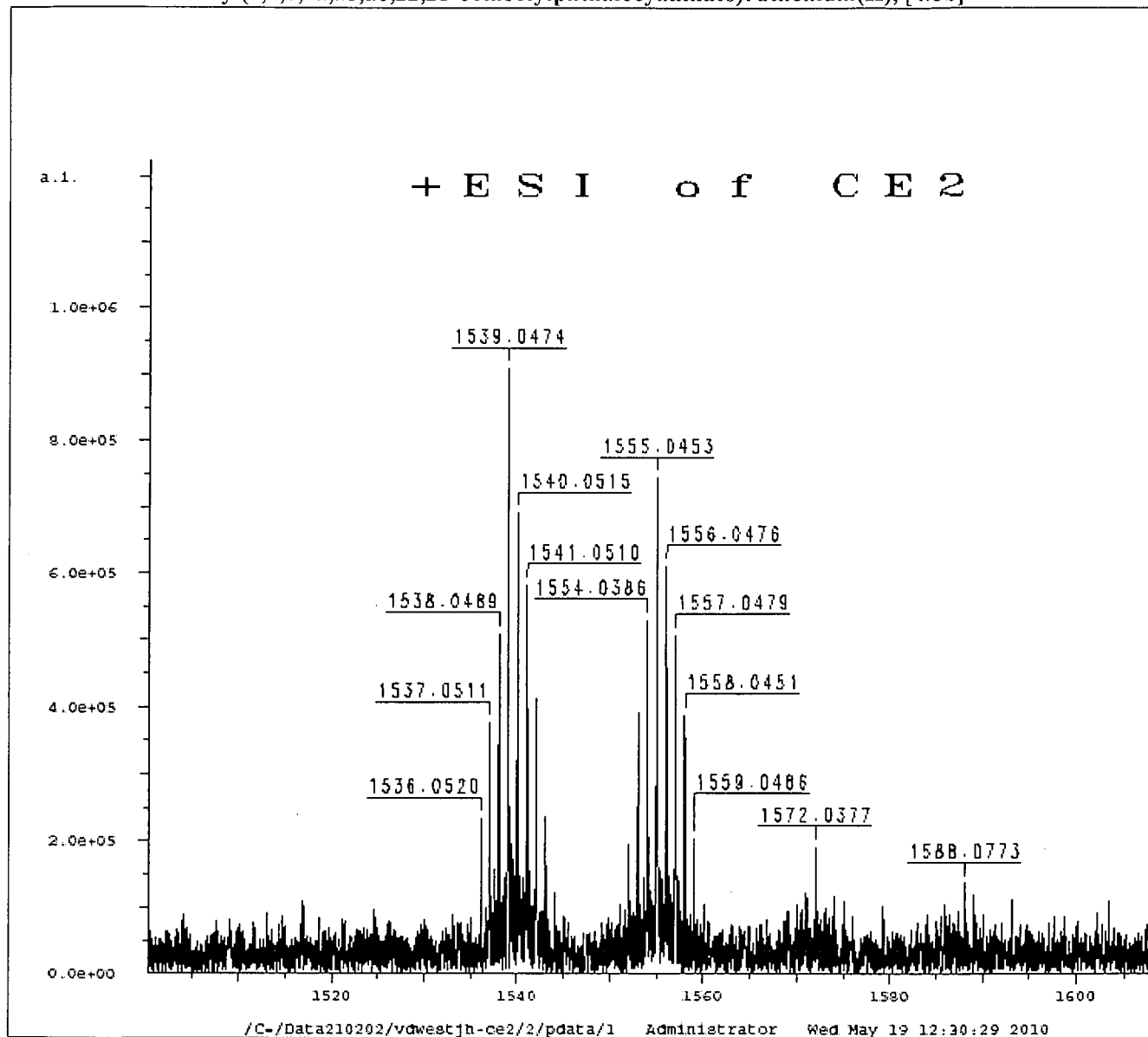
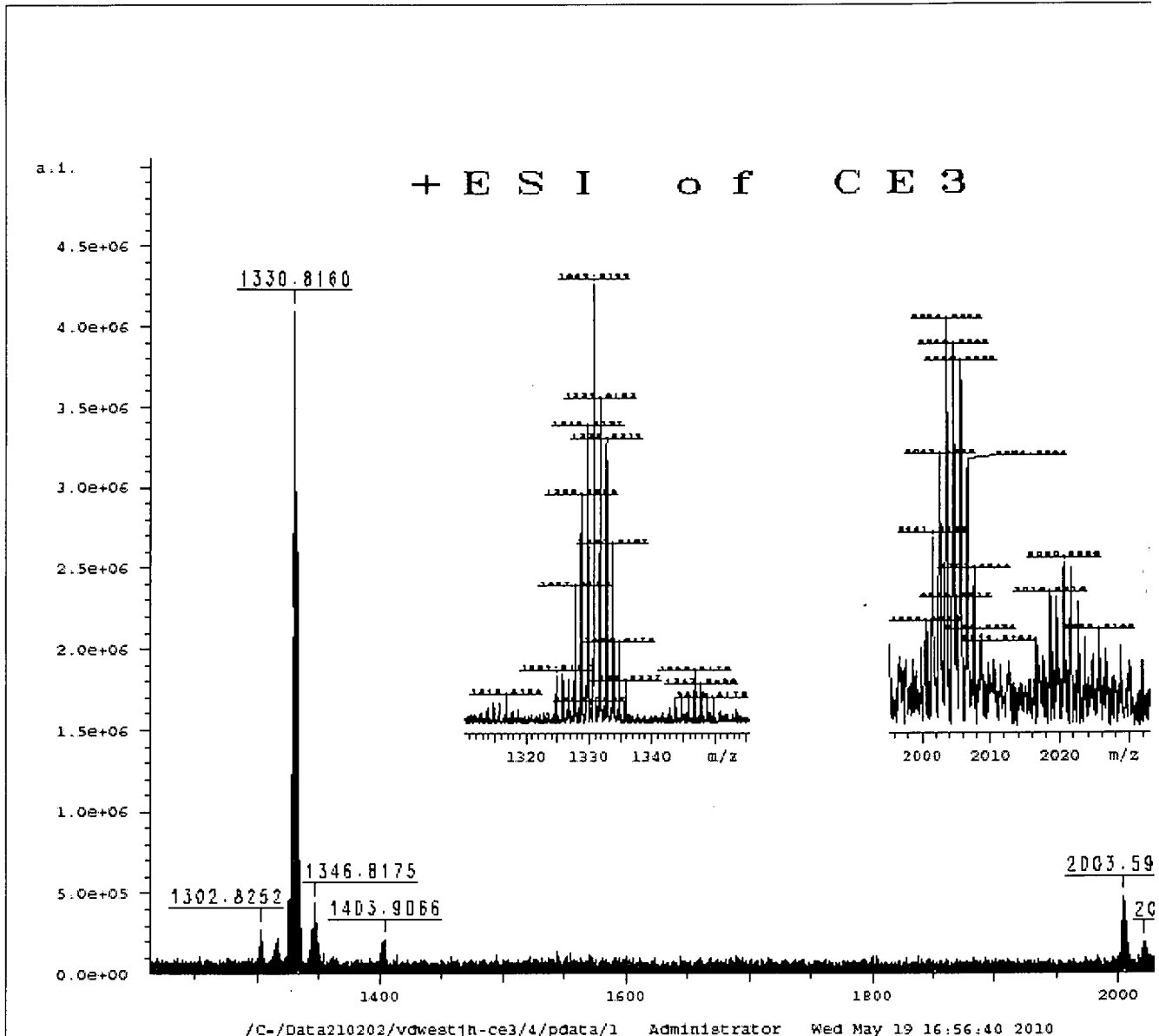


Plate 37: Carbonyl(1,4,8,11,15,18,22,25-octadodecylphthalocyanato)ruthenium(II),

[4.8c]



UV - UFS
BLOEMFONTEIN
INSTRUMENT-LIBRARY

Plate 38: Carbonyl(1,4,8,11,15,18,22,25-octaisopentylphthalocyaninato)ruthenium(II),
[4.8d].

